RISK OF INFLUENZA UNDER REALISTIC INFLUENZA VACCINATION INTERVENTIONS AMONG UNIVERSITY STUDENTS

Paul Nicholas Zivich

A dissertation submitted to the faculty at the University of North Carolina at Chapel Hill in partial fulfillment of the requirements for the degree of Doctor of Philosophy in the Department of Epidemiology in the Gillings School of Global Public Health.

Chapel Hill
2021

Approved by:

Allison E. Aiello

M. Alan Brookhart

Michael G. Hudgens

James Moody

David J. Weber

ABSTRACT

Paul Nicholas Zivich: Risk of Influenza Under Realistic Influenza Vaccination Interventions Among University Students
(Under the direction of Allison E Aiello)

Seasonal influenza causes substantial morbidity and mortality each year. One important group to consider is university students since their vaccination uptake is low, they experience high attack rates, they suffer substantial negative impacts on their well-being, and they may be important for further transmission. Rather than assess direct vaccine effectiveness, this work aimed to estimate the risk of influenza under large-scale changes in the distribution of influenza vaccination.

Using self-reported contact data from the eX-FLU cluster randomized trial on three-day self-isolation, we applied a recent extension of the targeted maximum likelihood estimation (TMLE) framework for dependent data. Hypothetical policies to increase vaccination focused on educational information regarding influenza, reducing non-financial barriers, and reducing financial barriers were compared. Each policy was further compared across a range of plausible shifts in the log-odds of influenza vaccination receipt. To guide the application of TMLE and approaches to account for measurement error of self-reported edges within eX-FLU, two simulation studies were conducted. To assess imputation and Bayesian procedures for measurement error, we conducted a simulation study of three network generative models with non-informative and informative measurement error. To assess TMLE for dependent data, we simulated four data-generating mechanisms in three different networks.

Both imputation and Bayesian approaches reduced bias and improved confidence limit coverage for all parameters in most scenarios. The TMLE for dependent data performed well

across scenarios with interference, but issues manifested when policies were not well-supported by the observed data. In the application of TMLE to the eX-FLU data, a reduction in the risk of laboratory-confirmed influenza was observed across policies. However, the estimates were consistent with little-to-no reduction. When accounting for measurement error of self-reported contacts via the Bayesian approach, a greater reduction in risk was observed but differences between policies were minor.

Our results are a robust analysis for a parameter of public health importance. The results of our simulations and analyses will serve as an example for future applications.

TABLE OF CONTENTS

LIST OF TABLES ix

LIST OF FIGURES xii

LIST OF ABBREVIATIONS xiv

CHAPTER 1: INTRODUCTION 1

1.1 Influenza 1

1.1.1 Virology 1

1.1.2 Pathogenesis 3

1.1.3 Epidemiology 4

1.2 Influenza Vaccine 5

1.2.1 Inactivated Vaccines 6

1.2.2 Live-Attenuated Vaccines 7

1.2.3 Vaccine Effectiveness 7

1.2.4 Vaccination Recommendations 9

1.3 Influenza and University Students 9

1.4 Difficulties in Measuring Vaccine Effectiveness 12

1.5 Measurement Error 15

1.5.1 Imputation Approach 16

1.5.2 Bayesian Approach 16

1.6 Synopsis 17

CHAPTER 2: STATEMENT OF SPECIFIC AIMS 18

CHAPTER 3: METHODS 21

3.1 Overview 21

3.2 Data Source 21
3.3 Outcome Assessment....24
3.4 Exposure Assessment....24
3.5 Covariate Assessment....25
3.6 Statistical Analyses....26
3.6.1 Approaches 28
3.6.2 Performance Metrics....30
3.6.3 Implementation Validation....33
3.6.4 Data-Generating Mechanisms 35
3.6.5 Policies....40
3.6.6 Network-TMLE....41
3.6.7 Missing Data....44
3.6.8 Measurement Error....49
CHAPTER 4: APPROACHES TO ACCOUNT FOR MEASUREMENT ERROR OF EDGES AND THEIR PERFORMANCE....53
4.1 Introduction....53
4.2 Methods 54
4.2.1 Imputation Approach....55
4.2.2 Bayesian Approach....56
4.2.3 Simulation Study....57
4.3 Results 60
4.3.1 Network-1 60
4.3.2 Network-2 61
4.3.3 Network-3 61
4.4 Discussion....62
4.4.1 Conclusions....64
4.5 Tables and Figures....65

CHAPTER 5: TARGETED MAXIMUM LIKELIHOOD ESTIMATION OF CAUSAL EFFECTS WITH INTERFERENCE 70

5.1 Introduction 70

5.2 Targeted Maximum Likelihood Estimation 71

5.2.1 Estimands and Assumptions 72

5.2.2 Estimation 72

5.3 Targeted Maximum Likelihood Estimation with Dependent Data 74

5.3.1 Estimands and Assumptions 75

5.3.2 Network-TMLE 76

5.4 Simulation Study Design 78

5.4.1 Networks 78

5.4.2 Data Generating Mechanisms 80

5.4.3 Performance Metrics 83

5.4.4 Software 84

5.5 Simulation Study Results 84

5.5.1 Statin and ASCVD 84

5.5.2 Naloxone and Opioid Overdose 85

5.5.3 Comprehensive Dietary Intervention and BMI 85

5.5.4 Vaccine and Infectious Disease Transmission 86

5.6 Discussion 86

5.7 Tables and Figures 89

CHAPTER 6: REALISTIC INTERVENTIONS ON THE DISTRIBUTION OF INFLUENZA VACCINATION AND RISK OF INFLUENZA AMONG UNIVERSITY STUDENTS 98

6.1 Introduction 98

6.2 Methods 99

6.2.1 Data Source 99

6.2.2 Policies 101

6.2.3 Targeted Maximum Likelihood Estimation 103
6.2.4 Missing Data....106
6.2.5 Sensitivity Analyses....106
6.3 Results....107
6.3.1 Vaccination Policies....107
6.3.2 Sensitivity Analyses....107
6.4 Discussion....108
6.4.1 Conclusions....110
6.5 Tables and Figures....111
CHAPTER 7: CONCLUSIONS....116
7.1 Study Findings....117
7.2 Strengths and Limitations....121
7.3 Public Health Implications....125
7.4 Future Research....127
7.5 Conclusions....129
APPENDIX 1: CHAPTER 4 SUPPLEMENTARY MATERIALS....130
APPENDIX 2: CHAPTER 5 SUPPLEMENTARY MATERIALS....143
Appendix 2.1: Validation Simulations and Demonstration of Double Robustness....143
Appendix 2.2: Data Generating Mechanisms....145
Appendix 2.3: Simulation Results for the Modified Clustered Power-Law Random Graph....146
Appendix 2.4: Simulation Results in Tabular Form....150
Appendix 2.5: Proposed Diagnostic Plot for Positivity....186
APPENDIX 3: CHAPTER 6 SUPPLEMENTARY MATERIALS....187
REFERENCES....190

LIST OF TABLES

Table 4.1: Confidence interval coverage of parameters for network-1 65

Table 4.2: Confidence interval coverage of parameters for network-2 66

Table 4.3: Confidence interval coverage of parameters for network-3 67

Table 6.1: Descriptive statistics for the eX-FLU analytic sample 111

Table 6.2: Students self-reported barriers to influenza vaccine receipt 112

Table A1.1: Bias for parameters for network-1 131

Table A1.2: Empirical standard error for parameters for network-1 132

Table A1.3: Confidence interval coverage for parameters for network-1 133

Table A1.4: Bias for parameters for network-2 134

Table A1.5: Empirical standard error for parameters for network-2 135

Table A1.6: Confidence interval coverage for parameters for network-2 136

Table A1.7: Bias for parameters for network-3 137

Table A1.8: Empirical standard error for parameters for network-3 138

Table A1.9: Confidence interval coverage for parameters for network-3 139

Table A2.2.1: Baseline confounder distributions by data-generating mechanisms 145

Table A2.4.1: IID-TMLE for statin data generating mechanism with a uniform random graph 150

Table A2.4.2: Network-TMLE with a series of logistic models for statin data generating mechanism with a uniform random graph 151

Table A2.4.3: Network-TMLE with a single Poisson model for statin data generating mechanism with a uniform random graph 152

Table A2.4.4: IID-TMLE for statin data generating mechanism with a clustered power-law random graph 153

Table A2.4.5: Network-TMLE for statin data generating mechanism with a clustered power-law random graph 154

Table A2.4.6: Network-TMLE for statin data generating mechanism with a clustered power-law random graph restricted by degree 155

Table A2.4.7: IID-TMLE for statin data generating mechanism with the eX-FLU network 156

Table A2.4.8: Network-TMLE for statin data generating mechanism with the eX-FLU network 157

Table A2.4.9: Network-TMLE for statin data generating mechanism with the eX-FLU network restricted by degree 158

Table 2.4.10: IID-TMLE for naloxone data generating mechanism with a uniform random graph 159

Table A2.4.11: Network-TMLE with a series of logistic models for naloxone data generating mechanism with a uniform random graph 160

Table A2.4.12: Network-TMLE with a single Poisson model for naloxone data generating mechanism with a uniform random graph 161

Table A2.4.13: IID-TMLE for naloxone data generating mechanism with a clustered power-law random graph 162

Table A2.4.14: Network-TMLE for naloxone data generating mechanism with a clustered power-law random graph 163

Table A2.4.15: Network-TMLE for naloxone data generating mechanism with a clustered power-law random graph restricted by degree 164

Table A2.4.16: IID-TMLE for naloxone data generating mechanism with the eX-FLU network 165

Table A2.4.17: Network-TMLE for naloxone data generating mechanism with the eX-FLU network 166

Table A2.4.18: Network-TMLE for naloxone data generating mechanism with the eX-FLU network restricted by degree 167

Table A2.4.19: IID-TMLE for diet data generating mechanism with a uniform random graph 168

Table A2.4.20: Network-TMLE with a series of logistic models for diet data generating mechanism with a uniform random graph 169

Table A2.4.21: Network-TMLE with a single logistic model for diet data generating mechanism with a uniform random graph 170

Table A2.4.22: IID-TMLE for diet data generating mechanism with a clustered power-law random graph 171

Table A2.4.23: Network-TMLE for diet data generating mechanism with a clustered power-law random graph 172

Table A2.4.24: Network-TMLE for diet data generating mechanism with a clustered power-law random graph restricted by degree 173

Table A2.4.25: IID-TMLE for diet data generating mechanism with the eX-FLU network 174

Table A2.4.26: Network-TMLE for diet data generating mechanism with the eX-FLU network 175

Table A2.4.27: Network-TMLE for diet data generating mechanism with the eX-FLU network restricted by degree 176

Table A2.4.28: IID-TMLE for vaccine data generating mechanism with a uniform random graph 177

Table A2.4.29: Network-TMLE with a series of logistic models for vaccine data generating mechanism with a uniform random graph 178

Table A2.4.30: Network-TMLE with a single Poisson model for vaccine data generating mechanism with a uniform random graph 179

Table A2.4.31: IID-TMLE for vaccine data generating mechanism with a clustered power-law random graph 180

Table A2.4.32: Network-TMLE for vaccine data generating mechanism with a clustered power-law random graph 181

Table A2.4.33: Network-TMLE for vaccine data generating mechanism with a clustered power-law random graph restricted by degree 182

Table A2.4.34: IID-TMLE for vaccine data generating mechanism with the eX-FLU network 183

Table A2.4.35: Network-TMLE for vaccine data generating mechanism with the eX-FLU network 184

Table A2.4.36: Network-TMLE for vaccine data generating mechanism with the eX-FLU network restricted by degree 185

LIST OF FIGURES

Figure 4.1: Examples of true, observed, and gold-standard networks 68

Figure 4.2: Bias of network parameters for network-1 68

Figure 4.3: Bias of network parameters for network-2 69

Figure 4.4: Bias for network parameters for network-3 69

Figure 5.1: Visualizations of networks used in simulations 89

Figure 5.2: Target maximum likelihood estimation for statins and atherosclerotic heart disease, and the uniform random graph 90

Figure 5.3: Target maximum likelihood estimation for statins and atherosclerotic heart disease, and the eX-FLU network 91

Figure 5.4: Target maximum likelihood estimation for naloxone and opioid overdose, and the uniform random graph 92

Figure 5.5: Target maximum likelihood estimation for naloxone and opioid overdose, and the eX-FLU network 93

Figure 5.6: Target maximum likelihood estimation for diet and body mass index, and the uniform random graph 94

Figure 5.7: Target maximum likelihood estimation for diet and body mass index and the eX-FLU network 95

Figure 5.8: Target maximum likelihood estimation for vaccination and infection and the uniform random graph 96

Figure 5.9: Target maximum likelihood estimation for vaccination and infection, and the eX-FLU network 97

Figure 6.1: Self-reported contacts between participants measured at the end of week one 113

Figure 6.2: Ten-week risk of influenza-like illness (A) and laboratory-confirmed influenza (B) under policies to increase log-odds of influenza vaccination 114

Figure 6.3: Measurement error sensitivity analysis of the ten-week risk of influenza-like illness (A) and laboratory-confirmed influenza (B) under policies to increase log-odds of influenza vaccination 115

Figure A1.1: Bias of estimated network parameters for network-1 140

Figure A1.2: Bias of estimated network parameters for network-2 141

Figure A1.3: Bias of estimated network parameters for network-3 142

Figure A2.1.1: Simulation results for Sofrygin and van der Laan 2017 mechanism 143

Figure A2.1.2: Simulation results for a unit-treatment effect only.....143

Figure A2.1.3: Simulation results for spillover effect only data generating mechanism 144

Figure A2.1.4: Simulation results for continuous outcome data generating mechanism 144

Figure A2.3.1: Target maximum likelihood estimation for statins and atherosclerotic heart disease, and the clustered power-law random graph 146

Figure A2.3.2: Target maximum likelihood estimation for naloxone and opioid overdose, and the clustered power-law random graph.....147

Figure A2.3.3: Target maximum likelihood estimation for diet and body mass index, and the clustered power-law random graph.....148

Figure A2.3.4: Target maximum likelihood estimation for vaccination and infection, and the clustered power-law random graph 149

Figure A2.5.1: Example of diagnostic plots for positivity issues for specific policies using the uniform random graph with statins 186

Figure A3.1: Diagnostic plots for MICE 187

Figure A3.2: Missing Vaccination Status Considered as Vaccinated.....188

Figure A3.3: Missing Vaccination Status Considered as Unvaccinated.....189

LIST OF ABBREVIATIONS

ACIP	United States Advisory Committee on Immunization Practices
ASCVD	Atherosclerotic cardiovascular disease
CDC	United States Centers for Disease Control and Prevention
CI	Confidence interval
ERGM	Exponential random graph model
ESE	Empirical standard error
GAM	Generalized additive model
HA	Hemagglutinin
IID	Independent and identically distributed
ILI	Influenza-like illness
MICE	Multiple imputation by chained equations
MIME	Multiple imputation for measurement error
NA	Neuraminidase
RDS	Respondent-driven sampling
RMSE	Root mean squared error
RNA	Ribonucleic acid
RSSI	Received signal strength indicator
SRS	Simple random sample
TMLE	Targeted maximum likelihood estimation
US	United States

CHAPTER 1: INTRODUCTION

Viral influenza is a worldwide infection that peaks in colder months in temperate climates and causes substantial morbidity and mortality. In the following section, influenza biology and epidemiology are reviewed. First, basic features of the influenza virus are reviewed; including virology, pathogenesis, and epidemiology. Next, influenza vaccination as a means to prevent influenza infection, morbidity, and mortality is discussed. Subsequently, the burden of influenza and influenza vaccination among university students is assessed. Lastly, limitations to current approaches to estimating the effects of influenza vaccination are reviewed.

1.1 Influenza

1.1.1 Virology

Influenza is a member of the orthomyxovirus family with a genome consisting of eight segments of negative-sense single-strand RNA and is a respiratory tract pathogen in humans.[1, 2] The RNA segments code for hemagglutinin (HA), neuraminidase (NA), RNA polymerase, matrix protein, membrane protein, non-structural proteins, and nuclear export protein.[2, 3] Influenza is further classified into four distinct types: A, B, C, and D; with symptomatic human influenza infections predominantly occurring as a result of types A and B. Although some severe cases of influenza C have been reported in children.[4] Due to antigenic diversity within influenza A, types are further distinguished by subtypes of HA and NA.[1, 3] Influenza A is unique in that it circulates in humans, wild aquatic birds, and domesticated animals.[5] In total, 16 different HA and 9 different NA serotypes are recognized. In contrast, influenza B and C appear restricted to circulation in humans and lack the same genetic and species diversity.[1]

Genetic diversity in influenza more broadly arises from *antigenic drift* and *antigenic shift*. *Antigenic shift* is a drastic change in the viral antigens, often resulting in reassortment (replacement of entire segments) or recombination (insertion of fragments within a segment).[1] The occurrence of antigenic shift can result in pandemic influenza since most or all humans have no prior immunity to a newly emerged or re-emerging serotype. Due to the ability of influenza A to circulate between multiple species, concerns regarding pandemic influenza are limited to type A. Influenza pandemics are separated by years or decades. Conversely, *antigenic drift* is the process of gradual mutations in the genome that occur due to errors during replication.[1] The gradual changes in the surface antigens of the virus allow for the evasion of host adaptive immunity[2] and necessitate the updating of the influenza antigens within the influenza vaccine. Changes in HA are monitored through global influenza virus surveillance programs. Hereafter, the focus is on seasonal influenza, since yearly influenza vaccination is the key preventive measure for seasonal influenza. While influenza vaccine development for potential emerging strains[6] or a universal influenza vaccine that is efficacious against all influenza type A viruses[7] are being pursued, these have yet to be realized. Currently, potential measures to prevent or mitigate a newly emergent pandemic influenza serotype consist of non-pharmaceutical measures (e.g., physical distancing, masks, hand hygiene, and surface disinfection[8-12]) and may include the use of antivirals for pre- or post-exposure prophylaxis.[13]

In humans, the influenza virus targets the respiratory tract for infection and productive replication. Infection begins with the influenza virus binding to the host cell, which is mediated by the HA protein binding to sialic acids on the surface of the host. After binding, the virus enters the cell via an endosome. The virus then changes the endosomal pH, fusing the viral membrane with the endosome membrane, releasing the viral genome. After release, viral RNA is taken to the nucleus of the infected cell, where replication of the viral RNA takes place. The viral genome is translated from negative-sense to positive-sense RNA then disseminated to the cytoplasm where translation into viral proteins takes place. The need for an intermediary

positive-sense RNA in genome replication and RNA polymerase's lack of a proofreading ability facilitate the rapid antigenic drift of influenza relative to other pathogens. Synthesized HA, NA, and M2 proteins are transported to and integrated into the cellular membrane. New negative-sense RNA segments are transported to the plasma membrane and bundled together. New virions then bud off the cell surface. NA then functions to prevent HA attachment with the sialic acid present on the surface of other virions or infected cells. Viral replication ends with cell death, releasing both pro-inflammatory cytokines and viral products.

To avoid detection by the host's innate immunity, the influenza virus inhibits several cell processes. The non-structural protein NS1 interrupts several signal cascades that result in the activation of host antiviral genes.[14-16] The non-structural proteins PB1 and PB2 further inhibit interferon production.[17, 18] Cell death eventually leads to the release of cytokines driving the migration of innate immune cells, such as natural killer cells and macrophages, responsible for viral clearance.

For the adaptive immune response, B cells produce antibodies that primarily target HA and NA proteins, with HA being preferentially targeted. While natural infection leads to a robust IgG antibody response with long-lasting B cell lines,[19, 20] the antigenic drift of the HA allows evasion of the adaptive immune response in subsequent years.[21] Another important element of clearing influenza infection is cell lysis of infected cells induced by CD8+ T cells. Unlike B cells, CD8+ T cells target non-structural proteins which are less subject to changes via antigenic drift. Finally, CD4+ T cells support both the humoral and cellular immune responses, but it remains unknown if CD4+ cells directly contribute to viral clearance.[22]

1.1.2 Pathogenesis

Influenza infection pathology ranges from asymptomatic infection of the upper respiratory tract to lethal viral or secondary bacterial pneumonia. Outside of the respiratory tract, influenza can also cause a variety of non-respiratory complications, including complications in the cardiovascular and nervous systems.[23, 24] On a cellular level, cell death results in the release

of inflammatory cytokines. While the release of cytokines and subsequent migration of immune cells to the lungs are necessary for host immune response, excessive release of these cytokines can result in severe disease and lung damage. If inflammation becomes systemic, severe respiratory distress and multiple organ failure can occur.[25] While influenza is often a self-limited disease, a variety of severe outcomes do occur. Even in absence of the more severe outcomes, the impact of influenza on individuals can manifest for multiple weeks.

A substantial portion of influenza cases may be asymptomatic.[26, 27] When symptomatic influenza infections occur, they are characterized by respiratory symptoms (e.g., runny nose, cough, and sore throat), muscle aches, fever, and chills,[1, 3] with cough being the most commonly reported symptom.[1] This constellation of respiratory symptoms is often referred to as "influenza-like illness" (ILI). Disease is generally self-limited, with symptoms lasting 3 to 5 days but can last up to a week.[3, 28]

Complications; which are more common in infants, older adults, and those with chronic illnesses; can prolong symptomatic illness. In more severe cases, influenza can lead to viral pneumonia. More commonly, influenza leads to secondary bacterial infections,[3] with synergistic interactions occurring with *Streptococcus pneumoniae*.[29, 30] Outside of the respiratory tract, influenza has been observed to lead to encephalitis, kidney damage, liver damage, and cardiac events, such as stroke and ischemic heart disease.[24]

Post-infection, a variety of sequelae have been observed. Coughing and lethargy can last up to two weeks post-infection.[28] More worryingly, an increased risk of myocardial disease has been observed in the following weeks post-infection.[23, 31] Neurological complications can also occur post-infection,[24] with Guillain-Barré syndrome as a prominent example.[32, 33]

1.1.3 Epidemiology

In the United States (US), seasonal influenza predominantly occurs between October to May each year.[1, 2] Currently, the primary circulating serotypes are influenza A H1N1, influenza A H3N2, and influenza B, with the dominant type of influenza A differing between seasons. A

substantial burden of morbidity and mortality results from seasonal influenza in the US. Each year, between 3% to 20% of the population are infected,[34, 35] more than 220,000 hospitalizations occur,[36] 3,000 to 49,000 deaths,[37] and $16.3 billion in lost productivity and loss of life.[38]

Human-to-human transmission predominantly occurs through respiratory secretions of infected individuals.[3] Aerosols are generated via talking, sneezing, and coughing, with each of those activities capable of airborne or droplet transmission.[39] Droplets can additionally contaminate the physical environment, including objects such as doorknobs, keyboards, and tables.[40, 41] Persistent contamination of objects has been reported.[42, 43] Touching contaminated fomites and then the mucous membranes of the face (i.e., nose, mouths, or eyes),[44] or re-aerosolization of virus present on fomites[45] are thought to also contribute to transmission.

After exposure, the incubation period to symptomatic disease is between 1 to 4 days. Importantly, evidence suggests that transmission occurs shortly before (about one day) the symptomatic phase begins.[3, 46] Pre-symptomatic shedding consists of fewer virions, indicating pre-symptomatic transmission may be limited to close and sustained contacts.[46] However, the importance and extent of pre-symptomatic transmission have been disputed.[47] Often the respiratory symptoms of ILI are used to identify influenza cases. However, symptoms used to define ILI can also result from other respiratory viruses (e.g., coronaviruses, respiratory syncytial virus, rhinovirus[48]), leading to potential misattribution of the causative pathogen.[1]

1.2 Influenza Vaccine

The primary preventative measure for seasonal influenza is through pharmaceutical means, namely the influenza vaccine.[3, 49] Because of the short incubation period of influenza, vaccination cannot be used for post-exposure prophylaxis. In the US, influenza vaccines are generally quadrivalent; with the trivalent vaccine consisting of two influenza A subtypes and one influenza B subtype, while the quadrivalent vaccine consists of an additional B subtype. Vaccines currently induce protective humoral immunity to the head of HA proteins. Because of the rapid changes in the HA head from antigenic drift, the protective effects of the influenza

vaccine are highly dependent on the similarity between the vaccine influenza antigens and the circulating types.[50] As a result, the protective effects of the influenza vaccine vary between seasons,[1, 51] with reported direct (e.g., unit-treatment) vaccine effectiveness as high as 80% and as low as 0%.[50] Additionally, this requires that individuals be vaccinated each year. As a result of antigenic drift, continuous monitoring of influenza vaccines is also necessary. To forecast which influenza serotypes will be circulating during the upcoming influenza season, international influenza surveillance systems monitor and project circulating influenza virus serotypes for the upcoming year.[52] These projections are used to determine which influenza types should be included in the vaccine. Importantly, the types of influenza circulating during the Fall and Winter months in the Southern Hemisphere can be used to predict influenza strains that will be circulating in the subsequent Fall and Winter months in the Northern Hemisphere. Currently available vaccines consist of inactivated (with multiple different manufacturing technologies) and live-attenuated vaccines.[52]

1.2.1 Inactivated Vaccines

Inactivated vaccines work by exposing individuals to HA and NA antigens to induce an adaptive immune response to those antigens. The immune response consists of antibody production targeting both HA and NA antigens. To induce a more robust immune response, inactivated vaccines generally include an adjuvant. In the US, the antigens included in inactivated vaccines are most commonly produced by growing influenza virus in chicken embryonated eggs. The use of chicken eggs to produce virions has come into question. In particular, it is thought that viral adaptions for growth in eggs via antigenic drift can result in vaccine strain mismatch.[53] Inactivated vaccines have also been manufactured by infecting cell lines with either the influenza virus directly or with modified baculoviruses that express HA proteins.[54] After amplification, the influenza virus is harvested and chemically inactivated. The inactivated influenza virus is then further broken into HA and NA subunits and partially purified.

1.2.2 Live-Attenuated Vaccines

Live-attenuated vaccines are similarly propagated in eggs, but instead mimic natural infection by activating the innate and adaptive immune system through exposure to an actively replicating virus. To prevent major adverse reactions from exposure to an active influenza virus, the virus included in the vaccine is attenuated via cold-adaptation, which consists of growing the virus at 25ºC.[55, 56] Due to the virus adaptions for replication in a cold environment, replication in environmental temperatures of the lower respiratory tract is impeded and prevents severe infection. Because live-attenuated vaccines mimic natural infection, activation of B cell and CD8+ T cell responses are both possible. However, a long-lasting CD8+ T cell response has not been observed to result from these vaccines.[57]

While a trivalent live-attenuated influenza vaccine was approved in 2003 in the US,[58] the poor performance of the live-attenuated vaccine against the continually circulating 2009 pandemic H1N1 was observed.[59-61] This led to the US Advisory Committee on Immunization Practices (ACIP) and the US Centers for Disease Control and Prevention (CDC) to recommend against the use of the attenuated nasal spray vaccine from 2016 to 2018.[62] Following 2018, the live-attenuated vaccine was again recommended,[63] but its use has been limited in the US.

1.2.3 Vaccine Effectiveness

In previous research, the influenza vaccine has been found to have protective effects for preventing influenza infection,[50, 64] reduction in severe outcomes,[65-67] and protection for close contacts and their surrounding community.[68-75] However, antigenic drift and the development of new vaccines necessitate continual monitoring of vaccine effectiveness. Vaccines are monitored by a variety of systems and methods.

As a proxy, inhibition titers via haemaggultination inhibition assays have been used a surrogate of vaccine effectiveness.[76] The advantage of this method of assessment is that the adaptive immune response can be quantified via a relatively inexpensive method.[77] Additionally, this method allows the assessment of vaccines to induce an immune response to potential

pandemic influenza serotypes that are not yet circulating in humans.[77] Evidence of antibodies that target HA can be used to support the licensure of influenza vaccines. However, the production of antibodies is of lesser interest relative to clinical end-points, such as infection, severe disease, death, and transmission.

A common clinical end-point for influenza vaccine effectiveness is the direct prevention of influenza infection for those who receive the vaccine compared to those who have not. Direct, or unit-treatment, vaccine effectiveness against infection has been quantified through several measures of influenza infection and study designs. While unit-treatment vaccine effectiveness against asymptomatic infection is of interest, studies to assess this are difficult to implement due to the need to test all participants at regular intervals.[78] However, most studies fail to capture asymptomatic cases due to symptom-based determinations of who is tested for influenza. Instead, symptomatic infections are often considered as the main end-point. Definitions of symptomatic influenza infection vary from the occurrence of ILI to laboratory-confirmed influenza. One noted issue in the use of ILI in place of laboratory-confirmation is that it is a non-specific condition. As a result, ILI may underestimate the true unit-treatment vaccine effectiveness against influenza infection.[79, 80] Laboratory-confirmed influenza avoids this issue, but accuracy is dependent on the type of test used.[81] Prevention of later end-points, such as hospitalization and death, is also of interest. These events are often captured via hospital-based studies or through the use of influenza surveillance systems.[82, 83]

To estimate the unit-treatment vaccine effectiveness for the preceding end-points, a variety of study designs have been used. Cohort studies, which follow a defined study population over an influenza season, can include active testing of any acute respiratory infections that occur or passive collection of influenza infections of those who sought care.[78] Other cohort studies have been nested in households, which allow the assessment of within-household transmission.[68, 84, 85] Case-control studies have also been used to estimate vaccine effectiveness.[78] Traditional case-control unit-treatment vaccine effectiveness studies sample

controls from the same source population of cases. A newer design is the test-negative case-control study. To account for bias in the selection of controls in terms of health-seeking behaviors or access to healthcare, test-negative studies identify controls from influenza-negative tests.[86, 87] Despite a rise in popularity of this design, key limitations for its application have been noted.[87-89] Lastly, influenza surveillance systems, which systematically collect all influenza cases within a defined catchment area, have been used to assess vaccine effectiveness on end-points like death. For example, the CDC's Influenza Hospitalization Surveillance Network has been used to estimate vaccine effectiveness against severe disease and death.[67, 82, 83]

1.2.4 Vaccination Recommendations

Preceding 2010, the seasonal influenza vaccine was only recommended for school-aged or younger children (6 months – 18 years), healthcare providers, pregnant women, older adults (≥50 years), and persons at higher risk for influenza-related complications (such as those with chronic disorders, immunosuppression, and conditions limiting respiratory function).[90] Since then, the seasonal influenza vaccine has been recommended by ACIP for all persons 6 months or older without medical contraindications.[91] Despite the updated recommendation, influenza vaccination uptake has remained at low levels among young adults.[92] One particularly important group of young adults included in the expanded recommendation is university students.

1.3 Influenza and University Students

University students are a vital population to consider for increasing influenza vaccination receipt. First, while vaccination uptake in university students has increased since the 2010 revised recommendations,[93] substantially less than half of college students receive a yearly influenza vaccine.[93-100] Second, attack rates in university students are comparable to high-risk groups, such as those 65 years or older.[101-103] A possible explanation for this observation is the extent of social contacts between large groups of students, the density of university housing, and close contacts with students in classes.[95, 102, 104-109] From a historical viewpoint, the mortality

among young adults during the 1918 influenza pandemic was substantially high[110] and had wide-ranging economic impacts. The emergence of a new pandemic influenza strains may place young adults at a similarly high mortality risk. While a universal vaccine is not yet available, the high mortality in this age group would suggest high priority when a universal influenza vaccine is widely available. Third, university student populations may disseminate influenza rapidly, as observed with the introduction of pandemic 2009 H1N1 to the US via university students returning from spring break in Mexico,[104] and other instances of pandemic influenza.[103] Fourth, influenza can have substantial negative impacts on work, school, and mental well-being of students.[96, 111] While other respiratory viruses manifest in similar ILI and missed days of school and work,[48, 111] prior research has found between 20 to 70% of ILI cases among university students have been attributed to influenza.[48, 111] Therefore, targeting the reduction of influenza has the potential to substantially reduce the impacts of ILI on university students. Also, students may serve as a source of infection for their university faculty or staff, who may be at high risk for influenza-related morbidity and mortality by virtue of older age or co-morbidities (e.g., immunosuppression or pregnancy). Lastly, university students often begin making independent health decisions at this stage in their lives. Since past vaccination is highly predictive of future vaccination behavior,[93, 112] encouraging influenza vaccination among this group may alter their future decision trajectory. To successfully increase influenza vaccination uptake among university students, hesitancy and barriers need to be addressed.

Previous research has indicated that low uptake of influenza vaccination more broadly may result from misinformation on risks and benefits associated with the vaccine,[100, 107, 113-118] convenience on when and where the vaccine can be received,[98, 113] and financial barriers.[94, 95] The decision to get vaccinated is linked to the perception that influenza is a serious illness, the influenza vaccine is effective, and the side-effects of the vaccine are minor.[113, 119] Lack of knowledge regarding influenza and the vaccine has been linked to not receiving the vaccine.[107, 113, 114] Educational campaigns should focus on vaccine safety,[100, 113, 114, 117, 118] effectiveness,[100,

[114, 117, 120] the threat of influenza,[114, 118, 120] and protecting others from influenza.[98, 114, 117] The usage of mass media, such as social media, public flyers, and television, has been shown to increase influenza knowledge and vaccine acceptance broadly.[97, 119, 121]

University students have been previously found to have fewer positive views on influenza vaccines,[113, 115] potentially due to fewer chronic conditions and having a lower perceived risk of serious influenza outcomes.[98, 115, 116, 119] A lack of convenience has also been reported as a barrier for influenza vaccination,[98] but not consistently.[113] Providing free influenza vaccination has had success in increasing vaccination uptake,[95] but costs have not always been perceived by students as a substantial barrier.[98, 113]

Previous campaigns to increase influenza vaccination among university students have targeted education regarding influenza and the vaccine, convenience, and costs. Among university students, mass media campaigns have raised influenza vaccination coverage.[94, 95] Media approaches have been reported as more successful when highlighting the benefits of the influenza vaccine.[93] For poster design, highlighting the benefits of the vaccine and the harms of influenza through text have been seen to be observed with increased intention to receive the influenza vaccine.[122] However, mass media campaigns have not always had success,[98, 107] potentially due to students already having some awareness of vaccination program services available to them.[98] Rather than a broad approach, some authors have suggested targeted educational campaigns, like collaborating with student organizations (e.g., fraternities or sororities).[107] Outside of media campaigns, using class time as an opportunity to provide educational materials on the influenza vaccine for medical and biology students has had success.[123] Convenience and cost barriers have also been addressed in tandem with educational campaigns. Costs have predominantly been targeted by providing the influenza vaccine at reduced or no cost to students. Another option is for universities to mandate influenza vaccination for students. After high-profile Mumps outbreaks at universities,[124, 125]

mandatory Measles-Mumps-Rubella vaccination for university students has been recommended as a means to increase vaccination and prevent outbreaks.[126] Something similar could be done in regards to influenza vaccination.

Previous research on policies that target one or more of these barriers have focused on influenza vaccination uptake as the outcome measure.[94, 95, 123] However, an outcome of greater public health importance is the overall reduction in risk of influenza resulting from increased uptake. By focusing on influenza risk, selecting between campaigns for more efficient use of resources may be possible. As an example, a hypothetical educational intervention may result in a similar reduction in influenza risk compared to vaccination clinics, but vaccination clinics may be substantially less costly.

1.4 Difficulties in Measuring Vaccine Effectiveness

In practice, there are several issues with the measurement of influenza vaccine effectiveness. First, it should be noted that vaccine effectiveness is often used to refer to a variety of different outcomes. Besides differing end-points, vaccine effectiveness can also be constructed with a variety of effect measures. For example, vaccine effectiveness is often defined as one minus the risk ratio, but odds ratios and incidence rate ratios are also used.[79, 127] Next, unit-treatment vaccine effectiveness is often focused on,[50, 128] including in university students.[129] Unit-treatment vaccine effectiveness corresponds to the average of changing each individual's vaccination status while holding the vaccination status of the remainder constant. However, this measure may be less relevant in the assessment of vaccination from a public health perspective. Instead, the risk of influenza under differing vaccination campaigns or policies is likely of greater interest. To further facilitate understanding why unit-treatment vaccine effectiveness may be of lesser public health interest, we rely on potential outcomes.

The potential outcomes framework was proposed by Jerzy Neyman in 1923 in the context of randomized trials.[130] Donald Rubin later extended the potential outcomes framework to include observational studies for point-exposures,[131] and James Robins further generalized

this framework for time-varying exposures.[132] Potential outcomes stipulate possible outcomes for a person under different exposures, treatments, interventions, or policies. Without a loss of generality, we refer explicitly to influenza vaccination. Let $Y_i(\boldsymbol{v})$ indicate the potential outcome Y for individual i, where $\boldsymbol{v}$ designates the vaccination status for every person within the defined population (i.e., $\boldsymbol{v} = \{v_1, v_2, \dots, v_i, \dots, v_n\}$). In other words, i's potential outcome is defined by the entirety of the population's vaccination. As will become useful later on, the potential outcomes can be rewritten as $Y_i(\boldsymbol{v}) = Y_i(v_i, v_{-i})$, where v_i is the vaccination of individual i and v_{-i} is the vaccination of all other units. Under the assumption of no interference, such that the potential outcome for i is independent of the vaccination of any other unit in the population,[133-135] individual i's potential outcome reduces to $Y_i(v_i)$. As has been long recognized in infectious disease research,[136] the assumption that the vaccination status of one person does not affect another person is often unreasonable. Therefore, the v_{-i} component of the potential outcome cannot be readily ignored.

The presence of the v_{-i} component also expands the possible estimands that one can consider studing.[137] As mentioned before, unit-treatment vaccine effectiveness is often estimated. Using the potential outcome notation, the unit-treatment effect can be expressed as $\Pr\big(Y(1, v_{-i})\big) - \Pr\big(Y(0, v_{-i})\big)$. In words, the unit-treatment effect is the expected population difference in the probability of Y contrasting vaccination to no vaccination, holding everyone else's vaccination as fixed. While the unit-treatment effect is commonly reported in vaccine and infectious disease epidemiology more broadly, utility of this estimand is limited from a public health standpoint.[138] Rather than considering some substantial change in the distribution of vaccination in the population, the unit-treatment effect focuses on a single unit. In settings where resources are not extremely constrained so that vaccination could only be increased by a single or few individuals, this measure likely has limited public health use.

In place of the unit-treatment effect, VanderWeele and Tchetgen have argued that the differences under changes in the distribution of vaccination (e.g., policies) are of greater public health importance.[138] Rather than holding v_{-i} as fixed, the risk under a different policy $\boldsymbol{v}^*$, indicated by $\Pr\big(Y(\boldsymbol{v}^*)\big)$, could be examined. As opposed to the unit-treatment effect, this value can correspond to large-scale changes in the distribution of vaccination in the population.

For estimation of $\Pr\big(Y(\boldsymbol{v}^*)\big)$ and other estimands that include v_{-i}, there have been two distinct approaches: partial interference and general interference. The partial interference assumption stipulates that the interference pattern consists of distinct groups where interference occurs *within* groups but *not between* groups.[133, 139] The partial interference assumption may be reasonable in settings where groups are geographically isolated (e.g., rural villages with few roads between them, etc.) or when interactions are highly dependent on environmental features (e.g., classrooms, places of employment, etc.). The independent and identically distributed group-level data then allows for the application of standard statistical theory.[133, 139-141] Approaches to estimation under partial interference have included two-stage randomized trials,[133, 140, 142] extensions to inverse probability weighting,[141, 143, 144] extensions to augmented inverse probability weighting,[145] and sensitivity analyses.[146]

While partial interference is reasonable in some scenarios, interference patterns do not always allow the separation of individuals into independent groups. General interference allows, in principle, for any two units in a population to affect each other. Consideration of all v_{-i} equally for $Y(v_i, v_{-i})$ is extraordinarily difficult (if not impossible). Therefore, general interference approaches instead restrict interference to a specific pattern with a known structure. This interference structure can be represented by a network where edges in the network indicate connections between units where effects can 'flow' through. Therefore, we only need to consider the components of v_{-i} for individuals directly or indirectly connected to i.

Methods for general interference may further be delineated by whether or not the vaccination is randomized by the investigator. In randomized experiments, methods can leverage the random assignment as the basis of inference.[147, 148] In settings of observational data, there have been two recently proposed approaches to allow for general interference: auto-g-computation, and network targeted maximum likelihood estimation (TMLE). Auto-g-computation is an extension to Robins' parametric g-formula to settings of general interference, with estimation proceeding by Gibbs sampling from a conditional auto-model.[149] This approach relies on the specification of a parametric auto-model for the outcome. Network-TMLE is an extension to TMLE framework for dependent data in the context of a network.[150-152] To make progress, network-TMLE restricts general interference to only exist for immediate contacts, referred to as weak dependence. Both of these approaches assume that the interference pattern, as expressed via a network, has been correctly measured.

1.5 Measurement Error

To measure contacts capable of infection transmission, like influenza, self-reported measures for contacts have often been used.[153, 154] Other work measuring face-to-face contacts via self-report and electronic sensor-collected data have found discrepancies between the two.[155-159] In particular, contacts of shorter duration were less likely to be self-reported.[158] Therefore, it is likely that measurement error of contacts poses a significant threat to the validity of approaches, like network-TMLE, when self-reported contact data is used.

More broadly, measurement error of edges has been recognized as an important limitation in network analyses. Previous simulation studies have focused on the performance of centrality measures (e.g., degree, betweenness, closeness, eigenvector centrality) with non-informative measurement error.[160-162] To analytically address measurement error, imputation[162, 163] and Bayesian approaches[164, 165] have been proposed. However, these approaches have not been explicitly compared in simulation studies.

1.5.1 Imputation Approach

Measurement error fits within the paradigm of missing data by stipulating that a perfect measure, referred to as the gold-standard, exists. This perfect measure is then missing for some (possibly all) of the study sample. The problem of measurement error is then to fill in the missing gold-standard measurements for the entire sample. This has been done using multiple imputation for measurement error (MIME); given that the correctly measured values are captured for a subsample.[166] This approach to thinking has been used to motivate imputation for measurement error for individual-specific covariates,[166-168] as well as edges in a network.[162]

For missing network data, multiple imputation approaches using exponential random graph models (ERGM) have been previously proposed.[163, 169] ERGM are a statistical model for network data for the prediction of ties between nodes in a network, which shares a similar interpretation to logistic regression models.[170] ERGM considers networks as a function of three broad categories of measures; density (number of edges), individual attributes, and geometric terms (higher-order interrelations between nodes). These models have been traditionally used to understand tie formation within networks. However, ERGM have also been used for multiple imputation of missing data.[169, 171-173] Use of ERGM as a way to correct for measurement error of edges has also been previously suggested.[169]

1.5.2 Bayesian Approach

Rather than explicitly framing measurement error as a missing data problem, Bayesian approaches attempt to reconstruct the true network from prior specifications.[165] Therefore, the collection or even existence of a gold-standard measure is not required. To estimate the true network, two models and corresponding prior distributions are specified.[165] The first model is the *measurement model*, which is the probability distribution for the measured edges given the true edges. The second model is the *network model*, which corresponds to the probability distribution of edge formation in the true network. Applying Bayes' rule, the true network can be consistently estimated with mismeasured edges, the specified models, and corresponding

priors. Draws from the joint posterior distribution are then used to estimate parameters of the true network. Bayesian approaches like this are expected to operate best when multiple measures of the same network are available to a researcher.[164] However, multiple measurements are uncommon in practice or may not possible. Therefore, performance of Bayesian approaches in the context of a single measurement are necessary.

1.6 Synopsis

In summation, influenza causes a substantial burden of morbidity and mortality each year. One important population to consider for the prevention of influenza is university students. Strategies that increase influenza vaccination to effectively reduce influenza risk are of interest. In order to assess possible policies to mitigate influenza cases among university students, methods are needed to allow for interference.

CHAPTER 2: STATEMENT OF SPECIFIC AIMS

This dissertation aims to estimate the risk of influenza under competing policies to increase influenza vaccination uptake among university students. In 2010, ACIP expanded influenza vaccination recommendations to include young adults.[91] Despite the updated recommendation, influenza vaccine receipt has remained at low levels among young adults,[174, 175] including university students.[93-95, 98] University students are an important population to consider for the prevention of influenza due to the high attack rate among university students[101-103]; university students may rapidly disseminate influenza to the surrounding community[103, 104]; influenza infection and symptoms have substantial negative impacts on work, school, and mental well-being of university students[96, 111]; and university students often begin making independent health decision at this stage in their lives.[93, 112]

To reliably estimate the risk of influenza under different policies, the approach must incorporate interference. Interference is the dependency of an individual's potential outcome on at least one other individual's exposure or treatment.[133] While long-recognized in infectious disease research,[136] interference has more recently been formalized through the potential outcomes framework.[133, 139] Despite this formalization, studies on influenza vaccination commonly ignore dependencies between observations.[176] Network-TMLE is a recently proposed extension to allow for network-dependent data in the TMLE framework. While network-TMLE has been previously demonstrated in selected simulations; simulations in more complex and real-world networks and an applied example of its usage are substantial gaps in the current literature. The lack of application of these methods to networks that more closely resemble

empirical network and real-world applications make it difficult to assess the importance and inhibit wider adoption of these approaches by epidemiologists.

Network-TMLE and other methods that rely on information within a network rely on the assumption that edges in the network are measured without error.[147, 151, 177] However, self-reported contacts have been found to differ from sensor-collected contacts,[155-159] likely indicating measurement error. To quantitatively address measurement error, imputation and Bayesian approaches have been suggested as options. However, these approaches have not been directly compared.

To reliably estimate the risk of influenza under competing influenza vaccination policies, this work pursues the following aims:

Aim 1: Compare approaches to address measurement error of edges in networks.

To address measurement error of edges, imputation and Bayesian approaches have been independently proposed. While proposed, the performance of these methods overall and in comparison to each other have not been systematically evaluated. Through a Monte Carlo simulation study, comparisons between these approaches were made for multiple measures and multiple network formation models.

Aim 2: Assess the finite-sample performance of network-TMLE.

While simulations have been conducted to evaluate the finite sample performance of network-TMLE; previous empirical studies have been limited to relatively simple random graphs, explored only a narrow set of data-generating mechanisms, and made no direct comparisons between network-TMLE and IID-TMLE. Through a Monte Carlo simulation study, the sample risk was estimated under varied data-generating mechanisms with a wide variety of networks, including a real-world network. Comparisons are further made between network-TMLE and IID-TMLE.

Aim 3: Estimate the risk of influenza under competing influenza vaccination policies.

Studies on vaccination often focus on the unit-treatment effect, which fails to address questions regarding large-scale changes in the distribution of vaccination. How vaccination uptake can best be increased to minimize influenza risk is of public health interest. Competing approaches can focus on providing information on the harm of influenza and the benefits of vaccination, reducing non-financial barriers to vaccine receipt, and reducing financial barriers to receipt. Influenza risk under policies that shift the log-odds of vaccination were assessed using network-TMLE and data collected in the eX-FLU cluster randomized trial.

CHAPTER 3: METHODS

3.1 Overview

To estimate the risk of influenza under competing policies to increase influenza vaccination uptake; data on demographics, behaviors, vaccination, respiratory illness, and contact data from the eX-FLU cluster randomized trial are used. Policies consist of approaches that shift the probability of vaccination uptake among different domains of self-reported reasons for not receiving the influenza vaccine. To allow for general interference, network-TMLE is used to estimate the risk under these different policies. As network-TMLE is a recently proposed estimator, we explore the finite sample properties under varied data-generating mechanisms and networks exhibiting different structural properties. Finally, network-TMLE assumes all edges in the network are measured without error. However, self-reported contacts have been previously shown to be subject to measurement error. To determine ways to address measurement error of edges, an additional simulation study on recently proposed imputation and Bayesian approaches was conducted.

3.2 Data Source

Data to estimate the risk of influenza under the competing policies comes from the eX-FLU study, a cluster-randomized trial on the feasibility and efficacy of three-day self-isolation on the spread of respiratory pathogens among university students.[154] At a midwestern university, students were recruited from six selected dormitories. The six dormitories were chosen based on their representativeness to the overall student population and their close physical proximity with each other. Students were recruited through chain referral sampling, which is highly efficient when attempting to enumerate networks. “Seed” students were recruited through

informational flyers, emails, and in-person informational tables. Recruited students were asked to nominate other students to participate in the study. Nominated students were then contacted via email. In total, there were 262 seed students and 328 nominated students. Enrolled students provided informed consent via an online form. To be eligible to participate, students had to be at least 18 years old.

Before recruitment, clusters were determined from features believed to influence how social interactions occurred (e.g., physical barriers within buildings, resident house assignment, geographic proximity of rooms). Each cluster was randomized to either self-imposed three-day self-isolation after the onset of symptomatic respiratory disease or to continue with their normal behavior when sick (control). Enrolled students were followed prospectively for ten-weeks (January – April 2013) for the development of respiratory infections.

At enrollment, students completed a survey and nominated social contacts. The enrollment survey collected information on health behaviors, psychosocial characteristics, knowledge regarding the transmission of influenza, and pandemic preparedness knowledge. Over the follow-up period, students were sent a survey via email on the Friday of each week. Study participants were also asked to complete a face-to-face contact diary. Information on location and relationship with contacts was also collected. While ILI symptoms were assessed in each weekly survey, students were asked to report the onset of coughing, sneezing, runny nose, fever or feverishness, chills, or body aches on the day of onset. These symptoms could be reported through phone, email, or a web-based reporting system. Students were considered ILI cases if they reported coughing plus at least one of the following symptoms: fever or feverishness, chills, or body aches. Once identified, ILI cases had nasal and throat swabs collected for testing. Additionally, healthy contacts of ILI cases in the previous week were also contacted for specimen collection. Therefore, asymptomatic infections could potentially be captured as well as symptomatic infections.

The intervention in the original study consisted of cluster randomization to either three-day self-isolation or control. The three-day isolation arm participants were provided an illness kit (consisting of study protocol instructions, thermometer, facemasks, information for preventing influenza transmission) at baseline. Upon meeting the definition of ILI case, those in the three-day isolation arm were asked to immediately begin the isolation protocol and remain in their dormitory room for three days. To facilitate adherence to isolation, students who developed ILI had provisions (e.g., snacks, beverages, etc.) and could be requested to provide a doctor's note verifying illness for professors or employers. For students in the control arm that became an ILI case, they were not asked to change their normal behavior while ill. However, they were provided basic information about ways to mitigate influenza transmission (i.e., hand hygiene, covering cough or sneezes).

A subsample of enrolled students (n=103) was also given smartphones with the iEpi application installed during the second week of follow-up. To identify participants in the iEpi subsample, groups of interconnected students were identified via the edge-betweenness community detection algorithm.[178] Participants were then randomly selected to participate, starting from the largest community, until 103 students were enrolled.[154] The iEpi application allowed for the collection of contacts, geographic information, and context-dependent surveys. Students were instructed to carry the phone with them at all times, charge the phone each night, and keep their phone in "discoverable" mode. Contact data was collected via Bluetooth signals. Briefly, each smartphone broadcasts a unique identifier to nearby devices. Broadcast signals travel a distance between 5-10 meters in normal operation and can travel through solid objects (e.g., walls, floors, etc.). Aside from broadcasting their unique identifier, the smartphone application also collected all incoming Bluetooth signals at a resolution of five minutes. From the unique identifier of captured signals, other participants' smartphones with the iEpi application could be identified and linked. Captured signals included a timestamp and the received signal

strength indicator (RSSI). RSSI is a unit-less measure of the strength of a Bluetooth signal. Therefore, highly-detailed contact information was captured for this subsample.

3.3 Outcome Assessment

At the onset of ILI, students were asked to report all symptoms to study staff. Self-reported ILI was defined as the presence of coughing with at least one of the following symptoms; fever or feverishness, body ache, or chills.[154] Students were able to report this information by phone, email, web-based reporting system, or in weekly surveys. The broad definition of ILI allowed for the capture of ILI cases both with and without fevers, and has been used in previous applications.[9, 10, 179]

A known problem with the use of ILI, a non-specific condition, to evaluate the influenza vaccine is that it can underestimate the true unit-treatment effect of the vaccine.[79, 80] Therefore, laboratory-confirmed influenza was also assessed. Upon becoming an ILI case, students had nasal and throat specimens collected. Nasal and throat swabs were combined and tested for both influenza A and influenza B via quantitative polymerase chain reaction. Polymerase chain reaction testing was done with primers and probes developed by the CDC Influenza Branch for universal detection of influenza A and influenza B viruses.[180] Additionally, health contacts of ILI cases had nasal and throat specimens collected, and tested. While not ILI cases, these students were included as laboratory-confirmed influenza if positive.

3.4 Exposure Assessment

The exposure of interest is receipt of the 2012-2013 influenza vaccine. In the original study, influenza vaccination was assessed via the enrollment survey (“Have you received a flu vaccination for the current 2012-2013 flu season?”). Among those unvaccinated, students were asked why they did not receive the influenza vaccine. Options included “because the flu shot causes the flu”, “because I don’t get the flu”, “because the flu shot does not work”, “because I didn’t know if I could get the flu shot”, “because I never got around to getting the flu shot”, “because I did not have transportation to go get the flu shot”, “because the hours when the flu

shot was available did not fit my schedule", "because the flu shot is too expensive", "because my health plan does not cover the flu shot", "because I do not have health insurance", and "because I am allergic to the flu shot". Reasons were further grouped into four categories: misinformation or myths regarding the vaccine (the flu shot causes the flu, I don't get the flu, the flu shot does not work, I didn't know if I could get the flu shot), non-financial barriers (I never got around to getting the flu shot, I did not have transportation to go get the flu shot, the hours when the flu shot was available did not fit my schedule), financial barriers (the flu shot is too expensive, my health plan does not cover the flu shot, I do not have health insurance), and allergies to the vaccine.

Previous studies found a protective unit-treatment effect for the vaccine during the 2012-2013 influenza season.[84, 181-184] Therefore, the vaccine is expected to directly protect against influenza for the season under study.

3.5 Covariate Assessment

Covariates included in the analysis were grouped as demographic, influenza risk factors, and health behaviors. Demographic factors collected include gender (male; female), race (Asian; Black or African American; Native American; Native Hawaiian / Pacific Islander; White; multi-racial), ethnicity (Hispanic; non-Hispanic), and dormitory. All demographic information was collected through self-report. Due to few participants identifying as Black or African American, Native American, Native Hawaiian / Pacific Islander, or multi-racial, these groups were combined.

Risk factors and health behaviors included stress, optimal hand hygiene, high-risk conditions, sleep quality, and alcohol use. Stress was measured via the Perceived Stress Scale-10.[185] Optimal hand hygiene was defined as self-reporting hand washing at least 5 times a day and at least 20 seconds for each hand hygiene event. High-risk conditions consisted of one of the following: asthma, reactive airway disease, Type 1 or 2 diabetes, and currently receiving HIV/AIDS or cancer treatment. Self-reported sleep quality was reported as very good, fairly

good, fairly bad, or very bad. Sleep quality categories were further reduced to good versus bad. Alcohol use was defined as self-reporting drinking alcohol at least once a week. In addition to risk factors and behaviors, information on the trial arm was also included.

Each week during follow-up, students were asked to self-report all face-to-face contacts with other study participants from the previous week. While a directed network of reported contacts was captured, the network was collapsed to an undirected network. Contact between students was assumed to have occurred as long as one student reported the contact. For the iEpi subsample, contacts were filtered by the recorded number of contacts between two participants within a week and the recorded RSSI values.

3.6 Statistical Analyses

All simulations and analyses were completed using Python 3.5.1, Python 3.6.6, and R 4.0.3. For Python, the following open-source libraries were used: NumPy,[186] SciPy,[187] statsmodels,[188] patsy,[189] NetworkX,[190] Sci-Kit Learn,[191] and pyGAM [192]. For R, the following open-source libraries were used: sna,[193] ergm,[194] rstan,[195] assortnet,[196] and DirectedClustering.[197]

Aim 1: Compare approaches to address measurement error of edges in networks.

For the following subsection, let $\mathbb{G}$ indicate the $N \times N$ adjacency matrix of the true network (i.e., no measurement error), where $\mathbb{G}_{ij}$ denotes the (i, j) entry and $\mathbb{G}_{ij} = 1$ indicates an edge and $\mathbb{G}_{ij} = 0$ otherwise. By definition, there are no self-loops ($\mathbb{G}_{ii} = 0$). The goal of the analysis is the estimation of a specific parameter (μ) and variance for that parameter ($Var(\mu)$). Let $\mathcal{G}$ indicate a single measurement of $\mathbb{G}$. When measurement error occurs, the two adjacency matrices will no longer match for every node pair (i.e., $\mathbb{G}_{ij} \neq \mathcal{G}_{ij}\ \exists\ i, j \in N$). Therefore, estimates of μ from $\mathcal{G}$ may be biased. Finally, let G indicate a perfectly measured network for n nodes (i.e., $\mathbb{G}_{ij} = G_{ij}\ \forall\ i, j \in n$), where $n < N$. Unlike $\mathcal{G}$, the gold-standard network G is only available for a portion of the population (e.g., G is a subgraph of $\mathbb{G}$).

To compare the performance of approaches to account for the measurement error of edges, a Monte Carlo simulation study was used. Comparisons were made for three different network generation models, consisting of 200 nodes. Network-1 was a stochastic block model based on whether nodes had matching values for a binary variable B and a categorical variable X. B was assigned to 62 (31%) of nodes, and X consisted of 4 categories with 50 nodes (25%) in each. The stochastic block model used to generate edges between nodes was:

$$\text{logit}\big(\Pr\big(\mathbb{G}_{ij}=1\big)\big) = -4.25 - 0.25\, I\big(B_i = B_j\big) + 1.25\, I\big(X_i = X_j\big)$$

where $I(Z=z)$ is the indicator function such that it is equal to 1 if the statement is true and 0 otherwise. Network-2 was generated using an ERGM with terms for matching values of B, matching values of X, and the squared difference of a continuous variable C

$$\text{logit}\big(\Pr\big(\mathbb{G}_{ij}=1\big|n,\mathbb{G}_{ij}^{c}\big)\big) = -4.5 + 0.1 \times I\big(B_i = B_j\big) + 1.25 \times I\big(X_i = X_j\big) - 0.5\big(C_i - C_j\big)^2$$

where n is the number of individuals (nodes) in the network, and $\mathbb{G}_{ij}^{c}$ denotes all dyad-pairs in the network aside from ij. Network-3 instead included terms for B and X, as well as Δ which models the number of closed triangles in the network. The ERGM used to generate network-3 was

$$\text{logit}\big(\Pr\big(\mathbb{G}_{ij}=1\big|n,\mathbb{G}_{ij}^{c}\big)\big) = -4.75 - 0.5 \times I\big(B_i = B_j\big) + 2.5 \times I\big(X_i = X_j\big) + 2.5\Delta$$

Network-3 has the addition of higher-order dependencies Δ (triangles) unlike the previous generation models.

Two types of measurement error were considered for each of the preceding networks: non-informative and informative measurement error. For non-informative measurement error, observed edges had a sensitivity of 0.85 and specificity of 0.99. For informative measurement error, errors were based on the node characteristic B, with pairs of nodes both having the same value of B (i.e., $B_i = B_j$) having a sensitivity of 0.90 and specificity of 0.995, whereas discordant pairs (i.e., $B_i \neq B_j$) had a sensitivity of 0.80 and specificity of 0.985. In total, six different scenarios were assessed through simulations, with each being simulated 1000 times.

3.6.1 Approaches

As a baseline comparator for all other approaches, parameters were estimated using the true network in each simulation (i.e., the network without any measurement error of edges). This approach was considered the best-case scenario in terms of performance.

As the stand-in for current practice, the parameters were estimated based on the observed edges, referred to as the Naïve approach. The Naïve approach does not attempt to account for measurement error. In addition to the Naïve approach, gold-standard subsamples were selected and used to estimate μ. The size of the gold-standard subsample available was varied changed between 80 (40%) and 120 (60%) nodes. Two different approaches to selecting the gold-standard nodes were compared: simple random sample (SRS) and respondent-driven sampling (RDS). The RDS procedure began with 10% of the subsample size selected as seeds. Each seed node nominated three nodes based on a random selection of nodes that it shared a true edge with. The procedure was repeated for nominated nodes until the gold-standard subsample size was met.

For the imputation approach, MIME was implemented with an ERGM (referred to as MIME-ERGM hereafter). ERGM are a parametric model for network data where the dependent variable is an edge.[170] These models have been traditionally used to understand tie formation within networks, but ERGM have also been used for multiple imputation of missing data.[169, 171-173] MIME-ERGM was implemented as follows. First, an ERGM was specified and estimated using only the nodes and edges from the gold-standard subsample, G. For specification of the model, the true data-generating model for the network was specified for network-1 and network-2. For network-3, MIME-ERGM included the geometrically weighted edgewise shared partners term rather than the triangle term due to model convergence issues. Next, G is extended to include all N nodes, with all edges not measured by the gold-standard measure considered as missing. The missing edges are then imputed using the estimated ERGM. MIME-ERGM differs from MIME in the context of independent data, which tends to include the information from the

measurements within this model.[166] Instead, the mismeasured network serves as the starting basis for the imputed networks from the ERGM. To allow for uncertainty in the predictions, MIME uses m imputations. Each imputed graph is indicated by $\tilde{G}_k$ for $k = 1, \ldots, m$ imputations. For each of the m imputations, the parameter of interest $\widehat{\mu_k}$ and $\widehat{Var}(\widehat{\mu_k})$ are estimated. To provide a single summary of all the imputations, the imputations are combined and summarized using Rubin's rule.[198] The overall point estimate for the parameter was the mean across all m imputations

$$\bar{\mu} = m^{-1} \sum_{k=1}^{m} \widehat{\mu_k}$$

The variance for this parameter is the within-imputation variance plus the between-imputation variance.

$$\overline{Var}(\bar{\mu}) = m^{-1} \sum_{k=1}^{m} \widehat{Var}(\widehat{\mu_k}) + (1 + m^{-1})(1 - m)^{-1} \sum_{k=1}^{m} (\widehat{\mu_k} - \bar{\mu})^2$$

MIME-ERGM was implemented using both methods of gold-standard subsample selection, and both subsample sizes.

The recently proposed Bayesian approach from Young et al. works by specifying two models and corresponding prior distributions.[165] Unlike MIME, no gold-standard subsample is required. The first model is the *measurement model*, which is the probability distribution for the observed edges in the observed network $\mathcal{G}$ as a function of the true network $\mathbb{G}$. With the prior θ, the measurement model can be written as $\Pr(\mathcal{G}_{ij} | \mathbb{G}_{ij}, \theta)$. The second model is the *network model*, which corresponds to the probability distribution of edges in $\mathbb{G}$. The network model is written as $\Pr(\mathbb{G}_{ij} | \lambda)$, with prior λ. Applying Bayes' rule, $\mathbb{G}$ can be consistently estimated with $\mathcal{G}$, the specified models, and the priors via:

$$\Pr(\mathbb{G}, \theta, \lambda | \mathcal{G}) = \frac{\Pr(\mathcal{G} | \mathbb{G}, \theta) \Pr(\mathbb{G} | \lambda) \Pr(\theta, \lambda)}{\Pr(\mathcal{G})}$$

Draws from the joint posterior distribution, $\Pr(\mathbb{G}, \alpha, \phi|\mathcal{G})$, are then used to estimate $\mathbb{G}$. Similar to MIME, multiple networks are generated. The parameters estimated from the m generated graphs were similarly summarized using Rubin's rule.[198]

3.6.2 Performance Metrics

Performance of approaches was compared for estimation of the following parameters: number of edges, density, assortativity coefficient, degree, and clustering coefficient. The number of edges was the number of unique edges in the network. Density is the number of edges occurring in the network divided by the total number of possible edges. The assortativity coefficient measures the tendency of individuals sharing an edge to also share similar traits or behaviors.[199] The assortativity coefficient is bounded between -1 and 1, indicating perfectly disassortative and assortative networks, respectively. The assortativity coefficient was calculated for the variable B. The mean degree was the mean of unique contacts for each node. The mean local clustering coefficient is the mean of the number of closed triangles that occur among a node's contacts divided by the total number of possible triangles.[200] A closed triangle is when a triad of nodes all share edges.

For all approaches, the variance for each parameter was estimated using a jackknife approach.[201-204] The jackknife operates by a leave-one-out procedure, where a single observation is removed then the parameter is re-estimated. After the leave-one-out procedure is completed for each observation, the estimated parameter for the full data set is subtracted from each leave-one-out iteration and then is squared. Finally, the squared differences are summed together and multiplied by a scaling factor. Instead of the usual scaling factor of $\frac{n-1}{n}$ used in IID data, the scaling factor of $\frac{n-2}{2n}$ was used instead.[204] The variances for the number of edges, density, degree, and clustering coefficient were estimated by removing a single node from the network.[204, 205] For the assortativity coefficient, a single edge was removed instead.[199]

The performance of each approach was evaluated for each parameter via the following metrics: bias, empirical standard error (ESE), and 95% confidence interval (CI) coverage. Bias was defined as the mean of the estimated parameter minus the true value for that parameter. The true value was determined from the average value from 10,000 true networks. ESE was defined as the standard error of the estimated parameter. 95% CI coverage was calculated as the proportion of CI that contained the true value for each measure.

Aim 2: Assess the finite-sample performance of network-TMLE.

Network-TMLE was implemented in Python with the following dependencies: NumPy,[186] SciPy,[187] statsmodels,[188] patsy,[189] and NetworkX.[190] To motivate the implementation, consider drawing inference about the effect of a binary exposure V on an outcome Y in an observational study. For individual $i = 1, \dots, n,$ let W_i indicate observed baseline covariate(s), V_i the observed exposure, and Y_i the observed outcome. Consider the setting where individuals are connected via a network of edges (e.g., an edge may indicate two individuals are friends within a social network, live within a certain distance of each other, or had a face-to-face conversation). Suppose the network structure is static (i.e., fixed over time) and can be summarized by an $n \times n$ adjacency matrix $\mathcal{G}$. Let $\mathcal{G}_{ij}$ denote the (i, j) entry of $\mathcal{G}$, where $\mathcal{G}_{ij} = 1$ if an edge exists between i and j. Assume no interference between individuals i and j if $\mathcal{G}_{ij} = 0$. Since interference is a relation between individuals, $\mathcal{G}_{ii} = 0 \; \forall \; i \in n$. Throughout, individual i's "immediate contacts" refers to individuals that have an edge with i. The potential outcomes may be denoted by $Y_i(v_i, v_i^s)$, with $v \in \mathcal{V} = \{0,1\}$ and $v^s \in \mathcal{V}^s$. Denote the conditional distribution of V given W under policy ω by $\Pr^*(V = v|W)$. For the aforementioned deterministic policy, $\Pr^*(V = 1|W) = 1$. Stochastic policies may also be of interest where $0 < \Pr^*(V = 1|W) < 1$. The target estimand is the conditional sample mean under policy ω, which can be expressed as $\psi^c = \frac{1}{n}\sum_{i=1}^{n} E\left[\sum_{a \in \mathcal{A}, a^s \in \mathcal{A}^s} Y_i(a, a^s) \Pr^*(A_i = a, A_i^s = a^s|W_i, W_i^s) \,|\boldsymbol{W}\right]$ where $\boldsymbol{W} = (W_1, W_2, \dots, W_n)$.[150]

Network-TMLE was implemented via the following procedure consisting of five steps. First an outcome model for $E[Y_i|V_i, V_i^S, W_i, W_i^S]$ is estimated by treating observations as if they were IID. From the estimated outcome model, predicted outcomes under the observed V_i and V_i^S for each unit are calculated, indicated by $\hat{Y}_i$.

Second, the weights can be expressed as

$$\frac{\Pr^*(V_i|W_i, W_i^S; \gamma^*) \Pr^*(V_i^S|V_i, W_i, W_i^S, \delta^*)}{\Pr(V_i|W_i, W_i^S; \gamma) \Pr(V_i^S|V_i, W_i, W_i^S; \delta)}$$

where γ, δ, γ^*, and δ^* denote the parameters for the model for $\Pr(V_i|W_i, W_i^S)$, $\Pr(V_i^S|V_i, W_i, W_i^S)$, $\Pr^*(V_i|W_i, W_i^S)$, and $\Pr^*(V_i^S|V_i, W_i, W_i^S)$, respectively. The model for $\Pr(V_i|W_i, W_i^S)$ can be estimated with a logistic regression model treating observations as IID. Different models may be assumed for estimating $\Pr(V_i^S|V_i, W_i, W_i^S)$. For example, if V_i^S is a binary variable indicating whether at least one of individual i's immediate contacts is exposed, then logistic regression might be used. If V_i^S is instead a count variable (e.g., indicating the number of immediate contacts exposed), then Poisson or negative binomial regression models might be assumed. Alternatively, restrictions on the functional form of V_i^S may be avoided by letting V_i^S equal the vector of exposures for individual i's immediate contacts. If the maximum number of contacts is b, then $\Pr(V_i^S|A_i, W_i, W_i^S)$ can be factored into b different binary conditional probabilities (i.e. $\Pr\left(V_i^{S(1)}\middle|V_i, W_i, W_i^S\right) \times \Pr\left(V_i^{S(2)}\middle|V_i, V_i^{S(1)}, W_i, W_i^S\right) \times \cdots \times \Pr\left(V_i^{S(b)}\middle|V_i, V_i^{S(1)}, \ldots, V_i^{S(b-1)}, W_i, W_i^S\right)$), where $V_i^{S(b)}$ indicates the exposure of contact b.[151] These conditional probabilities can then be estimated via logistic regression. To estimate the numerator, the following simulation procedure is used. A large number of copies of the data set indexed by k are generated. Next, the policy is applied to each k to generate V_{ik}^* and V_{ik}^{S*}. Then the parameters γ^* and δ^* are estimated by using the approach as the denominator, but using *all copies of the data simultaneously*. Then $\Pr^*(V_i|W_i, W_i^S; \gamma^*)$ and $\Pr^*(V_i^S|V_i, W_i, W_i^S, \delta^*)$ are estimated using $\widehat{\gamma^*}$, $\widehat{\delta^*}$, and the observed values of V_i and V_i^S.

For the third step, the following logistic regression model is estimated via weighted maximum likelihood

$$\text{logit}(Y_i) = \eta_0 + \text{logit}(\hat{Y}_i)$$

Fourth, the following procedure is used to estimate ψ for stochastic policies. The exposure under the policy, V_i^*, and the previously estimated outcome model are used to estimate the outcomes under the policy, $\hat{Y}_i^*$. The predicted $\hat{Y}_i^*$ is then updated via

$$\tilde{Y}_i^* = \text{expit}\left(\widehat{\eta_0} + \text{logit}(\hat{Y}_i^*)\right)$$

Finally, $\hat{\psi}$ can be estimated as the mean of $\tilde{Y}^*$. However, the estimated ψ only corresponds to a single draw of V^* from the policy. To account for the uncertainty in V_i^* for stochastic policies, the following Monte Carlo procedure is used. Generate $k = 1, \ldots, m$ different draws of V_{ik}^*, where V_{ik}^* denotes a single draw from $\text{Bernoulli}(\Pr^*(V_i = 1|W_i, W_i^S))$. Calculate the new summary measure V_{ik}^{S*} using V_{ik}^* and $\mathcal{G}$. Estimate $\hat{Y}_{ik}^*$ and $\tilde{Y}_{ik}^*$ with V_{ik}^* and V_{ik}^{S*}. The mean of the targeted predictions, $\hat{\psi}_k = \sum_{i=1}^n \tilde{Y}_{ik}^*/n$ is calculated for each k. The estimator for ψ is the mean of the m estimates, i.e., $\hat{\psi} = \sum_{k=1}^m \hat{\psi}_k/m$. To reduce computational burden, V_{ik}^* and V_{ik}^{S*} generated during the estimation of the weights' numerator are reused.

Lastly, $(1-\alpha)$ CI can be constructed by $\hat{\psi} \pm Z_{1-\alpha}\sqrt{\hat{\sigma}^2/n}$, where $Z_{1-\alpha/2}$ denotes the Z score for $1-\alpha/2$ entry. For the conditional sample mean, the variance is estimated by

$$\hat{\sigma}^2 = \frac{1}{n}\sum_{i=1}^{n}\left(\frac{\Pr^*(V_i|W_i)}{\Pr(V_i|W_i)}(Y_i - \hat{Y}_i)\right)^2$$

3.6.3 Implementation Validation

We conducted validation simulation studies for the implementation of network-TMLE. The validation simulations demonstrate our implementation producing expected results where TMLE for dependent data has been previously shown or in simple extensions.

The network for these simulations was a static network of n nodes with a uniform degree distribution with a maximum degree of two. Our simulations focus on the conditional sample

mean, so both the network and distribution of $\boldsymbol{W}$ were held constant. Simulations were conducted for sample sizes of 500 and 1000. Distributions of V and Y were generated 2000 times and network-TMLE was estimated within each simulated data set. We compared the four different possibilities of model specification: m and π correctly specified, only m correctly specified, only π correctly specified, and both m and π incorrect. Policies consisted of setting all individuals in the population to a single probability of V (i.e., $\Pr(V_i = 1|W_i, W_i^s) = \Pr(V = 1) = p$).

As a starting point, we re-created the simulations results reported in Sofrygin and van der Laan.[151] The data generating mechanism from Sofrygin and van der Laan was

$$\Pr(W_i = 1) = 0.35$$

$$\Pr(V_i = 1|W_i, W_i^s) = \text{expit}\left(-1.2 + 1.5W_i + 0.6\sum_{j=1}^{n} W_j\mathcal{G}_{ij}\right)$$

$$\Pr(Y_i = 1|V_i, V_i^s, W_i, W_i^s) = \text{expit}\left(-2.5 + 1.5W_i + 0.5V_i + 1.5\sum_{j=1}^{n} W_j\mathcal{G}_{ij} + 1.5\sum_{j=1}^{n} V_j\mathcal{G}_{ij}\right)$$

We then modified the data generating mechanism to only consist of a unit-treatment effect

$$\Pr(W_i = 1) = 0.35$$

$$\Pr(V_i = 1|W_i, W_i^s) = \text{expit}\left(-0.6 - 0.9W_i + 0.8\sum_{j=1}^{n} W_j\mathcal{G}_{ij}\right)$$

$$\Pr(Y_i = 1|V_i, W_i, W_i^s) = \text{expit}\left(-1.75 + 1.5W_i + 1.75V_i + 1.5\sum_{j=1}^{n} W_j\mathcal{G}_{ij}\right)$$

Next, we designed a scenario with only a spillover effect.

$$\Pr(W_i = 1) = 0.35$$

$$\Pr(V_i = 1|W_i, W_i^s) = \text{expit}\left(-0.6 - 0.9W_i + 0.8\sum_{j=1}^{n} W_j\mathcal{G}_{ij}\right)$$

$$\Pr(Y_i = 1|V_i^S, W_i, W_i^S) = \text{expit}\left(-1.75 + 1.5W_i + 1.5\sum_{j=1}^{n} W_j\mathcal{G}_{ij} - 1.5\sum_{j=1}^{n} V_j\mathcal{G}_{ij}\right)$$

Lastly, we created a modification that included a continuous Y

$$\Pr(W_i = 1) = 0.35$$

$$\Pr(A_i = 1|W_i, W_i^S) = \text{expit}\left(-1.2 + 1.5W_i + 0.4\sum_{j=1}^{n} W_j\mathcal{G}_{ij}\right)$$

$$Y_i = 20 - 5W_i + 5A_i + 1.5\sum_{j=1}^{n} W_j\mathcal{G}_{ij} + 1.5\sum_{j=1}^{n} A_j\mathcal{G}_{ij} + \epsilon_i$$

where $\epsilon_i \sim \text{Normal}(0,1)$.

3.6.4 Data-Generating Mechanisms

To assess the finite sample performance of network-TMLE outside of the implementation validation and contrast with IID-TMLE, a Monte Carlo simulation study was conducted. Comparisons were made using three networks with four different data-generating mechanisms, for a total of 12 scenarios.

Three different networks were used: a uniform random graph, a modified clustered power-law random graph, and the eX-FLU network[154] of self-reported contacts among undergraduate students. The uniform random graph followed a uniform degree distribution with a minimum degree of 1 and a maximum of 6. The modified clustered power-law random graph consisted of eight separately generated clustered power-law random subgraphs, with edges randomly generated between the random subgraphs. Each of the eight clustered power-law subgraphs was separately generated from a Barabasi-Albert random graph model with a set probability for closing triads between nodes.[206] For each node, three connections were generated and the probability of triad closure was set to 0.75. Lastly, the eX-FLU network was based on data from the eX-FLU cluster-randomized trial, a study to assess the efficacy of three-day self-isolation among university students.[154] Over the ten-week study period, enrolled

students reported face-to-face contacts each week. From the ten weeks of self-reported contacts, we generated a single static network and selected the largest connected component.

3.6.4.1 Statin and Cardiovascular Disease

First, statins on the risk of atherosclerotic cardiovascular disease (ASCVD) stood in for a setting with no interference, since the mechanism of action may reasonably allow researchers to believe that whether an individual's friends take a statin does not influence person i's risk of ASCVD. Let $W_{1,i}$ indicate age, $W_{2,i}$ indicate log-transformed low-density lipoprotein, $U_{1,i}$ indicate diabetes, $U_{2,i}$ indicate frailty, and $W_{5,i}$ indicate the calculated risk score for cardiovascular disease. These variables were generated from the following distributions.

$$W_{1,i} = \text{Uniform}(40, 60)$$

$$W_{2,i} = 0.005W_{1,i} + \text{Normal}(\log(100), 0.18)$$

$$\text{logit}\big(\Pr\big(U_{1,i} | \, W_{1,i}W_{2,i}\big)\big) = -4.23 + \ 0.03W_{2,i} - 0.02W_{1,i} + 0.0009W_{1,i}W_{1,i}$$

$$\text{logit}\big(U_{2,i}\big) = -5.5 + 0.05(X_i - 20) + 0.001X_iX_i + \text{Normal}(0,1)$$

$$\text{logit}(R_i) = 4.299 + 3.501U_{1,i} - 2.07\log\big(W_{1,i}\big) + 0.051\log\big(W_{1,i}\big)^2 + 4.090W_{2,i} - 1.04\log\big(W_{1,i}\big)W_{2,i} + 0.01U_{2,i}$$

These variables were generated once for each individual in each network and held constant across simulations. Statin prescription (indicated by V_i) was generated following

$$\begin{aligned}\text{logit}\big(\Pr\big(V_i = 1|W_{1,i}, W_{2,i}, W_{5,i}\big)\big) \\ = -5.3 + 0.2\,W_{2,i} + 0.15\big(W_{1,i} - 30\big) + 0.4\,I\big(0.05 \le W_{5,i} < 0.075\big) \\ + 0.9\,I\big(0.075 \le W_{5,i} < 0.2\big) + 1.5\,I\big(W_{5,i} \ge 0.2\big)\end{aligned}$$

Cardiovascular disease (indicated by Y_i) was generated following

$$\Pr\big(Y_i = 1|V_i, W_{1,i}, W_{2,i}, W_{5,i}\big) = \text{expit}\big(-5.05 - 0.8V_i + 0.37\,\sqrt{W_{1,i} - 39.9} + 0.75\,W_{2,i} + 0.75\,W_{5,i}\big)$$

3.6.4.2 Naloxone and Opioid Overdose Deaths

For spillover effect only, a data generating mechanism based on the effect of the nasal spray formulation of naloxone on subsequent opioid overdose deaths was created, since nasal spray formulations rely on another person for administration, with self-administration having occurred only in rare cases.[207] Let $W_{6,i}$ indicate gender, $W_{7,i}$ indicate recent release from prison, and $W_{8,i}$ recent overdose before study baseline. These variables were generated via the following

$$\Pr\left(W_{6,i} = 1\right) = 0.35$$

$$\text{logit}\left(\Pr\left(W_{7,i} = 1 | W_{6,i}^{s}\right)\right) = -1.1 + 0.5W_{6,i} + 0.1\frac{\sum_{j=1}^{n} W_{6,j}\mathcal{G}_{ij}}{\sum_{j=1}^{n}\mathcal{G}_{ij}}$$

$$\text{logit}\left(\Pr\left(W_{8,i} = 1 | W_{6,i}, W_{7,i}, W_{6,i}^{s}\right)\right) = -1.7 + 0.1W_{6,i} + 0.1\frac{\sum_{j=1}^{n} W_{6,j}\mathcal{G}_{ij}}{\sum_{j=1}^{n}\mathcal{G}_{ij}} + 0.6W_{7,i}$$

These variables were generated once for each individual in each network and held constant across simulations. Naloxone training and access (indicated by V_i) was generated following

$$\text{logit}\left(\Pr\left(V_i = 1 | W_{6,i}, W_{7,i}, W_{6,i}^{s}, W_{8,i}^{s}\right)\right)$$

$$= -1.3 - 1.5\, W_{7,i} + 1.5\, W_{7,i}W_{6,i} + 0.95\,\frac{\sum_{j=1}^{n} I\left(W_{6,j} = 1\right)\mathcal{G}_{ij}}{\sum_{j=1}^{n}\mathcal{G}_{ij}}$$

$$+ 0.95\frac{\sum_{j=1}^{n} I\left(W_{8,j} = 1\right)\mathcal{G}_{ij}}{\sum_{j=1}^{n}\mathcal{G}_{ij}}$$

Probability of opioid overdose was generated following

$$\text{logit}\left(\Pr\left(Y_i = 1 | V_i^{s}, W_{6,i}, W_{7,i}, W_{6,i}^{s}, W_{8,i}^{s}\right)\right)$$

$$= -1.1 - 0.2\sum_{j=1}^{n} I\left(V_j = 1\right)\mathcal{G}_{ij} + 1.7\, W_{7,i} - 0.9\, W_{6,i} + 0.75\,\frac{\sum_{j=1}^{n} I\left(W_{8,j} = 1\right)\mathcal{G}_{ij}}{\sum_{j=1}^{n}\mathcal{G}_{ij}}$$

$$- 0.75\frac{\sum_{j=1}^{n} I\left(W_{6,j} = 1\right)\mathcal{G}_{ij}}{\sum_{j=1}^{n}\mathcal{G}_{ij}}$$

3.6.4.3 Comprehensive Dietary Intervention and Body Mass Index

For simultaneous unit-treatment and spillover effects, a data generating mechanism based on a comprehensive dietary intervention on body mass index (BMI) was created, since previous work has also found that BMI to be socially clustered,[208, 209] with the transmission of obesity theorized to result from social pressures or the shared environments of social contacts.[209] Let $W_{6,i}$ indicate gender, $W_{9,i}$ indicate body mass index (BMI) at baseline, and $W_{10,i}$ indicate recent exercise at baseline. These variables were generated from the following distributions.

$$\Pr\left(W_{6,i} = 1\right) = 0.5$$

$$W_{9,i} = \text{LogNormal}(3.4, 0.2)$$

$$\text{logit}\left(\Pr\left(W_{10,i} = 1\right)\right) = -0.25$$

These variables were generated once for each individual in each network and held constant across simulations. Comprehensive dietary reform including caloric restriction and increased food quality (indicated by V_i) was generated following

$$\text{logit}\left(\Pr\left(V_i = 1 | W_{6,i}, W_{9,i}, W_{10,i}, W_{10,i}^{s}\right)\right)$$

$$= -0.5 + 0.05\left(W_{9,i} - 30\right) + 0.25 W_{6,i} W_{10,i} + 0.05 \frac{\sum_{j=1}^{n} I\left(W_{10,j} = 1\right) \mathcal{G}_{ij}}{\sum_{j=1}^{n} \mathcal{G}_{ij}}$$

BMI at end of the follow-up period depended on the following model

$$Y_i = 3 + W_{9,i} - 5V_i - 5\, I\left(3 < \sum_{j=1}^{n} I\left(V_j = 1\right) \mathcal{G}_{ij}\right) + 3W_{6,i} - 3W_{10,i} - 0.5 \sum_{j=1}^{n} I\left(W_{10,j} = 1\right) \mathcal{G}_{ij}$$

$$+ \frac{\sum_{j=1}^{n} \mathcal{G}_{ij}\left(W_{9,j} - W_{9,i}\right)}{\sum_{j=1}^{n} \mathcal{G}_{ij}} + \epsilon_i$$

where $\epsilon_i \sim \text{Normal}(0,1)$.

3.6.4.4 Vaccination and Infection

Lastly, a vaccine and infection mechanism was implemented via a Susceptible-Infected-Recovered (SIR) model, with this simulation mechanism corresponds to a simple model of human-to-human transmission. Let $W_{11,i}$ indicate asthma at baseline, and $W_{12,i}$ indicate hand hygiene. These variables were generated from the following distributions.

$$\Pr(W_{11,i}) = 0.15$$

$$\text{logit}(\Pr(W_{12,i} = 1|W_{11,i})) = -0.15 + 0.1W_{11,i}$$

These variables were generated once for each individual in each network and held constant across simulations. Vaccination status (indicated by V_i) was generated following

$$\text{logit}(\Pr(V_i = 1|W_{11,i}, W_{12,i}, W_{12,i}^S)) = -1.9 + 1.75W_{11,i} + 0.95W_{12,i} + 1.2\frac{\sum_{j=1}^{n} I(W_{12,j} = 1)\mathcal{G}_{ij}}{\sum_{j=1}^{n}\mathcal{G}_{ij}}$$

Individuals transitioned between three states: susceptible, infected, and recovered. Seven individuals were randomly chosen to be the initial infections. Individuals in the infected state were actively infectious for a period of five discrete time-steps after moving from the susceptible state. After the period of five discrete time-steps, individuals transitioned to the recovered state and were no longer infectious nor capable of being infected by contacts. All transmission events occurred over a period of ten time-steps. The probability of individual i becoming infected ($I_{i,t}$) at each discrete time-point by individual j was based on the following model

$$\text{logit}(\Pr(I_{i,t} = 1|Z_{j,t} = 1, \mathcal{G}_{ij} = 1, V_i, V_j, W_{11,i}, W_{12,i})) = -2.4 - 1.5V_i - 0.4V_j + 1.5W_{11,i} - 0.4W_{12,i}$$

where $Z_{j,t} = 1$ indicates whether j was in the infectious category at time t. Probabilities of becoming infected were assessed separately for each infected contact. Infected individuals were actively infectious for five discrete time-steps and the transmission process continued for a total of 20 discrete time-steps.

Aim 3: Estimate the risk of influenza under competing influenza vaccination policies.

In the following subsection, let V indicate influenza vaccination status, Y indicate influenza infection, T indicate trial arm for the cluster-randomized study, G indicate gender, C indicate class year, R indicate race, D indicate high risk, S indicate stress, H indicate optimal hand hygiene, A indicate alcohol use, Q indicate sleep quality, P indicate parental education, and B indicate the dorm. Additionally, let F indicate degree, where degree is the number of unique contacts, and $\mathcal{G}$ indicate the self-reported contact network at week one.

3.6.5 Policies

Previous work on influenza vaccination receipt among university students has focused on common misconceptions regarding the vaccine,[94, 95, 98, 100, 116, 120] the convenience of receipt,[94, 95, 98] and financial barriers.[94, 95] Therefore, we consider potential policies to address these reasons. Policy 1 consisted of a theoretical educational intervention to emphasize the benefits of the vaccine and dispelling common myths. Targeted students included those who reported at least one of the following: the influenza vaccine can cause the flu, that they do not get the flu, or that they did not know if they could receive the influenza vaccine. Policy 2 addressed non-financial barriers by targeting students who reported at least one of the following reasons for not receiving the influenza vaccine: did not get around to receiving the influenza vaccine, did not have transportation to go receive the vaccine, or the hours when the vaccine was available did not fit their schedule. Policy 3 addressed financial barriers and targeted students who reported that their health plan did not cover the vaccine or they did not have health insurance. Students who reported being allergic to the influenza vaccine were never vaccinated under any of the policies.

Since the effectiveness of the preceding policies in increasing vaccination is unknown and depends on how it is implemented, stochastic policies are considered instead. Individuals targeted by the policy had their log-odds of receiving the influenza vaccine increased. The following model was used to estimate the log-odds of vaccination

$$\Pr(V_i;\rho) = \text{expit}\Bigg(\rho_0 + \rho_1 G_i + \rho_2 I(R_i = 1) + \rho_3 I(R_i = 2) + \rho_4 D_i + \rho_5 S_i + \rho_6 H_i + \rho_7 A_i + \rho_8 Q_i$$

$$+ \rho_9 \sum_j T_j \mathcal{G}_{ij} + \rho_{10} \sum_j G_j \mathcal{G}_{ij} + \rho_{11} \sum_j D_j \mathcal{G}_{ij} + \rho_{12} \sum_j H_j \mathcal{G}_{ij} + \rho_{13} \sum_j A_j \mathcal{G}_{ij}$$

$$+ \rho_{14} \frac{\sum_j (S_i - S_j)^2 \mathcal{G}_{ij}}{F_i - 1} + \rho_{15} \sum_j I(R_j = 1)\mathcal{G}_{ij} + \rho_{16} \sum_j I(R_j = 2)\mathcal{G}_{ij} + \rho_{17} F_i + \rho_{18} G_i D_i$$

$$+ \rho_{19} A_i Q_i + \rho_{20} I(C_i = 1) + \rho_{21} I(C_i = 2) + \rho_{22} I(C_i = 3) + \rho_{23} I(C_i = 4) + \rho_{24} P_i\Bigg)$$

To allow for further flexibility in the model, each individual's log-odds of vaccination to be shifted under each policy was determined using 20-fold cross-validated super learner.[210] Super learner is a generalized stacking algorithm that allows for the combination of multiple predictive algorithms into a single prediction function, with asymptotic performance equivalent to the best performing algorithm included.[211] The super-learner implementation consisted of logistic regression, logistic generalized additive model (GAM),[192, 212] a single-layer eight-node neural-network,[191, 213] and a random forest classifier.[191, 214] The logistic GAM was further varied by smoothing parameters of 0.5, 0.75, 1.0, 1.5, and 2.0. Shifts in the log-odds for students targeted by the policy were varied from $\varpi = \{0, 0.25, 0.5, \ldots, 2.75, 3\}$. Students not targeted by the policy also had an increased log-odds of receiving the vaccine to reflect their potential benefit from the policy. However, their log-odds were only increased by a third of targeted students (i.e., $\varpi/3$).

3.6.6 Network-TMLE

To estimate the risk of influenza for each shift in the log-odds of vaccination under each of the policy variations, network-TMLE was used.[150-152] Network-TMLE was implemented via the following five steps.

Step 1: Outcome nuisance model: A logistic model for $\Pr(Y_i|V_i, V_i^s, W_i, W_i^s)$ was estimated handling each observation as if it were IID. The following model was estimated for the probability of influenza

$$\Pr(Y_i;\beta) = \text{expit}\Bigg(\beta_0 + \beta_1 V_i + \beta_2 \sum_j V_j \mathcal{G}_{ij} + \beta_3 V_i \sum_j V_j \mathcal{G}_{ij} + \beta_4 G_i + \beta_5 D_i + \beta_6 H_i + \beta_7 S_i + \beta_8 Q_i$$
$$+ \beta_9 A_i + \beta_{10} I(R_i = 1) + \beta_{11} I(R_i = 2) + \beta_{12} \sum_j T_j \mathcal{G}_{ij} + \beta_{13} \sum_j G_j \mathcal{G}_{ij} + \beta_{14} \sum_j D_j \mathcal{G}_{ij}$$
$$+ \beta_{15} \sum_j H_j \mathcal{G}_{ij} + \beta_{16} \sum_j A_j \mathcal{G}_{ij} + \beta_{17} \sum_j I\big(R_j = 1\big) \mathcal{G}_{ij} + \beta_{18} \sum_j I(R_i = 2) \mathcal{G}_{ij} + \beta_{19} F_i$$
$$+ \beta_{20} G_i A_i + \beta_{21} V_i A_i \Bigg)$$

To allow for further flexibility, super learner was used.[210, 211] To estimate the probability of influenza, a 20-fold super learner consisted of logistic regression, elastic-net regularized logistic regression,[215] and logistic GAM.[212] Two variations of elastic-net were included, with L1-L2 ratios of 0.25 and 0.75. Variations on the included logistic GAM with smoothing parameters of 0.5, 0.75, 1.0, 1.5, and 2.0.

Step 2: Exposure nuisance model: The weights can be written as

$$\frac{\Pr^*(V_i|W_i, W_i^s; \gamma^*) \Pr^*(V_i^s|A_i, W_i, W_i^s, \delta^*)}{\Pr(V_i|W_i, W_i^s; \gamma) \Pr(V_i^s|A_i, W_i, W_i^s; \delta)}$$

where γ, δ, γ^*, and δ^* denote the parameters for the model for $\Pr(A_i|W_i, W_i^s)$, $\Pr(A_i^s|A_i, W_i, W_i^s)$, $\Pr^*(A_i|W_i, W_i^s)$, and $\Pr^*(A_i^s|A_i, W_i, W_i^s)$, respectively. A logistic model for $\Pr(V_i|W_i, W_i^s)$ was estimated treating observations as IID. Since the summary measure $V_i^s = \sum_j I\big(\mathcal{G}_{ij} = 1\big) V_j$ was chosen for immediate contacts' vaccination, a Poisson for $\Pr(V_i^s|V_i, W_i, W_i^s)$ was estimated. The models were

$$\Pr(V_i;\gamma) = \text{expit}\Bigg(\gamma_0 + \gamma_1 G_i + \gamma_2 I(R_i = 1) + \gamma_3 I(R_i = 2) + \gamma_4 D_i + \gamma_5 S_i + \gamma_6 H_i + \gamma_7 A_i + \gamma_8 Q_i$$
$$+ \gamma_9 \sum_j T_j \mathcal{G}_{ij} + \gamma_{10} \sum_j G_j \mathcal{G}_{ij} + \gamma_{11} \sum_j D_j \mathcal{G}_{ij} + \gamma_{12} \sum_j H_j \mathcal{G}_{ij} + \gamma_{13} \sum_j A_j \mathcal{G}_{ij}$$
$$+ \gamma_{14} \frac{\sum_j (S_i - S_j)^2 \mathcal{G}_{ij}}{F_i - 1} + \gamma_{15} \sum_j I(R_j = 1)\mathcal{G}_{ij} + \gamma_{16} \sum_j I(R_j = 2)\mathcal{G}_{ij} + \gamma_{17} G_i A_i$$
$$+ \gamma_{18} V_i A_i \Bigg)$$

and

$$\log(E[V_i^S|\delta]) = \delta_0 + \delta_1 V_i + \delta_2 G_i + \delta_3 I(R_i = 1) + \delta_4 I(R_i = 2) + \delta_5 D_i + \delta_6 S_i + \delta_7 H_i + \delta_8 A_i + \delta_9 Q_i$$
$$+ \delta_{10} \sum_j T_j \mathcal{G}_{ij} + \delta_{11} \sum_j G_j \mathcal{G}_{ij} + \delta_{12} \sum_j D_j \mathcal{G}_{ij} + \delta_{13} \sum_j H_j \mathcal{G}_{ij} + \delta_{14} \sum_j A_j \mathcal{G}_{ij}$$
$$+ \delta_{15} \frac{\sum_j (S_i - S_j)^2 \mathcal{G}_{ij}}{F_i - 1} + \delta_{16} \sum_j I(R_j = 1)\mathcal{G}_{ij} + \delta_{17} \sum_j I(R_j = 2)\mathcal{G}_{ij} + \delta_{18} G_i A_i$$
$$+ \delta_{19} V_i A_i$$

To allow for flexibility in these models, super learner was similarly used. For $\Pr(V_i;\gamma)$, a 20-fold super learner consisted of logistic regression, elastic-net regularized logistic regression,[215] and logistic GAM.[212] Two variations of elastic-net were included, with L1-L2 ratios of 0.25 and 0.75. Variations on the included logistic GAM with smoothing parameters of 0.5, 0.75, 1.0, 1.5, and 2.0. For $\log(E[V_i^S|\delta])$, 20-fold super learner included Poisson regression and Poisson GAM with the following smoothing parameters: 0.5, 0.75, 1.0, 1.5, and 2.0.

Estimation of the numerator relies on a simulation approach due to the difficulty in specifying $\Pr^*(V_i|W_i, W_i^S;\gamma^*)$ and $\Pr^*(V_i^S|V_i, W_i, W_i^S, \delta^*)$ directly. First, 100 copies of the data set indexed by k are generated. Next, the policy ω is applied to each k to generate V_{ik}^* and V_{ik}^{S*}. Then γ^* and δ^* are estimated by using the same models as above, but are instead fit to *all*

copies of the data with ω applied simultaneously. Then $\Pr^*(V_i|W_i, W_i^s; \gamma^*)$ and $\Pr^*(V_i^s|V_i, W_i, W_i^s, \delta^*)$ are estimated using $\widehat{\gamma^*}$, $\widehat{\delta^*}$, and the observed values of V_i and V_i^s.

Step 3: Targeting: The outcome model and weights are then used to estimate the following model

$$\text{logit}(Y_i) = \eta_0 + \text{logit}\left(\hat{Y}_i\right)$$

via weighted maximum likelihood.

Step 4: Estimation: To estimate ψ for stochastic policies, network-TMLE is evaluated using a Monte Carlo procedure. Vaccination status under the policy (V_i^*) is determined for each individual by drawing from $\text{Bernoulli}(\Pr^*(V_i = 1|W_i, W_i^s))$ as determined by the policy for 100 different draws (indexed by k). From those draws, values of V_{ik}^* and V_{ik}^{*s} were determined. Then V_{ik}^*, V_{ik}^{*s}, and the estimated outcome model were used to estimate $\hat{Y}_{ik}^*$. The targeted predictions, $\tilde{Y}_{ik}^*$, are estimated via

$$\tilde{Y}_{ik}^* = \text{expit}\left(\widehat{\eta_0} + \text{logit}\left(\hat{Y}_{ik}^*\right)\right)$$

Then ψ_k is estimated by the mean of $\tilde{Y}_{ik}^*$. Finally, the overall estimate for ψ is the mean of all m estimates

$$\hat{\psi} = \frac{1}{100}\sum_{k=1}^{100} \hat{\psi}_k$$

To reduce computational burden, V_{ik}^* and V_{ik}^{s*} generated during the estimation of the weights' numerator are reused.

Step 5: Inference: The variance for the sample risk under the policy was estimated by

$$\hat{\sigma}^2 = \frac{1}{n}\sum_{i=1}^{n}\left(\frac{\Pr^*(V_i|W_i, W_i^s; \widehat{\gamma^*})\,\Pr^*\left(V_i^s\middle|A_i, W_i, W_i^s, \widehat{\delta^*}\right)}{\Pr(V_i|W_i, W_i^s; \hat{\gamma})\,\Pr\left(V_i^s\middle|A_i, W_i, W_i^s; \hat{\delta}\right)}\left(Y_i - \hat{Y}_i\right)\right)^2$$

3.6.7 Missing Data

To account for missing data, multiple imputation by chained equations (MICE) was used. Let $X_1, X_2, \ldots, X_r$ indicate the r covariates with missing data, and X_1^s indicate the corresponding

summary measure for X_1. For IID data, MICE works by first filling in the missing values via simple imputation.[216] Then the values are updated by setting one variable back to the original missingness pattern, fitting a regression model with the observed data, and filling in missing values for that variable with predictions from the fitted model. This process is repeated for each variable with missing data. The procedure is repeated for many cycles. Multiple imputed data sets are generated by repeating this same procedure. To address missing data while incorporating information from the network, the following extension to MICE was used

1. Fill-in all X with missing data via simple imputation and calculate X^s. For normally-distributed X, missing values were filled-in with the mean value of the observed values for that variable. For Poisson and multinomial, missing values were filled in with the mode. For binary variables, a weighted coin was flipped based on the overall probability of X.
2. Set X_1 where values were missing as missing
3. Regress the observed values of X_1 by a chosen model and set of variables
4. Replace the missing values of X_1 with predictions from the model fit in step 3. Update X_1^s based on the predictions
5. Repeat steps 2-4 for each variable $2,3 \ldots, r$. This marks the completion of a cycle
6. Repeat steps 2-5 for the designated number of cycles.

The extension to MICE adds the updating of X^s during steps 1 and 4. Therefore, information within X^s can be used to better predict the missing values of X. Explicitly, the procedure allows the leveraging of information, like assortativity, to improve predictive models. Because X_1^s can be included as a predictor of X_1, the number of cycles was increased from the recommendation of 10 cycles to 50 cycles. The above procedure was used to generate 100 data sets by independently repeating the above process for each data set.

In application to the eX-FLU data, MICE was used to address missingness in gender, class year, race, perceived stress, optimal hand hygiene, alcohol use, sleep quality, parental education, and influenza vaccination. Variables were imputed in the order presented. To impute gender, the following model was used

$$\Pr(G_i = 1) = \text{expit}\left(\beta_0 + \beta_1 \sum_j G_j \mathcal{G}_{ij} + \beta_2 V_i + \beta_3 \sum_j V_j \mathcal{G}_{ij} + \beta_4 S_i + \beta_5 H_i + \beta_6 A_i + \beta_7 Q_i + \beta_8 Y_i + \beta_9 D_i + \beta_{10} F_i\right)$$

For class year

$$\text{logit}\left(\frac{\Pr(C_i = 2)}{\Pr(C_i = 1)}\right) = \left(\beta_{0,2} + \beta_{1,2} S_i + \beta_{2,2} A_i + \beta_{3,2} F_i\right)$$

$$\text{logit}\left(\frac{\Pr(C_i = 3)}{\Pr(C_i = 1)}\right) = \left(\beta_{0,3} + \beta_{1,3} S_i + \beta_{2,3} A_i + \beta_{3,3} F_i\right)$$

$$\text{logit}\left(\frac{\Pr(C_i = 4)}{\Pr(C_i = 1)}\right) = \left(\beta_{0,4} + \beta_{1,4} S_i + \beta_{2,4} A_i + \beta_{3,4} F_i\right)$$

$$\text{logit}\left(\frac{\Pr(C_i \geq 5)}{\Pr(C_i = 1)}\right) = \left(\beta_{0,5} + \beta_{1,5} S_i + \beta_{2,5} A_i + \beta_{3,5} F_i\right)$$

For race

$$\text{logit}\left(\frac{\Pr(R_i = 1)}{\Pr(R_i = 0)}\right)$$

$$= \Bigg(\beta_{0,1} + \beta_{1,1} \sum_j I(R_j = 0)\mathcal{G}_{ij} + \beta_{2,1} \sum_j I(R_j = 1)\mathcal{G}_{ij} + \beta_{3,1} \sum_j I(R_j = 2)\mathcal{G}_{ij}$$

$$+ \beta_{4,1} \sum_j I(R_j = 0)\mathcal{G}_{ij} \sum_j I(R_j = 1)\mathcal{G}_{ij} + \beta_{5,1} \sum_j I(R_j = 0)\mathcal{G}_{ij} \sum_j I(R_j = 2)\mathcal{G}_{ij}$$

$$+ \beta_{6,1} \sum_j I(R_j = 1)\mathcal{G}_{ij} \sum_j I(R_j = 2)\mathcal{G}_{ij} + \beta_{7,1} V_i + \beta_{8,1} S_i + \beta_{9,1} H_i + \beta_{10,1} A_i + \beta_{11,1} Q_i$$

$$+ \beta_{12,1} Y_i \Bigg)$$

$$\text{logit}\left(\frac{\Pr(R_i = 2)}{\Pr(R_i = 0)}\right)$$

$$= \Bigg(\beta_{0,2} + \beta_{1,2} \sum_j I(R_j = 0)\mathcal{G}_{ij} + \beta_{2,2} \sum_j I(R_j = 1)\mathcal{G}_{ij} + \beta_{3,2} \sum_j I(R_j = 2)\mathcal{G}_{ij}$$

$$+ \beta_{4,2} \sum_j I(R_j = 0)\mathcal{G}_{ij} \sum_j I(R_j = 1)\mathcal{G}_{ij} + \beta_{5,2} \sum_j I(R_j = 0)\mathcal{G}_{ij} \sum_j I(R_j = 2)\mathcal{G}_{ij}$$

$$+ \beta_{6,2} \sum_j I(R_j = 1)\mathcal{G}_{ij} \sum_j I(R_j = 2)\mathcal{G}_{ij} + \beta_{7,2} V_i + \beta_{8,2} S_i + \beta_{9,2} H_i + \beta_{10,2} A_i + \beta_{11,2} Q_i$$

$$+ \beta_{12,2} Y_i \Bigg)$$

For stress

$$E[S_i] = \beta_0 + \beta_1 G_i + \beta_2 \sum_j G_j \mathcal{G}_{ij} + \beta_3 \sum_j \frac{(S_i - S_j)\mathcal{G}_{ij}}{F_i} + \beta_4 Y_i + \beta_5 C_i + \beta_6 I(R_i = 1) + \beta_7 I(R_i = 2)$$

$$+ \beta_8 D_i + \beta_9 F_i + \beta_{10} P_i$$

For hand hygiene

$$\Pr(H_i = 1) = \text{expit}\Bigg(\beta_0 + \beta_1 \sum_j H_j \mathcal{G}_{ij} + \beta_2 G_i + \beta_3 \sum_j G_j \mathcal{G}_{ij} + \beta_4 A_i + \beta_5 V_i + \beta_6 \sum_j V_j \mathcal{G}_{ij} + \beta_7 D_i + \beta_8 \sum_j D_j \mathcal{G}_{ij} + \beta_9 Y_i\Bigg)$$

For alcohol use

$$\Pr(A_i = 1) = \text{expit}\Bigg(\beta_0 + \beta_1 \sum_j A_j \mathcal{G}_{ij} + \beta_2 H_i + \beta_3 \sum_j H_j \mathcal{G}_{ij} + \beta_4 V_i + \beta_5 \sum_j V_j \mathcal{G}_{ij} + \beta_6 C_i + \beta_7 I(R_i = 1) + \beta_8 I(R_1 = 2) + \beta_9 Y_i + \beta_9 P_i + \beta_{10} F_i\Bigg)$$

For sleep quality

$$\Pr(Q_i = 1) = \text{expit}\Bigg(\beta_0 + \beta_1 \sum_j Q_j \mathcal{G}_{ij} + \beta_2 S_i + \beta_3 C_i + \beta_4 A_i + \beta_5 V_i + \beta_6 \sum_j A_j \mathcal{G}_{ij} + \beta_7 \sum_j V_j \mathcal{G}_{ij} + \beta_8 I(R_i = 1) + \beta_9 I(R_i = 2)\Bigg)$$

For parental education

$$\Pr(P_i = 1) = \text{expit}\Bigg(\beta_0 + \beta_1 C_i + \beta_2 I(R_i = 1) + \beta_3 I(R_i = 2) + \beta_4 \sum_j I(R_i = 0)\mathcal{G}_{ij} + \beta_5 \sum_j I(R_i = 1)\mathcal{G}_{ij} + \beta_6 \sum_j I(R_i = 2)\mathcal{G}_{ij} + \beta_7 Q_i + \beta_8 A_i + \beta_9 \sum_j A_j \mathcal{G}_{ij}\Bigg)$$

For influenza vaccination

$$\Pr(V) = \text{expit}\left(\beta_0 + \beta_1 \sum_j V_j \mathcal{G}_{ij} + \beta_2 I(R_i = 1) + \beta_3 I(R_i = 2) + \beta_4 D_i + \beta_6 \sum_j D_j \mathcal{G}_{ij} + \beta_5 A_i \right.$$

$$\left. + \beta_6 \sum_j A_j \mathcal{G}_{ij} + \beta_7 H_i + \beta_8 \sum_j H_j \mathcal{G}_{ij} + \beta_9 G_i + \beta_{10} Y_i + \beta_{11} P_i + \beta_{12} F_i \right)$$

3.6.8 Measurement Error

Network-TMLE assumes that the observed network is the true network (i.e., there is no measurement error). However, previous studies have found substantial measurement error when comparing self-reported contacts to electronic sensors.[155-159] To address measurement error of the self-reported contacts, a Bayesian approach to reconstruct the true network.[165]

To reconstruct the true network, two models are used: the *measurement model* and the *network model*. Priors need to be chosen for each of these models. The measurement model describes how the self-reported contacts in the network, $\mathcal{G}_{ij}$, depend on the true contacts, $\mathbb{G}_{ij}$. The data model can be written as

$$\Pr(\mathcal{G}_{ij} | \mathbb{G}_{ij}, \theta)$$

where θ is the prior. Another way of describing these probabilities is sensitivity (when $\mathbb{G}_{ij} = 1$) and one minus specificity (when $\mathbb{G}_{ij} = 0$). For both sensitivity and one minus specificity, beta distributions were specified. The network model describes the probabilities of contacts within the network as a function of the covariates. The network model can be written as

$$\Pr(\mathbb{G}_{ij} | W_i, W_j, \lambda)$$

where λ is the prior for the network model.

From the measurement and network models, application of Bayes rule results in

$$\Pr(\mathbb{G}_{ij}, \theta, \lambda | \mathcal{G}_{ij}) = \frac{\Pr(\mathcal{G}_{ij} | \mathbb{G}_{ij}, W, \theta) \Pr(\mathbb{G}_{ij} | W, \lambda) \Pr(\theta, \lambda)}{\Pr(\mathcal{G}_{ij})}$$

The probability for each edge within the network can then be calculated by

$$\Pr(\mathbb{G}_{ij}|\mathcal{G}_{ij}) = \int \Pr(\mathbb{G}_{ij}, \theta, \lambda|\mathcal{G}_{ij})\, \mathrm{d}\theta \mathrm{d}\lambda$$

The resulting matrix then contains the probability of an each for each pair of nodes in the network. Edges then can be drawn from Bernoulli distributions for each pair of nodes to generate an estimate of the true network. In the case of an undirected network, draws are for the upper triangle of the matrix. To allow for uncertainty in the reconstructed network, multiple networks are generated.

In application to the eX-FLU contact network, the goal is to address measurement error of self-reported contacts at week one. While at first glance the contact network being reconstructed may be viewed a scenario of multiple noisy measures of the same structure, this is not the case. While the eX-FLU network is measured over multiple weeks, there is no reason to believe that there is a constant contact network across all weeks. In fact, the contact network is expected to vary between weeks as a result of the self-isolation in the study. Therefore, the assumption of multiple measurements of a single underlying network is unreasonable. Instead, only a single measurement of the contact network is available. However, reconstructing the network from a single measurement for each edge is a difficult task.[164] To make the problem more feasible, informed priors on sensitivity and specificity are used.

To inform the selection of priors for the measurement model, data from the iEpi sub-sample of the eX-FLU study was used. For weeks four to ten of follow-up, sensitivity and specificity were calculated for self-reported edges in comparison to iEpi collected edges. Since Bluetooth signals can pass through solid objects (e.g., walls), what was deemed to be a real contact as measured by Bluetooth was restricted by RSSI. To be considered a valid contact, the RSSI for the Bluetooth RSSI had to be greater than or equal to -70. Furthermore, two individuals were considered as having had contact that week if more than ten captured signals were recorded that week to further reduce incorrectly recorded contacts via iEpi. From these iEpi restricted contacts, the number of contacts captured by both self-report and Bluetooth for each

week divided by the number of Bluetooth contacts for each week was used to estimate sensitivity. Specificity was similarly estimated by dividing the number of no-contact captured by self-report and Bluetooth by the number of no-contact captured by Bluetooth. The prior distribution for sensitivity was $\mathrm{Beta}(7243, 2757)$ and for one minus specificity was $\mathrm{Beta}(103, 9897)$.

For the network model, the stochastic block model was specified as

$$\Pr(\mathbb{G}_{ij}|\lambda) = \mathrm{expit}\Big(\lambda_0 + \lambda_1 I(B_i = B_j) + \lambda_2 I(C_i = C_j) + \lambda_3 I(G_i = G_j) + \lambda_4 I(R_i = R_j) + \lambda_5 I(V_i = V_j) + \lambda_6 I(A_i + A_j > 0)\Big)$$

For λ_0 a $\mathrm{Cauchy}(-4.5, 10)$ prior was used. For the remainder of λ terms, the priors were $\mathrm{Cauchy}(0, 2.5)$. The choice of priors for this model was based on recommendations for weakly informative priors in the context of a logistic regression model.[217] However, λ_0 was centered at -4.5 rather than 0 since networks are often sparse.

To combine the measurement error sensitivity analyses and allow for the uncertainty resulting from the MICE procedure, each of the 100 MICE imputations was used to estimate the preceding Bayesian network reconstruction approach, for a total of 10,000 data sets. A single point and variance estimate were obtained via the nested multiple imputation rule.[218, 219] For the p graphs from each of the q MICE data sets, the point estimate was calculated as

$$\hat{\psi} = \frac{1}{pq}\sum_{j}^{q}\sum_{i}^{p}\hat{\psi}_{i,j} = \frac{1}{q}\sum_{j}^{q}\hat{\psi}_j$$

The variance for the point estimate was estimated as

$$\widehat{Var}(\hat{\psi}) = \frac{1}{pq}\sum_{j}^{q}\sum_{i}^{p}\widehat{Var}(\hat{\psi}_{i,j}) + (1+q^{-1})\frac{1}{q-1}\sum_{j}^{q}(\hat{\psi}_j - \hat{\psi})^2$$

$$+ (1-p^{-1})\frac{1}{q}\sum_{j}^{q}\frac{1}{p-1}\sum_{i}^{p}(\hat{\psi}_{i,j} - \hat{\psi}_j)^2$$

which consists of the complete variance, between-MICE block variance, and within-MICE block variance, respectively.

CHAPTER 4: APPROACHES TO ACCOUNT FOR MEASUREMENT ERROR OF EDGES AND THEIR PERFORMANCE

4.1 Introduction

Measurement error, a difference between the true value and a measured value, poses a threat to the validity of network analyses on two levels: measurement error for attributes of individuals (or nodes) and measurement error of the relations between individuals (or edges).[162] As the problem of measurement error of edges is unique to network analysis, our focus is on this type of measurement error hereafter. Measurement error of edges occurs in a variety of contexts. Examples include self-reported face-to-face contacts,[155-159] design of questionnaires to collect friendships,[220] reciprocity of friendships,[221] electronic communications to measure tie strength,[222] and protein-protein interactions in cells.[223]

When measurement error occurs, parameters estimated using the observed network may no longer be valid for the true network. Previous simulation studies on measurement error have focused on the bias of centrality measures, with performance depending on the underlying structure of the network and whether edges are false positives or false negatives.[160-162] However, these results are predicated on measurement error being non-informative or random. In applications with systematic or informative measurement error, these results may no longer apply. Altogether, these prior results indicate measurement error poses a threat to the validity of routinely reported network measures.

While no measurement error of edges has often been taken for granted by researchers, there have been recent proposals to account for measurement error. Outside of study design aspects to reduce the occurrence of measurement error (e.g., questionnaire design, measuring more central nodes for greater accuracy, etc.[220]); two broad categories of approaches to

analytically account for measurement error are imputation and Bayesian approaches. MIME works by framing measurement error as a missing data problem. MIME has been demonstrated and used to correct for measurement error with an internal or external validation subsample outside of network settings,[166, 168, 224-226] and has been suggested as an approach for measurement error of edges in networks.[162] In contrast, Bayesian approaches work by leveraging prior knowledge regarding both the network formation process and the uncertainty of measurements.[164, 227, 228] While the previous approaches have been described in contrast to each other, no explicit comparisons in terms of performance have been conducted.

In this simulation study, we compare both MIME and Bayesian approaches to account for measurement error of edges in the context of a single measured network. Both non-informative and informative measurement error were assessed. Performance was compared for global, relational, and individual-level parameters.

4.2 Methods

Let $\mathbb{G}$ indicate the true network (i.e., no measurement error) with the $N \times N$ adjacency matrix, where $\mathbb{G}_{ij}$ denotes the (i,j) entry and $\mathbb{G}_{ij} = 1$ indicates an edge and $\mathbb{G}_{ij} = 0$ otherwise (Figure 4.1). By definition, there are no self-loops ($\mathbb{G}_{ii} = 0$). The goal of the analysis is the estimation of a parameter (μ) and variance for that parameter ($Var(\mu)$). Let $\mathcal{G}$ indicate a single measurement of $\mathbb{G}$. When measurement error occurs, the two adjacency matrices will no longer match for every node pair (i.e., $\mathbb{G}_{ij} \neq \mathcal{G}_{ij}\ \exists\ i,j \in N$). Therefore, estimates of μ based on $\mathcal{G}$ may be biased. Finally, let G indicate a perfectly measured network with the $n \times n$ adjacency matrix (i.e., $\mathbb{G}_{ij} = G_{ij}\ \forall\ i,j \in n$), where $n < N$. Unlike $\mathcal{G}$, the gold-standard network G is only available for a portion of the population. Scenarios like this may occur when a gold-standard measure is expensive to collect or is invasive. The motivating question is how $\mathcal{G}$ or G can be used to learn μ.

4.2.1 Imputation Approach

Assuming that an error-free measure of edges exists and that measure is only available for some portion of the study sample, measurement error can be framed as a missing data problem. The gold-standard graph G can be expanded to include all nodes in N and filling in edges involving the added nodes as missing. Therefore, measurement error becomes a problem of filling in those missing edges.

4.2.1.1 General Procedure

To account for measurement error of edges, we propose the following procedure. First, a statistical model is specified (e.g., ERGM,[229] additive and multiplicative effect models,[230] etc.) and estimated using the observed parts of G. Next, G is extended to include all N nodes. Afterwards, missing edges are imputed based on the statistical model. To allow for uncertainty in the predictions, MIME uses m imputations. Each imputed graph is indicated by $\tilde{G}_k$ for $k = 1, \ldots, m$ imputations. For each of the m imputations, the parameter of interest $\widehat{\mu_k}$ and $\widehat{Var}(\widehat{\mu_k})$ are calculated. To provide a single summary of the multiple imputations, the imputations are combined using Rubin's rule.[198] The point estimate for the parameter of interest is the mean across all m imputations

$$\bar{\mu} = m^{-1} \sum_{k=1}^{m} \widehat{\mu_k}$$

The variance for this parameter is the within-imputation variance plus the between-imputation variance

$$\overline{Var}(\bar{\mu}) = m^{-1} \sum_{k=1}^{m} \widehat{Var}(\widehat{\mu_k}) + (1 + m^{-1})(1 - m)^{-1} \sum_{k=1}^{m} (\widehat{\mu_k} - \bar{\mu})^2$$

While the preceding procedure is general in terms of the chosen statistical model, we implemented MIME with an ERGM. ERGM are a parametric model for network data where the dependent variable is the edges.[170] These models have been traditionally used to understand tie formation within networks; however, ERGM have also been used for multiple imputation of

missing data.[169, 171-173] ERGM-based imputation for measurement error has been previously suggested,[169] but no published implementation strategy exists to our knowledge.

For the implementation of MIME-ERGM, the estimated ERGM only includes information captured in G (i.e., edges from $\mathcal{G}$ do not contribute to the model). This differs from other MIME approaches, which tend to include the information from the measurements within this model.[166] Instead, information from $\mathcal{G}$ is used during the generation of $\tilde{G}_k$, with the mismeasured edges in $\mathcal{G}$ used as the basis for the imputed graphs.

4.2.2 Bayesian Approach

In contrast to MIME procedure, the Bayesian procedure proposed by Young et al. does not require a gold-standard measure, and instead works by specifying two models and corresponding prior distributions.[227] The first model is the *measurement model*, which is the prior probability distribution for the observed edges in $\mathcal{G}$ as a function of $\mathbb{G}$. With the prior λ, the measurement model can be written as $\Pr(\mathcal{G}_{ij}|\mathbb{G}_{ij}, \lambda)$. The second model is the *network model*, which corresponds to the probability distribution of edges in $\mathbb{G}$. The network model is written as $\Pr(\mathbb{G}_{ij}|\theta)$, with prior ϕ. Applying Bayes' rule, $\mathbb{G}$ can be consistently estimated with $\mathcal{G}$, the specified models, and the priors via:

$$\Pr(\mathbb{G}, \lambda, \theta|\mathcal{G}) = \frac{\Pr(\mathcal{G}|\mathbb{G}, \lambda)\Pr(\mathbb{G}|\theta)\Pr(\lambda, \theta)}{\Pr(\mathcal{G})}$$

Draws from the joint posterior distribution, $\Pr(\mathbb{G}, \lambda, \theta|\mathcal{G})$, are then used to estimate $\mathbb{G}$. Similar to MIME, multiple networks are generated. In the simulations, the multiple generated graphs were summarized using Rubin's rule as before.

As discussed in other work,[164, 228] Bayesian approaches like the one above are expected to operate best when multiple measures of the same network are available. However, multiple measurements are uncommon in practice or may not possible in some scenarios. In the context of a single measurement of a network, estimation of these models to account for measurement

error is difficult. Increased reliance on priors and specification of the network model becomes necessary.[164]

4.2.3 Simulation Study

To assess the performance of the different approaches to handling measurement error, we conducted a simulation study for three networks consisting of 200 nodes. Estimates of network measures were compared to the true values, where true values for the measures of interest were based on the mean value from 10,000 graphs generated from the true network generating model.

4.2.3.1 Network Measures

Focus was on three distinct levels of network measures: global (number of edges, density), relational (assortativity coefficient), and individual measures (degree, clustering coefficient). The number of edges was the number of unique edges that existed in the network. Density is the number of edges occurring in the network divided by the total number of possible edges. The assortativity coefficient is a measure of the tendency of individuals connected in a network to share similar traits or behaviors bounded between -1 and 1.[199] The assortativity coefficient was calculated for the variable B. The mean degree was the mean of unique contacts for each node. The mean local clustering coefficient is the mean of the number of closed triangles that occur among a node's contacts divided by the total number of possible triangles.[200] A closed triangle is when a triad of nodes all share edges.

Variances for each of the parameters were estimated using a jackknife approach.[201-204] The jackknife works through a leave-one-out approach, where a single observation is removed then the parameter of interest is re-calculated. After the leave-one-out procedure is repeated for all observations, the overall estimate is subtracted from each leave-one-out iteration and then is squared. Finally, these squared changes are summed together and multiplied by a scaling factor. Instead of the usual scaling factor of $\frac{n-1}{n}$ used in IID data, a scaling factor of $\frac{n-2}{2n}$ was

used instead.[204] The variances for edges, density, degree, and clustering coefficient were estimated by removing a single node.[204, 205] For the assortativity coefficient, a single edge was removed instead.[199]

4.2.3.2 Networks

Three different network models were assessed in the simulation study. Network-1 is a stochastic block model based on whether nodes had matching values for a binary variable B and a categorical variable X. B was assigned to 62 (31%) of nodes, and X consisted of 4 categories with 50 nodes in each. The stochastic block model used to generate edges between nodes was:

$$\text{logit}\big(\Pr\big(\mathbb{G}_{ij}=1\big)\big) = -4.25 - 0.25\, I\big(B_i = B_j\big) + 1.25\, I\big(X_i = X_j\big)$$

Network-2 was generated using a ERGM with terms for matching values of B, matching values of X, and the squared difference of a continuous variable C

$$\text{logit}\big(\Pr\big(\mathbb{G}_{ij}=1\big|n, \mathbb{G}_{ij}^{c}\big)\big) = -4.5 + 0.1 \times I\big(B_i = B_j\big) + 1.25 \times I\big(X_i = X_j\big) - 0.5\big(C_i - C_j\big)^2$$

where n is the number of individuals in the network, and $\mathbb{G}_{ij}^{c}$ denotes all dyad-pairs in the network aside from ij. Network-3 instead included terms for B and X, as well as Δ which models the number of closed triangles in the network. The ERGM used to generate network-3 was

$$\text{logit}\big(\Pr\big(\mathbb{G}_{ij}=1\big|n, \mathbb{G}_{ij}^{c}\big)\big) = -4.75 - 0.5 \times I\big(B_i = B_j\big) + 2.5 \times I\big(X_i = X_j\big) + 2.5\Delta$$

Network-3 has the addition of higher-order dependencies (triangles) unlike the previous generation models.

4.2.3.3 Measurement Error

For measurement error of the true networks, two types of errors were considered: non-informative and informative measurement error. For non-informative measurement error, observed edges had a sensitivity of 0.85 and specificity of 0.99. For informative measurement error, errors were based on the node characteristic B, with pairs of nodes both having the same

value of B (i.e., $B_i = B_j$) having a sensitivity of 0.90 and specificity of 0.995, whereas discordant pairs (i.e., $B_i \neq B_j$) had a sensitivity of 0.80 and specificity of 0.985.

4.2.3.4 Gold-Standard Selection

The gold-standard subsample available was varied between 80 (40%) and 120 (60%) nodes. Two different approaches to selecting the gold-standard nodes were compared: simple random sample (SRS) and respondent-driven sampling (RDS). The RDS procedure began with 10% of the subsample size selected as seeds. Each seed node nominated three nodes based on random selection of nodes that it shared a true edge with. The procedure was repeated for nominated nodes until the gold-standard subsample size was met.

4.2.3.5 Approaches

Within the scenarios, we compared the following approaches measurement from the true network, measurements from the observed network (Naïve), MIME-ERGM, and Bayesian models. As a baseline comparator for performance, approaches were compared with the true network, which is the best-case scenario. As the current standard for measurement error, the network parameters were estimated based on the observed edges.

MIME-ERGM was implemented by including terms for the two indicator variables in network-1. For network-2, MIME-ERGM used the correct specification of the network generating model. Finally, MIME-ERGM for network-3 included the geometrically weighted edgewise shared partners (GWESP) rather than Δ due to model convergence issues. MIME-ERGM was implemented with both SRS (MIME-ERGM-SRS) and RDS (MIME-ERGM-RDS) approaches to selecting the gold-standard subsample. In our implementation, 100 imputed graphs were generated and then summarized.

For the Bayesian procedure, Beta distribution priors for the measurement model were centered on the true sensitivity and specificity. Additionally, the priors were restricted such that the sensitivity was always less than the specificity. For non-informative measurement error,

sensitivity and specificity were generated from $\mathrm{Beta}(8500,1500)$ and $\mathrm{Beta}(100,9900)$, respectively. For informative error, sensitivity was generated from $\mathrm{Beta}(9000,1000)$ and $\mathrm{Beta}(8000,2000)$, and specificity from $\mathrm{Beta}(50,9950)$ and $\mathrm{Beta}(150,9850)$. For the network model, the following distribution was used

$$\Pr(\mathbb{G}|\boldsymbol{W};\phi) = \mathrm{logit}\left(\phi_0 + \boldsymbol{\phi_w}\boldsymbol{W_{ij}}\right)$$

where $\boldsymbol{W}$ indicates the vector of all pairwise covariates for the corresponding model. For network-3, the Bayesian procedure did not include a term to capture Δ. The priors were $\phi_0 = \mathrm{Cauchy}(-4.5, 5)$ and $\phi_w = \mathrm{Cauchy}(0, 2.5)$. Cauchy distributions were chosen for their heavier tails than the normal distribution and based on recommendations in the context of logistic regression.[217] The prior for ϕ_0 was centered at -4.5 rather than zero since networks were sparse. Similarly, 100 networks were generated and summarized within each iteration.

4.2.3.6 Performance Metrics

To compare the performance between methods, we used the following metrics: bias, ESE, and 95% CI coverage. Bias was defined as the mean of the estimated parameter minus the true parameter. ESE was estimated by the standard deviation of the simulation estimates for each parameter. CI coverage was calculated as the proportion of 95% CIs containing the true value of the parameter.

4.3 Results

4.3.1 Network-1

As expected, little bias for all parameters (Figure 4.2) and adequate CI coverage for most parameters (Table 4.1) occurred when the true network was used to estimate the parameters. However, CI coverage for the assortativity coefficient was only 83%. For all parameters, the Naïve approach was biased for both non-informative and informative measurement error (Figure 4.2). Similarly, CI coverage was below expected levels for all parameters besides the clustering coefficient.

MIME-ERGM-SRS had little bias for all the assessed parameters, with ESE decreasing as a greater portion of the population was included in the gold-standard subsample (Figure 4.2). Despite adequate performance in terms of bias, CI coverage was below expected levels (Table 4.1). Increasing the percent of the gold-standard available from 40% to 60% improved coverage, but CI coverage was still below the expected level for density. Performance for MIME-ERGM-SRS was similar with informative measurement error. Results for gold-standard subsample measures and MIME-ERGM-RDS are available in Appendix 1.

For non-informative measurement error, the Bayesian procedure had bias, ESE, and CI coverage slightly better than MIME-ERGM-SRS with 60% of the gold-standard available. Performance was similar for informative measurement error.

4.3.2 Network-2

Similar to network-1, the Naïve approach was biased for all measures (Figure 4.3) and had poor CI coverage for both types of measurement error (Table 4.2). MIME-ERGM-SRS had minimal bias for all parameters but below expected levels of CI coverage. Increasing the subsample size to 60% improved performance but CI coverage was still below expected levels for density. For the Bayesian procedure, there was little bias and CI coverage was greatly improved over the naïve estimator but still below the true network.

4.3.3 Network-3

The Naïve approach had some bias for all parameters (Figure 4.4). For both non-informative and informative measurement error, the clustering coefficient was substantially under-estimated. CI coverage was improved for density, assortativity, and degree in contrast to previous scenarios (Table 4.3).

For MIME-ERGM-SRS, the estimated number of edges, density, and degree were over-estimated, with poor CI coverage. The estimated clustering coefficient was closer to the truth compared to other methods but still underestimated the true value. These results were consistent for both types of measurement error explored.

For the Bayesian approach, bias was minimal for all parameters besides the clustering coefficient (Figure 4.3). The clustering coefficient was further under-estimated relative to the Naïve approach. CI coverage was below levels observed in the previous networks, but was above MIME-ERGM-SRS (Table 4.3). Performance was similar for informative measurement error.

4.4 Discussion

The best solution for measurement error is to prevent its occurrence. However, direct observation of the true network is not always possible due to costs, logistics, privacy concerns, or other reasons. After the data has been collected, an analyst has two choices regarding measurement error: do nothing or do something. While the former has been common in network analysis, ignoring the existence of measurement error can lead to biased estimates, as demonstrated in our simulations. In lieu of perfect measurement of the entire network, two approaches to account for measurement error in the context of a single faulty measurement of a network were compared. These approaches out-performed the Naïve approach in most contexts. Therefore, these approaches or further adaptations of them may be considered as ways to address measurement error analytically.

Similar to preceding studies, our simulations demonstrate that bias can result from measurement error of edges within a network. Borgatti et al. explored the robustness of centrality measures (degree, betweenness, closeness, and eigenvector centrality); with all centrality measures having similar performance and monotonic decline in performance with increasing measurement error.[160] Furthermore, the authors found dense networks were more robust to lower specificity, and sparse networks robust to lower sensitivity. However, their results are predicated on non-informative measurement error, the Erdős-Rényi graph model, and only a single type of error (edge addition or edge deletion) occurring. Wang et al. considered two real-world networks instead and found inconsistent performance of centrality measures related to the degree distributions.[162] These results are similar to the simulation

experiments of Frantz et al., which also found the performance of centrality measures linked to the structure of the true network.[161] Our simulations further these results with both imperfect sensitivity-specificity and informative measurement error. We found bias was dependent on the chosen parameter; the true, underlying structure of the network; and whether measurement error was informative.

To motivate the use of procedures like MIME, measurement error of edges was framed as a missing data problem. While measurement error can be framed as a missing data problem, there are important distinctions to note. First is the distinction in the context of each. For example, not reporting a friendship due to limits on the number of nominations possible constitutes measurement error. Whereas an individual not reporting any friends because they decline to complete the survey is missing data. Second, how bias occurs from measurement error is distinct. For missing edges, those values are unknown and a complete-case analysis is possible. For measurement error of edges, a measure is available for all edges. Unless a gold-standard measure is proposed (which may not be available for anyone), measurement error does not immediately appear as missing data. Therefore, when contrasting with previous simulation studies on missing edge data.[231-236] those results are comparable to the results from the gold-standard subsample (as opposed to the Naïve approach).

The proposed MIME-ERGM procedure was able to address the bias of measures but had limited performance in terms of CI coverage in our simulations. There are several limitations to the MIME-ERGM procedure with implications for practice. First, MIME-ERGM had difficulty concerning CI coverage when only 40% of the network had the gold-standard measure available. This difficulty arises due to the available data to estimate the ERGM. Specifically, 40% of the nodes being part of the gold-standard measure consists of less than 16% of the possible edges for a network of 200 nodes. This issue is further exacerbated in sparse networks since relatively few edges are available. Therefore, MIME needs to consider the *proportion of edges* available rather than the *proportion of nodes*. Next, MIME-ERGM did not perform well

when the subsample was selected via RDS. Additionally, the RDS procedure used relied on the underlying network to complete the referral process, which may not be possible to implement in practice. The requirement of a SRS for a substantial portion of the network may be difficult to achieve in practice. Lastly, MIME-ERGM performed poorly when the network had higher-order dependencies. Other statistical models may perform better in this context. Future work may consider comparing the performance of MIME with other statistical models that do not require explicit specification of higher-order terms (e.g., additive and multiplicative effect models[230]).

The Bayesian procedure performed adequately even in the context of a single measured network. In contrast to MIME, the Bayesian procedure has the advantage of not requiring a subsample of the network to be measured perfectly. Therefore, the use or even existence of a gold-standard measure is not required. This advantage comes at the cost of the Bayesian procedure being reliant on the specification of the priors for both measurement and network models. In the context of a single measured network, we found the Bayesian procedure proposed by Young et al.[165] to be reliant on the measurement model priors and the specification of the network model. Without accurate and strong informative priors on the measurement model, biased results can occur. Due to the heavy reliance on priors, we recommend a combination of values for the sensitivity and specificity priors are contrasted.

4.4.1 Conclusions

Measurement error of edges is a difficult problem when only a single measurement of the network is available. Despite the difficulty, the pursuit of corrective approaches for measurement error is worthwhile. The MIME and Bayesian approaches compared here are two promising avenues to address measurement error analytically that rely on different sets of assumptions.

4.5 Tables and Figures

Table 4.1: Confidence interval coverage of parameters for network-1

	Edges	Density	Assortativity	Degree	Cluster
True	100%	94%	83%	99%	95%
Random Error					
Naïve*	6%	0%	67%	0%	99%
MIME-s40%†	92%	71%	73%	80%	100%
MIME-s60%†	100%	90%	88%	96%	100%
Bayes	100%	90%	87%	95%	100%
Conditional Error					
Naïve*	19%	0%	23%	0%	99%
MIME-s40%†	93%	73%	74%	83%	100%
MIME-s60%†	99%	91%	90%	96%	100%
Bayes	99%	89%	87%	96%	100%

MIME: multiple imputation for measurement error. CI coverage was calculated as the percent of 95% CI that contained the true value. Random error consisted of measurement error occurring completely at random. Conditional error consisted of measurement error occurring conditional on the node attributes of pairs

* Naïve consisted of the parameters estimated using the observed (mismeasured) network
† The gold-standard for the MIME procedure consisted of a simple random subsample for the designated percentage of nodes in the network.

Table 4.2: Confidence interval coverage of parameters for network-2

	Edges	Density	Assortativity	Degree	Cluster
True	100%	96%	83%	100%	93%
Random Error					
Naïve*	1%	0%	79%	0%	99%
MIME-s40%†	92%	71%	74%	80%	100%
MIME-s60%†	99%	92%	91%	96%	100%
Bayes	97%	87%	88%	93%	100%
Conditional Error					
Naïve*	3%	0%	1%	0%	99%
MIME-s40%†	93%	75%	73%	82%	100%
MIME-s60%†	99%	91%	91%	96%	100%
Bayes	99%	89%	84%	95%	100%

MIME: multiple imputation for measurement error. CI coverage was calculated as the percent of 95% CI that contained the true value. Random error consisted of measurement error occurring completely at random. Conditional error consisted of measurement error occurring conditional on the node attributes of pairs

* Naïve consisted of the parameters estimated using the observed (mismeasured) network
† The gold-standard for the MIME procedure consisted of a simple random subsample for the designated percentage of nodes in the network.

Table 4.3: Confidence interval coverage of parameters for network-3

	Edges	Density	Assortativity	Degree	Cluster
True	100%	95%	86%	100%	99%
Random Error					
Naïve*	100%	70%	78%	92%	0%
MIME-s40%†	35%	15%	64%	22%	24%
MIME-s60%†	31%	10%	84%	15%	60%
Bayes	99%	67%	90%	87%	0%
Conditional Error					
Naïve*	100%	76%	77%	95%	0%
MIME-s40%†	33%	14%	65%	18%	25%
MIME-s60%†	29%	8%	82%	13%	60%
Bayes	98%	67%	89%	88%	0%

MIME: multiple imputation for measurement error. CI coverage was calculated as the percent of 95% CI that contained the true value. Random error consisted of measurement error occurring completely at random. Conditional error consisted of measurement error occurring conditional on the node attributes of pairs

* Naïve consisted of the parameters estimated using the observed (mismeasured) network
† The gold-standard for the MIME procedure consisted of a simple random subsample for the designated percentage of nodes in the network.

Figure 4.1: Examples of true, observed, and gold-standard networks

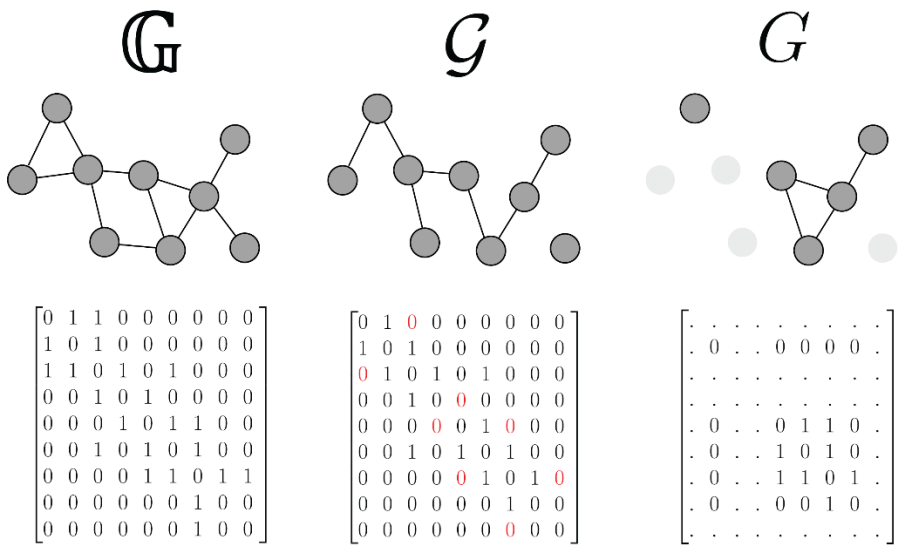

$\mathbb{G}$ is the true network, $\mathcal{G}$ is the mismeasured network, and G is the gold-standard subsample. Edges that are mismeasured are indicated in red for $\mathcal{G}$.

Figure 4.2: Bias of network parameters for network-1

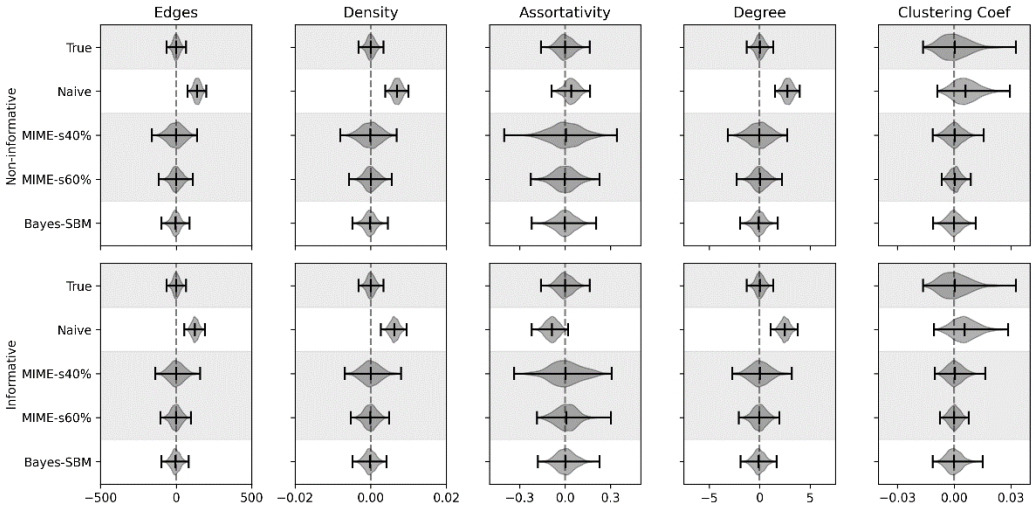

True: parameters were estimated using the true network. Naïve: parameters were estimated using the full mismeasured network. MIME: parameters were estimated using multiple imputation for measurement error with an ERGM. The gold-standard subsample was selected as a simple random sample. The percentage indicates the proportion of nodes included in the subsample. Bayes: stochastic block model Bayesian estimation. Coef: coefficient

Figure 4.3: Bias of network parameters for network-2

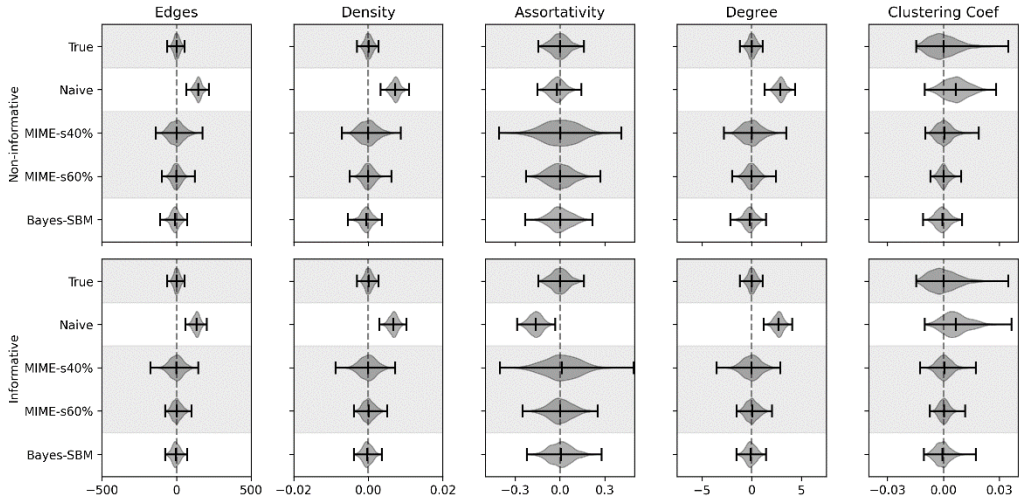

True: parameters were estimated using the true network. Naïve: parameters were estimated using the full mismeasured network. MIME: parameters were estimated using multiple imputation for measurement error with an ERGM. The gold-standard subsample was selected as a simple random sample. The percentage indicates the proportion of nodes included in the subsample. Bayes: stochastic block model Bayesian estimation. Coef: coefficient

Figure 4.4: Bias for network parameters for network-3

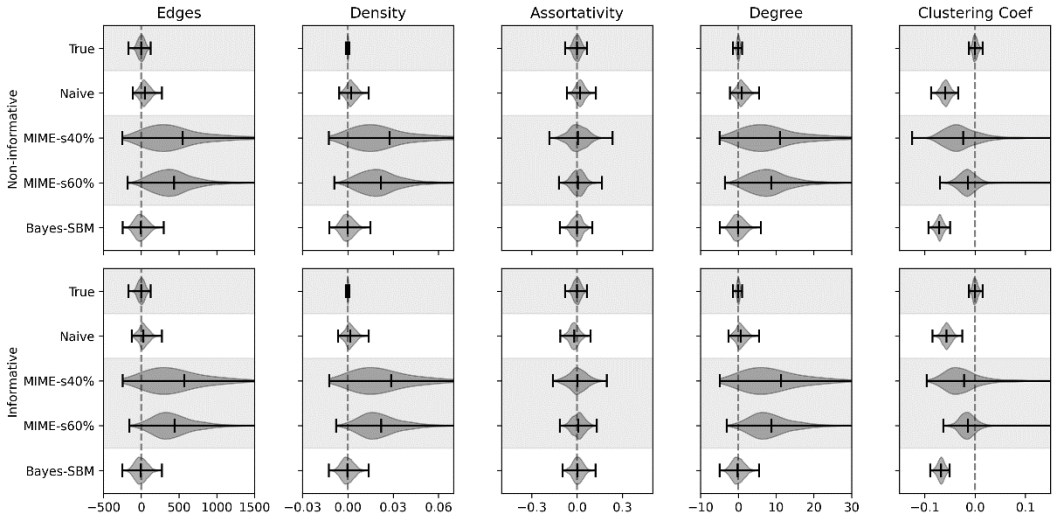

True: parameters were estimated using the true network. Naïve: parameters were estimated using the full mismeasured network. MIME: parameters were estimated using multiple imputation for measurement error with an ERGM. The gold-standard subsample was selected as a simple random sample. The percentage indicates the proportion of nodes included in the subsample. Bayes: stochastic block model Bayesian estimation. Coef: coefficient

CHAPTER 5: TARGETED MAXIMUM LIKELIHOOD ESTIMATION OF CAUSAL EFFECTS WITH INTERFERENCE

5.1 Introduction

Causal effect estimation often relies on the assumption of no interference, such that an individual's potential outcomes are independent of all other individuals' exposure.[133-135] However, interference exists across many areas of medicine and public health, most notably in infectious disease and medical social sciences. Examples include interference between people who inject drugs at risk of HIV,[237, 238] students within the same school,[239] and between individuals connected within social networks.[240] The ongoing global SARS-CoV-2 pandemic has brought further attention to interference; evaluation of physical distancing and shelter-in-place policies have highlighted how such policies or lack thereof can impact other nearby geographic regions.[241, 242] In addition to infectious disease, interference occurs across substantive areas, with examples including household opioid use in pharmacoepidemiology,[243] passive tobacco smoke exposure in cancer epidemiology,[244, 245] and behaviors among children within classrooms in developmental psychology.[246]

When interference is present, multiple estimands may be considered.[133, 137] One estimand of public health importance is the mean of an outcome under a specific policy. For example, what would the three-month risk of influenza have been if 60% of the population had received the influenza vaccine? To estimate this quantity or other related estimands, methods allowing for interference have been developed for two broad settings: partial interference and general interference. The partial interference assumption stipulates interference occurs *within but not between* groups,[133, 247] which allows for the application of standard statistical theory.[139-141, 145] While the partial interference assumption is sometimes reasonable, interference patterns

do not always allow the separation of individuals into independent groups. General interference allows, in principle, for any two units in a population to affect each other. Methods for general interference may further be delineated by whether or not the exposure is randomized. In randomized experiments, methods can leverage the random assignment as the basis of inference.[147, 148] In the observational setting, extensions of IID-TMLE have recently been developed to allow for general interference.[150-152]

In this chapter, we present empirical studies of network-TMLE. While simulations have been conducted to evaluate the finite sample performance of network-TMLE,[150, 151] previous empirical studies have been limited to relatively simple random networks. In practice, networks often exhibit more complex properties,[231, 248, 249] limiting the utility of previous simulation studies to guide application. Additionally, previous simulations have explored only a narrow set of data generating mechanisms and made no direct comparisons between network-TMLE and IID-TMLE. To address these gaps, we conducted simulations for the estimation of the sample mean under varied data generating mechanisms with a wider variety of networks, including an observed network of face-to-face contacts among university students. Two variations on policies were assessed: setting all individuals to some constant probability of exposure, and shifting the propensity score distribution. For each scenario, both network-TMLE and IID-TMLE were evaluated.

5.2 Targeted Maximum Likelihood Estimation

TMLE is a doubly-robust substitution estimator that incorporates an outcome model and a propensity score (or exposure) model through a targeting step.[250, 251] These models are often referred to as nuisance models since they are not of direct interest. The double-robustness property means that as long as one nuisance model is correctly specified, then the estimator will be statistically consistent. TMLE has the advantage of retaining root-n convergence rates even when data-adaptive machine learning estimators are used for fitting the nuisance models.[250, 252, 253] In the absence of interference, TMLE methods have been developed for average causal

effects,[250] causal effects under different longitudinal treatment plans,[254] and stochastic policies.[255] The following is a brief review of IID-TMLE for stochastic policies.

5.2.1 Estimands and Assumptions

Consider drawing inference about the effect of a binary exposure V on an outcome Y in an observational study. For individual $i = 1, \dots, n,$ let W_i indicate observed baseline covariate(s), V_i the observed exposure, and Y_i the observed outcome. Assume (W_i, V_i, Y_i) for $i = 1, \dots, n$ are independent and identically distributed and there is no interference. Let $Y_i(v)$ indicate the potential outcome for individual i had, possibly counter to fact, their exposure been $v \in \mathcal{V} = \{0,1\}$. The goal is to draw inference about the mean outcome under a policy, denoted in general by ω, which alters or shifts the distribution of V. For example, the target estimand might be a deterministic policy where everyone is exposed. Denote the conditional distribution of V given W under policy ω by $\Pr^*(V = v|W)$. For the aforementioned deterministic policy, $\Pr^*(V = 1|W) = 1$. Stochastic policies may also be of interest where $0 < \Pr^*(V = 1|W) < 1$. The target estimand is the average outcome under policy ω, which may be defined by the population mean $\psi^p = E[\sum_{v\in\mathcal{V}} Y(v) \Pr^*(V = v|W)]$, the sample mean $\psi^s = \frac{1}{n}\sum_{i=1}^{n}(\sum_{v\in\mathcal{V}} Y_i(v) \Pr^*(V_i = v|W_i))$, or the conditional sample mean $\psi^c = \frac{1}{n}\sum_{i=1}^{n} E[\sum_{v\in\mathcal{V}} Y_i(v) \Pr^*(V_i = v|W_i)\,|W_i]$. In general, the target estimand is denoted by ψ. To draw inference about ψ, assume:

1. If $V_i = v$ then $Y_i = Y_i(v)$
2. $Y(v) \perp V|W$ for all $v \in \mathcal{V}$
3. If $\Pr^*(V = v|W) > 0$ then $\Pr(V = v|W) > 0$, for all $v \in \mathcal{V}$

where assumption 1 is causal consistency,[256] 2 is conditional exchangeability,[257] and 3 is the positivity assumption for stochastic policies.[150, 255]

5.2.2 Estimation

IID-TMLE can be divided into five steps: outcome model estimation, weight estimation, targeting, estimation of ψ, and inference. The steps for point estimation of the mean are the

same for ψ^p, ψ^s, and ψ^c; with differences occurring in variance estimation.[258] Therefore, we only distinguish between the estimands during estimation of the variance. In the case of a continuous Y, the observed values of Y are first rescaled to lie in $(0,1)$, which is necessary for the targeting step.

IID-TMLE begins with the estimation of an outcome model for $E[Y_i|V_i, W_i]$, using either a parametric model or machine learning. Predicted values from the outcome model ($\hat{Y}_i$) are then generated using the estimated model. Next an exposure model for $\Pr(V_i|W_i)$ is estimated with either a parametric model or machine learning. For each individual, the following weight is computed

$$\frac{\Pr^*(V_i|W_i)}{\widehat{\Pr}(V_i|W_i)}$$

where the denominator is computed based on the estimated exposure model and the numerator (the policy of interest) is assumed to be known. Next the logistic regression model

$$\text{logit}(Y_i) = \eta_0 + \text{logit}\left(\hat{Y}_i\right)$$

is fit using weighted maximum likelihood. The estimated intercept $\widehat{\eta_0}$ can be thought of as a correction term for the outcome predictions. When $\hat{Y}_i$ is close to the observed outcomes, then $\widehat{\eta_0}$ will be near zero. When the outcome model is incorrectly specified and the exposure model is correct, $\widehat{\eta_0}$ shifts the values of $\text{logit}\left(\hat{Y}_i\right)$.

To estimate ψ for a deterministic policy, the following procedure is used. The exposure under ω, denoted by V_i^*, and the estimated outcome model are used to impute the outcomes under ω, denoted by $\hat{Y}_i^*$. Next, the targeted predictions are computed via

$$\tilde{Y}_i^* = \text{expit}\left(\widehat{\eta_0} + \text{logit}\left(\hat{Y}_i^*\right)\right)$$

and ψ is estimated as the mean of the targeted predictions,

$$\hat{\psi} = \frac{1}{n}\sum_{i=1}^{n} \tilde{Y}_i^*$$

For stochastic policies, the estimation procedure above requires modification. Because the distribution of V^* is no longer degenerate under a stochastic policy, the following Monte Carlo approach is used. For $k = 1, \ldots, m$ sample V_{ik}^* from $\text{Bernoulli}(\Pr^*(V_i = 1|W_i))$. For each V_{ik}^*, compute the imputed outcome and targeted prediction for individual i, say $\hat{Y}_{ik}^*$ and $\tilde{Y}_{ik}^*$, as in the deterministic policy estimation procedure above. Then $\tilde{Y}_i^*$ is calculated by $\tilde{Y}_i^* = \sum_{k=1}^{m} \tilde{Y}_{ik}^*/m$ and the estimator for ψ is the mean of the targeted predictions as before.

Lastly, $(1-\alpha)$ CI can be constructed by $\hat{\psi} \pm z_{1-\alpha/2}\sqrt{\hat{\sigma}^2/n}$, where $z_{1-\alpha/2}$ denotes the $1-\alpha/2$ quantile of a standard normal distribution and $\hat{\sigma}^2$ is an estimand-specific variance estimator. For the population mean ψ^p the variance is estimated by[255]

$$\hat{\sigma}_p{}^2 = \frac{1}{n}\sum_{i=1}^{n}\left(\frac{\Pr^*(V_i|W_i)}{\widehat{\Pr}(V_i|W_i)}\left(Y_i - \hat{Y}_i\right) + \tilde{Y}_i^* - \hat{\psi}\right)^2$$

and for the conditional sample mean ψ^c the variance is estimated by[258]

$$\hat{\sigma}_c{}^2 = \frac{1}{n}\sum_{i=1}^{n}\left(\frac{\Pr^*(V_i|W_i)}{\widehat{\Pr}(V_i|W_i)}\left(Y_i - \hat{Y}_i\right)\right)^2$$

Since the sample mean variance is non-identifiable and the asymptotic variance of the conditional mean is always greater than or equal to the sample mean asymptotic variance, the sample mean variance may be conservatively estimated by the conditional sample mean variance estimator.[258]

5.3 Targeted Maximum Likelihood Estimation with Dependent Data

In the presence of interference, the potential outcomes depend on both an individual's exposure and the exposure of others. Consider the setting where individuals are connected via a network of edges (e.g., an edge may indicate two individuals are friends within a social network, live within a certain distance of each other, or had a face-to-face conversation). Suppose the network structure is static (i.e., fixed over time) and can be summarized by an $n \times n$ adjacency matrix $\mathcal{G}$. Let $\mathcal{G}_{ij}$ denote the (i,j) entry of $\mathcal{G}$, where $\mathcal{G}_{ij} = 1$ if an edge exists

between i and j. Assume no interference between individuals i and j if $\mathcal{G}_{ij} = 0$. Since interference is a relation between individuals, $\mathcal{G}_{ii} = 0 \; \forall \; i \in n$. Throughout, individual i's "immediate contacts" refers to individuals that have an edge with i.

From $\mathcal{G}$ and the covariates, various summary measures can be calculated. The total number of immediate contacts for individual i (also referred to as degree) is defined as $F_i = \sum_{j=1}^{n} \mathcal{G}_{ij}$. The exposure status for i's immediate contacts can be expressed by different summary measures, which are functions of $(V_1, V_2, \dots, V_n)$ and $\mathcal{G}$, and in general will be denoted by V_i^s with possible realization $v_i^s \in \mathcal{V}^s$. For example, $V_i^s = \sum_{j=1}^{n} V_j \, \mathcal{G}_{ij}$ is the number of individual i's immediate contacts with $V = 1$. Similarly, let W_i^s denote a general summary measure of baseline covariates W for i's immediate contacts.

5.3.1 Estimands and Assumptions

In the presence of interference, the potential outcomes for individual i can be denoted by $Y_i(v_i, v_{-i})$, where v_{-i} indicates the exposure for all individuals excluding i. Assume an exposure mapping[147] such that only the summary measure of an individual's immediate contacts is necessary to define all of an individual's potential outcomes (referred to as weak dependence hereafter), in which case the potential outcomes may be denoted by $Y_i(v_i, v_i^s)$, with $v \in \mathcal{V} = \{0,1\}$ and $v^s \in \mathcal{V}^s$. The target estimand is the average outcome under policy ω for the sample, which may be defined as the sample mean $\psi^s = \frac{1}{n}\sum_{i=1}^{n} E\left[\sum_{v \in \mathcal{V}, v^s \in \mathcal{V}^s} Y_i(v, v^s) \Pr^*(V_i = v, V_i^s = v^s | W_i, W_i^s)\right]$ or the conditional sample mean $\psi^c = \frac{1}{n}\sum_{i=1}^{n} E\left[\sum_{v \in \mathcal{V}, v^s \in \mathcal{V}^s} Y_i(v, v^s) \Pr^*(V_i = v, V_i^s = v^s | W_i, W_i^s) \, | \boldsymbol{W}\right]$ where $\boldsymbol{W} = (W_1, W_2, \dots, W_n)$.[150] In general, the target estimand is denoted by ψ as before. To draw inference about ψ, we assume

1. If $V_i = v, \; V_i^s = v^s$ then $Y_i = Y_i(v, v^s)$
2. $Y(v, v^s) \perp V, V^s | W, W^s$
3. If $\Pr^*(V = v, V^s = v^s | W, W^s) > 0$ then $\Pr(V = v, v^s = v^s | W, W^s) > 0$, for all $v \in \mathcal{V}$, $v^s \in \mathcal{V}^s$

where assumption 1 is causal consistency, 2 is conditional exchangeability, and 3 is the positivity assumption for stochastic policies.

5.3.2 Network-TMLE

Network-TMLE extends the TMLE framework to dependent data by allowing V_i to depend on W_i and W_i^S; and Y_i to depend on V_i, V_i^S, W_i, and W_i^S. Similar to IID-TMLE, network-TMLE is doubly robust and is divided into five steps: estimate the outcome model, estimate the weights, targeting, estimation of ψ, and inference. As before, point estimation for ψ^S and ψ^C remains the same for both, with differences occurring for estimation of the variance.

Step 1) Estimate the outcome model. A model for $E[Y_i|A_i, A_i^S, W_i, W_i^S]$ can be estimated handling each observation as if it were IID (see Section 4 of van der Laan[152]). For example, ordinary least squares could be used to estimate the parameters of the model

$$E[Y_i|V_i, V_i^S, W_i, W_i^S; \beta] = \beta_0 + \beta_1 V_i + \beta_2 V_i^S + \beta_3 W_i + \beta_4 W_i^S + \beta_5 F_i$$

After estimating the model parameters, predicted outcomes under the observed V_i and V_i^S for each unit are calculated, indicated by $\hat{Y}_i$.

Step 2) Estimate the weights. The weights can be expressed as

$$\frac{\pi^*(W_i, W_i^S;\ \gamma^*, \delta^*)}{\pi(W_i, W_i^S; \gamma, \delta)} = \frac{\Pr^*(V_i|W_i, W_i^S; \gamma^*)\ \Pr^*(V_i^S|V_i, W_i, W_i^S, \delta^*)}{\Pr(V_i|W_i, W_i^S; \gamma)\ \Pr(V_i^S|V_i, W_i, W_i^S; \delta)}$$

where γ, δ, γ^*, and δ^* denote the parameters for the model for $\Pr(V_i|W_i, W_i^S)$, $\Pr(V_i^S|V_i, W_i, W_i^S)$, $\Pr^*(V_i|W_i, W_i^S)$, and $\Pr^*(V_i^S|V_i, W_i, W_i^S)$, respectively. The model for $\Pr(V_i|W_i, W_i^S)$ can be estimated with a logistic regression model treating observations as IID. Different models may be assumed for estimating $\Pr(V_i^S|V_i, W_i, W_i^S)$. For example, if V_i^S is a binary variable indicating whether at least one of individual i's immediate contacts is exposed, then logistic regression might be used. If V_i^S is instead a count variable (e.g., indicating the number of immediate contacts exposed), then Poisson or negative binomial regression models might be assumed. Alternatively, restrictions on the functional form of V_i^S may be avoided by letting V_i^S equal the vector of exposures for individual i's immediate contacts. If the maximum number of contacts is

b, then $\Pr(V_i^s|V_i, W_i, W_i^s)$ can be factored into b different binary conditional probabilities (i.e. $\Pr\left(V_i^{s(1)}\middle|V_i, W_i, W_i^s\right) \times \Pr\left(V_i^{s(2)}\middle|V_i, V_i^{s(1)}, W_i, W_i^s\right) \times \cdots \times \Pr\left(V_i^{s(b)}\middle|V_i, V_i^{s(1)}, \ldots, V_i^{s(b-1)}, W_i, W_i^s\right)$), where $V_i^{s(b)}$ indicates the exposure of contact b[151]. These conditional probabilities can then be estimated via logistic regression.

Estimation of the numerator of the weights relies on a simulation approach since policies are often specified as $\Pr^*(V = v|W, W^s)$ as opposed to $\Pr^*(V = v, V^s = v^s|W, W^s)$, and depend on the distribution of $\boldsymbol{W}$ in the network. To estimate $\pi^*(W_i, W_i^s; \gamma^*, \delta^*)$ via simulation, a large number of copies of the data set indexed by k are generated as follows. First, V_{ik}^* is sampled from $\text{Bernoulli}(\Pr^*(V_i = 1|W_i, W_i^s))$ for each k and the summary measure V_{ik}^{*s} is calculated. Then γ^* and δ^* are estimated by using the approach as before, but using all copies of the data simultaneously. Then $\pi^*(W_i, W_i^s; \gamma^*, \delta^*)$ is estimated with $\widehat{\gamma^*}$, $\widehat{\delta^*}$, and the observed values of V_i and V_i^s.

Step 3) Targeting. To target, the following logistic regression model is fit using weighted maximum likelihood,

$$\text{logit}(Y_i) = \eta_0 + \text{logit}\left(\hat{Y}_i\right)$$

Step 4) Estimation of ψ. As before, stochastic policies are evaluated using a Monte Carlo approach. For $k = 1, \ldots, m$ sample V_{ik}^* from $\text{Bernoulli}(\Pr^*(V_i = 1|W_i, W_i^s))$, and calculate the summary measures for V_{ik}^{*s}. For each V_{ik}^* and V_{ik}^{*s}, compute the imputed outcome, $\hat{Y}_{ik}^*$, using the previously estimated outcome model. The targeted prediction, $\tilde{Y}_{ik}^*$, is then computed by

$$\tilde{Y}_{ik}^* = \text{expit}\left(\widehat{\eta_0} + \text{logit}\left(\hat{Y}_{ik}^*\right)\right)$$

The mean of the targeted predictions, $\hat{\psi}_k = \sum_{i=1}^n \tilde{Y}_{ik}^*/n$ is calculated for each k. The estimator for ψ is the mean of the m estimates, i.e., $\hat{\psi} = \sum_{k=1}^m \hat{\psi}_k/m$. To reduce computational burden, V_{ik}^* and V_{ik}^{s*} generated during the estimation of the weights' numerator are reused.

Step 5) Inference for ψ. For the sample mean, the estimates of the variance rely on strong assumptions which may be unrealistic in many settings[150] or approximate an upper bound which may be uninformative in practice.[151] Therefore, the conditional sample mean may be the preferred target of inference. For the conditional sample mean, the variance is estimated by[151]

$$\hat{\sigma}_s{}^2 = \frac{1}{n}\sum_{i=1}^{n}\left(\frac{\pi^*\left(W_i, W_i^S; \widehat{\gamma^*}, \widehat{\delta^*}\right)}{\pi\left(W_i, W_i^S; \hat{\gamma}, \hat{\delta}\right)}\left(Y_i - \hat{Y}_i\right)\right)^2$$

with $(1-\alpha)$ CI constructed by $\hat{\psi} \pm z_{1-\alpha/2}\sqrt{\hat{\sigma}_c{}^2/n}$.

5.4 Simulation Study Design

For estimation of ψ^c, network-TMLE and IID-TMLE were compared across networks and data generating mechanisms for a total of 12 scenarios. All simulations were repeated 4000 times. We considered two different policy types. For the first policy, all individuals in the network were assigned the same probability of exposure, $\Pr^*(V_i = 1|W_i, W_i^S) = \Pr^*(V_i = 1) = p$. For the second policy, each individual's log-odds of exposure was shifted by a constant value, $\Pr^*(V_i = 1|W_i, W_i^S) = \text{expit}(\text{logit}(\Pr(V_i = 1|W_i, W_i^S)) + q)$. Shifts in the log-odds of exposure were used to ensure all probabilities under the policy remained between $(0, 1)$. The true values of the conditional sample mean for each policy were obtained empirically. Exposure was randomly distributed within the network according to the policy, with the network and $\boldsymbol{W}$ held fixed. The outcomes were evaluated from the true outcome model and the mean of ψ^c across 10,000 different data sets for each policy was used as the true value.

5.4.1 Networks

Three different networks were used: a uniform random graph, a modified clustered power-law random graph, and the eX-FLU network[154] of self-reported contacts among undergraduate students (Figure 5.1). The uniform random graph followed a uniform degree distribution with a minimum degree of 1 and a maximum of 6. The modified clustered power-law

random graph consisted of eight separately generated clustered power-law random subgraphs, with edges randomly generated between the random subgraphs. Each of the eight clustered power-law subgraphs was separately generated from a Barabasi-Albert random graph model with a set probability for closing triads between nodes.[206] For each node, three connections were generated and the probability of triad closure was set to 0.75. The advantage of this approach is that the random graph takes on common characteristics of empirical networks, including a power-law degree distribution, a high clustering coefficient, and an underlying community structure. Lastly, the eX-FLU network was based on data from the eX-FLU cluster-randomized trial, a study to assess the efficacy of three-day self-isolation among university students.[154] Over the ten-week study period, enrolled students reported face-to-face contacts each week. From the ten weeks of self-reported contacts, we generated a single static network and selected the largest connected component.

For the uniform random graph, two versions of network-TMLE were evaluated. The two versions entailed different approaches to estimating $\Pr(V_i^s|V_i, W_i, W_i^s)$. In one version of network-TMLE, the distribution of V_i^s was factored into $b = 6$ different binary conditional distributions and estimated by a series of six logistic models. For the other version of TMLE, a single model was used with the regression model based on the summary measure of V_i^s in the outcome model. Due to the skewed degree distributions of the clustered power-law random graph and eX-FLU network, only the single model for $\Pr(V_i^s|V_i, W_i, W_i^s)$ was used. Instead, restrictions based on the maximum degree were compared. Nodes with degrees above the maximum had their value for V held as fixed and considered as background features (i.e., no inference is made for these nodes). For the clustered power-law random graph, nodes with a degree above 18 were considered as features of the background (1%). Similarly, nodes with a degree greater than 23 were considered as background features for the eX-FLU network (5%).

5.4.2 Data Generating Mechanisms

Four data generating mechanisms inspired by real-world scenarios were considered. Each data generating mechanism was selected to feature different possible exposure effects, including individual-specific (i.e., unit-treatment) effects and spillover effects from contacts. Below is a brief narrative description of each.

5.4.2.1 Statin and Cardiovascular Disease

To simulate a no interference setting, a data generating mechanism based on a hypothetical study on statin initiation and subsequent ASCVD was created. Statins are a cholesterol-lowering drug that have been shown to reduce cardiovascular disease risk[259] by reducing cholesterol synthesis.[260] The mechanism of action may reasonably allow researchers to believe that whether i's friends take a statin has no influence on i's risk of ASCVD. Therefore, ASCVD risk was independent of immediate contacts in our simulation. Confounders were based on the 2018 primary prevention guidelines for the management of blood cholesterol[261] and included age, low-density lipoprotein levels, and ASCVD risk score.

Let $W_{1,i}$ indicate age, $W_{2,i}$ indicate log-transformed low-density lipoprotein, and $W_{5,i}$ indicate risk score. The conditional probability of taking a statin was specified by:

$$\text{logit}(\Pr(V_i = 1|L_i, X_i, R_i)) = -5.3 + 0.15\big(W_{1,i} - 30\big) + 0.2\, W_{2,i} + 0.4\, I\big(0.05 \leq W_{5,i} < 0.075\big) + 0.9\, I\big(0.075 \leq W_{5,i} < 0.2\big) + 1.5\, I\big(W_{5,i} \geq 0.2\big)$$

The conditional probability of ASCVD was specified by:

$$\text{logit}\big(\Pr\big(Y_i = 1|V_i, W_{1,i}, W_{2,i}, W_{5,i}\big)\big) = -5.05 - 0.8V_i + 0.37\sqrt{W_{1,i} - 39.9} + 0.75W_{2,i} + 0.75W_{5,i}$$

5.4.2.2 Naloxone and Opioid Overdose

For spillover effect only, a data generating mechanism based on the effect of naloxone on subsequent opioid overdose deaths was created. Opioid overdose deaths have dramatically increased in recent years.[262, 263] Naloxone has been used as an emergency intervention to rapidly reverse opioid overdoses by blocking opioids receptors[264] and has been made

increasingly available to the general population to prevent overdose deaths.[265, 266] Nasal spray formulations rely on another person for administration, with self-administration having occurred only in rare cases.[207] Therefore, the prevention of opioid overdose deaths with naloxone is an example where the protective effect may operate solely via spillover effects. Confounders included gender, recent overdose, and recent release from prison, which have been observed as predictors of opioid overdose in previous studies.[267, 268] In the context of this mechanism, the interference pattern could be thought of as a co-injection network.

Let $W_{6,i}$ indicate gender, $W_{7,i}$ indicate recent release from prison, and $W_{8,i}$ indicate recent overdose. The conditional probability of naloxone was generated according to:

$$\text{logit}\big(\Pr\big(V_i = 1 | W_{6,i}, W_{7,i}, W_{6,i}^s, W_{8,i}^s\big)\big) = -1.3 - 1.5\, W_{7,i} + 1.5\, W_{6,i} W_{7,i} + 0.95\, \frac{\sum_{j=1}^{n} I\big(W_{6,j} = 1\big)\mathcal{G}_{ij}}{\sum_{j=1}^{n} \mathcal{G}_{ij}}$$

$$+0.95 \frac{\sum_{j=1}^{n} I\big(W_{8,j} = 1\big)\mathcal{G}_{ij}}{\sum_{j=1}^{n} \mathcal{G}_{ij}}$$

The conditional probability of death from opioid overdose was specified by:

$$\text{logit}\big(\Pr\big(Y_i = 1 | V_i^s, W_{6,i}, W_{7,i}, W_{6,i}^s, W_{8,i}^s\big)\big)$$

$$= -1.1 - 0.2 \sum_{j=1}^{n} I\big(V_j = 1\big)\mathcal{G}_{ij} + 1.7\, W_{7,i} - 0.9\, W_{6,i} + 0.75\, \frac{\sum_{j=1}^{n} I\big(W_{8,j} = 1\big)\mathcal{G}_{ij}}{\sum_{j=1}^{n} \mathcal{G}_{ij}}$$

$$- 0.75 \frac{\sum_{j=1}^{n} I\big(W_{6,j} = 1\big)\mathcal{G}_{ij}}{\sum_{j=1}^{n} \mathcal{G}_{ij}}$$

5.4.2.3 Comprehensive Dietary Intervention and Body Mass Index

For simultaneous unit-treatment and spillover effects, a data generating mechanism based on a comprehensive dietary intervention on body mass index (BMI) was created. Research has found BMI to be socially clustered,[208, 209] with the transmission of obesity theorized to result from social pressures or the shared environments of social contacts.[209] Comprehensive dietary interventions that limit caloric intake and increase the quality of food may reduce BMI.[269] Our simulation focuses on a theoretical dietary intervention that impacts an

individual's BMI as well as their immediate friends' BMI. Confounders included baseline BMI, gender, and baseline exercise. In this context, the interference pattern can be viewed as a network of friendships.

Let $W_{6,i}$ indicate gender, $W_{9,i}$ indicate baseline BMI, and $W_{10,i}$ indicate exercise at baseline. The conditional probability of starting the proposed diet at baseline was specified by:

$$\text{logit}\big(\Pr\big(V_i = 1 | W_{6,i}, W_{9,i}, W_{10,i}, W_{10,i}^{s}\big)\big)$$

$$= -0.5 + 0.05\big(W_{9,i} - 30\big) + 0.25 W_{6,i} W_{10,i} + 0.05 \frac{\sum_{j=1}^{n} I\big(W_{10,j} = 1\big)\mathcal{G}_{ij}}{\sum_{j=1}^{n} \mathcal{G}_{ij}}$$

BMI at follow-up was generated by:

$$Y_i = 3 + W_{9,i} - 5V_i - 5\, I\left(3 < \sum_{j=1}^{n} I\big(V_j = 1\big)\mathcal{G}_{ij}\right) + 3W_{6,i} - 3W_{10,i} - 0.5 \sum_{j=1}^{n} I\big(W_{10,j} = 1\big)\mathcal{G}_{ij}$$

$$+ \frac{\sum_{j=1}^{n} \mathcal{G}_{ij}\big(W_{9,j} - W_{9,i}\big)}{\sum_{j=1}^{n} \mathcal{G}_{ij}} + \epsilon_i$$

where $\epsilon_i \sim \text{Normal}(0, 1)$.

5.4.2.4 Infectious Disease Transmission

The fourth simulation mechanism entailed a Susceptible-Infected-Recovered (SIR) model of human-to-human transmission of an infectious agent. The hypothetical vaccine followed a 'leaky' model, such that the vaccine reduced the probability of infection given a single exposure to an infectious agent.[270] The spillover effect of the vaccine was composed of contagion (vaccinated individuals were less likely to become infected and thus less likely to transmit) and infectiousness effects (vaccinated-but-infected individuals had reduced probability of transmitting the disease).[271]

The stochastic SIR model was implemented as follows. Seven individuals were randomly selected as initial infections. Actively infectious individuals infected their immediate contacts based on a probability of transmission conditional on characteristics of the infected and uninfected individuals. Infected individuals were actively infectious for a period of five discrete

time-steps after becoming infected, and recovered after the infectiousness period (no longer infectious nor capable of being infected by contacts). All transmission events occurred over a period of ten time-steps. Unlike the previous data generating mechanisms, the infection transmission mechanism does not necessarily adhere to the weak dependence assumption. By chance, infections can spread beyond immediate contacts.

Let $W_{11,i}$ indicate asthma, and $W_{12,i}$ indicate hand hygiene. The probability of being vaccinated was specified by:

$$\text{logit}\left(\Pr\left(V_i = 1 | W_{11,i}, W_{12,i}, W_{12,i}^s\right)\right) = -1.9 + 1.75W_{11,i} + 0.95W_{12,i} + 1.2\frac{\sum_{j=1}^{n} I\left(W_{12,j} = 1\right)\mathcal{G}_{ij}}{\sum_{j=1}^{n}\mathcal{G}_{ij}}$$

and the probability of individual i becoming infected at discrete time-point t ($I_{i,t}$) by individual j was generated by:

$$\text{logit}\left(\Pr\left(I_{i,t} = 1 \middle| Z_{j,t} = 1, \mathcal{G}_{ij} = 1, V_i, V_j, W_{11,i}, W_{12,i}\right)\right) = -2.4 - 1.5V_i - 0.4V_j + 1.5W_{11,i} - 0.4W_{12,i}$$

where $Z_{j,t} = 1$ indicates whether j was in the infectious category at time t. For individuals with multiple infectious contacts, probabilities were independently resolved for each contact. Note this is not the outcome model used in network-TMLE. Instead, network-TMLE used the following outcome model:

$$\begin{aligned}\text{logit}\left(\Pr\left(Y_i = 1 | V_i, V_i^s, W_{11,i}, W_{12,i}, W_{11,i}^s, W_{12,i}^s, F_i\right)\right) \\ = \beta_0 + \beta_1 V_i + \beta_2\frac{\sum_{j=1}^{n} I\left(V_j = 1\right)\mathcal{G}_{ij}}{\sum_{j=1}^{n}\mathcal{G}_{ij}} + \beta_3 W_{11,i} + \beta_4\frac{\sum_{j=1}^{n} I\left(W_{11,j} = 1\right)\mathcal{G}_{ij}}{\sum_{j=1}^{n}\mathcal{G}_{ij}} + \beta_5 W_{12,i} \\ + \beta_6\frac{\sum_{j=1}^{n} I\left(W_{12,j} = 1\right)\mathcal{G}_{ij}}{\sum_{j=1}^{n}\mathcal{G}_{ij}} + \beta_7 F_i\end{aligned}$$

where Y_i is the indicator variable of ever infected by the end of follow-up.

5.4.3 Performance Metrics

To compare network-TMLE and IID-TMLE, the following metrics were used: bias, ESE, and 95% CI coverage. Bias was defined as the mean of $\hat{\psi}^c$ minus ψ^c for each ω. ESE was estimated by the standard deviation of the simulation estimates for each policy scenario. CI

coverage was calculated as the proportion of 95% CIs containing the true mean of the outcome. Tables containing these and other selected metrics are available in Appendix 2.4.

5.4.4 Software

All simulations were conducted using Python 3.5.1 with the following libraries: NumPy,[186] SciPy,[187] statsmodels,[188] patsy,[189] and NetworkX.[190] Since no current implementation of network-TMLE was available in Python, we designed one. Our implementation was validated by replicating the simulations from Sofrygin and van der Laan[151] (Appendix 2.1).

5.5 Simulation Study Results

5.5.1 Statin and ASCVD

For the hypothetical study of statins, the assumption regarding no interference for IID-TMLE is valid. The estimated risk of ASCVD for IID-TMLE exhibited little bias and the corresponding 95% CIs had approximately nominal coverage levels across all networks and policies (Figure 5.2A, Figure 5.3A). Results for the clustered power-law random graph are in Appendices 2.3 and 2.4.

Network-TMLE also exhibited little bias, but had greater ESE relative to IID-TMLE. The network-TMLE CI coverage approximated the nominal level for policies where the probability of exposure was similar to the proportion exposed in the observed data. However, CI coverage was less than the nominal level for policies where substantially more individuals would be exposed relative to the observed data for the uniform random graph (Figure 5.2). On the other hand, CI coverage exceeded the nominal level for policies where the probability of exposure was not similar to the observed data for the eX-FLU graph (Figure 5.3). Results for the power-law random graph were similar to the eX-FLU graph results (Figure A2.3.1). Additional simulations were conducted restricting the degree in the eX-FLU network and power-law graphs. Restricting inference to individuals with a degree of 18 or less for the power-law graph resulted in improved performance for network-TMLE (Table A2.4.6). However, inflated coverage levels where the probability of exposure was not similar to the observed data persisted when

restricting inference to individuals with a degree of 23 or less for the eX-FLU graph (Table A2.4.9).

5.5.2 Naloxone and Opioid Overdose

For simulations of naloxone and opioid overdose (where there was a spillover effect only), IID-TMLE exhibited biased point estimates and CI coverage well below the nominal level (Figure 5.4A, Figure 5.5A, Figure A2.3.2A). IID-TMLE only performed well for policies where the probability of exposure was close to the observed proportion exposed.

For the uniform random graph, network-TMLE exhibited negligible bias and CI coverage approximating the nominal level for policies where the likelihood of exposure was not substantially different from the observed proportion exposure (Figure 5.4). For the eX-FLU network, network-TMLE had minimal bias, and the corresponding CIs had approximately nominal coverage for most policies (Figure 5.5). Results were similar when the degree of the eX-FLU network was restricted (Table A2.4.18). Performance of network-TMLE for the power-law random graph (Figure A2.3.2, Table A2.3.14-15) was comparable to results from the eX-FLU graph simulations.

5.5.3 Comprehensive Dietary Intervention and BMI

For simulations of a comprehensive dietary intervention on BMI with both unit-treatment and spillover effects, IID-TMLE performed poorly across all networks (Figure 5.6A, Figure 5.7A, Figure A2.3.3A), with biased point estimates and CI coverage levels far from the nominal level. Conversely, network-TMLE point estimates exhibited minimal bias and the corresponding CIs had approximately 95% nominal coverage, with some slight undercoverage for the uniform random graph and high exposure policies (Figure 5.6B-C, Figure 5.7B-C, Figure A2.3.3B-C). Results for the restricted degree power-law random graph and eX-FLU network graph were similar (Tables A2.4.26-27, A2.4.23-24).

5.5.4 Vaccine and Infectious Disease Transmission

Results for the infectious disease transmission simulations are presented in Figure 5.8, 5.9, and Appendix 2.4. As expected, IID-TMLE again exhibited bias and the corresponding CI coverage was less than the nominal level except for policies where the likelihood of exposure was similar to the observed proportion exposed. On the other hand, network-TMLE had little bias across networks, although 95% CIs also had lower coverage for policies with exposure distributed dissimilar to the observed data.

5.6 Discussion

The recent extension of TMLE for inference about the sample mean under stochastic policies with dependent data performed well in simulation studies for a variety of data generating mechanisms based on real-world examples. The simulation scenarios included different network structures as well as unit-treatment and spillover effects. These results demonstrate the potential utility of network-TMLE over a wide range of realistic settings. Software implementing network-TMLE in Python is freely available, which may help facilitate greater use of these methods.

While network-TMLE performed better than IID-TMLE in settings where interference was present, the network-TMLE CIs often failed to provide nominal coverage levels for policies where the probability of exposure was substantially different from the observed proportion exposed. Thus, care should be exercised when employing network-TMLE for inference about policies “far” from the observed data. A simple diagnostic plot may be helpful by comparing histograms of the summary measure V^s stratified by V for the observed data versus the corresponding distributions expected under the policy of interest. Examples of the proposed diagnostic plot are provided in Appendix 2.5. Similarly, restricting inference to individuals below a specified degree may improve confidence interval coverage for networks with skewed degree distributions. While individuals above the maximum degree are then considered to be fixed

features of the network and the target parameter has a modified interpretation, the improvements in CI coverage may nonetheless be preferred.

Limiting inference to policies "close" to the observed data is recommended when using network-TMLE to ensure valid inferences. Focusing on policies which modestly perturb the exposure distribution may also be more relevant from a policy perspective. In contrast, in the absence of interference, commonly targeted estimands like the average causal effect contrast two extreme exposure distributions: everyone exposed versus no one exposed.[255, 272-274] Such extreme counterfactual exposure settings may be unrealistic or irrelevant in practice. For instance, when assessing the effect of smoking during pregnancy on some health outcome, the counterfactual scenario where all individuals smoke is likely unrealistic. Rather, there may be more interest in the effect of policies or interventions which modestly decrease the likelihood of smoking during pregnancy. As another example, consider policies encouraging influenza vaccination. Previous interventions to increase vaccination rates have resulted in only minor to moderate increases in the vaccine receipt.[94, 95, 275, 276] Therefore, the counterfactual scenario of everyone in the population being vaccinated may be of less relevance, in addition to being difficult to draw valid inferences about.

Future work could consider the following. First, additional empirical studies of network-TMLE are needed incorporating model selection, particularly for summary measures of exposure since the correct functional form for V^s is typically unknown. To reduce model misspecification errors, machine learning can be paired with network-TMLE. For instance, flexible estimation of $\Pr(V_i^s|V_i, W_i, W_i^s)$ could be accomplished with a conditional density super learner.[277, 278] Further simulations studies could be considered for extensions of network-TMLE which relax the weak dependence assumption by incorporating longitudinal data.[150] Additional empirical evaluation could be conducted of network-TMLE for other estimands such as marginal unit-treatment effects (i.e. direct effects).[151] Generalization of network-TMLE to other related

estimands (i.e., spillover effects, total effects) is also of interest. Finally, direct comparisons between network-TMLE and auto-g-computation, a recent extension of the parametric g-formula for general interference,[149] could be undertaken.

5.7 Tables and Figures

Figure 5.1: Visualizations of networks used in simulations

A: uniform random network, B: clustered power-law random network, C: eX-FLU observed network

Figure 5.2: Target maximum likelihood estimation for statins and atherosclerotic heart disease, and the uniform random graph

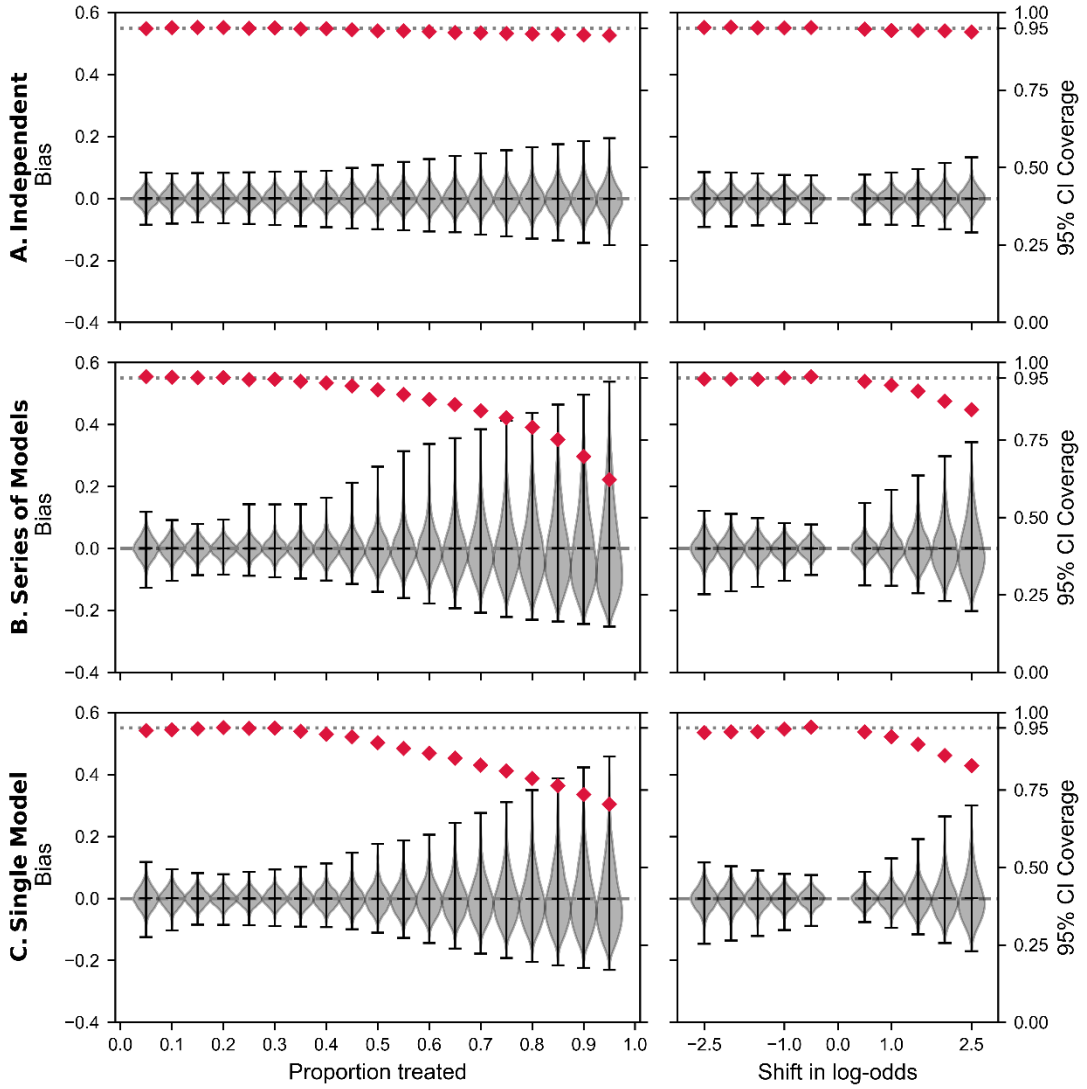

Left y-axes and violin plots correspond to bias, defined as the estimated conditional sample mean minus the true conditional sample mean. The right y-axes and red diamonds correspond to 95% confidence interval (CI) coverage. The first column corresponds to all individuals in the population having the same set probability of statins. The second column corresponds to the shift in log-odds of the predicted probability of statins for each individual. The proportion of statins in the observed data was 25%.

A: Targeted maximum likelihood estimation under the assumption of independent observations. B: Network-TMLE with a series of logistic models for statin use of immediate contacts. C: Network-TMLE with a Poisson model for statin use of immediate contacts.

Figure 5.3: Target maximum likelihood estimation for statins and atherosclerotic heart disease, and the eX-FLU network

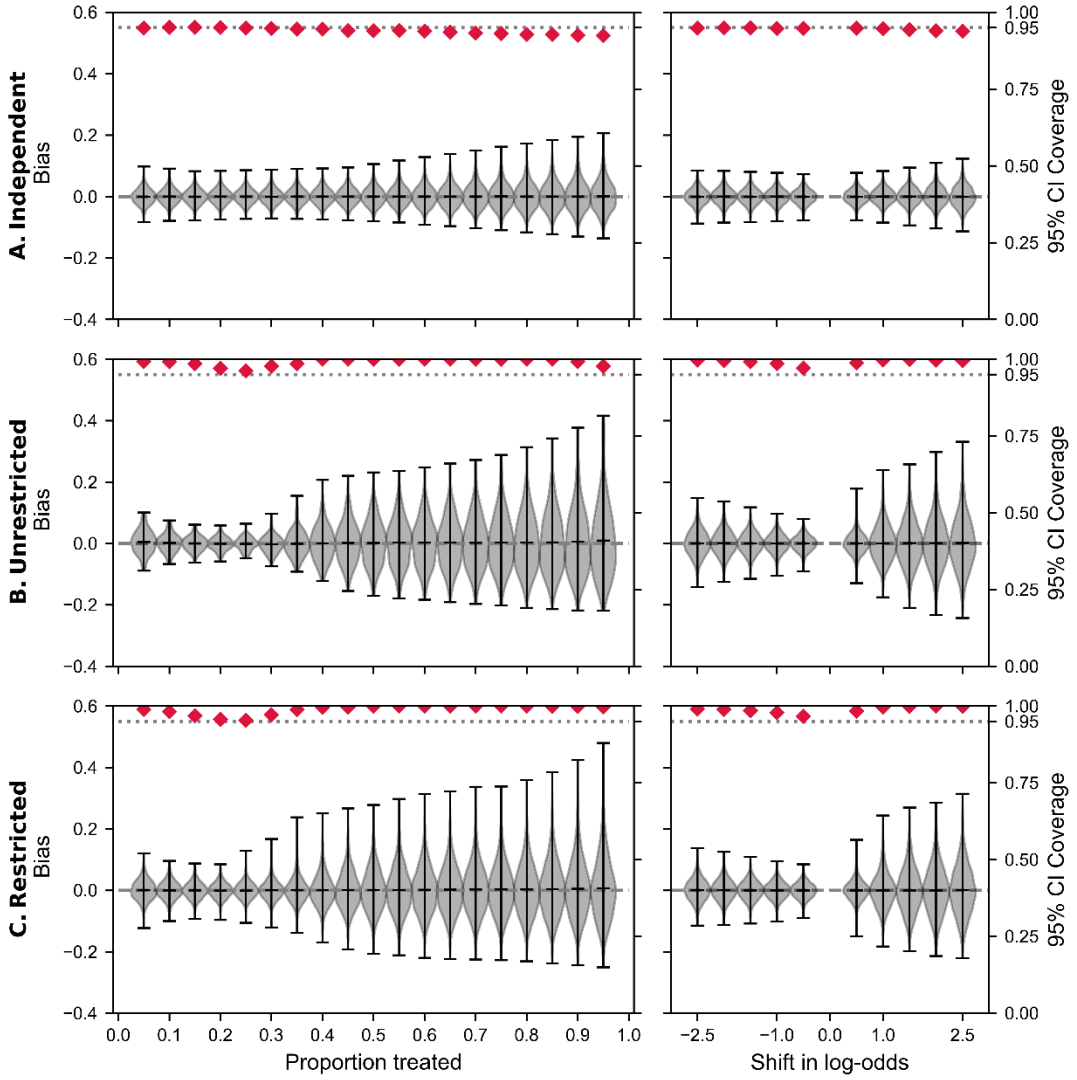

Left y-axes and violin plots correspond to bias, defined as the estimated conditional sample mean minus the true conditional sample mean. The right y-axes and red diamonds correspond to 95% confidence interval (CI) coverage. The first column corresponds to all individuals in the population having the same set probability of statins. The second column corresponds to the shift in log-odds of the predicted probability of statins for each individual. The proportion of statins in the observed data was 24%.

A: Targeted maximum likelihood estimation under the assumption of independent observations. B: Network-TMLE with a Poisson model for statin use of immediate contacts. No restrictions on maximum degree were placed. C: Network-TMLE with a Poisson model for statin use of immediate contacts. The maximum degree for participants was restricted to be 22 or less.

Figure 5.4: Target maximum likelihood estimation for naloxone and opioid overdose, and the uniform random graph

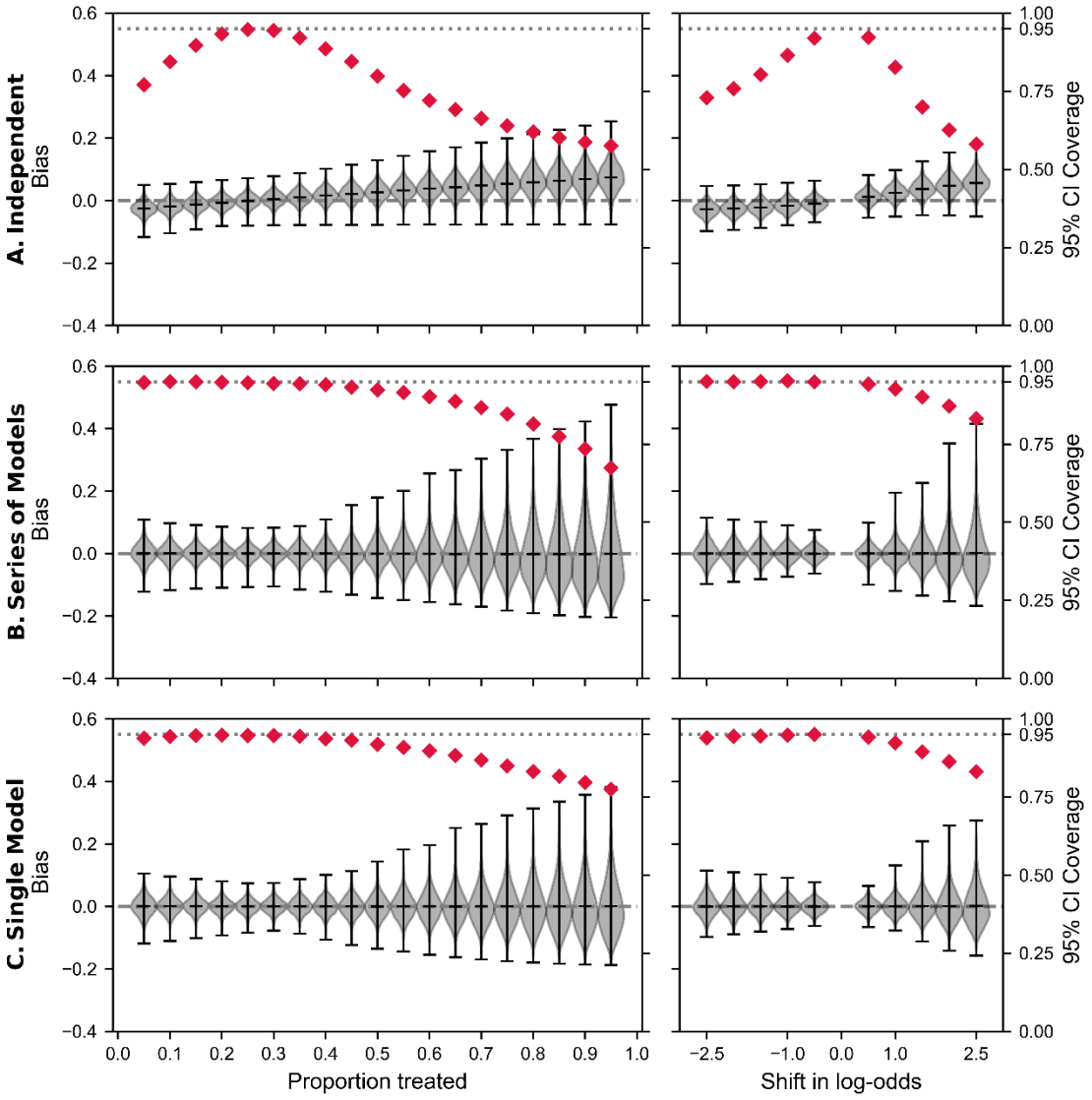

Left y-axes and violin plots correspond to bias, defined as the estimated conditional sample mean minus the true conditional sample mean. The right y-axes and red diamonds correspond to 95% confidence interval (CI) coverage. The first column corresponds to all individuals in the population having the same set probability of naloxone. The second column corresponds to the shift in log-odds of the predicted probability of naloxone for each individual. The proportion of naloxone in the observed data was 26%.

A: Targeted maximum likelihood estimation under the assumption of independent observations. B: Network-TMLE with a series of logistic models for naloxone use of immediate contacts. C: Network-TMLE with a Poisson model for naloxone use of immediate contacts.

Figure 5.5: Target maximum likelihood estimation for naloxone and opioid overdose, and the eX-FLU network

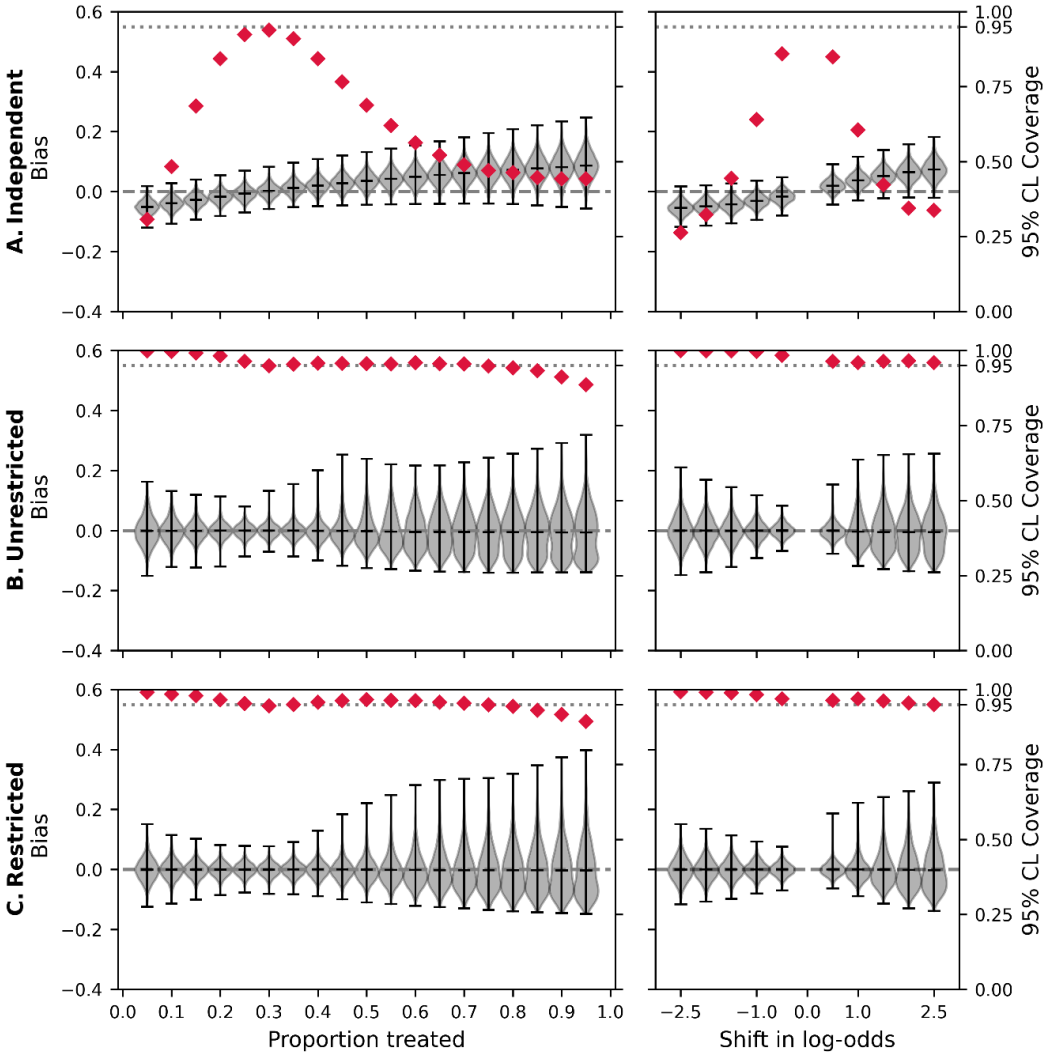

Left y-axes and violin plots correspond to bias, defined as the estimated conditional sample mean minus the true conditional sample mean. The right y-axes and red diamonds correspond to 95% confidence interval (CI) coverage. The first column corresponds to all individuals in the population having the same set probability of naloxone. The second column corresponds to the shift in log-odds of the predicted probability of naloxone for each individual. The proportion of naloxone in the observed data was 28%.

A: Targeted maximum likelihood estimation under the assumption of independent observations. B: Network-TMLE with a Poisson model for naloxone use of immediate contacts. No restrictions on maximum degree were placed. C: Network-TMLE with a Poisson model for naloxone use of immediate contacts. The maximum degree for participants was restricted to be 22 or less.

Figure 5.6: Target maximum likelihood estimation for diet and body mass index, and the uniform random graph

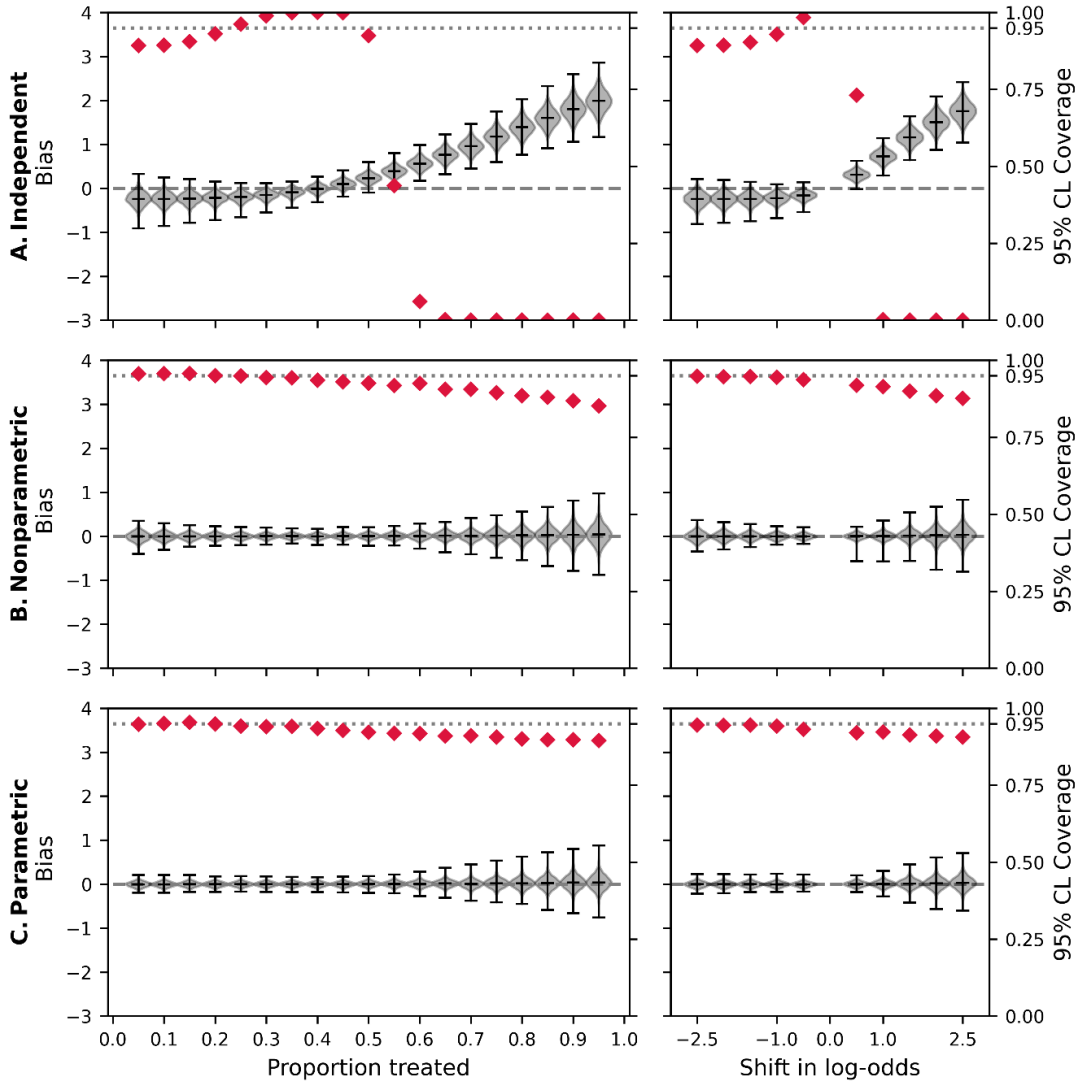

Left y-axes and violin plots correspond to bias, defined as the estimated conditional sample mean minus the true conditional sample mean. The right y-axes and red diamonds correspond to 95% confidence interval (CI) coverage. The first column corresponds to all individuals in the population having the same set probability of diet. The second column corresponds to the shift in log-odds of the predicted probability of diet for each individual. The proportion on a diet in the observed data was 40%. A: Targeted maximum likelihood estimation under the assumption of independent observations. B: Network-TMLE with a series of logistic models for diet of immediate contacts. C: Network-TMLE with a logistic model for diet of immediate contacts.

Figure 5.7: Target maximum likelihood estimation for diet and body mass index and the eX-FLU network

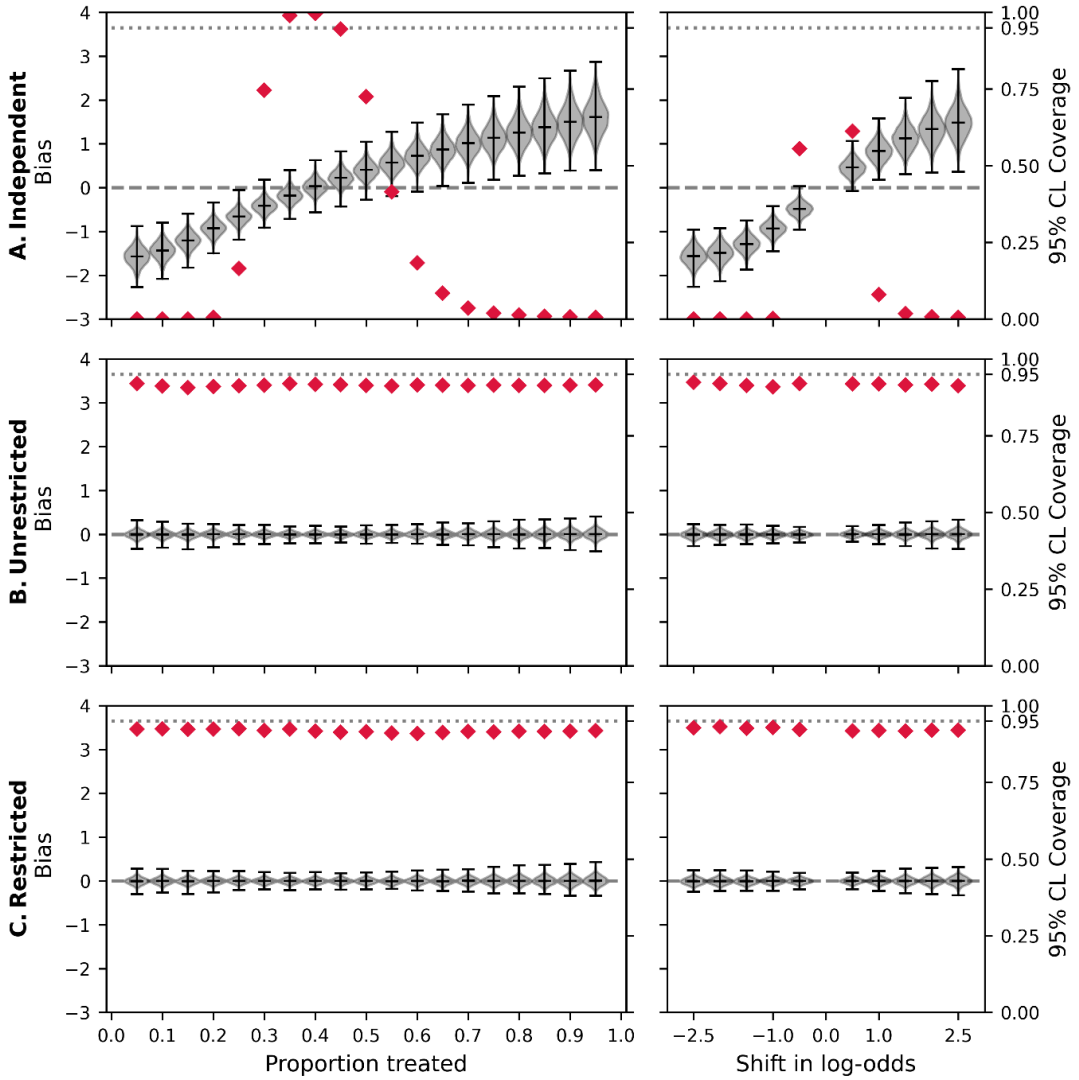

Left y-axes and violin plots correspond to bias, defined as the estimated conditional sample mean minus the true conditional sample mean. The right y-axes and red diamonds correspond to 95% confidence interval (CI) coverage. The first column corresponds to all individuals in the population having the same set probability of diet. The second column corresponds to the shift in log-odds of the predicted probability of diet for each individual. The proportion on a diet in the observed data was 40%. A: Targeted maximum likelihood estimation under the assumption of independent observations. B: Network-TMLE with a logistic model for diet of immediate contacts. No restrictions on maximum degree were placed. C: Network-TMLE with a logistic model for diet of immediate contacts. The maximum degree for participants was restricted to be 22 or less.

Figure 5.8: Target maximum likelihood estimation for vaccination and infection and the uniform random graph

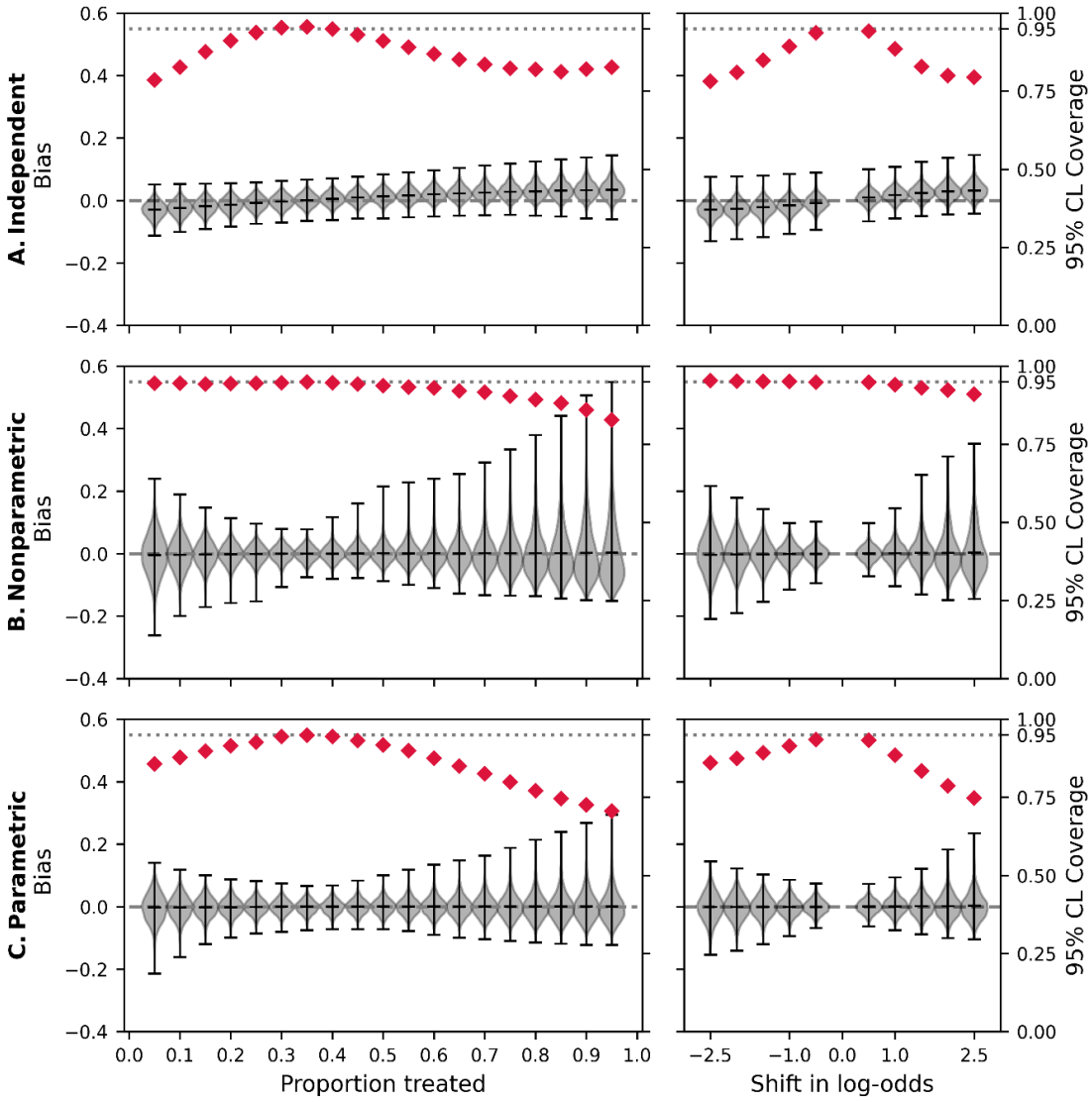

Left y-axes and violin plots correspond to bias, defined as the estimated conditional sample mean minus the true conditional sample mean. The right y-axes and red diamonds correspond to 95% confidence interval (CI) coverage. The first column corresponds to all individuals in the population having the same set probability of vaccination. The second column corresponds to the shift in log-odds of the predicted probability of vaccination for each individual. The proportion vaccinated in the observed data was 35%.
A: Targeted maximum likelihood estimation under the assumption of independent observations. B: Network-TMLE with a series of logistic models for vaccination of immediate contacts. C: Network-TMLE with a Poisson model for vaccination of immediate contacts.

Figure 5.9: Target maximum likelihood estimation for vaccination and infection, and the eX-FLU network

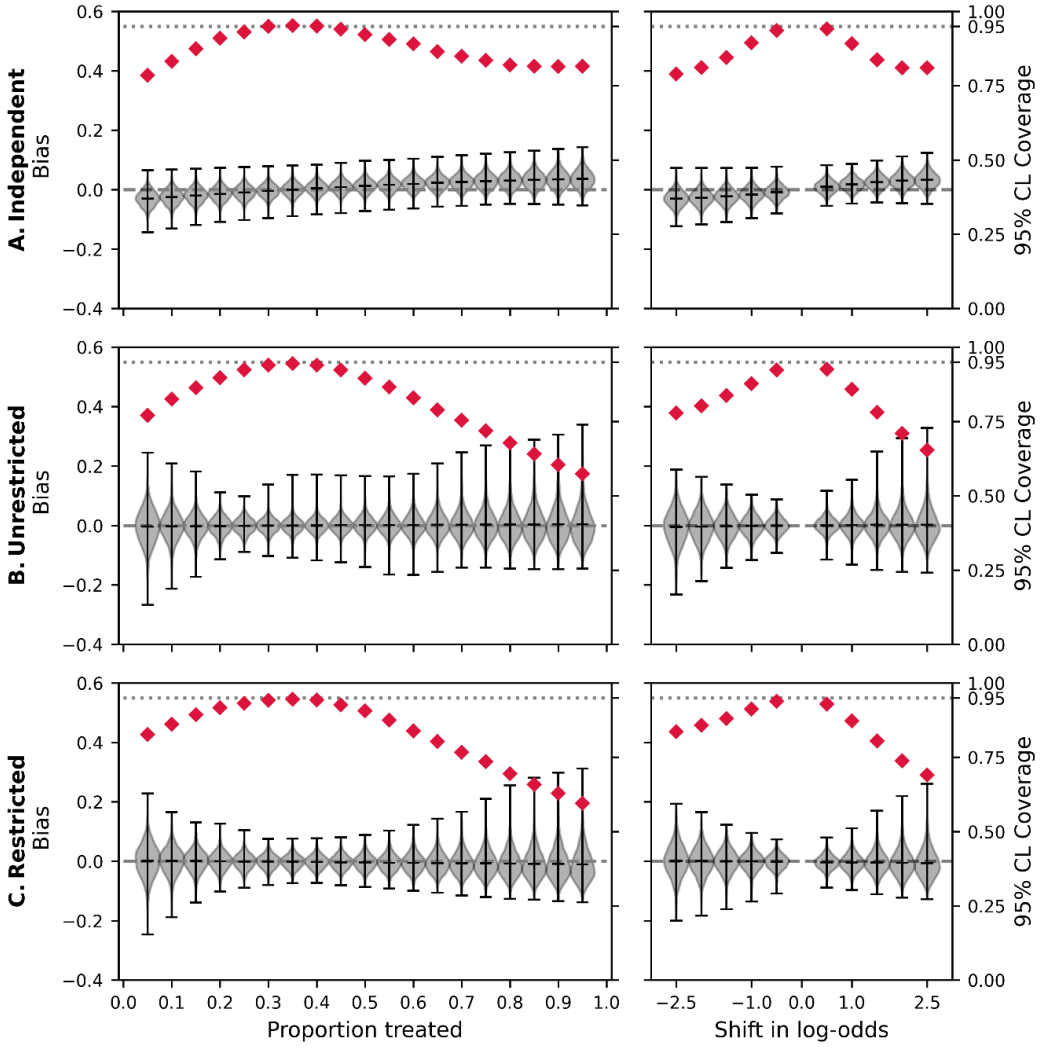

Left y-axes and violin plots correspond to bias, defined as the estimated conditional sample mean minus the true conditional sample mean. The right y-axes and red diamonds correspond to 95% confidence interval (CI) coverage. The first column corresponds to all individuals in the population having the same set probability of vaccination. The second column corresponds to the shift in log-odds of the predicted probability of vaccination for each individual. The proportion vaccinated in the observed data was 36%.
A: Targeted maximum likelihood estimation under the assumption of independent observations. B: Network-TMLE with a Poisson model for vaccination of immediate contacts. No restrictions on maximum degree were placed. C: Network-TMLE with a Poisson model for vaccination of immediate contacts. The maximum degree for participants was restricted to be 22 or less.

CHAPTER 6: REALISTIC INTERVENTIONS ON THE DISTRIBUTION OF INFLUENZA VACCINATION AND RISK OF INFLUENZA AMONG UNIVERSITY STUDENTS

6.1 Introduction

Vaccine and infectious disease epidemiology often focus on the direct or unit-treatment effect. The unit-treatment effect contrasts vaccine to no vaccine, holding all else constant.[137] Since interference (an individual's potential outcome depends on at least one other individual[133, 279]) likely exists for infectious diseases, the unit-treatment effect no longer collapses to the average treatment effect.[280] Whereas the average treatment effect would contrast everyone being vaccinated versus no one being vaccinated, the unit-treatment is instead the expected value of vaccination contrasted with no vaccination for each individual holding the vaccination status of the remainder of the population as fixed. However, large-scale distributional changes in the vaccine uptake are often of greater public health interest. Despite this elevated importance, few studies focus on these large-scale changes. Here we demonstrate an applied example of evaluating large-scale changes in the context of influenza vaccination among university students.

In 2010, the Advisory Committee on Immunization Practices expanded the recommendations for the influenza vaccine to include all persons older than 6 months and without contraindications.[91] University students are an important population to consider since they have elevated influenza risk[101-103]; less than half receive the yearly vaccine[93-100]; suffer negative impacts on their well-being from symptomatic influenza[96, 111]; and university students may rapidly disseminate influenza to the surrounding community[103, 104]. Previous research on influenza vaccination hesitancy and reported reasons for not receiving the vaccine has found that university students often report common misconceptions regarding the vaccine,[94, 95, 98, 100,

[116, 120] convenience of receipt,[94, 95, 98] or financial barriers.[94, 95] Research on addressing these barriers to vaccination have focused on vaccination receipt as the outcome as opposed to influenza infection.[94, 95] However, these results may be misleading in terms of the expected reduction in influenza. The distribution of vaccination within the set of contacts between students likely influences the overall risk.[137, 281] Therefore, strategies to increase influenza vaccination uptake may vary in their effectiveness of reducing the risk of influenza. For example, a strategy to reduce non-financial barriers to influenza vaccination may increase the overall vaccination uptake to a greater extent than an educational strategy, but the education strategy may nonetheless be more effective at reducing the risk of influenza due to the structure of the network. Focus solely on vaccination receipt as the end-point fails to capture this information.

In this chapter, we estimate the risk of influenza under different, realistic large-scale changes in the distribution of influenza vaccination uptake among students at a midwestern university. The large-scale changes shifted the probability distribution of vaccination informed by students' self-reported reasons for not receiving the vaccine, while also respecting contraindications. For estimation, we applied network-TMLE. Additionally, we assessed the sensitivity of our results due to missing data on vaccination, and measurement error of both influenza and self-reported contacts.

6.2 Methods

6.2.1 Data Source

Data for the analysis comes from the eX-FLU study, a cluster-randomized trial on three-day self-isolation to prevent the spread of respiratory pathogens among university students.[154] Briefly, students were recruited from one of six dormitories, with dormitories selected based on their physical proximity to each other and their representativeness of the undergraduate student population. Students were recruited through a chain referral sampling procedure; with seed students recruited through informational flyers, emails, and in-person informational tables at the dormitories. After enrollment, students were asked to nominate other students to participate. In

total there were 262 seeds and 328 nominees. Clusters were defined by environmental features believed to shape social interactions (e.g., physical barriers, resident house appointments, geographic proximity). Each cluster was randomized to either self-imposed three-day self-isolation after the onset of symptomatic respiratory illness or to continue their normal behavior while ill. To facilitate adherence in the self-isolation arm, students who developed ILI had provisions (e.g., snacks, beverages, etc.) and could be requested to provide a doctor's note verifying illness for professors or employers. Enrolled students were followed for ten-weeks of the Spring semester (January to April 2013, excluding Spring Break) for the development of respiratory illness.

6.2.1.1 Measures

Demographic factors collected include gender (male; female), race (white; black; Asian; other), ethnicity (Hispanic; non-Hispanic). Common risk factors and health behaviors related to respiratory infection were also collected. These factors included: stress (continuous), optimal hand hygiene (yes; no), high-risk conditions (yes; no), sleep quality (good; bad), and alcohol use (continuous). Stress was measured via the Perceived Stress Scale-10.[185] Optimal hand hygiene was defined as self-reporting hand washing at least 5 times a day and at least 20 seconds. High-risk conditions consisted of one of the following: asthma, reactive airway disorder, Type 1/2 diabetes, currently receiving HIV/AIDS or cancer treatment. Self-reported sleep quality was dichotomized as good or bad. Alcohol use was defined as self-reporting drinking alcohol at least once a week.

Influenza vaccination (yes; no) was defined as self-reported receipt of the 2012-2013 influenza vaccine before baseline. ILI was defined as the presence of coughing plus at least one of the following symptoms: fever, body aches, or chills. ILI is a non-specific condition and underestimates the true vaccine effect for actual influenza-caused illness.[80] Therefore, we also considered laboratory-confirmed influenza. Influenza was considered laboratory-confirmed if

any nasal or throat specimens collected with six days of the onset of illness were positive via quantitative polymerase chain reaction.[154]

6.2.1.2 Contact Data

Each week during follow-up, students were asked to self-report all face-to-face contacts with other study participants from the previous week. To enhance participant recall, previously reported contacts were listed. Additionally, a subsample (n=103) had contacts recorded via the smartphone's Bluetooth capabilities with the iEpi system.[154] To impose a clear time ordering between contacts and the outcomes, we considered only reported contacts during the first week of follow-up.

To describe the patterns of contacts, the number of isolates, assortativity by vaccination, and degree are reported. Isolates are students who had not reported contacts. Assortativity, the tendency for individuals connected in a network to share similar traits and behaviors, was assessed for vaccination status via the assortativity coefficient.[199] The assortativity coefficient is bounded between -1 and 1, where -1 and 1 indicate perfectly disassortative and assortative networks, respectively. An assortativity coefficient of 0 indicates there is no overall observed contact pattern by vaccination.

6.2.2 Policies

Previous work on influenza vaccination receipt among university students has focused on common misconceptions regarding the vaccine,[94, 95, 98, 100, 116, 120] the convenience of receipt,[94, 95, 98] and financial barriers.[94, 95] Therefore, we consider potential policies to address these reasons. The policies consist of both deterministic and stochastic components. Deterministic components set the vaccination status of an individual; whereas stochastic components assign individuals a probability of receiving the vaccine. For the deterministic component, all students that reported being allergic to the influenza vaccine were never vaccinated. For the stochastic component of the policy, individuals targeted by the policy had their log-odds of receiving the influenza vaccine increased. Each individual's predicted log-odds

of vaccination to be shifted was determined using super learner.[210] The 20-fold super learner consisted of logistic regression, logistic GAM,[212] a neural-network with a single layer with eight nodes, and a random forest classifier.[214] We considered increases in the log-odds between $\varpi = \{0, 0.25, 0.5, \ldots, 2.75, 3\}$. Students not targeted by the policy also had an increased log-odds of receiving the vaccine to reflect their potential benefit from the policy. However, their log-odds were only increased by a third (i.e., $\varpi/3$).

6.2.2.1 Policy 1

Prior research has indicated that misinformation on harms posed by the vaccine, and perceived lack of risk for influenza are common.[100, 116, 120] Other research indicates information on limiting transmission to contacts could potentially increase vaccine receipt.[98] Therefore, policy 1 consisted of a theoretical educational intervention to emphasize the benefits of the vaccine and dispel common myths. Targeted students included those who reported at least one of the following: the influenza vaccine can cause the flu, that they do not get the flu, or that they did not know if they could receive the influenza vaccine.

6.2.2.2 Policy 2

Other studies have reported barriers like the convenience of when or where to get the vaccine may reduce vaccine receipt.[94, 95, 98] Policy 2 addressed non-financial barriers by targeting students who reported at least one of the following reasons for not receiving the influenza vaccine: did not get around to receiving the influenza vaccine, did not have transportation to go receive the vaccine, or the hours when the vaccine was available did not fit their schedule.

6.2.2.3 Policy 3

While costs have been less often reported as a barrier in previous research,[94, 98] we also assessed a policy to address financial barriers. Financial barriers reported by students consisted of their health plan did not cover the vaccine or they did not have health insurance.

6.2.3 Targeted Maximum Likelihood Estimation

6.2.3.1 Potential Outcomes

Let W indicate baseline covariates, V indicate influenza vaccination, and Y indicate observed influenza. Let $\mathcal{G}$ be a $n \times n$ adjacency matrix, so that $\mathcal{G}_{ij} = 1$ indicates contact between individuals i and j, $\mathcal{G}_{ij} = 0$ otherwise. The potential outcomes are $Y_i(v_i, v_{-i})$; where v_i is the vaccination status of individual i and v_{-i} is the vaccination status of the remainder of the population. In the context of no interference, $Y_i(v_i, v_{-i})$ simplifies to $Y_i(v_i)$. However, the assumption of no interference is unreasonable since the influenza infection of person i may depend on the vaccination status of person j.

Rather than no interference, weak dependence (only person i's immediate contacts may affect i) was assumed instead. Under weak dependence, the potential outcomes are no longer defined by the entirely of v_{-i}; but instead are $Y_i(v_i, v_i^s)$, where v_i^s is a summary measure of the vaccination status of all persons j where $\mathcal{G}_{ij} = 1$. Since interest is in stochastic policies, v and v^s are replaced by $\Pr^*(V, V^s|W, W^s)$, which indicates the conditional distribution of vaccination under the policy of interest. The estimand is

$$\psi = \frac{1}{n}\sum_{i=1}^{n} E\left[\sum_{v\in\mathcal{V}, v^s\in\mathcal{V}^s} Y_i(v, v^s)\Pr^*\left(V_i = v, V_i^s = v^s \middle| W_i, W_i^s\right)|\boldsymbol{W}\right]$$

where $\boldsymbol{W} = (W_1, W_2, \ldots, W_n)$. To draw inference for ψ, extensions of causal consistency, conditional exchangeability, and positivity to weak dependence were assumed.

We take this opportunity to demonstrate why the unit-treatment effect is insufficient to address our question. Under weak dependence, the sample unit-treatment effect is

$$\frac{1}{n}\sum_{i=1}^{n} Y_i(v_i = 1, v_i^s) - Y_i(v_i = 0, v_i^s)$$

The unit-treatment effect holds the vaccination status of immediate contacts as fixed, only contrasting that individual's vaccination.

6.2.3.2 Estimation

To estimate ψ, a recent extension of TMLE to weak dependence was used.[150, 151, 282] Briefly, network-TMLE can be divided into four steps: outcome model estimation, weight estimation, targeting, and estimation of ψ. Network-TMLE begins with estimation of an outcome model for $\Pr(Y_i|V_i, V_i^s, W_i, W_i^s)$; where V_i^s and W_i^s are summary measures of i's immediate contacts' V and W, respectively. The model can be estimated by treating observations as if they were IID. After estimation of an outcome model, predicted values of the outcome ($\hat{Y}_i$) are then generated.

Next, weights are calculated as

$$\frac{\Pr^*(V_i, V_i^s|W_i, W_i^s)}{\Pr(V_i, V_i^s|W_i, W_i^s)}$$

where the numerator is the distribution of vaccination under the policy and the denominator is based on the observed distribution of vaccination. The denominator probability is factored into $\Pr(V_i|W_i, W_i^s)$ and $\Pr(V_i^s|V_i, W_i, W_i^s)$. Each part can be estimated from the observed data treating the observations as IID. Since the summary measure for immediate contacts' vaccination was a sum of those who were vaccinated, $\Pr(V_i^s|V_i, W_i, W_i^s)$ was estimated using a Poisson distribution. To estimate the numerator, a simulation procedure was used. A large number of copies of the data are generated, and the policy of interest was applied to each copy. Then the factored numerator is evaluated by fitting models as before, but to all copies of the data at once. The fitted models and observed V_i and V_i^s are then used to predict the numerator probability.

Next, the targeting step is accomplished by estimating the following logistic regression model via weighted maximum likelihood

$$\text{logit}(Y_i) = \eta_0 + \text{logit}\left(\hat{Y}_i\right)$$

The estimated intercept $\widehat{\eta_0}$ can be thought of as a correction term for the outcome predictions, with $\widehat{\eta_0}$ shifting the values of $\hat{Y}_i$ when the outcome model is misspecified.

Because interest is in a policy with a stochastic component, the updated values of vaccination, V_i^*, are no longer degenerate. Therefore, a Monte Carlo simulation procedure is used to estimate ψ. First, generate $k = 1,2,\ldots,m$ different draws of V_{ik}^* from $\text{Bernoulli}(\Pr^*(V_i = 1|W_i, W_i^S))$ and calculate V_{ik}^{*S} using V_{ik}^*. Next, the estimated probability of influenza under the policy, $\hat{Y}_{ik}^*$, is predicted from the previously estimated outcome model, V_{ik}^*, and V_{ik}^{S*}. $\hat{Y}_{ik}^*$ is then updated via $\widehat{\eta_0}$

$$\tilde{Y}_{ik}^* = \text{expit}\left(\widehat{\eta_0} + \text{logit}\left(\hat{Y}_{ik}^*\right)\right)$$

Then ψ_k is estimated by the mean of $\tilde{Y}_{ik}^*$. Finally, the overall estimate for ψ is the mean of all m estimates

$$\hat{\psi} = \frac{1}{m}\sum_{k=1}^{m}\hat{\psi}_k$$

To reduce computational burden, V_{ik}^* and V_{ik}^{S*} generated during the estimation of the weights' numerator were reused.

While estimators of both population and sample variance estimators are available,[150] we opted for inference on the sample risk. Assumptions necessary for the population variance estimator to be validly estimated (e.g., $\boldsymbol{W}$ is IID, and latent variable dependence in the network only occurs up to second-order contacts) are unlikely in this setting. The sample variance estimator does not restrict the distribution of $\boldsymbol{W}$ in the network nor requires such limited latent variable dependence.[150]

To allow for flexibility in the estimated nuisance models, we used super learner.[210, 211] Briefly, the 20-fold super learners for $\Pr(Y_i|V_i, V_i^S, W_i, W_i^S)$ and $\Pr(V_i|W_i, W_i^S)$ consisted of logistic regression, elastic-net regularized logistic regression,[215] and logistic GAM.[212] Two variations of elastic-net were included, with L1-L2 ratios of 0.25 and 0.75. Variations on the included logistic GAM with smoothing parameters of 0.5, 0.75, 1.0, 1.5, and 2.0. For $\Pr(V_i^S|V_i, W_i, W_i^S)$, the 20-

fold super learner consisted of Poisson regression and Poisson GAM with the same smoothing parameters as before.

6.2.4 Missing Data

Problems of missing data in networks are magnified since complete-case analyses that drop individuals with missing data change the topology of the network. To address missing data, a modified version of MICE was used. Imputations were summarized using Rubin's Rule.[198]

6.2.5 Sensitivity Analyses

In sensitivity analyses, the focus was on missing data on vaccination and measurement error of the network. Vaccination had the largest extent of missing data of variables in the analysis. While imputed vaccination was used in the primary analyses, we explored estimation under the two extremes of all those with missing vaccination being vaccinated or being unvaccinated.

Network-TMLE requires that the underlying network is correctly measured. Past research has shown that self-reported contacts are often underestimated when compared to other sources of data.[155, 158, 159] To address measurement error of self-reported contacts, we used a recently proposed Bayesian approach.[227] From each of the previous MICE imputations, a probability for each contact was estimated. These probabilities were estimated by combining a measurement model and network model. Priors for the measurement model were estimated using the Bluetooth and self-reported contacts from the iEpi subsample over the follow-up period. For the measurement model, a sensitivity of 0.7243 and specificity of 0.9897 for self-reported contacts were used. For the network model, a stochastic block model with terms for dormitory, class year, gender, race, and vaccination were used. Additionally, a term was added whether either of the students drank alcohol, based on previous observations that students who drink alcohol have more social contacts.[283] From these estimated probabilities, 100 different networks were generated. Summarization across the generated networks and missing data imputations were done using the nested variation of Rubin's Rule.[218]

6.3 Results

Of the 454 students who completed the baseline survey, 402 (89%) reported either receiving or not receiving the influenza vaccine. Of those, 161 (40%) reported receiving the vaccine (Table 6.1). There was a total of 190 (42%) ILI and 17 (4%) laboratory-confirmed influenza cases. Two (11%) of the laboratory-confirmed influenza cases were not ILI cases (i.e., asymptomatic cases). Of those who reported not receiving the vaccine, the most commonly cited reasons were tied to the convenience of accessing the vaccine (Table 6.2). Only two students reported being allergic to the vaccine.

In the self-reported contact network, there were 828 edges with 71 isolates (Figure 6.1). The largest component of the network consisted of 311 students. Contacts were not assortative by vaccination for either the observed vaccination (-0.01; 95% CI: -0.06, 0.05) or imputed vaccination (-0.02; 95% CI: -0.10, 0.05). The degree distribution for the network was highly skewed, with many students reporting only a few contacts and a few students reporting a large number. Students with more than 13 contacts (3%) had their vaccination status held constant under all policies assessed.

6.3.1 Vaccination Policies

The policies considered shifted vaccination uptake from 40% up to 67% for the greatest increase in log-odds. As shown in Figure 6.2A, no difference in the risk of ILI occurred across the various shifts in log-odds or the variations between policies. For laboratory-confirmed influenza, a minor downward trend in risk occurred for all policies (Figure 6.2B). However, the estimated reduction was also consistent with no reduction in the risk of influenza.

6.3.2 Sensitivity Analyses

When comparing the extremes of all students with missing vaccination status as vaccinated or unvaccinated, the results were substantively similar (Figure A3.2, Figure A3.3). For the analyses of accounting for measurement error of self-reported contacts, a greater reduction in risk of influenza, as defined both by ILI and laboratory-confirmation, was observed

(Figure 6.3). At a shift of three in the log-odds, the risk of laboratory-confirmed influenza was 0.02 (95% CI: 1%, 4%) for both policy 1 and policy 2.

6.4 Discussion

In this chapter, we demonstrated a recent extension to the TMLE framework to networks with the estimated risk of influenza under realistic policies among university students, including issues of missing data and measurement error, which are common in practice. Our primary results indicate a small reduction in the risk of laboratory-confirmed influenza. The reduction in the risk of influenza was greater when accounting for measurement error of self-reported contacts. However, results from both analyses are imprecise and are consistent with little-to-no reduction in overall risk. Furthermore, we did not observe any functional difference in the risk of influenza between the different policies to increase influenza vaccination uptake across the increases in log-odds of vaccination.

Prior research has indicated a protective unit-treatment effect of the influenza vaccine during the 2012-2013 influenza season,[64] and protective spillover effects in households[68] and communities.[70] Therefore, a reduction in the risk of influenza when increasing vaccination uptake would be expected. The relatively few influenza cases limit our ability to detect overall reductions in the risk of influenza. The lack of a reduction in ILI also results from most ILI cases being caused by another respiratory pathogen (e.g., respiratory syncytial virus, seasonal coronavirus, adenovirus), highlighting the limitation of ILI as a proxy for influenza among university students. There are also several sources of systematic biases that could explain only a small reduction in influenza risk being observed.

First, weak dependence stipulates that only immediate contacts' vaccination matters. While a weaker restriction than no interference, weak dependence may not be valid since the risk-period (10 weeks) is longer than the combined incubation and infectious periods for influenza.[284] Relatedly, Spring Break may have impacted the results since the network may be heavily disrupted by travel and outside contacts. However, only one influenza case occurred in

the week immediately following Spring Break. Second, measurement error of the network remains. All contacts regardless of distance and time spent in contact are assumed to be equivalent in the model. However, both of these factors may play a role in transmission of respiratory pathogens. Third, model misspecification is possible. While a flexible super-learner was used, data-adaptive algorithms were limited, since methods like cross-fitting[285] have yet to be extended for network-TMLE. Furthermore, misspecification of the summary measures is a concern. We specified V_i^s as a sum of immediate contacts' vaccination and used a Poisson model to estimate $\Pr(V_i^s|V_i, W_i, W_i^s)$. Use of a conditional density super-learner would allow for weaker assumptions for that model.[278] Fourth, information on influenza vaccination was only available via self-report. Self-reported influenza vaccine has been shown to adequately correspond to actual receipt; but sensitivity and specificity has varied across studies when compared to medical records.[286, 287] While medical records have been viewed as a true indicator of receipt, medical records miss other avenues outside of doctor offices and hospitals (e.g., pharmacies, vaccination clinics). Among the students in this study, 53 reported vaccine receipt at locations that would have been missed using medical records.

While our analysis does not provide a clear answer to the question of which policies of increasing influenza vaccination among university students to best minimize the risk of influenza among those students, our work contributes to application of better approaches for the assessment causal effects for vaccination and other settings with interference. The assumption of no interference is unwarranted in infectious disease epidemiology and with recent methodological extensions for partial or general interference, its continued issuance is rapidly becoming less acceptable. Despite these developments, the assumption of no interference is still common in application. By allowing for interference, we were able to focus on the risk of influenza under a variety of policies. Through approaches like ours, selection among competing policies can be done more effectively. Lastly, our analysis compliments previous theoretical and

simulation work on network-TMLE by demonstrating its application with approaches to address systematic biases common in practice to address a question of public health importance.

6.4.1 Conclusions

Studies on contagious outcomes often leave the parameter of interest implicit as the unit-treatment effect; which is the marginal expectation of the outcome when changing a single unit's exposure status holding the exposure of the remainder of the population constant. While this value can be important in assessment during development of vaccines or treatments, or under extreme constraints on possible policies; the unit-treatment effect may be of less interest to public health practitioners or policy makers when compared to the risk under policies that shift exposure, treatment, or vaccination distributions. Here we focused on large-scale changes in influenza vaccination uptake and subsequent risk of influenza among university students. Our results indicate a reduction in the risk of laboratory-confirmed influenza, but these results are consistent with no reduction. While our analysis does not inform strict selection between policies to increase influenza vaccination may be most beneficial to pursue among university students, it does exemplify what could be gained by focusing on other parameters available with interference.

6.5 Tables and Figures

Table 6.1: Descriptive statistics for the eX-FLU analytic sample

	Overall (n=454)		Vaccinated (n=161)	
	N	%	N	%
Three-Day Isolation	225	50%	81	50%
ILI case*	190	42%	65	40%
Lab-confirmed Flu†	17	4%	2	1%
Female	269	60%	104	65%
Missing	6		1	
Race				
Asian	78	18%	34	22%
Black or African American	40	9%	10	6%
Native American	1	0%	0	0%
Native Hawaiian / Pacific Islander	1	0%	0	0%
White	294	67%	106	68%
Multi-racial	23	5%	7	4%
Missing	17		4	
Hispanic	20	5%	5	3%
Missing	25		6	
Age	19	[18, 19]	18	[18, 19]
Class Year				
Freshman	256	57%	97	61%
Sophomore	111	25%	35	22%
Junior	32	7%	12	8%
Senior	40	9%	14	9%
5+ years	10	2%	2	1%
Missing	5		1	
High Risk‡	100	22%	55	34%
Perceived Stress Scale-10	16.5	[12.0, 20.0]	16	[13.0, 20.0]
Missing	24		4	
Optimal Hand Hygiene#	107	27%	40	28%
Missing	59		19	
Alcohol Use	155	37%	51	33%
Missing	31		7	
Good Sleep Quality	340	77%	125	79%
Missing	15		2	
Unique Contacts††	2	[1, 5]	2	[1, 4]
Unique Vaccinated Contacts††	1	[0, 2]	1	[0, 2]

The sample consists of the 454 of 590 (77%) enrolled participants who completed the baseline survey.

* ILI consisted of self-reported coughing and one of the following: fever, body aches, or chills
† Influenza was laboratory-confirmed via quantitative PCR
‡ High risk was defined as the presence of one of the following: asthma, reactive airway disorder, Type 1/2 diabetes, currently receiving HIV/AIDS or cancer treatment
# Optimal hand hygiene was defined as self-reporting hand washing at least 5 times a day and spending at least 20 seconds for each hand hygiene event
** Good sleep quality was defined as self-reported fair or good sleep quality.
†† Unique contacts were defined at week two of follow-up.

Table 6.2: Students self-reported barriers to influenza vaccine receipt

	N	%
Education Policy*	50	20.7%
Convenience Policy†	93	38.6%
Reduced Cost Policy‡	18	7.5%
Allergic to Vaccine#	2	0.8%

Policies were based on self-reported reasons why the student did not receive the influenza vaccine for 2012-2013. 241 students reported not receiving the vaccine

* The intervention targets students who reported one of the following: the influenza vaccine causes influenza, they don't get influenza, or they didn't know they could get the influenza vaccine

† The intervention targets students who reported one of the following: never got around to getting the vaccine, did not have transportation to get the influenza vaccine, or the hours the vaccine was available were inconvenient

‡ The intervention targets students who reported one of the following: their health plan did not cover the influenza vaccine, or they did not have health insurance

Those who reported being allergic to the influenza vaccine were not vaccinated under any intervention strategy

Figure 6.1: Self-reported contacts between participants measured at the end of week one

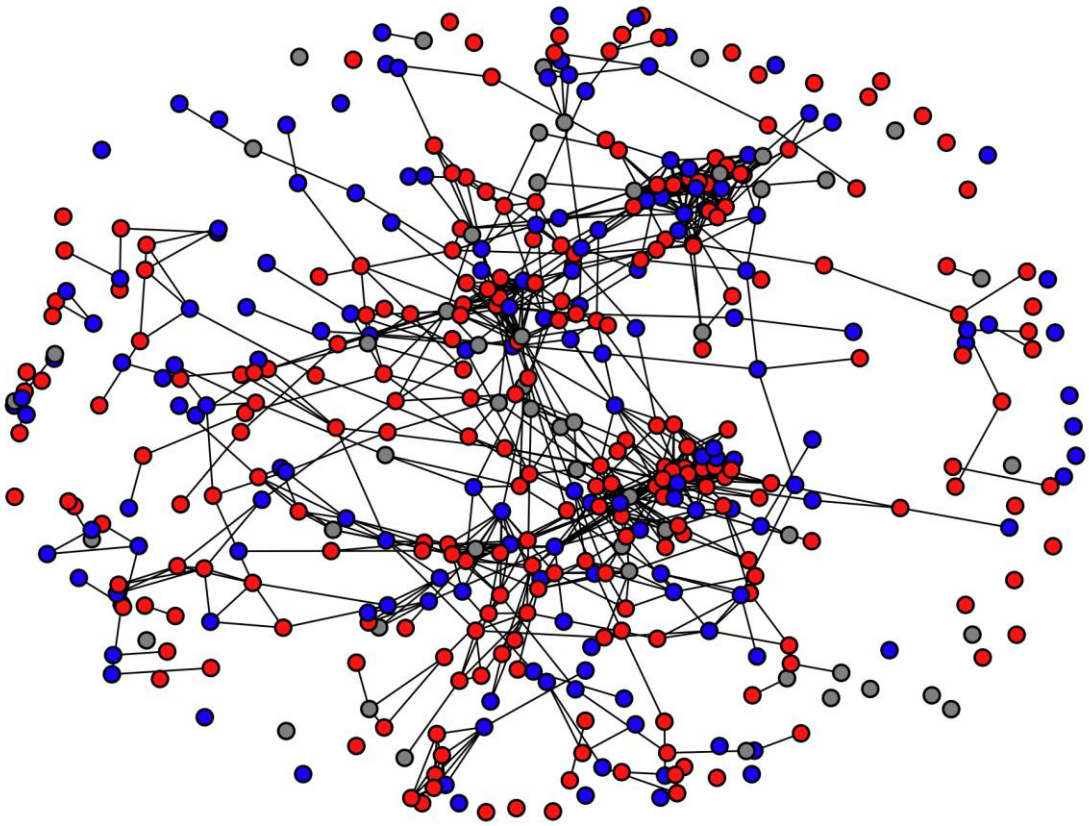

Blue indicates individuals who reported influenza vaccination, red indicates individuals who reported not receiving the influenza vaccine, and gray indicates individuals with missing influenza vaccination status. 71 students had no reported contacts.

Figure 6.2: Ten-week risk of influenza-like illness (A) and laboratory-confirmed influenza (B) under policies to increase log-odds of influenza vaccination

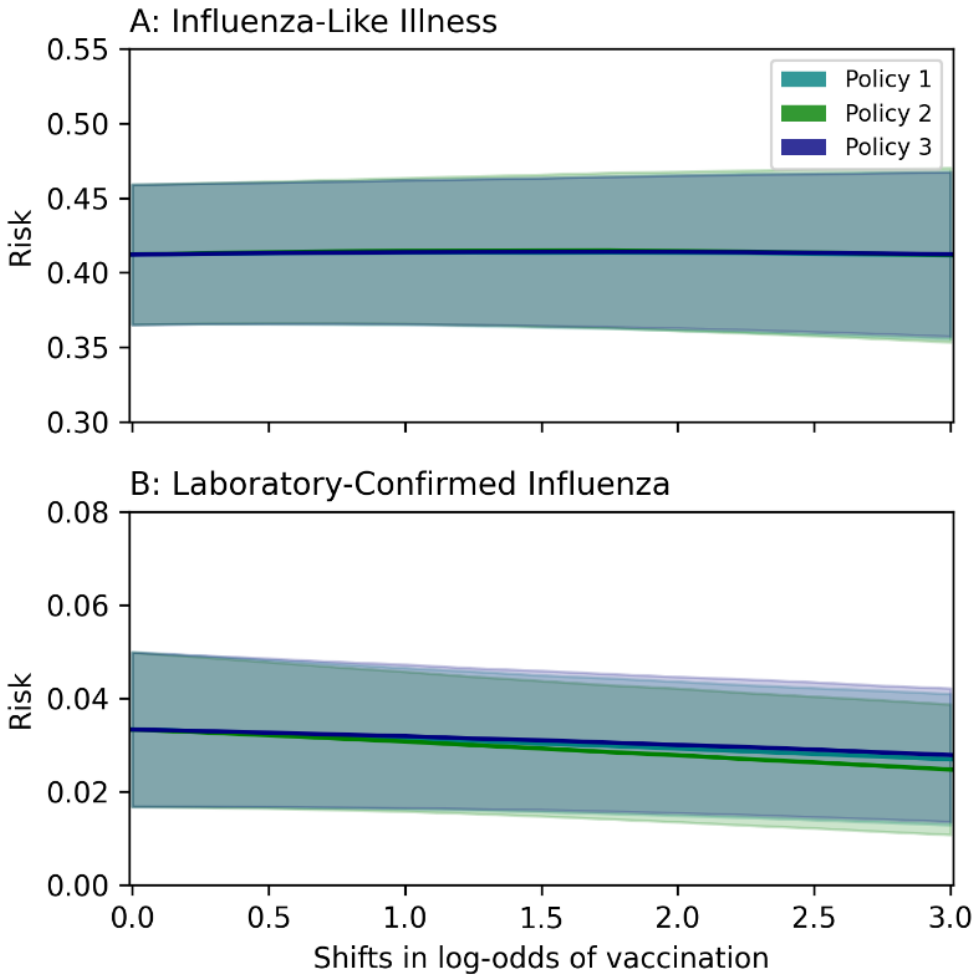

Shaded regions indicated 95% CI. ILI was defined as the presence of coughing plus at least one of the following symptoms: fever, body aches, or chills. Laboratory-confirmation of influenza was determined via quantitative polymerase chain reaction
Policy 1: theoretical policy to emphasize benefits of the vaccine and dispelling common myths.
Policy 2: theoretical policy to address non-financial barriers to vaccination
Policy 3: theoretical policy to address financial barriers to vaccination

Figure 6.3: Measurement error sensitivity analysis of the ten-week risk of influenza-like illness (A) and laboratory-confirmed influenza (B) under policies to increase log-odds of influenza vaccination

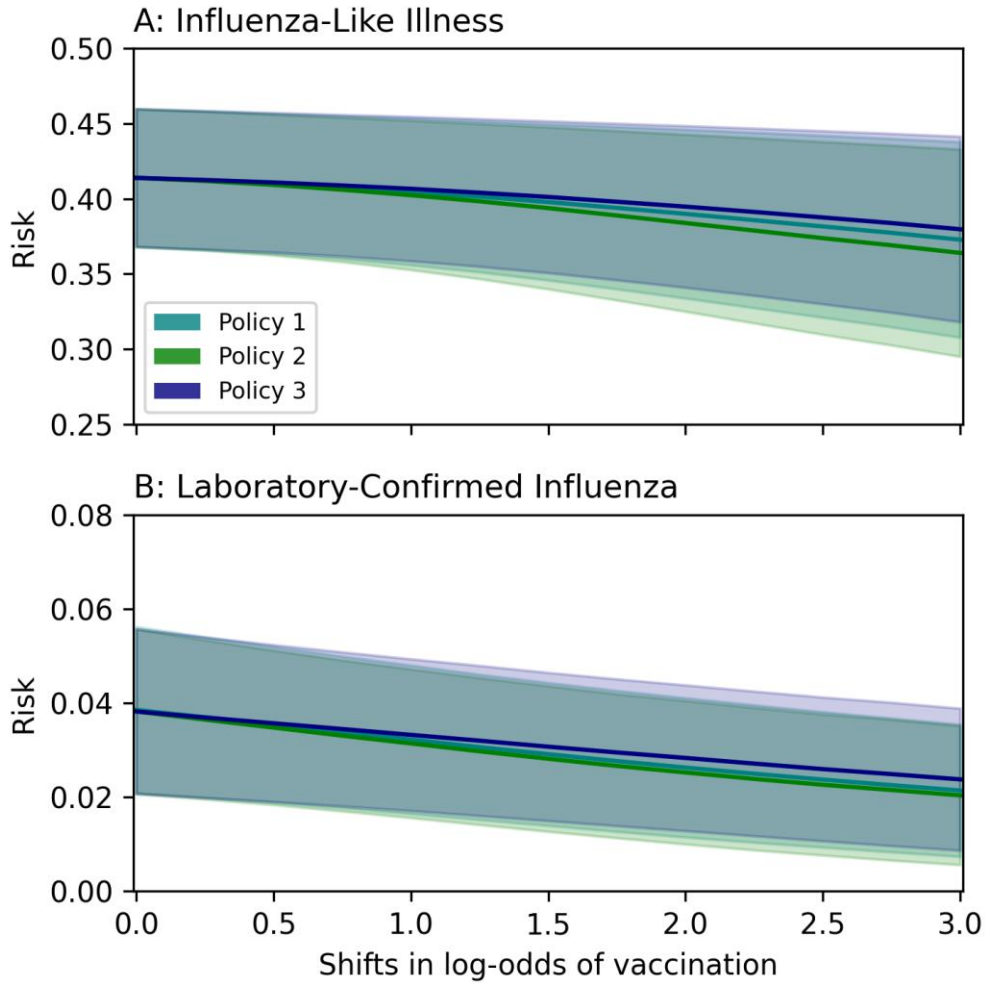

Shaded regions indicated 95% CI. ILI was defined as the presence of coughing plus at least one of the following symptoms: fever, body aches, or chills. Laboratory-confirmation of influenza was determined via quantitative polymerase chain reaction.
Policy 1: theoretical policy to emphasize benefits of the vaccine and dispelling common myths.
Policy 2: theoretical policy to address non-financial barriers to vaccination
Policy 3: theoretical policy to address financial barriers to vaccination

CHAPTER 7: CONCLUSIONS

University students have sub-optimal influenza vaccination rates, a high influenza attack rate, and may be an important demographic population for transmission of influenza.[93-95, 98, 99, 101-104] This dissertation aimed to compare different strategies or policies of increasing influenza vaccination among university students and the subsequent risk of influenza. To estimate influenza risk, we used a recent extension of TMLE for dependent data and implemented a Bayesian procedure to reduce measurement error associated with self-reported contacts. To guide the application of those methods, two simulation studies were conducted. In summary, the work presented here exemplifies a practical analysis focused on estimands important for public health decisions with applications for vaccination and infectious disease risk.

This work addressed the estimation of the risk of influenza through three aims. First, a simulation study was conducted to compare imputation and Bayesian approaches to address measurement of edges in a network. While both MIME and Bayesian procedures could be used to address measurement error of edges, we found the Bayesian approach to have more stable performance and avoid the need for the extensive collection of a gold-standard measure from a random sample of the population. However, informative priors for sensitivity and specificity were necessary for the context of a single observation of a network. Second, another simulation study was conducted to evaluate the finite-sample performance of network-TMLE. Previous studies had only explored few data-generating mechanisms or simple random graphs. Network-TMLE outperformed an IID-TMLE across multiple settings with spillover effects. However, we found the performance of Network-TMLE to diminish for policies where individuals had probabilities close to one for exposure (e.g., CI coverage dropped below expected levels for policies where

nearly all individuals were exposed). The reduced performance is likely due to a lack of statistical support in the data, where no individuals had a majority of their contacts exposed but had nearly all of their contacts exposed under the policy. Performance differed by the exposure summary measure and the structure of the network, which had differing support requirements. Furthermore, restriction by degree generally improved performance for skewed degree distributions. Finally, we applied what was learned in the simulation studies to estimate changes in the risk of influenza under various policies to improve influenza vaccination uptake across a range of plausible values. In the primary analysis, results were consistent with little-to-no difference in risk of both ILI and laboratory-confirmed influenza for all policy variations. When accounting for measurement error, a greater reduction in the risk was observed. Previous evidence has found discrepancies between self-reported and sensor-collected contacts.[155-159] Additionally, differences were observed with the eX-FLU data when comparing self-reported contacts versus those recorded by Bluetooth. The difference between the primary and measurement error results indicates sensitivity of the findings to assumptions regarding the measurement of the network, and that measurement error was likely an issue. Approaches to assess the sensitivity of findings to measurement error should be regularly used with network-TMLE in practice.

7.1 Study Findings

In Chapter 4, estimation of common descriptive parameters of a network was shown to potentially be biased when either non-informative or informative measurement error of edges was present. The extent of bias varied by both the parameter, the true structure of the network, and whether measurement error was informative. Previous studies on the robustness of centrality measures (degree, betweenness, closeness, and eigenvector centrality) have found the impact of measurement error depends on the structure of the true network and the exact measure being used.[160-162] However, these studies focused on non-informative measurement error and centrality measures. Our simulation results extend these previous studies by

considering the impact of imperfect sensitivity and specificity jointly, informative measurement error, and other common network parameters beyond centrality. Consistent with the previous work, bias due to measurement error of edges was observed to be dependent on the chosen measure; the true, underlying structure of the network; and whether measurement error was informative.

To analytically address measurement error of edges, two proposed approaches were directly compared. MIME-ERGM was able to address measurement error, but its performance was limited by several caveats. First, MIME-ERGM had sub-par CI coverage when the gold-standard subsample consisted of only 40% of the network. Next, performance was poor in terms of both bias and CI coverage when the gold-standard subsample was selected by RDS. Lastly, MIME-ERGM had difficulties when the true network contained higher-order dependencies between nodes (i.e., triangles). Despite the inclusion of the geometrically weighted edgewise shared partners term, performance was inadequate.

Even in the context of a single measured network, the Bayesian procedure was found to perform adequately in almost all scenarios. A key advantage of the Bayesian approach over MIME, is that a gold-standard measure need not be available (nor even exist). However, this advantage comes at the price of heavy reliance on priors when only a single observation of the network is available. Without informative priors, difficulty in reconstructing the network may occur. Additionally, the Bayesian procedure failed to capture triangles, since a triangle term was not included in the network model.

In Chapter 5, we conducted an extensive simulation study regarding the performance of network-TMLE. Preceding simulation studies on the finite sample performance of network-TMLE had only considered relatively simple random graphs, few data-generating mechanisms, and made no direct comparisons to other estimators.[150, 151] Our simulation study expanded this previous work by using three networks that exhibited different structural properties (including a real-world contact network among university students), assessing various combinations of unit-

treatment and spillover effect combinations, using a Susceptible-Infected-Recovered model as a data generating mechanism, directly comparing network-TMLE with IID-TMLE, comparing different stochastic policy specifications, and providing an implementation of network-TMLE in Python. These simulations can help to further guide the application of network-TMLE.

When data was IID, IID-TMLE performed as expected, with little bias and near 95% CI coverage. When spillover effects were included in the data generating mechanism, IID-TMLE was biased, either under-estimating or over-estimating the mean depending on the specified policy. The poor performance was most stark for the scenario of a continuous outcome. These simulations demonstrate the danger of ignoring spillover effects when assessing mean outcomes under differing policies.

Network-TMLE was demonstrated under various unit-treatment and spillover effects, and outperformed IID-TMLE in terms of bias and CI coverage when spillover effects were present. This illustrates the importance of considering interference. For both the naloxone-opioid overdose and diet-BMI mechanisms, bias was minimal and CI coverage was near expected levels. For the uniform random graph, the non-parametric modeling approach for the exposure summary measure had worse CI coverage compared to the parametric model for policies where a large proportion of the population was exposed. For the clustered power-law random graph and the eX-FLU network, restricting by degree improved CI coverage for the naloxone-opioid overdose mechanism. For diet-BMI (where the summary measure for diet was a threshold), the performance was similar when restricting by degree or not. For the vaccine and infection transmission mechanism, 95% CI coverage was reduced, particularly at the extremes of the stochastic policies. However, the non-parametric model for the uniform graph and transmission mechanism led to improved coverage, indicative of potential misspecification of the summary measure for the exposure. For the statin-ASCVD mechanism, we found network-TMLE performance to have little bias, but increased ESE relative to IID-TMLE and decreased CI coverage for policies where all individuals had a high probability of receiving statins. These

results are likely due to issues of data sparsity that result from immediate contacts' exposure increasing the dimensionality of the model relative to the IID-TMLE approach.

These simulations suggest the following guidelines for application. First, restrictions by degree should be used when the exposure summary measure consists of multiple categories and the degree distribution of the network is skewed. When only a few individuals have many contacts and the summary measure consists of a count of exposed contacts, those few individuals may not have a 'stand-in' within the network. Instead, those individuals can be considered as a background feature and inference is performed for the remainder of nodes. When individuals with outlying values for degree are included, network-TMLE performed less well. Second, practical violations of positivity may be more common since policies change both individual and immediate contacts' exposures. For example, a policy that increases the probability of vaccination applies to both an individual's vaccination and their contacts' vaccination, both which define an individual's potential outcome. While stochastic policies rely on less support than deterministic ones, when exposure or treatment is less common, estimating the mean for a policy where most of the population is exposed may not be adequately supported by the data. For example, if influenza vaccination is uncommon in a population, then few individuals will have all of their immediate contacts vaccinated.
For assessment of a policy where nearly all individuals received the influenza vaccine, nearly all individuals will have their immediate contacts vaccinated. Therefore, the observed data may not contain information for those types of policies. To help assess support for policies, the following diagnostic plot procedure can be used. The values for the chosen summary measure are plotted stratified by the exposure for the observed data. Similarly, the stratified exposure summary measure under the policy is plotted. If little overlap occurs between the distributions of summary measures, this can be indicative of issues. Lastly, focusing on shifts in the log-odds of exposure may be more reasonable to assess compared to setting all individuals in the population to a constant probability.

In Chapter 6, the lessons learned from the previous simulation studies were used to estimate the risk of influenza under different distributions of influenza vaccination among university students. In the primary analysis, no difference in the risk of ILI across the various policies was observed. For laboratory-confirmed influenza, a minor decrease in risk occurred for all policies. However, the estimates in risk for both definitions of influenza were imprecise and the confidence intervals were consistent with no reduction in the risk of influenza.

To address measurement error of self-reported contacts, the Bayesian procedure for measurement assessed in Chapter 4 was used. Data collected from the iEpi subsample was further used to inform priors on the sensitivity and specificity of self-reported contacts for the measurement model. For the estimated network model, contacts were largely driven by dormitory assignment but were also related to gender, race, class year, and alcohol use. When accounting for measurement error, the reduction in risk of influenza (defined in terms of both ILI and laboratory-confirmation) was further reduced for policies with greater shifts in the log-odds. The greater reduction in influenza risk, in-line with theoretical expectations on the influenza vaccine, indicates that measurement error due to the self-reporting of contacts biased the primary results. Policies targeting the different categories of students had little difference between them. Therefore, our results do not provide a clear strategy to reduce influenza risk. It should also be noted that the conclusions from both the primary and measurement error analyses were consistent with a small or no reduction in the risk of influenza in the population.

7.2 Strengths and Limitations

This work provides a notable contribution to studying influenza vaccination and methodological approaches for infectious disease epidemiology studies more generally. The statistical analyses presented here focus on an estimand of import for public health decision making – what the risk of influenza would have been under changes in the distribution of influenza vaccination accounting for contacts between students. Previous work on influenza vaccination more broadly has tended to focus on the unit-treatment effect of the influenza

vaccine,[50, 128, 129] which may be of lesser interest for public health decision making. While the policies assessed are somewhat non-specific in their exact application (e.g., what the educational materials would contain, how a vaccination clinic would be publicized, etc.), there are several advantages to our approach. First, the policies focused on reported reasons for not receiving the influenza vaccine and adhered to the contraindications for the vaccine.[288] Second, shifts in log-odds for each policy were further varied across a range of plausible values. The focus on stochastic policies stands in contrast to the usual focus on all-exposed or none-exposed estimands, which are optimistic in the sense of possible changes in the distribution of exposures.[255, 272-274] Previous approaches to increase influenza vaccination uptake have resulted in only minor to moderate increases in vaccine receipt.[94, 95, 275, 276] Therefore, scenarios of everyone receiving the influenza vaccine are of little interest. By exploring variations in shifting the log-odds of vaccination, how effective the policy would have to be at increasing vaccine uptake was also compared and suggested that continuing to increase the probabilities of vaccination uptake continued to reduce the risk of influenza.

There are also several advantages of the eX-FLU study design that contributed important elements to our analyses. Firstly, the nasal and throat specimen collection strategy of the original eX-FLU study allowed for the capture of asymptomatic influenza infections. Second, electronic sensor collected contacts were captured. While these measurements were not available for the full population, they did allow for informed priors for the sensitivity and specificity of self-reported contacts in this population. Third, the eX-FLU study consisted of rigorous follow-up of a large and geographically fixed study population.

Regarding the analytical approach of this work, several quantitative approaches were used to address potential biases. Furthermore, the finite-sample performance of the methods used was assessed through extensive simulation studies. First, the performance of network-TMLE and two competing approaches to quantitatively accounting for measurement error of edges were assessed in a variety of contexts. These simulation studies contributed to the

application of those methods in a practical setting. The simulation study of network-TMLE was an extensive assessment, included a real-world network, and explicitly compared performance with a TMLE that assumed data was IID. The measurement error of edges simulation study compared multiple approaches for various parameters in multiple network generation models. Second, measurement error for influenza and the contacts was explored. As previous work has indicated, defining influenza by the presence of ILI misattributes respiratory symptoms to influenza[48] and can result in underestimates of the effectiveness of influenza vaccination.[80] For this reason, laboratory-confirmed influenza was assessed in addition to ILI. Finally, self-reported contacts have been observed as underestimates compared to electronic sensors in other works.[155-159] To account for measurement error of self-reported contacts, a Bayesian approach was used,[165] which was further informed by the iEpi subsample.

Our analyses regarding influenza risk have several limitations. During the 2012-2013 influenza season, both the inactivated and live attenuated influenza vaccines were available.[288] Unfortunately, information on the type of influenza vaccine students received was not collected. Previous studies on the unit-treatment effect of the influenza vaccine have found differences in effectiveness for children and adolescents.[60, 289, 290] If these differences extend to young adults, then the inability to distinguish between the two vaccines in our analysis can be viewed as a violation of the treatment-variation irrelevance assumption.[256, 291] A potential way to side-step this issue is to re-interpret the results for the risk of influenza as a weighted average of the different types of vaccines, where the unobserved weights correspond to the probability of receiving each vaccine that naturally occurred in the population.[292, 293] This interpretation may questionable for approaches like vaccination clinics since only a singular type of influenza vaccine may be offered at those sites.

Conditional exchangeability necessitates that potential outcomes are independent of vaccination. Under weak dependence, this independence is extended to the vaccination of immediate contacts. While we included a variety of previously identified risk factors and health

behaviors, the concern of unobserved confounders remains. One issue is that follow-up for influenza infection did not start until January, but the influenza season starts in the Autumn. Therefore, preceding influenza cases (and subsequent immunity to circulating influenza during the follow-up period) could have been more common in the unvaccinated individuals and led to an over-estimate of the risk. Additionally, all contacts were considered equivalent, but differences in their context (e.g., indoor versus outdoor, dormitory room versus classroom) likely have differential probabilities of influenza transmission. Lastly, the collapsing of several categorical variables into fewer categories (e.g., race, high-risk conditions) assumes that those collapsed categories are homogenous. However, that may not be the case.

Relatedly, models were used for both the exposure and outcome. While several flexible algorithms were included in a super learner, the algorithms that could be included in the super learner were restricted to be Donsker. Restrictions on the complexity of algorithms in necessary without extension of procedures like cross-fitting.[252, 285] Related to the issue of the model specification, is the specification of the summary measure of immediate contacts' vaccination. While a non-parametric approach for estimation of the exposure summary measure exists, its application is precluded from use with highly skewed degree distributions. Finally, the assumption of weak dependence limits interference to the vaccination of immediate contacts. This assumption is unlikely since the follow-up period is longer than the combined incubation and infectiousness period of influenza.[284] Under the assumption that influenza vaccination is protective for contacts, the transmission of influenza would be reduced among further out contacts. Therefore, the violation of the weak dependence may mean the risk of influenza under the policies is lower than estimated.

With regards to missing data, an extension of MICE was used to account for multiple variables with missing data. For MICE to address missing data, the imputation models must include all variables that are common causes of both the values being missing and the missing values themselves. Additionally, the use of parametric models requires that the models are

flexible enough to capture the true distribution. Unfortunately, the complexity of some models was restricted due to model convergence issues. Another missing data issue is the students who were not enrolled in the study. While students were recruited from six dormitories, not everyone in each dormitory was enrolled. Therefore, unobserved links capable of influenza transmission likely exist.

Furthermore, our estimate is for the sample risk. In other words, the targeted quantity was the risk of influenza for the students in the study. Therefore, our results cannot be extended outside of the sample. Whether and under what assumptions our results could be generalized or transported to other populations is an open question. Even if our inferential model was for a larger population than the sample, there remains the issue of inconsistent matching between the vaccine strain and the circulating influenza strain each year. During poor strain matching years, the reduction in risk of influenza may be substantially lessened compared to seasons with ideal strain matching. Additionally, the severity of the preceding influenza season may further enhance or reduce vaccination uptake either directly or through effective communication regarding harms.

Finally, the ability to differentiate between policies in terms of reducing the risk of influenza was hampered by the relatively few laboratory-confirmed influenza cases. Since only about 4% of students had laboratory-confirmed influenza, the maximum reduction that could have been observed was 4%. While ILI was more common, it is subject to measurement error when used as a proxy for influenza.[80]

7.3 Public Health Implications

Focus solely on the unit-treatment effect may undervalue the benefits of the influenza vaccine. By ignoring protective spillover effects, the benefits to increasing overall vaccination uptake may be underestimated. Realistic increases in the log-odds of vaccination among university students resulted in a reduced risk of influenza. This difference was more pronounced when accounting for measurement error of self-reported contacts. However, stark differences

between policies in terms of the subsequent influenza risk were not observed. Therefore, a clear preference in policy approach was not indicated.

More broadly, the methodological approaches detailed here can be applied to a variety of settings. Despite the long-recognized existence of interference in infectious disease epidemiology,[136] the implications of interference and dependence between individuals are often ignored. As an illustrative example of this issue, consider the early research on concurrent sexual partners as a risk factor for HIV infection. Early research studies concluded that concurrent sexual partnerships were not significantly associated with increased acquisition of HIV infection.[294-296] However, these conclusions were in contrast to mathematical modeling studies from around the same time.[297, 298] While several explanations for the discrepant results exist, one reason is that empirical studies did not account for the structure of sexual networks.[299, 300] A more recent observational study that incorporated information on the structure of the underlying sexual network did find concurrency to be associated with increased HIV transmission.[301] This example highlights the need to think beyond the individual when studying infectious diseases.

The ongoing SARS-CoV-2 pandemic has only further stressed the importance of considering dependencies between individuals for infectious disease research. As another illustrative example, consider the effectiveness of face masks. When evaluating the effectiveness of masks, the distinction between protection for the wearer (unit-treatment effects) and protection for the wearer's contacts (spillover effects) is vital.[302, 303] For laboratory-confirmed influenza, the current evidence is consistent with a minor protective effect of individuals but pooled estimates across randomized control trials are still imprecise (risk ratio 0.78; 95% CI: 0.51-1.20).[304] But even barring protection for the wearer, the widespread use of masks could be beneficial due to reduced SARS-CoV-2 or influenza transmission from infectious individuals. By reducing the virus particles exhaled, transmission from asymptomatic or symptomatic individuals can be reduced or prevented.[305, 306] Because of these competing mechanisms for

what constitutes protectiveness of masks or other interventions, studies to address unit-treatment, spillover effects, and their combination are needed.

Interference also extends beyond infectious diseases, with examples including household opioid use in pharmacoepidemiology,[243] passive tobacco smoke exposure in cancer epidemiology,[244, 245] and behavior among children within classrooms in developmental psychology.[246] Even in the absence of interference, dependencies between observations can be of concern. Network dependence, when social connections give rise to statistical dependencies, can lead to both spurious associations and invalid variance estimates even without the occurrence of interference.[307] The occurrence of network dependence has been illustrated with the Framingham Heart Study,[307] which has been extensive used under the assumption that enrolled individuals were IID. The assumption of no interference and no network dependence may be unlikely in many substantive topic areas in epidemiology.

From the vantage point of these analytical difficulties, the simulation studies and application of network-TMLE to address a question regarding influenza vaccination can be viewed as a step towards more rigorously applied research in infectious diseases and epidemiology more broadly.

7.4 Future Research

Influenza vaccine research would benefit from a focus on other estimands in addition to the unit-treatment effect. We demonstrated a method for general interference; however, other approaches for general interference and partial interference are available.[139-141, 145, 149, 308, 309] Partial interference study designs have been used to quantify the spillover effect of increasing influenza vaccination among children.[71-75] Vaccine and infectious disease research more generally, would benefit from greater adoption of these analytical approaches. Examining vaccine effects through the lens of interference also has implications regarding studies of unit-treatment vaccine effectiveness as well. While comparisons in systematic reviews and meta-analyses directly compare unit-treatment vaccine effectiveness across studies,[50] those

estimates may not be comparable due to differences in uptake the vaccination status of the population or how vaccination is distributed. Specifically, the v_{-i} part of the potential outcomes, $Y_i(v_i, v_{-i})$, may be dissimilar across individual studies. Ultimately, a deeper focus on interference and its implications can serve to improve influenza vaccine research and infectious disease research more broadly.

Regarding the application of network-TMLE, there are several areas where further simulation studies would be beneficial. First, best practices regarding model selection for the exposure and outcomes models need further development. The selection of summary measures, particularly for the summary measure for the exposure, requires further exploration. Network-TMLE requires that summary measures are correctly specified. However, knowing the correct summary measure may be difficult if not impossible, particularly in settings of infection transmission. Sensitivity to misspecification of the summary measure with flexible models and alternative approaches for estimation of exposure summary measure model (e.g., conditional density super learner[277, 278]) are remaining gaps. Second, whether and how the population variance can be estimated under weaker conditions would be beneficial. The current requirements of the confounders being IID limit its potential use. Third, other estimands should also be explored. A procedure has been described for estimating marginal unit-treatment effects,[151] but how network-TMLE can be generalized to other related estimands (i.e., spillover effects, total effects) is also of interest. Fourth, the performance of network-TMLE should be explored when the network is only partially observed. Lastly, a longitudinal extension of network-TMLE is needed. By defining the risk period into smaller intervals and applying a longitudinal network-TMLE, the weak dependence assumption could be made more plausible.

For addressing measurement error of edges, implementations of MIME that use different statistical models should be assessed. For example, additive and multiplicative effect models have been proposed as an alternative to ERGM more generally. These models have the advantage of avoiding the need to explicitly specify features of the network like triangles.

Therefore, the performance of MIME may be improved in clustered networks if additive and multiplicative effect models are used instead. In regards to the Bayesian approach to addressing measurement error, allowing for more flexible models to capture features like triangles in the network model is needed. Furthermore, the expansion of a Bayesian model to incorporate other systematic errors, such as missing data or measurement error of node attributes, would be beneficial for practice.

7.5 Conclusions

Our work is the first, to our knowledge, to assess the risk of influenza under policies shifting in the probability of students receiving the influenza vaccine. Preceding work has either focused on vaccination receipt as the outcome[94, 95] or has focused exclusively on the unit-treatment (i.e., direct) effectiveness of the influenza vaccine.[129] Informed by the preceding work, several distinct strategies were conceptualized and explored over a range of plausible shifts in the log-odds of vaccination. To accomplish this, we used several recently developed methods, including Bayesian approaches to account for measurement error and an extension of TMLE for dependent data. To inform our application of these methods, we conducted extensive simulation studies regarding performance. While our analyses are perhaps less informative regarding the selection of a singular strategy to increase influenza vaccination to reduce influenza risk among university students, the simultaneous application of network-TMLE and approaches to measurement error of edges is notable. The results of our simulations and analyses can serve as an example for future applications in vaccine and infectious disease research more broadly.

APPENDIX 1: CHAPTER 4 SUPPLEMENTARY MATERIALS

For network-3, MIME-ERGM-SRS failed to converge 119 times for non-informative measurement error with 40% of the gold-standard, 39 times for non-informative measurement error with 60% of the gold-standard, 108 times for informative measurement error with 40% of the gold-standard, and 35 times for informative measurement error with 60% of the gold-standard. MIME-ERGM-RDS failed to converge 7 times for non-informative measurement error with 40% of the gold-standard, and 8 times for informative measurement error with 40% of the gold-standard. None of the other approaches failed to converge.

Table A1.1: Bias for parameters for network-1

	Edges	Density	Assortativity	Degree	Cluster
True	0.2	0.004	0.000	0.00	0.000
Non-informative					
Naïve*	138.6	0.007	0.040	2.77	0.006
Gold-standard SRS 40%	-326.8	0.000	-0.016	-4.68	-0.010
Gold-standard SRS 60%	-248.6	0.000	-0.006	-3.10	-0.005
Gold-standard RDS 40%†	-269.2	0.018	-0.005	-1.80	0.012
Gold-standard RDS 60%†	-178.3	0.010	-0.007	-0.76	0.007
MIME-SRS-40%	-1.71	0.000	0.005	-0.03	0.000
MIME-SRS-60%	1.54	0.000	-0.002	0.03	0.000
MIME-RDS-40%†	356.1	0.018	0.012	7.12	0.023
MIME-RDS-60%†	193.1	0.010	0.009	3.86	0.013
Bayes	-5.0	0.000	-0.002	-0.10	0.000
Informative					
Naïve*	124.5	0.006	-0.088	2.49	0.006
Gold-standard SRS 40%	-326.8	0.000	-0.016	-4.68	-0.010
Gold-standard SRS 60%	-248.6	0.000	-0.006	-3.10	-0.005
Gold-standard RDS 40%†	-269.2	0.018	-0.005	-1.80	0.012
Gold-standard RDS 60%†	-178.2	0.010	-0.007	-0.76	0.007
MIME-SRS-40%	0.7	0.000	0.004	0.02	0.000
MIME-SRS-60%	-1.8	0.000	0.007	-0.35	0.000
MIME-RDS-40%†	353.3	0.018	0.011	7.07	0.023
MIME-RDS-60%†	194.4	0.010	0.009	3.89	0.013
Bayes	-4.5	0.000	0.003	-0.09	0.000

SRS: simple random sample, RDS: respondent-driven sampling, MIME: multiple imputation for measurement error. Non-informative consisted of measurement error occurring randomly. Informative consisted of measurement error occurring conditional on node pairs having the same values of B. Bias was defined as the estimate parameter from the corresponding method minus the true parameter. The true parameter was calculated as the mean parameter from 10,000 generated networks.

* Naïve consisted of the parameters estimated using the observed (mismeasured) network
† Respondent-driven sampling consisted of 10% of the subsample size being selected as seeds. Each seed node then nominated three nodes based on random selection of nodes that it shared a true edge with. The procedure was repeated for nominated nodes until the gold-standard subsample size was met.

Table A1.2: Empirical standard error for parameters for network-1

	Edges	Density	Assortativity	Degree	Cluster
True	20.1	0.001	0.049	0.40	0.008
Non-informative					
Naïve*	21.6	0.001	0.042	0.43	0.007
Gold-standard SRS 40%	7.6	0.002	0.120	0.38	0.013
Gold-standard SRS 60%	11.9	0.002	0.079	0.40	0.011
Gold-standard RDS 40%†	7.0	0.002	0.085	0.35	0.020
Gold-standard RDS 60%†	10.6	0.001	0.066	0.35	0.013
MIME-SRS-40%	50.4	0.003	0.107	1.01	0.004
MIME-SRS-60%	32.9	0.002	0.072	0.66	0.003
MIME-RDS-40%†	45.2	0.002	0.074	0.90	0.004
MIME-RDS-60%†	29.6	0.001	0.058	0.59	0.003
Bayes	27.2	0.001	0.061	0.55	0.004
Informative					
Naïve*	21.0	0.001	0.039	0.42	0.006
Gold-standard SRS 40%	7.6	0.002	0.120	0.38	0.013
Gold-standard SRS 60%	11.9	0.002	0.079	0.40	0.011
Gold-standard RDS 40%†	7.0	0.002	0.085	0.35	0.020
Gold-standard RDS 60%†	10.6	0.001	0.066	0.35	0.013
MIME-SRS-40%	49.5	0.002	0.106	0.99	0.004
MIME-SRS-60%	31.8	0.002	0.070	0.64	0.003
MIME-RDS-40%†	44.9	0.002	0.076	0.90	0.004
MIME-RDS-60%†	30.2	0.002	0.057	0.60	0.003
Bayes	27.5	0.001	0.060	0.55	0.004

SRS: simple random sample, RDS: respondent-driven sampling, MIME: multiple imputation for measurement error. Non-informative consisted of measurement error occurring randomly. Informative consisted of measurement error occurring conditional on node pairs having the same values of B. Bias was defined as the estimate parameter from the corresponding method minus the true parameter. The true parameter was calculated as the mean parameter from 10,000 generated networks.

* Naïve consisted of the parameters estimated using the observed (mismeasured) network
† Respondent-driven sampling consisted of 10% of the subsample size being selected as seeds. Each seed node then nominated three nodes based on random selection of nodes that it shared a true edge with. The procedure was repeated for nominated nodes until the gold-standard subsample size was met.

Table A1.3: Confidence interval coverage for parameters for network-1

	Edges	Density	Assortativity	Degree	Cluster
True	100%	94%	83%	99%	95%
Non-informative					
Naïve*	6%	0%	67%	0%	99%
Gold-standard SRS 40%	0%	94%	82%	0%	49%
Gold-standard SRS 60%	0%	96%	83%	0%	78%
Gold-standard RDS 40%†	0%	0%	84%	12%	94%
Gold-standard RDS 60%†	0%	0%	83%	88%	96%
MIME-SRS-40%	92%	71%	73%	80%	100%
MIME-SRS-60%	100%	90%	88%	96%	100%
MIME-RDS-40%†	0%	0%	74%	0%	22%
MIME-RDS-60%†	0%	0%	89%	0%	100%
Bayes	100%	90%	87%	95%	100%
Informative					
Naïve*	19%	0%	23%	0%	99%
Gold-standard SRS 40%	0%	94%	82%	0%	49%
Gold-standard SRS 60%	0%	96%	83%	0%	76%
Gold-standard RDS 40%†	0%	0%	84%	12%	94%
Gold-standard RDS 60%†	0%	0%	83%	88%	96%
MIME-SRS-40%	93%	73%	74%	83%	100%
MIME-SRS-60%	99%	91%	90%	96%	100%
MIME-RDS-40%†	0%	0%	71%	0%	21%
MIME-RDS-60%†	0%	0%	89%	0%	100%
Bayes	99%	89%	87%	96%	100%

SRS: simple random sample, RDS: respondent-driven sampling, MIME: multiple imputation for measurement error. Non-informative consisted of measurement error occurring randomly. Informative consisted of measurement error occurring conditional on node pairs having the same values of B. CI coverage was calculated as the percent of 95% CI that contained the true value.

* Naïve consisted of the parameters estimated using the observed (mismeasured) network
† Respondent-driven sampling consisted of 10% of the subsample size being selected as seeds. Each seed node then nominated three nodes based on random selection of nodes that it shared a true edge with. The procedure was repeated for nominated nodes until the gold-standard subsample size was met.

Table A1.4: Bias for parameters for network-2

	Edges	Density	Assortativity	Degree	Cluster
True	1.1	0.000	-0.001	0.00	0.000
Non-informative					
Naïve*	144.5	0.007	-0.019	2.89	0.007
Gold-standard SRS 40%	-283.0	0.000	-0.008	-4.06	-0.009
Gold-standard SRS 60%	-215.3	0.000	-0.007	-2.69	-0.005
Gold-standard RDS 40%†	-225.3	0.018	-0.008	-1.18	0.009
Gold-standard RDS 60%†	-144.5	0.010	-0.007	-0.33	0.007
MIME-SRS-40%	0.6	0.000	0.003	0.01	0.000
MIME-SRS-60%	-0.3	0.000	0.000	-0.01	0.000
MIME-RDS-40%†	354.7	0.018	-0.003	7.09	0.023
MIME-RDS-60%†	192.8	0.010	-0.004	3.86	0.013
Bayes	-10.4	-0.001	0.003	-0.21	-0.001
Informative					
Naïve*	133.9	0.007	-0.163	2.68	0.007
Gold-standard SRS 40%	-283.0	0.000	-0.008	-4.06	-0.009
Gold-standard SRS 60%	-215.3	0.000	-0.007	-2.69	-0.005
Gold-standard RDS 40%†	-225.3	0.018	-0.008	-1.18	0.009
Gold-standard RDS 60%†	-144.5	0.010	-0.007	-0.33	0.007
MIME-SRS-40%	-0.5	0.000	0.013	-0.01	0.001
MIME-SRS-60%	1.8	0.000	0.002	0.04	0.000
MIME-RDS-40%†	354.5	0.018	-0.004	7.09	0.023
MIME-RDS-60%†	191.1	0.010	0.000	3.82	0.013
Bayes	-5.2	0.000	0.007	-0.11	-0.001

SRS: simple random sample, RDS: respondent-driven sampling, MIME: multiple imputation for measurement error. Non-informative consisted of measurement error occurring randomly. Informative consisted of measurement error occurring conditional on node pairs having the same values of B. Bias was defined as the estimate parameter from the corresponding method minus the true parameter. The true parameter was calculated as the mean parameter from 10,000 generated networks.

* Naïve consisted of the parameters estimated using the observed (mismeasured) network
† Respondent-driven sampling consisted of 10% of the subsample size being selected as seeds. Each seed node then nominated three nodes based on random selection of nodes that it shared a true edge with. The procedure was repeated for nominated nodes until the gold-standard subsample size was met.

Table A1.5: Empirical standard error for parameters for network-2

	Edges	Density	Assortativity	Degree	Cluster
True	18.1	0.001	0.055	0.36	0.008
Non-informative					
Naïve*	21.9	0.001	0.046	0.44	0.007
Gold-standard SRS 40%	7.5	0.002	0.137	0.38	0.012
Gold-standard SRS 60%	11.0	0.002	0.087	0.37	0.011
Gold-standard RDS 40%†	6.3	0.002	0.096	0.32	0.019
Gold-standard RDS 60%†	9.5	0.001	0.069	0.32	0.013
MIME-SRS-40%	46.8	0.002	0.119	0.94	0.004
MIME-SRS-60%	29.2	0.001	0.079	0.58	0.002
MIME-RDS-40%†	41.7	0.002	0.081	0.83	0.004
MIME-RDS-60%†	27.7	0.001	0.061	0.55	0.002
Bayes	26.6	0.001	0.070	0.53	0.003
Informative					
Naïve*	21.7	0.001	0.042	0.43	0.007
Gold-standard SRS 40%	7.5	0.002	0.137	0.38	0.012
Gold-standard SRS 60%	11.0	0.002	0.087	0.37	0.011
Gold-standard RDS 40%†	6.3	0.002	0.096	0.32	0.019
Gold-standard RDS 60%†	9.5	0.001	0.069	0.32	0.013
MIME-SRS-40%	45.2	0.002	0.118	0.90	0.004
MIME-SRS-60%	30.0	0.002	0.078	0.60	0.003
MIME-RDS-40%†	42.1	0.002	0.078	0.84	0.004
MIME-RDS-60%†	27.2	0.001	0.062	0.55	0.002
Bayes	25.1	0.001	0.076	0.50	0.004

SRS: simple random sample, RDS: respondent-driven sampling, MIME: multiple imputation for measurement error. Non-informative consisted of measurement error occurring randomly. Informative consisted of measurement error occurring conditional on node pairs having the same values of B. Bias was defined as the estimate parameter from the corresponding method minus the true parameter. The true parameter was calculated as the mean parameter from 10,000 generated networks.

* Naïve consisted of the parameters estimated using the observed (mismeasured) network
† Respondent-driven sampling consisted of 10% of the subsample size being selected as seeds. Each seed node then nominated three nodes based on random selection of nodes that it shared a true edge with. The procedure was repeated for nominated nodes until the gold-standard subsample size was met.

Table A1.6: Confidence interval coverage for parameters for network-2

	Edges	Density	Assortativity	Degree	Cluster
True	100%	96%	83%	100%	93%
Non-informative					
Naïve*	1%	0%	79%	0%	99%
Gold-standard SRS 40%	0%	93%	82%	0%	35%
Gold-standard SRS 60%	0%	94%	84%	0%	73%
Gold-standard RDS 40%†	0%	0%	82%	55%	89%
Gold-standard RDS 60%†	0%	0%	85%	99%	96%
MIME-SRS-40%	92%	71%	74%	80%	100%
MIME-SRS-60%	99%	92%	91%	96%	100%
MIME-RDS-40%†	0%	0%	74%	0%	23%
MIME-RDS-60%†	0%	0%	90%	0%	100%
Bayes	97%	87%	88%	93%	100%
Informative					
Naïve*	3%	0%	1%	0%	99%
Gold-standard SRS 40%	0%	93%	82%	0%	35%
Gold-standard SRS 60%	0%	94%	84%	0%	73%
Gold-standard RDS 40%†	0%	0%	82%	55%	89%
Gold-standard RDS 60%†	0%	0%	85%	99%	96%
MIME-SRS-40%	93%	75%	73%	82%	100%
MIME-SRS-60%	99%	91%	91%	96%	100%
MIME-RDS-40%†	0%	0%	75%	0%	22%
MIME-RDS-60%†	0%	0%	91%	0%	100%
Bayes	99%	89%	84%	95%	100%

SRS: simple random sample, RDS: respondent-driven sampling, MIME: multiple imputation for measurement error. Non-informative consisted of measurement error occurring randomly. Informative consisted of measurement error occurring conditional on node pairs having the same values of B. CI coverage was calculated as the percent of 95% CI that contained the true value.

* Naïve consisted of the parameters estimated using the observed (mismeasured) network
† Respondent-driven sampling consisted of 10% of the subsample size being selected as seeds. Each seed node then nominated three nodes based on random selection of nodes that it shared a true edge with. The procedure was repeated for nominated nodes until the gold-standard subsample size was met.

Table A1.7: Bias for parameters for network-3

	Edges	Density	Assortativity	Degree	Cluster
True	-1.1	0.000	0.000	-0.01	0.000
Non-informative					
Naïve*	45.9	0.002	0.020	0.92	-0.059
Gold-standard SRS 40%	-800.0	0.000	-0.010	-11.49	-0.032
Gold-standard SRS 60%	-608.3	0.000	-0.002	-7.61	-0.010
Gold-standard RDS 40%†	-705.5	0.030	-0.001	-6.78	0.043
Gold-standard RDS 60%†	-481.9	0.018	0.001	-3.40	0.025
MIME-SRS-40%	550.3	0.028	0.005	11.01	-0.024
MIME-SRS-60%	435.4	0.022	0.006	8.71	-0.014
MIME-RDS-40%†	954.8	0.048	0.017	19.09	-0.025
MIME-RDS-60%†	708.1	0.036	0.016	14.16	-0.017
Bayes	-3.3	0.000	0.000	-0.07	-0.071
Informative					
Naïve*	32.0	0.002	-0.019	0.64	-0.057
Gold-standard SRS 40%	-800.0	0.000	-0.010	-11.49	-0.032
Gold-standard SRS 60%	-608.3	0.000	-0.002	-7.61	-0.010
Gold-standard RDS 40%†	-705.5	0.030	-0.001	-6.78	0.043
Gold-standard RDS 60%†	-481.9	0.018	0.001	-3.40	0.025
MIME-SRS-40%	568.0	0.029	0.004	11.36	-0.022
MIME-SRS-60%	441.2	0.022	0.008	8.82	-0.014
MIME-RDS-40%†	947.4	0.048	0.016	18.95	-0.026
MIME-RDS-60%†	707.9	0.036	0.015	14.16	-0.017
Bayes	-6.6	0.000	0.004	-0.13	-0.068

SRS: simple random sample, RDS: respondent-driven sampling, MIME: multiple imputation for measurement error. Non-informative consisted of measurement error occurring randomly. Informative consisted of measurement error occurring conditional on node pairs having the same values of B. Bias was defined as the estimate parameter from the corresponding method minus the true parameter. The true parameter was calculated as the mean parameter from 10,000 generated networks.

* Naïve consisted of the parameters estimated using the observed (mismeasured) network
† Respondent-driven sampling consisted of 10% of the subsample size being selected as seeds. Each seed node then nominated three nodes based on random selection of nodes that it shared a true edge with. The procedure was repeated for nominated nodes until the gold-standard subsample size was met.

Table A1.8: Empirical standard error for parameters for network-3

	Edges	Density	Assortativity	Degree	Cluster
True	43.2	0.000	0.023	0.35	0.004
Non-informative					
Naïve*	62.8	0.003	0.029	1.26	0.008
Gold-standard SRS 40%	18.2	0.006	0.075	0.91	0.033
Gold-standard SRS 60%	32.5	0.005	0.049	7.69	0.022
Gold-standard RDS 40%†	23.6	0.007	0.057	1.18	0.026
Gold-standard RDS 60%†	37.7	0.005	0.042	1.26	0.016
MIME-SRS-40%	617.4	0.031	0.060	12.35	0.039
MIME-SRS-60%	338.5	0.017	0.040	6.77	0.020
MIME-RDS-40%†	298.7	0.015	0.048	5.97	0.015
MIME-RDS-60%†	223.9	0.011	0.033	4.48	0.009
Bayes	78.3	0.004	0.033	1.57	0.007
Informative					
Naïve*	63.0	0.003	0.031	1.26	0.008
Gold-standard SRS 40%	18.2	0.006	0.075	0.91	0.033
Gold-standard SRS 60%	32.5	0.005	0.049	7.69	0.022
Gold-standard RDS 40%†	23.6	0.007	0.057	1.18	0.026
Gold-standard RDS 60%†	37.7	0.005	0.042	1.26	0.016
MIME-SRS-40%	663.4	0.033	0.059	13.27	0.043
MIME-SRS-60%	341.9	0.017	0.040	6.83	0.018
MIME-RDS-40%†	320.8	0.016	0.049	6.42	0.015
MIME-RDS-60%†	202.3	0.010	0.034	4.05	0.008
Bayes	78.0	0.004	0.034	1.56	0.007

SRS: simple random sample, RDS: respondent-driven sampling, MIME: multiple imputation for measurement error. Non-informative consisted of measurement error occurring randomly. Informative consisted of measurement error occurring conditional on node pairs having the same values of B. Bias was defined as the estimate parameter from the corresponding method minus the true parameter. The true parameter was calculated as the mean parameter from 10,000 generated networks.

* Naïve consisted of the parameters estimated using the observed (mismeasured) network
† Respondent-driven sampling consisted of 10% of the subsample size being selected as seeds. Each seed node then nominated three nodes based on random selection of nodes that it shared a true edge with. The procedure was repeated for nominated nodes until the gold-standard subsample size was met.

Table A1.9: Confidence interval coverage for parameters for network-3

	Edges	Density	Assortativity	Degree	Cluster
True	100%	95%	86%	100%	99%
Non-informative					
Naïve*	100%	70%	78%	92%	0%
Gold-standard SRS 40%	0%	86%	84%	0%	89%
Gold-standard SRS 60%	0%	84%	87%	0%	97%
Gold-standard RDS 40%†	0%	0%	88%	1%	89%
Gold-standard RDS 60%†	0%	1%	87%	28%	91%
MIME-SRS-40%	35%	15%	64%	22%	24%
MIME-SRS-60%	31%	10%	84%	15%	60%
MIME-RDS-40%†	0%	0%	66%	0%	13%
MIME-RDS-60%†	1%	0%	85%	0%	40%
Bayes	99%	67%	90%	87%	0%
Informative					
Naïve*	100%	76%	77%	95%	0%
Gold-standard SRS 40%	0%	86%	84%	0%	89%
Gold-standard SRS 60%	0%	84%	87%	0%	97%
Gold-standard RDS 40%†	0%	0%	88%	1%	89%
Gold-standard RDS 60%†	0%	1%	87%	28%	91%
MIME-SRS-40%	33%	14%	65%	18%	25%
MIME-SRS-60%	29%	8%	82%	13%	60%
MIME-RDS-40%†	0%	0%	66%	0%	14%
MIME-RDS-60%†	0%	0%	84%	0%	36%
Bayes	99%	67%	90%	88%	0%

SRS: simple random sample, RDS: respondent-driven sampling, MIME: multiple imputation for measurement error. Non-informative consisted of measurement error occurring randomly. Informative consisted of measurement error occurring conditional on node pairs having the same values of B. CI coverage was calculated as the percent of 95% CI that contained the true value.

* Naïve consisted of the parameters estimated using the observed (mismeasured) network
† Respondent-driven sampling consisted of 10% of the subsample size being selected as seeds. Each seed node then nominated three nodes based on random selection of nodes that it shared a true edge with. The procedure was repeated for nominated nodes until the gold-standard subsample size was met.

Figure A1.1: Bias of estimated network parameters for network-1

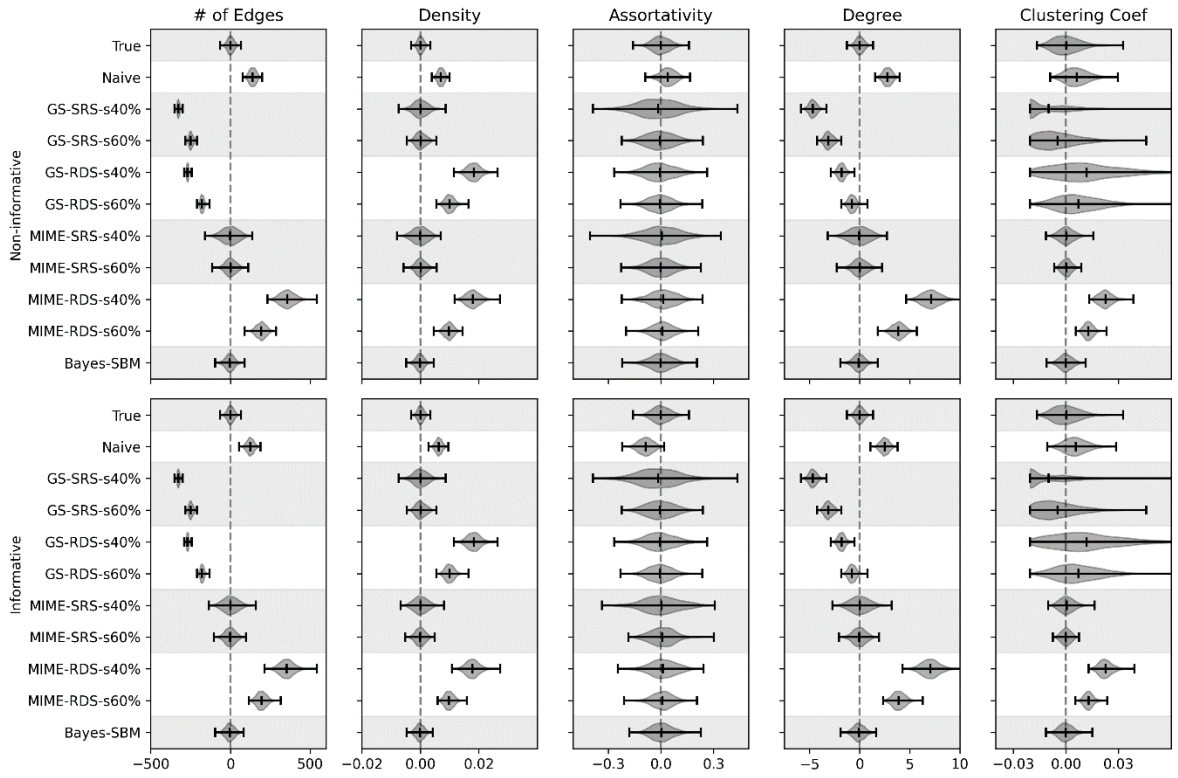

True: parameters were estimated using the true network. Naïve: parameters were estimated using the full mismeasured network. MIME: parameters were estimated using multiple imputation for measurement error with an ERGM. The gold-standard subsample was selected as a simple random sample. The percentage indicates the proportion of nodes included in the subsample. Bayes: stochastic block model Bayesian estimation.

Figure A1.2: Bias of estimated network parameters for network-2

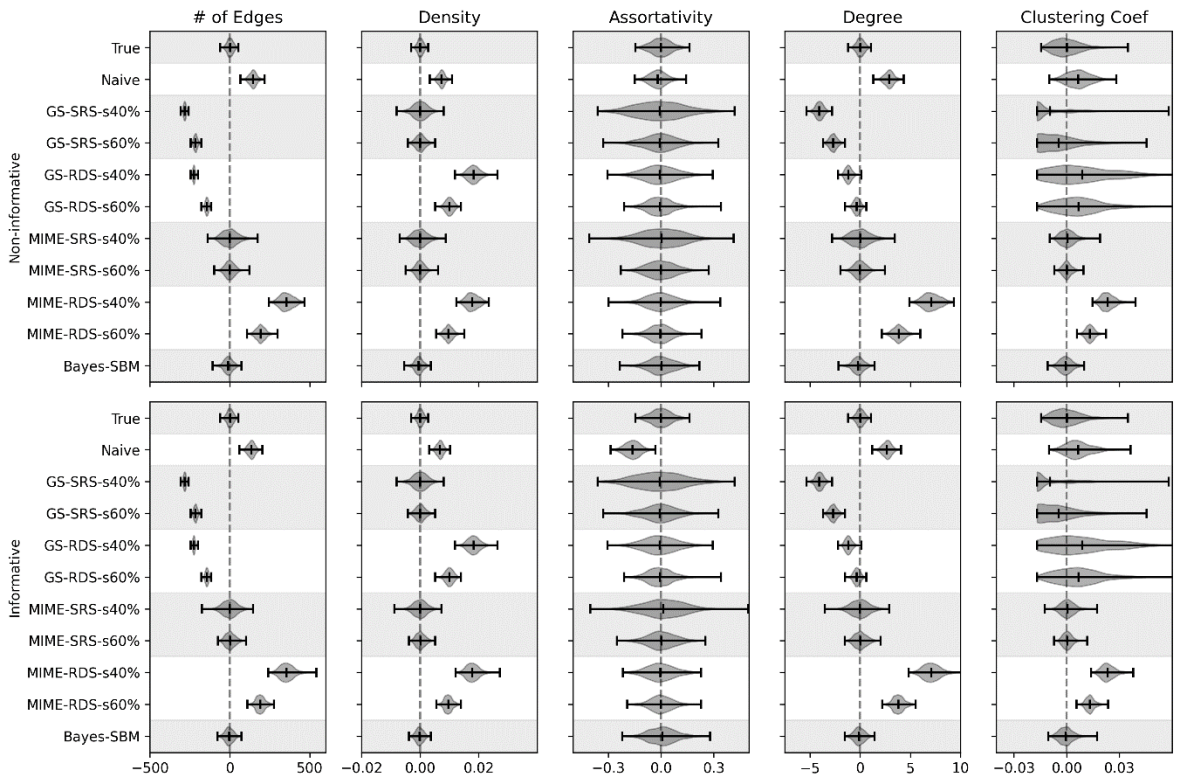

True: parameters were estimated using the true network. Naïve: parameters were estimated using the full mismeasured network. MIME: parameters were estimated using multiple imputation for measurement error with an ERGM. The gold-standard subsample was selected as a simple random sample. The percentage indicates the proportion of nodes included in the subsample. Bayes: stochastic block model Bayesian estimation.

Figure A1.3: Bias of estimated network parameters for network-3

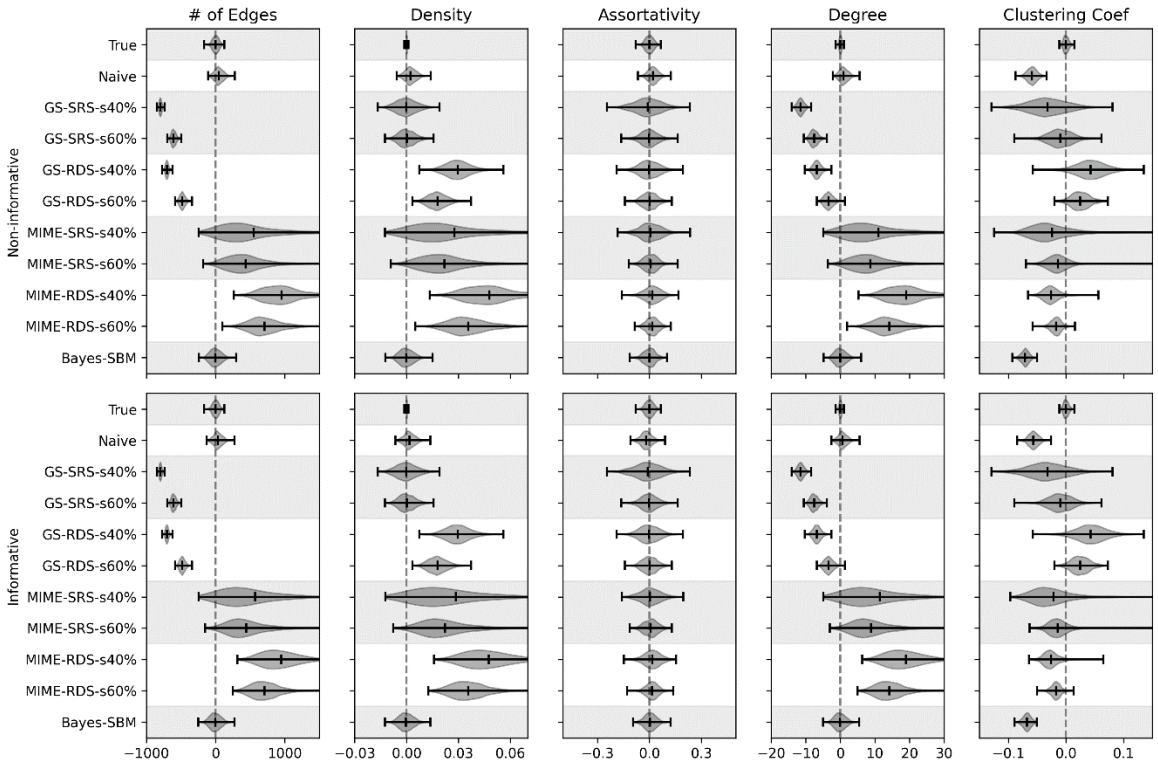

True: parameters were estimated using the true network. Naïve: parameters were estimated using the full mismeasured network. MIME: parameters were estimated using multiple imputation for measurement error with an ERGM. The gold-standard subsample was selected as a simple random sample. The percentage indicates the proportion of nodes included in the subsample. Bayes: stochastic block model Bayesian estimation.

APPENDIX 2: CHAPTER 5 SUPPLEMENTARY MATERIALS

Appendix 2.1: Validation Simulations and Demonstration of Double Robustness

Figure A2.1.1: Simulation results for Sofrygin and van der Laan 2017 mechanism

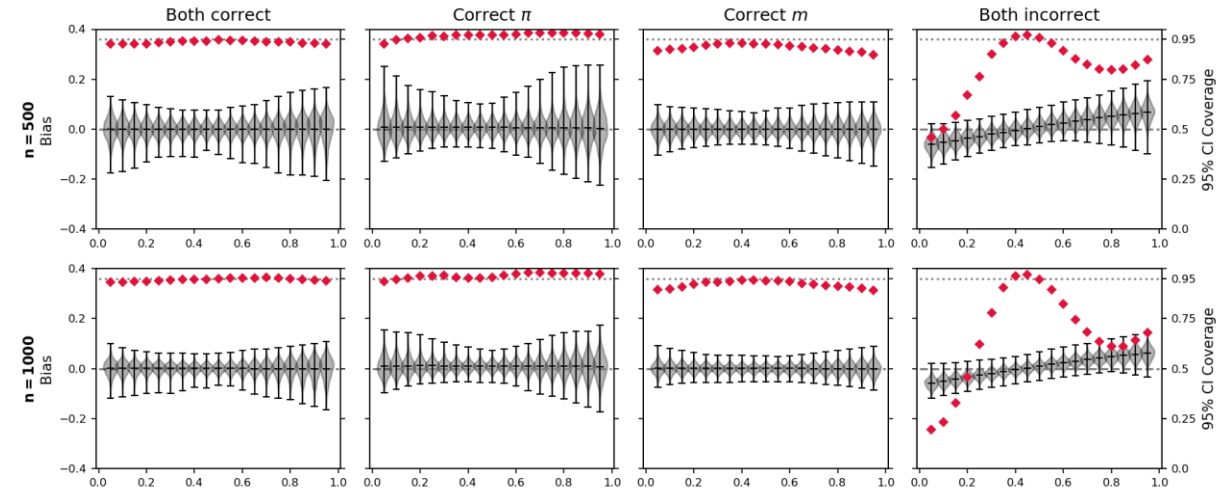

Left y-axes and violin plots correspond to bias, defined as the estimated conditional sample mean minus the true conditional sample mean. The right y-axes and red diamonds correspond to 95% CI coverage. Columns refer to which of the nuisance models (π is the treatment and m is the outcome) are correctly specified.

Figure A2.1.2: Simulation results for a unit-treatment effect only

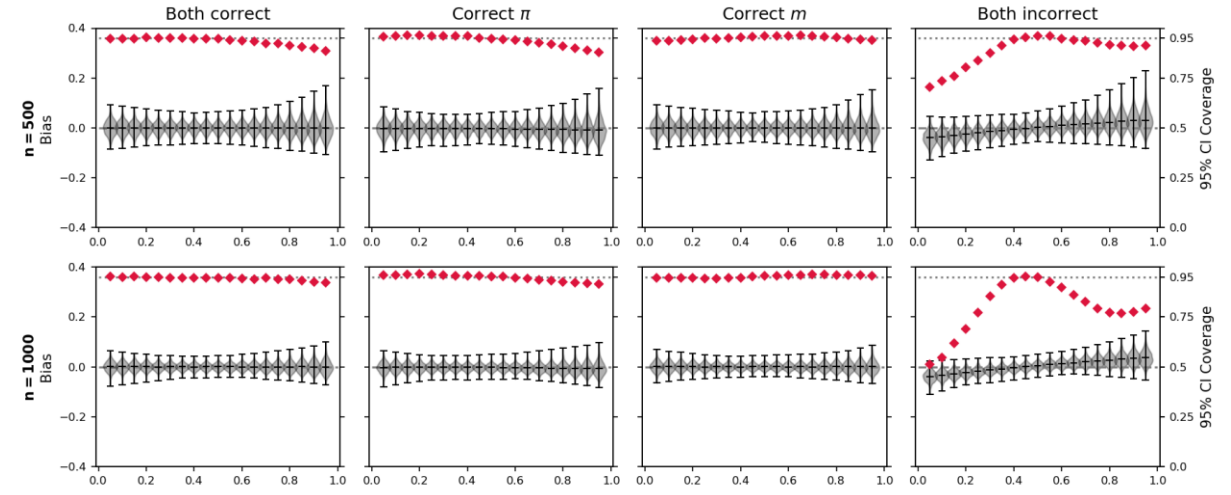

Left y-axes and violin plots correspond to bias, defined as the estimated conditional sample mean minus the true conditional sample mean. The right y-axes and red diamonds correspond to 95% CI coverage.

Figure A2.1.3: Simulation results for spillover effect only data generating mechanism

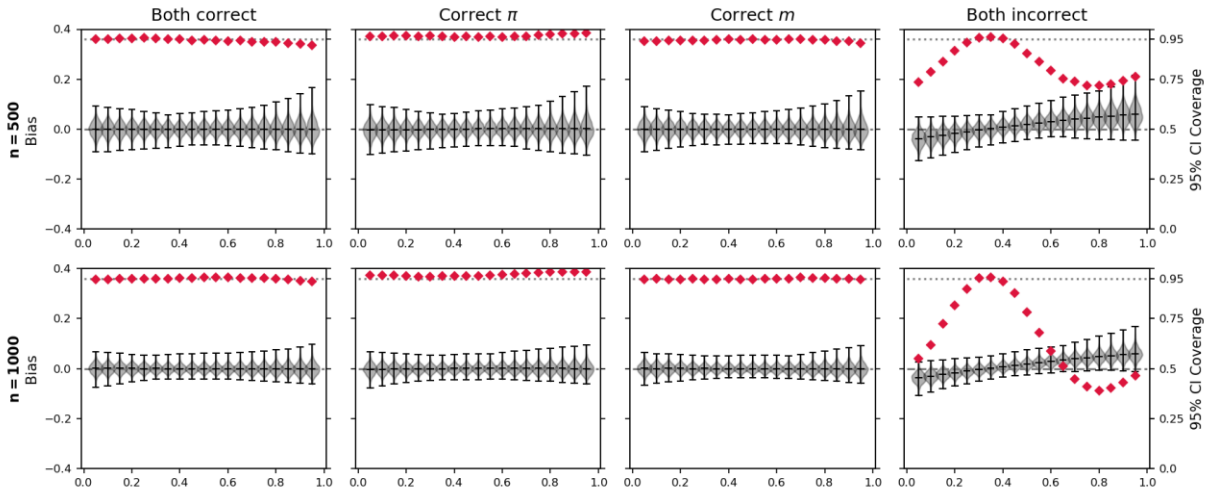

Left y-axes and violin plots correspond to bias, defined as the estimated conditional sample mean minus the true conditional sample mean. The right y-axes and red diamonds correspond to 95% CI coverage.

Figure A2.1.4: Simulation results for continuous outcome data generating mechanism

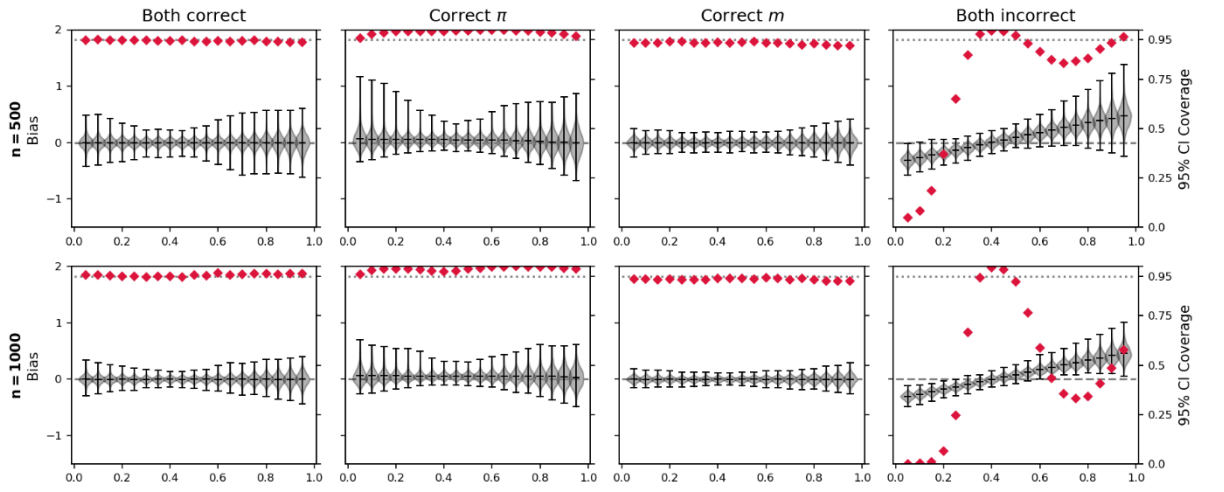

Left y-axes and violin plots correspond to bias, defined as the estimated conditional sample mean minus the true conditional sample mean. The right y-axes and red diamonds correspond to 95% CI coverage.

Appendix 2.2: Data Generating Mechanisms

Table A2.2.1: Baseline confounder distributions by data-generating mechanisms

	Uniform (n=500) % / median (IQR)	Clustered Power-Law (n=500) % / median (IQR)	eX-FLU (n=467) % / median (IQR)
Statin DGM			
Age	50 (45, 55)	49 (44, 55)	50 (44, 55)
log(LDL)	4.9 (4.7, 5.0)	4.8 (4.7, 5.0)	4.9 (4.7, 5.0)
Risk score	0.05 (0.03, 0.11)	0.06 (0.03, 0.13)	0.06 (0.03, 0.13)
Naloxone DGM			
Gender	29%	37%	30%
Recently released from prison	31%	31%	28%
Prior overdose	20%	22%	20%
Diet DGM			
Gender	50%	49%	47%
Baseline BMI	30 (26, 34)	30 (26, 34)	29 (25, 33)
Exercise	47%	42%	47%
Transmission DGM			
Asthma	15%	14%	18%
Hand hygiene	43%	47%	44%

DGM: data generating mechanism, CVD: cardiovascular disease, IQR: interquartile range, log(LDL): log-transformed low-density lipoprotein, BMI: body mass index

Appendix 2.3: Simulation Results for the Modified Clustered Power-Law Random Graph

Figure A2.3.1: Target maximum likelihood estimation for statins and atherosclerotic heart disease, and the clustered power-law random graph

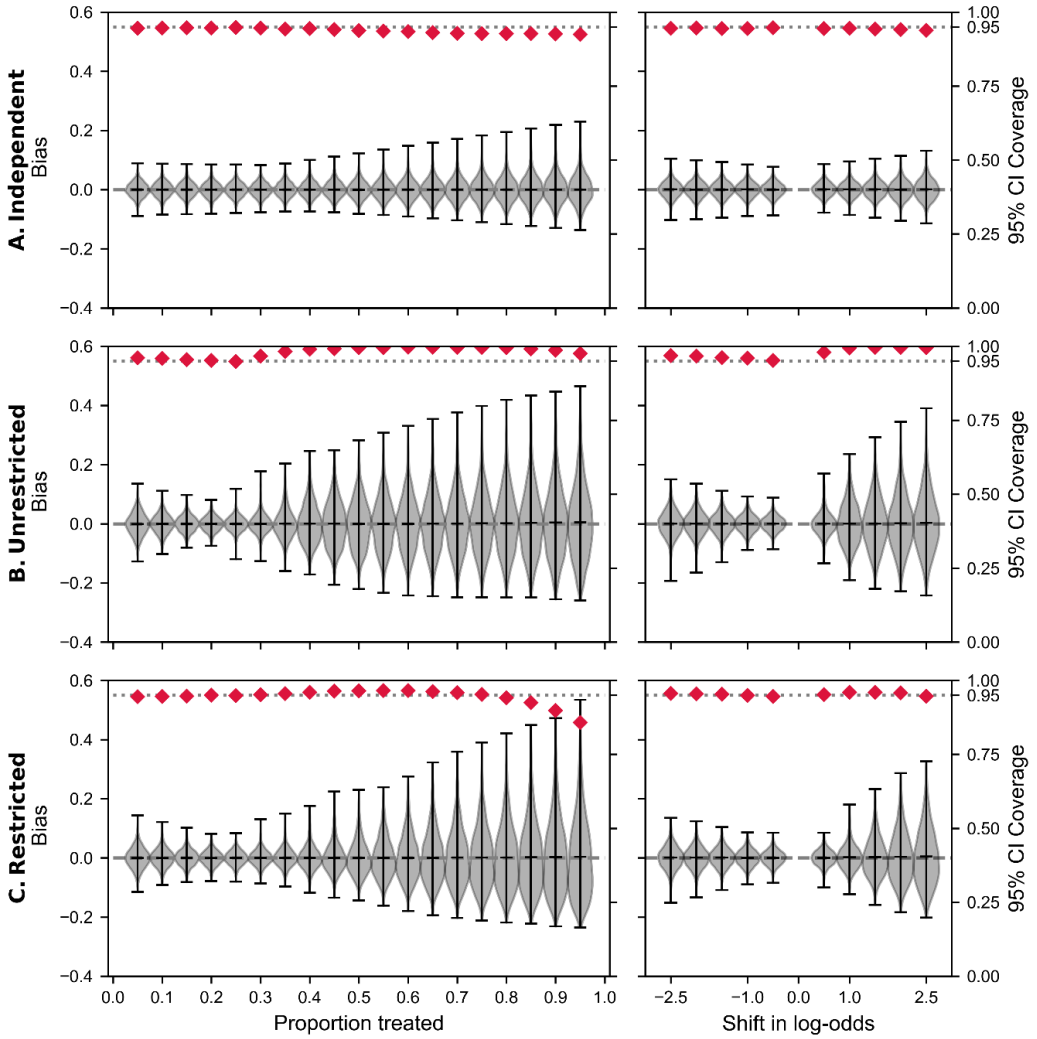

Left y-axes and violin plots correspond to bias, defined as the estimated conditional sample mean minus the true conditional sample mean. The right y-axes and red diamonds correspond to 95% CI coverage. The first column corresponds to all individuals in the population having the same set probability of statins. The second column corresponds to the shift in log-odds of the predicted probability of statins for each individual. The proportion of statins in the observed data was 24%. A: Targeted maximum likelihood estimation under the assumption of independent observations. B: Network-TMLE with a Poisson model for statin use of immediate contacts. C: Network-TMLE with a Poisson model for statin use of immediate contacts. The maximum degree for participants was restricted to be 18 or less.

Figure A2.3.2: Target maximum likelihood estimation for naloxone and opioid overdose, and the clustered power-law random graph

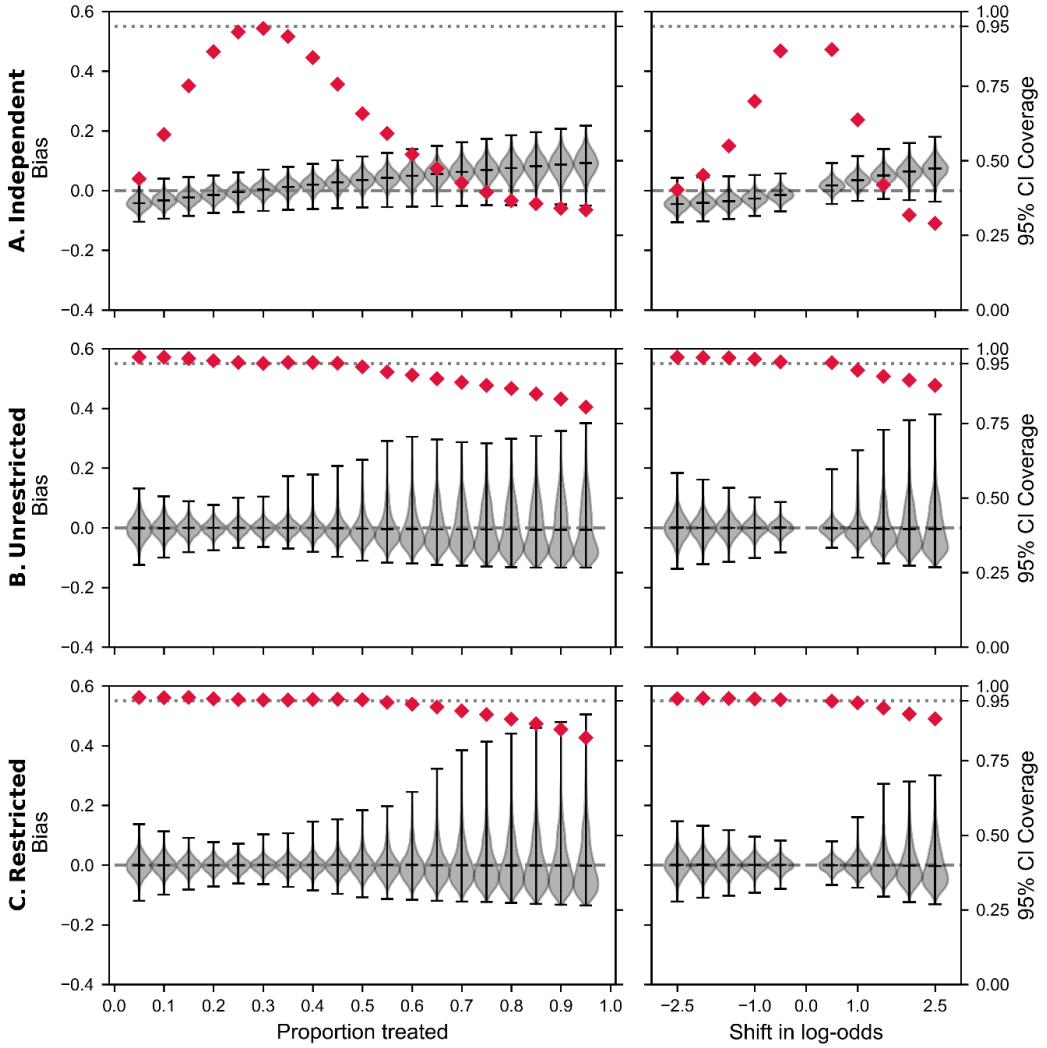

Left y-axes and violin plots correspond to bias, defined as the estimated conditional sample mean minus the true conditional sample mean. The right y-axes and red diamonds correspond to 95% CI coverage. The first column corresponds to all individuals in the population having the same set probability of naloxone. The second column corresponds to the shift in log-odds of the predicted probability of naloxone for each individual. The proportion of naloxone in the observed data was 29%. A: Targeted maximum likelihood estimation under the assumption of independent observations. B: Network-TMLE with a Poisson model for naloxone use of immediate contacts. C: Network-TMLE with a Poisson model for naloxone use of immediate contacts. The maximum degree for participants was restricted to be 18 or less.

Figure A2.3.3: Target maximum likelihood estimation for diet and body mass index, and the clustered power-law random graph

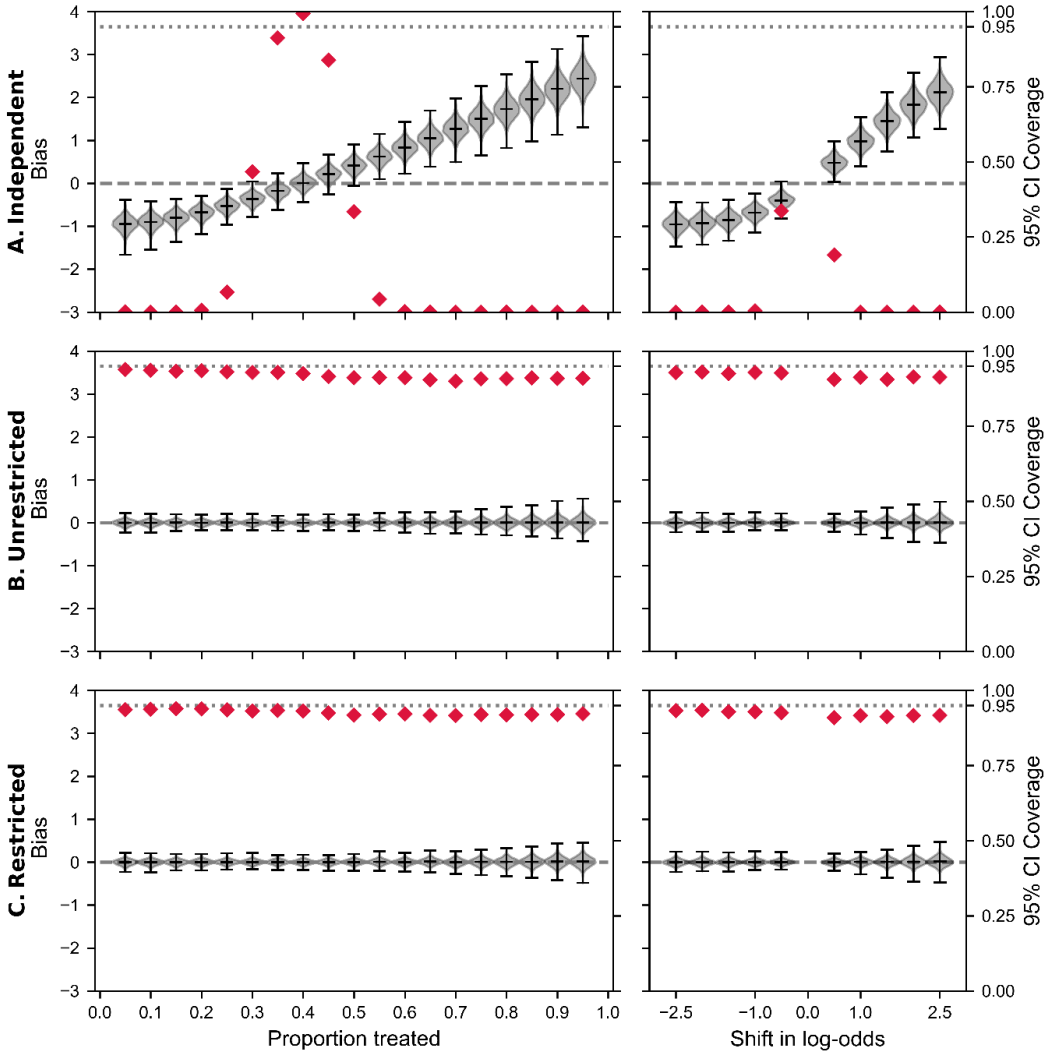

Left y-axes and violin plots correspond to bias, defined as the estimated conditional sample mean minus the true conditional sample mean. The right y-axes and red diamonds correspond to 95% CI coverage. The first column corresponds to all individuals in the population having the same set probability of diet. The second column corresponds to the shift in log-odds of the predicted probability of diet for each individual. The proportion on a diet in the observed data was 40%.
A: Targeted maximum likelihood estimation under the assumption of independent observations. B: Network-TMLE with a logistic model for diet of immediate contacts. No restrictions on maximum degree were placed. C: Network-TMLE with a logistic model for diet of immediate contacts. The maximum degree for participants was restricted to be 18 or less.

Figure A2.3.4: Target maximum likelihood estimation for vaccination and infection, and the clustered power-law random graph

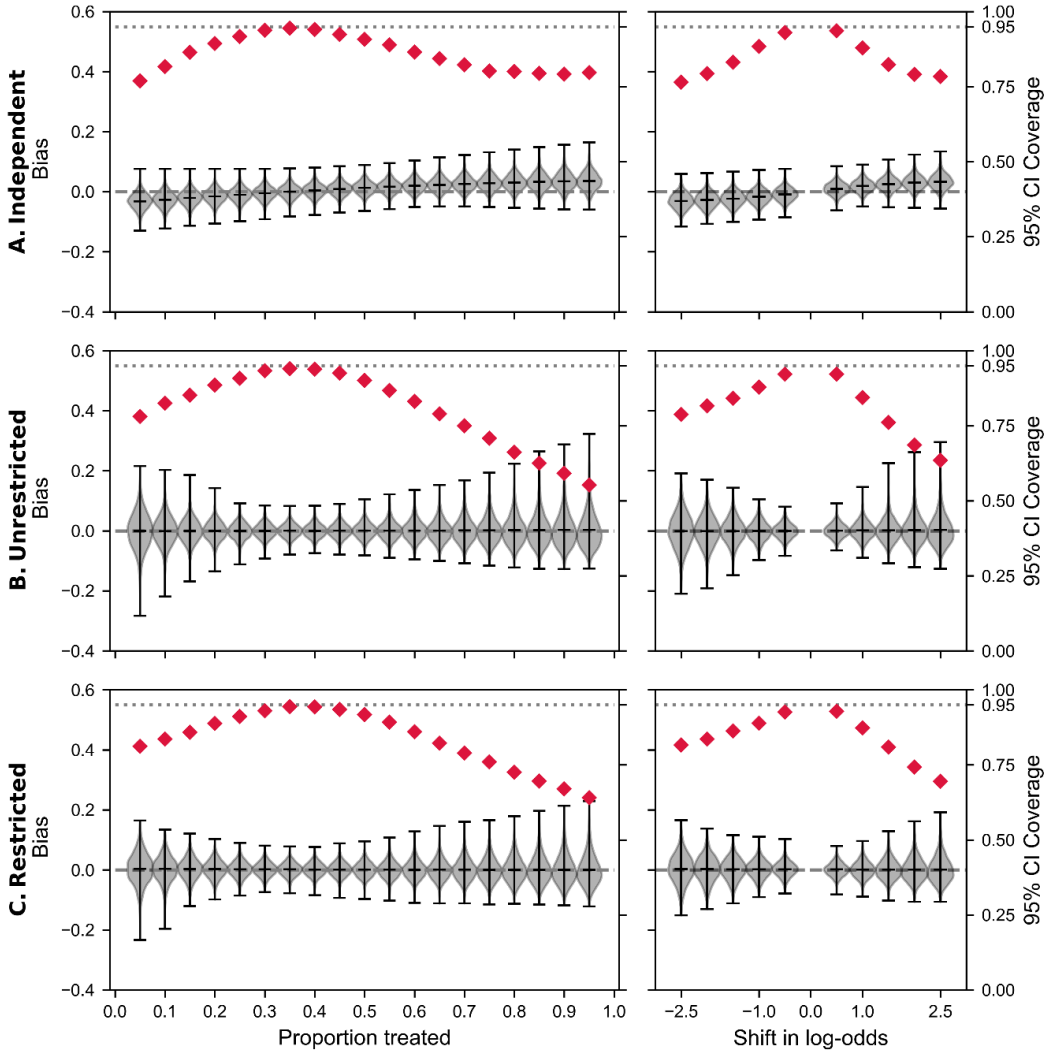

Left y-axes and violin plots correspond to bias, defined as the estimated conditional sample mean minus the true conditional sample mean. The right y-axes and red diamonds correspond to 95% CI coverage. The first column corresponds to all individuals in the population having the same set probability of vaccination. The second column corresponds to the shift in log-odds of the predicted probability of vaccination for each individual. The proportion vaccinated in the observed data was 36%. A: Targeted maximum likelihood estimation under the assumption of independent observations. B: Network-TMLE with a Poisson model for vaccination of immediate contacts. C: Network-TMLE with a Poisson model for vaccination of immediate contacts. The maximum degree for participants was restricted to be 18 or less.

Appendix 2.4: Simulation Results in Tabular Form

Table A2.4.1: IID-TMLE for statin data generating mechanism with a uniform random graph

	Bias	ESE	ASE	CLD	Coverage	Non-informative	Fail
Proportion							
0.05	0.001	0.025	0.025	0.096	94.8%	0	0
0.10	0.001	0.024	0.024	0.093	95.2%	0	0
0.15	0.000	0.023	0.023	0.090	95.2%	0	0
0.20	0.000	0.023	0.023	0.089	95.2%	0	0
0.25	0.001	0.023	0.023	0.088	94.9%	0	0
0.30	0.001	0.023	0.023	0.089	95.1%	0	0
0.35	0.000	0.023	0.023	0.091	94.8%	0	0
0.40	0.000	0.024	0.024	0.095	94.9%	0	0
0.45	0.000	0.025	0.025	0.099	94.5%	0	0
0.50	0.000	0.027	0.026	0.104	94.1%	0	0
0.55	0.000	0.028	0.028	0.109	94.2%	0	0
0.60	0.000	0.030	0.030	0.116	93.9%	0	0
0.65	0.000	0.032	0.031	0.123	93.6%	0	0
0.70	-0.001	0.034	0.033	0.130	93.5%	0	0
0.75	-0.001	0.036	0.035	0.138	93.2%	0	0
0.80	-0.001	0.038	0.037	0.146	93.1%	0	0
0.85	0.000	0.040	0.039	0.154	92.9%	0	0
0.90	-0.001	0.043	0.042	0.163	92.8%	0	0
0.95	-0.001	0.045	0.044	0.172	92.7%	0	0
Shift in log-odds							
-2.5	0.000	0.025	0.025	0.097	95.2%	0	0
-2	0.000	0.024	0.024	0.095	95.3%	0	0
-1.5	0.000	0.023	0.024	0.093	95.1%	0	0
-1	0.000	0.023	0.023	0.089	95.1%	0	0
-0.5	0.000	0.022	0.022	0.086	95.2%	0	0
0.5	0.000	0.022	0.022	0.084	94.7%	0	0
1	0.000	0.023	0.023	0.090	94.3%	0	0
1.5	0.000	0.026	0.025	0.099	94.2%	0	0
2	0.000	0.029	0.028	0.112	94.1%	0	0
2.5	0.000	0.032	0.032	0.125	93.8%	0	0

IID-TMLE: independent and identically distributed targeted maximum likelihood estimation, ESE: empirical standard error, ASE: average standard error, CLD: confidence limit difference, Coverage: 95% confidence interval coverage of the true parameter, Non-informative: the lower confidence limit was less than 0 and the upper confidence limit was greater than 1, Fail: estimator failed to produce an estimate.

Table A2.4.2: Network-TMLE with a series of logistic models for statin data generating mechanism with a uniform random graph

	Bias	ESE	ASE	CLD	Coverage	Non-informative	Fail
Proportion							
0.05	0.001	0.033	0.033	0.131	95.5%	0	0
0.10	0.001	0.028	0.028	0.112	95.3%	0	0
0.15	0.001	0.025	0.026	0.100	95.2%	0	0
0.20	0.000	0.024	0.024	0.095	95.2%	0	0
0.25	0.000	0.024	0.024	0.095	94.6%	0	0
0.30	0.000	0.026	0.026	0.101	94.6%	0	0
0.35	0.000	0.029	0.028	0.111	94.0%	0	0
0.40	0.000	0.034	0.032	0.125	93.4%	0	0
0.45	-0.001	0.040	0.037	0.144	92.4%	0	0
0.50	-0.001	0.047	0.042	0.166	91.2%	0	0
0.55	0.000	0.056	0.048	0.190	89.8%	0	0
0.60	-0.001	0.064	0.054	0.213	88.1%	0	0
0.65	0.000	0.073	0.060	0.236	86.5%	0	0
0.70	0.000	0.083	0.066	0.257	84.5%	0	0
0.75	0.000	0.093	0.070	0.274	82.2%	0	0
0.80	0.000	0.103	0.073	0.286	79.2%	0	0
0.85	0.001	0.114	0.075	0.294	75.2%	0	0
0.90	0.001	0.126	0.075	0.295	69.7%	0	0
0.95	0.002	0.141	0.074	0.291	62.3%	0	0
Shift in log-odds							
-2.5	0.000	0.036	0.036	0.140	94.7%	0	0
-2	0.000	0.033	0.033	0.130	94.6%	0	0
-1.5	0.000	0.030	0.030	0.118	94.6%	0	0
-1	0.000	0.026	0.027	0.104	95.2%	0	0
-0.5	0.000	0.024	0.024	0.093	95.4%	0	0
0.5	0.000	0.027	0.026	0.102	94.0%	0	0
1	0.000	0.037	0.035	0.135	92.8%	0	0
1.5	0.000	0.053	0.048	0.187	90.7%	0	0
2	0.001	0.072	0.061	0.240	87.5%	0	0
2.5	0.001	0.090	0.071	0.279	84.8%	0	0

Network-TMLE: targeted maximum likelihood estimation for dependent data, ESE: empirical standard error, ASE: average standard error, CLD: confidence limit difference, Coverage: 95% confidence interval coverage of the true parameter, Non-informative: the lower confidence limit was less than 0 and the upper confidence limit was greater than 1, Fail: estimator failed to produce an estimate.

Table A2.4.3: Network-TMLE with a single Poisson model for statin data generating mechanism with a uniform random graph

	Bias	ESE	ASE	CLD	Coverage	Non-informative	Fail
Proportion							
0.05	0.001	0.033	0.032	0.125	94.2%	0	0
0.10	0.001	0.028	0.027	0.107	94.5%	0	0
0.15	0.001	0.025	0.024	0.096	94.8%	0	0
0.20	0.000	0.023	0.023	0.090	95.2%	0	0
0.25	0.001	0.023	0.023	0.089	95.0%	0	0
0.30	0.001	0.024	0.023	0.091	95.0%	0	0
0.35	0.000	0.026	0.025	0.098	94.0%	0	0
0.40	0.000	0.029	0.027	0.107	93.0%	0	0
0.45	-0.001	0.033	0.030	0.119	92.2%	0	0
0.50	-0.001	0.039	0.034	0.133	90.3%	0	0
0.55	-0.001	0.045	0.038	0.149	88.5%	0	0
0.60	-0.001	0.051	0.042	0.165	86.9%	0	0
0.65	-0.001	0.059	0.046	0.182	85.3%	0	0
0.70	-0.001	0.066	0.051	0.198	83.0%	0	0
0.75	-0.002	0.074	0.054	0.213	81.2%	0	0
0.80	-0.001	0.082	0.058	0.226	78.8%	0	0
0.85	-0.001	0.090	0.061	0.238	76.4%	0	0
0.90	-0.001	0.099	0.063	0.247	73.6%	0	0
0.95	-0.001	0.108	0.065	0.256	70.4%	0	0
Shift in log-odds							
-2.5	0.000	0.036	0.034	0.134	93.5%	0	0
-2	0.000	0.033	0.032	0.124	93.8%	0	0
-1.5	0.000	0.030	0.029	0.113	93.8%	0	0
-1	0.000	0.026	0.026	0.100	94.7%	0	0
-0.5	0.000	0.023	0.023	0.089	95.3%	0	0
0.5	0.000	0.023	0.023	0.089	93.8%	0	0
1	0.000	0.030	0.028	0.108	92.2%	0	0
1.5	0.001	0.042	0.036	0.141	89.7%	0	0
2	0.001	0.057	0.045	0.178	86.2%	0	0
2.5	0.002	0.073	0.054	0.210	82.9%	0	0

Network-TMLE: targeted maximum likelihood estimation for dependent data, ESE: empirical standard error, ASE: average standard error, CLD: confidence limit difference, Coverage: 95% confidence interval coverage of the true parameter, Non-informative: the lower confidence limit was less than 0 and the upper confidence limit was greater than 1, Fail: estimator failed to produce an estimate.

Table A2.4.4: IID-TMLE for statin data generating mechanism with a clustered power-law random graph

	Bias	ESE	ASE	CLD	Coverage	Non-informative	Fail
Proportion							
0.05	0.000	0.025	0.024	0.096	94.6%	0	0
0.10	0.000	0.024	0.024	0.092	94.7%	0	0
0.15	0.000	0.023	0.023	0.090	94.8%	0	0
0.20	0.000	0.023	0.023	0.089	94.7%	0	0
0.25	0.000	0.023	0.023	0.089	94.9%	0	0
0.30	0.000	0.023	0.023	0.090	94.6%	0	0
0.35	0.000	0.024	0.024	0.092	94.3%	0	0
0.40	0.000	0.025	0.024	0.096	94.4%	0	0
0.45	0.000	0.026	0.026	0.100	94.1%	0	0
0.50	0.000	0.027	0.027	0.106	93.8%	0	0
0.55	0.000	0.029	0.028	0.112	93.6%	0	0
0.60	0.000	0.031	0.030	0.118	93.4%	0	0
0.65	0.000	0.033	0.032	0.125	93.1%	0	0
0.70	0.000	0.035	0.034	0.133	92.9%	0	0
0.75	0.000	0.037	0.036	0.141	92.7%	0	0
0.80	0.000	0.039	0.038	0.149	92.7%	0	0
0.85	0.000	0.041	0.040	0.158	92.8%	0	0
0.90	0.000	0.044	0.043	0.167	92.7%	0	0
0.95	0.000	0.046	0.045	0.176	92.5%	0	0
Shift in log-odds							
-2.5	0.001	0.025	0.025	0.097	94.6%	0	0
-2	0.000	0.025	0.024	0.095	94.7%	0	0
-1.5	0.000	0.024	0.024	0.092	94.5%	0	0
-1	0.000	0.023	0.023	0.089	94.5%	0	0
-0.5	0.000	0.022	0.022	0.086	94.7%	0	0
0.5	0.000	0.022	0.022	0.084	94.5%	0	0
1	0.001	0.023	0.023	0.089	94.6%	0	0
1.5	0.000	0.026	0.025	0.099	94.3%	0	0
2	0.000	0.029	0.028	0.111	94.1%	0	0
2.5	0.000	0.033	0.032	0.126	93.9%	0	0

IID-TMLE: independent and identically distributed targeted maximum likelihood estimation, ESE: empirical standard error, ASE: average standard error, CLD: confidence limit difference, Coverage: 95% confidence interval coverage of the true parameter, Non-informative: the lower confidence limit was less than 0 and the upper confidence limit was greater than 1, Fail: estimator failed to produce an estimate.

Table A2.4.5: Network-TMLE for statin data generating mechanism with a clustered power-law random graph

	Bias	ESE	ASE	CLD	Coverage	Non-informative	Fail
Proportion							
0.05	-0.001	0.038	0.041	0.161	96.1%	0	0
0.10	0.000	0.030	0.032	0.125	95.9%	0	0
0.15	0.000	0.026	0.026	0.104	95.5%	0	0
0.20	0.000	0.023	0.024	0.093	95.2%	0	0
0.25	0.000	0.024	0.024	0.094	94.9%	0	0
0.30	0.000	0.031	0.034	0.131	96.7%	0	0
0.35	0.000	0.048	0.062	0.242	98.2%	0	0
0.40	0.000	0.064	0.104	0.407	99.0%	1	0
0.45	0.000	0.074	0.143	0.560	99.2%	8	0
0.50	0.000	0.079	0.173	0.679	99.5%	27	0
0.55	0.000	0.083	0.196	0.768	99.6%	72	0
0.60	0.000	0.086	0.212	0.830	99.7%	124	0
0.65	0.000	0.089	0.222	0.872	99.7%	173	0
0.70	0.001	0.093	0.229	0.898	99.7%	213	0
0.75	0.001	0.097	0.233	0.912	99.6%	232	0
0.80	0.002	0.101	0.233	0.913	99.5%	226	0
0.85	0.003	0.106	0.230	0.903	99.1%	210	0
0.90	0.004	0.112	0.224	0.879	98.7%	181	0
0.95	0.005	0.120	0.212	0.832	97.6%	127	0
Shift in log-odds							
-2.5	0.001	0.041	0.046	0.181	96.8%	0	0
-2	0.001	0.037	0.041	0.162	96.7%	0	0
-1.5	0.000	0.032	0.036	0.139	96.2%	0	0
-1	0.000	0.028	0.029	0.115	96.0%	0	0
-0.5	0.000	0.024	0.024	0.095	95.3%	0	0
0.5	0.001	0.036	0.041	0.163	98.0%	0	0
1	0.000	0.068	0.123	0.483	99.5%	0	0
1.5	0.001	0.082	0.189	0.739	99.6%	42	0
2	0.002	0.089	0.220	0.864	99.6%	162	0
2.5	0.003	0.097	0.232	0.910	99.5%	218	0

Network-TMLE: targeted maximum likelihood estimation for dependent data, ESE: empirical standard error, ASE: average standard error, CLD: confidence limit difference, Coverage: 95% confidence interval coverage of the true parameter, Non-informative: the lower confidence limit was less than 0 and the upper confidence limit was greater than 1, Fail: estimator failed to produce an estimate.

Table A2.4.6: Network-TMLE for statin data generating mechanism with a clustered power-law random graph restricted by degree

	Bias	ESE	ASE	CLD	Coverage	Non-informative	Fail
Proportion							
0.05	0.000	0.035	0.034	0.135	94.5%	0	0
0.10	0.000	0.029	0.029	0.113	94.6%	0	0
0.15	0.000	0.025	0.025	0.099	94.7%	0	0
0.20	0.000	0.024	0.023	0.092	95.0%	0	0
0.25	0.000	0.023	0.023	0.091	94.8%	0	0
0.30	0.000	0.025	0.025	0.099	95.2%	0	0
0.35	0.001	0.029	0.030	0.119	95.5%	0	0
0.40	0.000	0.037	0.039	0.154	96.0%	0	0
0.45	0.000	0.046	0.051	0.201	96.4%	0	0
0.50	0.000	0.056	0.065	0.255	96.5%	0	0
0.55	0.000	0.065	0.079	0.310	96.6%	0	0
0.60	0.001	0.074	0.092	0.362	96.6%	1	0
0.65	0.001	0.081	0.104	0.407	96.3%	3	0
0.70	0.001	0.089	0.113	0.443	95.9%	3	0
0.75	0.001	0.096	0.120	0.469	95.3%	3	0
0.80	0.001	0.103	0.124	0.486	94.1%	6	0
0.85	0.002	0.111	0.126	0.493	92.5%	5	0
0.90	0.003	0.119	0.125	0.491	89.9%	5	0
0.95	0.003	0.130	0.122	0.480	85.8%	4	0
Shift in log-odds							
-2.5	0.001	0.036	0.037	0.146	95.6%	0	0
-2	0.001	0.034	0.034	0.135	95.4%	0	0
-1.5	0.001	0.030	0.031	0.121	95.3%	0	0
-1	0.000	0.027	0.027	0.105	94.9%	0	0
-0.5	0.000	0.024	0.023	0.092	94.6%	0	0
0.5	0.001	0.025	0.025	0.099	95.2%	0	0
1	0.002	0.039	0.042	0.167	96.0%	0	0
1.5	0.003	0.061	0.074	0.292	96.0%	0	0
2	0.004	0.081	0.104	0.407	95.8%	3	0
2.5	0.005	0.095	0.121	0.475	94.6%	8	0

Network-TMLE: targeted maximum likelihood estimation for dependent data, ESE: empirical standard error, ASE: average standard error, CLD: confidence limit difference, Coverage: 95% confidence interval coverage of the true parameter, Non-informative: the lower confidence limit was less than 0 and the upper confidence limit was greater than 1, Fail: estimator failed to produce an estimate.

Table A2.4.7: IID-TMLE for statin data generating mechanism with the eX-FLU network

		Bias	ESE	ASE	CLD	Coverage	Non-informative	Fail
Proportion								
	0.05	0.000	0.025	0.025	0.099	94.9%	0	0
	0.10	0.000	0.024	0.024	0.095	95.1%	0	0
	0.15	0.000	0.023	0.024	0.093	95.1%	0	0
	0.20	0.000	0.023	0.023	0.092	95.1%	0	0
	0.25	0.000	0.023	0.023	0.092	94.9%	0	0
	0.30	0.000	0.024	0.024	0.093	94.8%	0	0
	0.35	0.000	0.024	0.024	0.096	94.5%	0	0
	0.40	0.001	0.025	0.025	0.099	94.6%	0	0
	0.45	0.000	0.027	0.026	0.104	94.0%	0	0
	0.50	0.000	0.028	0.028	0.109	94.1%	0	0
	0.55	0.001	0.030	0.029	0.115	94.1%	0	0
	0.60	0.000	0.032	0.031	0.122	93.9%	0	0
	0.65	0.000	0.034	0.033	0.130	93.6%	0	0
	0.70	0.000	0.036	0.035	0.138	93.3%	0	0
	0.75	0.001	0.038	0.037	0.146	93.2%	0	0
	0.80	0.000	0.040	0.039	0.155	92.8%	0	0
	0.85	0.000	0.043	0.042	0.163	92.8%	0	0
	0.90	0.000	0.045	0.044	0.173	92.5%	0	0
	0.95	0.001	0.048	0.046	0.182	92.4%	0	0
Shift in log-odds								
	-2.5	-0.001	0.025	0.026	0.100	94.9%	0	0
	-2	0.000	0.025	0.025	0.098	94.9%	0	0
	-1.5	0.000	0.024	0.024	0.095	94.9%	0	0
	-1	0.000	0.023	0.023	0.092	94.7%	0	0
	-0.5	0.000	0.023	0.023	0.089	94.7%	0	0
	0.5	0.000	0.022	0.022	0.087	94.9%	0	0
	1	0.000	0.024	0.024	0.092	94.7%	0	0
	1.5	0.000	0.026	0.026	0.102	94.4%	0	0
	2	0.000	0.030	0.029	0.115	94.0%	0	0
	2.5	0.000	0.034	0.033	0.130	93.9%	0	0

IID-TMLE: independent and identically distributed targeted maximum likelihood estimation, ESE: empirical standard error, ASE: average standard error, CLD: confidence limit difference, Coverage: 95% confidence interval coverage of the true parameter, Non-informative: the lower confidence limit was less than 0 and the upper confidence limit was greater than 1, Fail: estimator failed to produce an estimate.

Table A2.4.8: Network-TMLE for statin data generating mechanism with the eX-FLU network

	Bias	ESE	ASE	CLD	Coverage	Non-informative	Fail
Proportion							
0.05	0.005	0.039	0.060	0.233	99.3%	0	0
0.10	0.002	0.030	0.042	0.163	99.3%	0	0
0.15	0.000	0.024	0.031	0.122	98.5%	0	0
0.20	-0.001	0.021	0.026	0.100	97.0%	0	0
0.25	-0.002	0.021	0.026	0.102	96.3%	0	0
0.30	-0.003	0.028	0.038	0.147	97.8%	0	0
0.35	-0.001	0.042	0.068	0.268	98.5%	0	0
0.40	0.000	0.056	0.119	0.467	100.0%	1	0
0.45	0.002	0.065	0.174	0.681	100.0%	8	0
0.50	0.001	0.071	0.217	0.852	100.0%	16	0
0.55	0.003	0.074	0.254	0.996	100.0%	30	0
0.60	0.003	0.076	0.279	1.094	100.0%	42	0
0.65	0.003	0.080	0.296	1.159	100.0%	51	0
0.70	0.002	0.083	0.304	1.192	100.0%	53	0
0.75	0.003	0.087	0.306	1.201	100.0%	50	0
0.80	0.003	0.092	0.304	1.192	100.0%	47	0
0.85	0.004	0.097	0.298	1.166	100.0%	42	0
0.90	0.006	0.105	0.286	1.122	99.3%	35	0
0.95	0.009	0.117	0.267	1.048	97.8%	27	0
Shift in log-odds							
-2.5	0.000	0.042	0.070	0.275	99.8%	0	0
-2	0.001	0.038	0.061	0.239	99.6%	0	0
-1.5	0.000	0.034	0.050	0.195	99.2%	0	0
-1	0.001	0.029	0.038	0.149	98.6%	0	0
-0.5	0.000	0.024	0.028	0.109	97.1%	0	0
0.5	0.000	0.032	0.045	0.175	98.8%	0	0
1	0.001	0.057	0.135	0.530	99.8%	56	0
1.5	0.001	0.070	0.232	0.910	99.9%	594	0
2	0.001	0.077	0.281	1.102	99.8%	1129	0
2.5	0.001	0.084	0.296	1.160	99.6%	1266	0

Network-TMLE: targeted maximum likelihood estimation for dependent data, ESE: empirical standard error, ASE: average standard error, CLD: confidence limit difference, Coverage: 95% confidence interval coverage of the true parameter, Non-informative: the lower confidence limit was less than 0 and the upper confidence limit was greater than 1, Fail: estimator failed to produce an estimate.

Table A2.4.9: Network-TMLE for statin data generating mechanism with the eX-FLU network restricted by degree

	Bias	ESE	ASE	CLD	Coverage	Non-informative	Fail
Proportion							
0.05	0.000	0.033	0.044	0.172	98.9%	0	0
0.10	0.000	0.028	0.035	0.136	98.2%	0	0
0.15	0.000	0.026	0.029	0.113	96.9%	0	0
0.20	-0.001	0.025	0.026	0.100	95.7%	0	0
0.25	-0.001	0.025	0.026	0.101	95.4%	0	0
0.30	0.001	0.030	0.033	0.130	97.2%	0	0
0.35	0.001	0.039	0.052	0.205	98.9%	0	0
0.40	0.001	0.050	0.085	0.335	99.6%	9	0
0.45	0.001	0.060	0.129	0.506	99.7%	47	0
0.50	0.001	0.066	0.175	0.688	100.0%	163	0
0.55	0.001	0.070	0.219	0.857	100.0%	377	0
0.60	0.002	0.072	0.254	0.996	100.0%	698	0
0.65	0.002	0.074	0.281	1.102	100.0%	976	0
0.70	0.003	0.075	0.300	1.175	100.0%	1206	0
0.75	0.003	0.078	0.311	1.221	100.0%	1335	0
0.80	0.003	0.080	0.317	1.241	100.0%	1368	0
0.85	0.004	0.084	0.315	1.236	100.0%	1300	0
0.90	0.005	0.090	0.307	1.202	99.9%	1136	0
0.95	0.006	0.098	0.286	1.121	99.7%	881	0
Shift in log-odds							
-2.5	0.000	0.035	0.049	0.191	99.1%	0	0
-2	0.000	0.032	0.044	0.173	99.0%	0	0
-1.5	0.000	0.030	0.039	0.151	98.6%	0	0
-1	0.000	0.027	0.032	0.126	97.9%	0	0
-0.5	0.000	0.024	0.026	0.103	96.6%	0	0
0.5	0.000	0.031	0.038	0.151	98.4%	0	0
1	0.000	0.054	0.105	0.410	99.7%	15	0
1.5	0.000	0.069	0.205	0.802	99.9%	305	0
2	0.000	0.075	0.276	1.082	100.0%	981	0
2.5	0.001	0.079	0.310	1.214	100.0%	1398	0

Network-TMLE: targeted maximum likelihood estimation for dependent data, ESE: empirical standard error, ASE: average standard error, CLD: confidence limit difference, Coverage: 95% confidence interval coverage of the true parameter, Non-informative: the lower confidence limit was less than 0 and the upper confidence limit was greater than 1, Fail: estimator failed to produce an estimate.

Table 2.4.10: IID-TMLE for naloxone data generating mechanism with a uniform random graph

	Bias	ESE	ASE	CLD	Coverage	Non-informative	Fail
Proportion							
0.05	-0.025	0.021	0.021	0.082	77.1%	0	0
0.10	-0.019	0.020	0.020	0.079	84.5%	0	0
0.15	-0.013	0.020	0.020	0.077	89.7%	0	0
0.20	-0.007	0.019	0.020	0.077	93.4%	0	0
0.25	-0.001	0.020	0.020	0.077	94.7%	0	0
0.30	0.005	0.020	0.020	0.079	94.4%	0	0
0.35	0.011	0.021	0.021	0.082	92.1%	0	0
0.40	0.017	0.022	0.022	0.086	88.6%	0	0
0.45	0.022	0.023	0.023	0.091	84.5%	0	0
0.50	0.027	0.025	0.025	0.097	79.9%	0	0
0.55	0.033	0.026	0.026	0.103	75.2%	0	0
0.60	0.038	0.028	0.028	0.109	72.0%	0	0
0.65	0.043	0.030	0.030	0.116	69.1%	0	0
0.70	0.049	0.032	0.032	0.124	66.3%	0	0
0.75	0.054	0.034	0.034	0.132	63.9%	0	0
0.80	0.059	0.036	0.036	0.139	62.0%	0	0
0.85	0.064	0.038	0.038	0.148	60.1%	0	0
0.90	0.069	0.040	0.040	0.156	58.7%	0	0
0.95	0.074	0.042	0.042	0.164	57.5%	0	0
Shift in log-odds							
-2.5	-0.028	0.021	0.021	0.083	73.0%	0	0
-2	-0.025	0.021	0.021	0.082	75.9%	0	0
-1.5	-0.022	0.020	0.020	0.080	80.4%	0	0
-1	-0.017	0.020	0.020	0.078	86.5%	0	0
-0.5	-0.009	0.019	0.020	0.077	92.0%	0	0
0.5	0.012	0.020	0.021	0.081	92.2%	0	0
1	0.025	0.022	0.022	0.088	82.7%	0	0
1.5	0.037	0.025	0.025	0.099	70.0%	0	0
2	0.048	0.028	0.029	0.112	62.7%	0	0
2.5	0.057	0.032	0.032	0.125	58.1%	0	0

IID-TMLE: independent and identically distributed targeted maximum likelihood estimation, ESE: empirical standard error, ASE: average standard error, CLD: confidence limit difference, Coverage: 95% confidence interval coverage of the true parameter, Non-informative: the lower confidence limit was less than 0 and the upper confidence limit was greater than 1, Fail: estimator failed to produce an estimate.

Table A2.4.11: Network-TMLE with a series of logistic models for naloxone data generating mechanism with a uniform random graph

	Bias	ESE	ASE	CLD	Coverage	Non-informative	Fail
Proportion							
0.05	0.001	0.030	0.031	0.122	94.8%	0	0
0.10	0.001	0.026	0.026	0.103	95.1%	0	0
0.15	0.001	0.023	0.023	0.091	94.9%	0	0
0.20	0.001	0.021	0.022	0.085	94.9%	0	0
0.25	0.000	0.021	0.021	0.084	94.7%	0	0
0.30	0.000	0.023	0.023	0.088	94.4%	0	0
0.35	0.000	0.025	0.025	0.097	94.4%	0	0
0.40	0.000	0.029	0.028	0.109	94.1%	0	0
0.45	0.000	0.034	0.032	0.124	93.2%	0	0
0.50	-0.001	0.039	0.036	0.141	92.4%	0	0
0.55	0.000	0.046	0.041	0.160	91.6%	0	0
0.60	-0.001	0.052	0.045	0.178	90.2%	0	0
0.65	-0.001	0.059	0.050	0.196	88.8%	0	0
0.70	-0.001	0.066	0.054	0.212	86.7%	0	0
0.75	-0.001	0.073	0.057	0.225	84.7%	0	0
0.80	-0.001	0.081	0.060	0.236	81.5%	0	0
0.85	-0.001	0.090	0.062	0.243	77.5%	0	0
0.90	-0.001	0.099	0.063	0.246	73.5%	0	0
0.95	-0.001	0.111	0.063	0.245	67.5%	0	0
Shift in log-odds							
-2.5	0.000	0.032	0.033	0.130	95.1%	0	0
-2	0.000	0.030	0.031	0.120	95.0%	0	0
-1.5	0.000	0.027	0.027	0.107	95.1%	0	0
-1	0.000	0.024	0.024	0.093	95.3%	0	0
-0.5	0.000	0.021	0.021	0.082	95.0%	0	0
0.5	0.000	0.023	0.022	0.086	94.2%	0	0
1	0.000	0.032	0.029	0.114	92.7%	0	0
1.5	0.001	0.046	0.040	0.156	90.1%	0	0
2	0.001	0.062	0.051	0.199	87.2%	0	0
2.5	0.002	0.077	0.059	0.229	83.1%	0	0

Network-TMLE: targeted maximum likelihood estimation for dependent data, ESE: empirical standard error, ASE: average standard error, CLD: confidence limit difference, Coverage: 95% confidence interval coverage of the true parameter, Non-informative: the lower confidence limit was less than 0 and the upper confidence limit was greater than 1, Fail: estimator failed to produce an estimate.

Table A2.4.12: Network-TMLE with a single Poisson model for naloxone data generating mechanism with a uniform random graph

	Bias	ESE	ASE	CLD	Coverage	Non-informative	Fail
Proportion							
0.05	0.001	0.030	0.029	0.115	93.9%	0	0
0.10	0.001	0.025	0.025	0.098	94.4%	0	0
0.15	0.001	0.022	0.022	0.087	94.7%	0	0
0.20	0.001	0.021	0.021	0.081	94.8%	0	0
0.25	0.000	0.020	0.020	0.080	94.7%	0	0
0.30	0.000	0.021	0.021	0.082	94.7%	0	0
0.35	0.000	0.023	0.022	0.087	94.5%	0	0
0.40	0.001	0.026	0.024	0.096	93.7%	0	0
0.45	0.000	0.029	0.027	0.106	93.2%	0	0
0.50	0.000	0.034	0.030	0.119	91.9%	0	0
0.55	0.000	0.038	0.034	0.133	91.0%	0	0
0.60	0.000	0.044	0.037	0.147	89.9%	0	0
0.65	0.000	0.049	0.041	0.161	88.4%	0	0
0.70	0.000	0.055	0.044	0.174	86.9%	0	0
0.75	0.000	0.061	0.047	0.186	85.0%	0	0
0.80	0.000	0.066	0.050	0.196	83.2%	0	0
0.85	0.001	0.072	0.052	0.205	81.7%	0	0
0.90	0.001	0.078	0.054	0.213	79.7%	0	0
0.95	0.001	0.084	0.056	0.219	77.5%	0	0
Shift in log-odds							
-2.5	0.000	0.032	0.031	0.122	94.0%	0	0
-2	0.000	0.029	0.029	0.113	94.5%	0	0
-1.5	0.000	0.026	0.026	0.102	94.6%	0	0
-1	0.000	0.023	0.023	0.089	94.9%	0	0
-0.5	0.000	0.020	0.020	0.079	95.0%	0	0
0.5	0.000	0.020	0.020	0.078	94.2%	0	0
1	0.000	0.026	0.024	0.095	92.4%	0	0
1.5	0.001	0.036	0.031	0.122	89.5%	0	0
2	0.001	0.049	0.039	0.152	86.4%	0	0
2.5	0.001	0.060	0.045	0.177	83.2%	0	0

Network-TMLE: targeted maximum likelihood estimation for dependent data, ESE: empirical standard error, ASE: average standard error, CLD: confidence limit difference, Coverage: 95% confidence interval coverage of the true parameter, Non-informative: the lower confidence limit was less than 0 and the upper confidence limit was greater than 1, Fail: estimator failed to produce an estimate.

Table A2.4.13: IID-TMLE for naloxone data generating mechanism with a clustered power-law random graph

	Bias	ESE	ASE	CLD	Coverage	Non-informative	Fail
Proportion							
0.05	-0.042	0.020	0.020	0.079	44.0%	0	0
0.10	-0.033	0.020	0.019	0.076	58.8%	0	0
0.15	-0.023	0.019	0.019	0.074	75.1%	0	0
0.20	-0.014	0.019	0.019	0.073	86.5%	0	0
0.25	-0.005	0.019	0.019	0.074	93.1%	0	0
0.30	0.003	0.019	0.019	0.075	94.3%	0	0
0.35	0.012	0.020	0.020	0.078	91.6%	0	0
0.40	0.020	0.021	0.021	0.081	84.5%	0	0
0.45	0.027	0.022	0.022	0.085	75.6%	0	0
0.50	0.035	0.023	0.023	0.090	65.8%	0	0
0.55	0.042	0.025	0.024	0.096	59.1%	0	0
0.60	0.049	0.026	0.026	0.102	52.1%	0	0
0.65	0.056	0.028	0.028	0.108	47.4%	0	0
0.70	0.062	0.030	0.029	0.115	42.6%	0	0
0.75	0.069	0.032	0.031	0.122	39.4%	0	0
0.80	0.075	0.033	0.033	0.129	36.6%	0	0
0.85	0.081	0.035	0.035	0.137	35.6%	0	0
0.90	0.087	0.037	0.037	0.145	34.0%	0	0
0.95	0.092	0.039	0.039	0.152	33.5%	0	0
Shift in log-odds							
-2.5	-0.045	0.020	0.020	0.080	40.3%	0	0
-2	-0.042	0.020	0.020	0.078	45.1%	0	0
-1.5	-0.036	0.019	0.020	0.077	55.0%	0	0
-1	-0.027	0.019	0.019	0.074	69.9%	0	0
-0.5	-0.015	0.018	0.018	0.072	86.8%	0	0
0.5	0.017	0.019	0.019	0.075	87.2%	0	0
1	0.034	0.021	0.021	0.081	63.7%	0	0
1.5	0.050	0.023	0.023	0.091	41.9%	0	0
2	0.064	0.027	0.026	0.103	31.8%	0	0
2.5	0.074	0.030	0.030	0.116	29.0%	0	0

IID-TMLE: independent and identically distributed targeted maximum likelihood estimation, ESE: empirical standard error, ASE: average standard error, CLD: confidence limit difference, Coverage: 95% confidence interval coverage of the true parameter, Non-informative: the lower confidence limit was less than 0 and the upper confidence limit was greater than 1, Fail: estimator failed to produce an estimate.

Table A2.4.14: Network-TMLE for naloxone data generating mechanism with a clustered power-law random graph

	Bias	ESE	ASE	CLD	Coverage	Non-informative	Fail
Proportion							
0.05	-0.001	0.036	0.042	0.166	97.2%	0	0
0.10	-0.001	0.029	0.032	0.126	97.2%	0	0
0.15	-0.001	0.024	0.026	0.102	96.7%	0	0
0.20	-0.001	0.021	0.022	0.087	96.0%	0	0
0.25	0.000	0.020	0.020	0.079	95.4%	0	0
0.30	0.000	0.020	0.020	0.078	95.0%	0	0
0.35	0.000	0.022	0.023	0.088	95.4%	0	0
0.40	-0.001	0.029	0.029	0.114	95.4%	0	0
0.45	-0.002	0.038	0.040	0.155	95.1%	0	0
0.50	-0.003	0.047	0.052	0.205	93.9%	0	0
0.55	-0.004	0.054	0.065	0.256	92.2%	1	0
0.60	-0.005	0.060	0.077	0.303	91.2%	1	0
0.65	-0.005	0.065	0.087	0.343	90.0%	4	0
0.70	-0.006	0.069	0.095	0.373	88.8%	6	0
0.75	-0.006	0.073	0.101	0.395	87.7%	5	0
0.80	-0.006	0.076	0.104	0.408	86.6%	6	0
0.85	-0.006	0.080	0.105	0.413	84.9%	5	0
0.90	-0.006	0.084	0.104	0.409	83.1%	6	0
0.95	-0.007	0.089	0.101	0.397	80.5%	5	0
Shift in log-odds							
-2.5	0.000	0.040	0.046	0.182	97.1%	0	0
-2	0.000	0.035	0.041	0.160	97.0%	0	0
-1.5	0.000	0.030	0.034	0.133	97.0%	0	0
-1	0.000	0.024	0.027	0.106	96.5%	0	0
-0.5	0.000	0.020	0.021	0.083	95.6%	0	0
0.5	-0.001	0.024	0.024	0.094	95.3%	0	0
1	-0.003	0.045	0.051	0.198	92.8%	1	0
1.5	-0.004	0.060	0.079	0.311	90.8%	3	0
2	-0.004	0.068	0.097	0.379	89.4%	8	0
2.5	-0.005	0.074	0.104	0.407	87.7%	8	0

Network-TMLE: targeted maximum likelihood estimation for dependent data, ESE: empirical standard error, ASE: average standard error, CLD: confidence limit difference, Coverage: 95% confidence interval coverage of the true parameter, Non-informative: the lower confidence limit was less than 0 and the upper confidence limit was greater than 1, Fail: estimator failed to produce an estimate.

Table A2.4.15: Network-TMLE for naloxone data generating mechanism with a clustered power-law random graph restricted by degree

	Bias	ESE	ASE	CLD	Coverage	Non-informative	Fail
Proportion							
0.05	-0.001	0.032	0.034	0.134	96.1%	0	0
0.10	-0.001	0.026	0.028	0.109	96.1%	0	0
0.15	-0.001	0.023	0.024	0.093	96.1%	0	0
0.20	0.000	0.020	0.021	0.083	95.7%	0	0
0.25	0.000	0.019	0.020	0.078	95.5%	0	0
0.30	0.000	0.020	0.020	0.078	95.2%	0	0
0.35	0.000	0.021	0.021	0.084	95.2%	0	0
0.40	0.000	0.024	0.024	0.096	95.4%	0	0
0.45	0.000	0.029	0.030	0.116	95.6%	0	0
0.50	0.001	0.035	0.036	0.142	95.4%	0	0
0.55	0.000	0.042	0.044	0.173	94.5%	0	0
0.60	0.000	0.049	0.053	0.206	93.9%	0	0
0.65	0.000	0.056	0.061	0.239	92.9%	0	0
0.70	-0.001	0.062	0.068	0.268	91.7%	0	0
0.75	-0.001	0.068	0.075	0.292	90.4%	1	0
0.80	-0.002	0.073	0.079	0.311	88.9%	2	0
0.85	-0.002	0.078	0.083	0.324	87.3%	2	0
0.90	-0.002	0.083	0.085	0.331	85.4%	1	0
0.95	-0.002	0.089	0.085	0.333	82.7%	2	0
Shift in log-odds							
-2.5	0.000	0.035	0.037	0.144	95.7%	0	0
-2	0.001	0.032	0.033	0.130	95.9%	0	0
-1.5	0.000	0.028	0.029	0.113	95.8%	0	0
-1	0.000	0.023	0.024	0.095	95.6%	0	0
-0.5	0.000	0.020	0.020	0.079	95.4%	0	0
0.5	0.000	0.020	0.020	0.079	94.9%	0	0
1	-0.001	0.030	0.032	0.124	94.3%	0	0
1.5	-0.002	0.046	0.051	0.200	92.6%	1	0
2	-0.003	0.059	0.068	0.266	90.6%	1	0
2.5	-0.003	0.068	0.078	0.304	89.0%	2	0

Network-TMLE: targeted maximum likelihood estimation for dependent data, ESE: empirical standard error, ASE: average standard error, CLD: confidence limit difference, Coverage: 95% confidence interval coverage of the true parameter, Non-informative: the lower confidence limit was less than 0 and the upper confidence limit was greater than 1, Fail: estimator failed to produce an estimate.

Table A2.4.16: IID-TMLE for naloxone data generating mechanism with the eX-FLU network

	Bias	ESE	ASE	CLD	Coverage	Non-informative	Fail
Proportion							
0.05	-0.051	0.021	0.020	0.080	30.8%	0	0
0.10	-0.039	0.020	0.020	0.077	48.4%	0	0
0.15	-0.028	0.020	0.019	0.076	68.5%	0	0
0.20	-0.017	0.019	0.019	0.075	84.3%	0	0
0.25	-0.007	0.020	0.019	0.076	92.4%	0	0
0.30	0.003	0.020	0.020	0.078	93.8%	0	0
0.35	0.012	0.021	0.021	0.080	91.0%	0	0
0.40	0.020	0.022	0.021	0.084	84.4%	0	0
0.45	0.028	0.023	0.023	0.089	76.6%	0	0
0.50	0.036	0.025	0.024	0.094	68.8%	0	0
0.55	0.042	0.026	0.026	0.100	62.0%	0	0
0.60	0.049	0.028	0.027	0.107	56.3%	0	0
0.65	0.056	0.030	0.029	0.113	52.2%	0	0
0.70	0.062	0.032	0.031	0.121	48.9%	0	0
0.75	0.067	0.034	0.033	0.128	47.0%	0	0
0.80	0.072	0.036	0.035	0.136	46.3%	0	0
0.85	0.077	0.038	0.037	0.144	44.7%	0	0
0.90	0.082	0.040	0.039	0.152	44.3%	0	0
0.95	0.087	0.042	0.041	0.160	44.3%	0	0
Shift in log-odds							
-2.5	-0.055	0.021	0.021	0.082	26.3%	0	0
-2	-0.050	0.021	0.020	0.080	32.3%	0	0
-1.5	-0.042	0.020	0.020	0.079	44.4%	0	0
-1	-0.031	0.019	0.020	0.077	64.0%	0	0
-0.5	-0.016	0.019	0.019	0.075	86.0%	0	0
0.5	0.020	0.019	0.020	0.077	84.9%	0	0
1	0.037	0.021	0.022	0.084	60.6%	0	0
1.5	0.052	0.024	0.024	0.095	42.3%	0	0
2	0.065	0.027	0.028	0.108	34.4%	0	0
2.5	0.074	0.031	0.031	0.121	33.8%	0	0

IID-TMLE: independent and identically distributed targeted maximum likelihood estimation, ESE: empirical standard error, ASE: average standard error, CLD: confidence limit difference, Coverage: 95% confidence interval coverage of the true parameter, Non-informative: the lower confidence limit was less than 0 and the upper confidence limit was greater than 1, Fail: estimator failed to produce an estimate.

Table A2.4.17: Network-TMLE for naloxone data generating mechanism with the eX-FLU network

	Bias	ESE	ASE	CLD	Coverage	Non-informative	Fail
Proportion							
0.05	-0.001	0.047	0.104	0.407	99.9%	0	0
0.10	-0.001	0.037	0.069	0.272	99.7%	0	0
0.15	-0.001	0.030	0.047	0.183	99.2%	0	0
0.20	-0.001	0.025	0.032	0.127	98.3%	0	0
0.25	-0.001	0.022	0.024	0.095	96.4%	0	0
0.30	0.000	0.021	0.022	0.085	94.9%	0	0
0.35	-0.001	0.024	0.025	0.097	95.5%	0	0
0.40	-0.001	0.032	0.036	0.142	95.8%	0	0
0.45	-0.002	0.043	0.057	0.223	95.7%	1	0
0.50	-0.002	0.053	0.084	0.328	95.6%	1	0
0.55	-0.004	0.058	0.110	0.430	95.6%	5	0
0.60	-0.005	0.061	0.131	0.513	95.9%	7	0
0.65	-0.005	0.063	0.147	0.576	95.6%	10	0
0.70	-0.005	0.065	0.158	0.618	95.5%	17	0
0.75	-0.005	0.066	0.164	0.643	94.8%	20	0
0.80	-0.006	0.068	0.166	0.651	94.3%	23	0
0.85	-0.006	0.071	0.165	0.647	93.3%	22	0
0.90	-0.006	0.074	0.160	0.626	91.2%	19	0
0.95	-0.007	0.079	0.149	0.585	88.6%	17	0
Shift in log-odds							
-2.5	-0.001	0.049	0.117	0.458	99.9%	3	0
-2	-0.001	0.044	0.097	0.382	99.9%	0	0
-1.5	-0.001	0.037	0.073	0.285	99.9%	0	0
-1	0.000	0.028	0.047	0.185	99.7%	0	0
-0.5	0.000	0.021	0.028	0.111	98.4%	0	0
0.5	-0.001	0.027	0.033	0.128	96.4%	0	0
1	-0.004	0.052	0.094	0.367	96.0%	1	0
1.5	-0.005	0.061	0.149	0.583	96.4%	19	0
2	-0.005	0.064	0.172	0.674	96.6%	30	0
2.5	-0.006	0.066	0.177	0.694	96.0%	37	0

Network-TMLE: targeted maximum likelihood estimation for dependent data, ESE: empirical standard error, ASE: average standard error, CLD: confidence limit difference, Coverage: 95% confidence interval coverage of the true parameter, Non-informative: the lower confidence limit was less than 0 and the upper confidence limit was greater than 1, Fail: estimator failed to produce an estimate.

Table A2.4.18: Network-TMLE for naloxone data generating mechanism with the eX-FLU network restricted by degree

	Bias	ESE	ASE	CLD	Coverage	Non-informative	Fail
Proportion							
0.05	-0.001	0.037	0.053	0.207	99.0%	0	0
0.10	-0.001	0.030	0.040	0.155	98.5%	0	0
0.15	-0.001	0.025	0.031	0.121	98.0%	0	0
0.20	-0.001	0.022	0.025	0.099	96.6%	0	0
0.25	0.000	0.021	0.022	0.087	95.3%	0	0
0.30	-0.001	0.021	0.021	0.083	94.5%	0	0
0.35	0.000	0.023	0.023	0.090	95.0%	0	0
0.40	0.000	0.026	0.028	0.109	95.8%	0	0
0.45	0.000	0.032	0.036	0.140	96.3%	0	0
0.50	-0.001	0.039	0.047	0.184	96.6%	0	0
0.55	-0.001	0.047	0.060	0.234	96.4%	0	0
0.60	-0.002	0.054	0.073	0.286	96.3%	4	0
0.65	-0.002	0.059	0.085	0.335	95.8%	5	0
0.70	-0.002	0.064	0.096	0.377	95.4%	4	0
0.75	-0.003	0.068	0.105	0.410	94.9%	5	0
0.80	-0.003	0.072	0.111	0.434	94.4%	7	0
0.85	-0.003	0.076	0.114	0.448	93.1%	11	0
0.90	-0.003	0.081	0.116	0.453	91.7%	15	0
0.95	-0.004	0.087	0.114	0.449	89.4%	18	0
Shift in log-odds							
-2.5	-0.001	0.038	0.056	0.220	99.2%	0	0
-2	0.000	0.035	0.049	0.193	99.0%	0	0
-1.5	0.000	0.030	0.040	0.159	98.8%	0	0
-1	0.000	0.025	0.031	0.123	98.3%	0	0
-0.5	0.000	0.021	0.024	0.092	96.9%	0	0
0.5	0.000	0.022	0.024	0.093	96.4%	0	0
1	0.000	0.036	0.045	0.178	96.9%	0	0
1.5	-0.001	0.052	0.079	0.309	96.2%	0	0
2	-0.002	0.062	0.104	0.408	95.5%	5	0
2.5	-0.003	0.068	0.116	0.456	94.9%	10	0

Network-TMLE: targeted maximum likelihood estimation for dependent data, ESE: empirical standard error, ASE: average standard error, CLD: confidence limit difference, Coverage: 95% confidence interval coverage of the true parameter, Non-informative: the lower confidence limit was less than 0 and the upper confidence limit was greater than 1, Fail: estimator failed to produce an estimate.

Table A2.4.19: IID-TMLE for diet data generating mechanism with a uniform random graph

		Bias	ESE	ASE	CLD	Coverage	Fail
Proportion							
	0.05	-0.242	0.151	0.222	0.870	89.3%	0
	0.10	-0.241	0.136	0.212	0.830	89.4%	0
	0.15	-0.234	0.121	0.203	0.795	90.5%	0
	0.20	-0.220	0.108	0.195	0.766	93.1%	0
	0.25	-0.194	0.097	0.189	0.742	96.2%	0
	0.30	-0.152	0.089	0.185	0.725	98.9%	0
	0.35	-0.091	0.083	0.183	0.716	99.9%	0
	0.40	-0.009	0.083	0.182	0.713	100.0%	0
	0.45	0.098	0.086	0.183	0.718	99.9%	0
	0.50	0.234	0.093	0.186	0.730	92.4%	0
	0.55	0.389	0.103	0.191	0.749	43.8%	0
	0.60	0.561	0.116	0.198	0.774	6.1%	0
	0.65	0.763	0.130	0.206	0.806	0.2%	0
	0.70	0.957	0.145	0.215	0.842	0.0%	0
	0.75	1.177	0.161	0.225	0.883	0.0%	0
	0.80	1.390	0.177	0.237	0.928	0.0%	0
	0.85	1.601	0.194	0.249	0.976	0.0%	0
	0.90	1.804	0.211	0.262	1.027	0.0%	0
	0.95	1.990	0.229	0.276	1.081	0.0%	0
Shift in log-odds							
	-2.5	-0.244	0.150	0.221	0.866	89.2%	0
	-2	-0.244	0.140	0.214	0.840	89.3%	0
	-1.5	-0.239	0.126	0.205	0.805	90.3%	0
	-1	-0.223	0.107	0.194	0.762	92.9%	0
	-0.5	-0.163	0.088	0.184	0.723	98.4%	0
	0.5	0.307	0.091	0.185	0.727	73.1%	0
	1	0.727	0.120	0.201	0.787	0.2%	0
	1.5	1.160	0.152	0.221	0.866	0.0%	0
	2	1.508	0.179	0.241	0.943	0.0%	0
	2.5	1.755	0.201	0.257	1.006	0.0%	0

IID-TMLE: independent and identically distributed targeted maximum likelihood estimation, ESE: empirical standard error, ASE: average standard error, CLD: confidence limit difference, Coverage: 95% confidence interval coverage of the true parameter, Fail: estimator failed to produce an estimate.

Table A2.4.20: Network-TMLE with a series of logistic models for diet data generating mechanism with a uniform random graph

		Bias	ESE	ASE	CLD	Coverage	Fail
Proportion							
	0.05	-0.004	0.099	0.102	0.400	95.7%	0
	0.10	-0.004	0.082	0.084	0.330	95.7%	0
	0.15	-0.002	0.070	0.071	0.278	95.7%	0
	0.20	-0.001	0.061	0.061	0.241	95.0%	0
	0.25	0.000	0.056	0.055	0.215	95.0%	0
	0.30	0.000	0.052	0.050	0.198	94.4%	0
	0.35	0.001	0.050	0.048	0.189	94.4%	0
	0.40	0.000	0.050	0.048	0.187	93.5%	0
	0.45	0.001	0.052	0.049	0.192	93.0%	0
	0.50	0.006	0.056	0.052	0.203	92.6%	0
	0.55	0.007	0.062	0.056	0.221	91.8%	0
	0.60	0.004	0.071	0.063	0.247	92.5%	0
	0.65	0.016	0.083	0.072	0.282	90.6%	0
	0.70	0.007	0.097	0.083	0.325	90.6%	0
	0.75	0.017	0.115	0.096	0.378	89.4%	0
	0.80	0.020	0.135	0.112	0.439	88.5%	0
	0.85	0.025	0.159	0.130	0.509	88.0%	0
	0.90	0.033	0.186	0.149	0.586	86.8%	0
	0.95	0.037	0.217	0.171	0.669	85.2%	0
Shift in log-odds							
	-2.5	-0.001	0.100	0.100	0.392	94.8%	0
	-2	-0.001	0.089	0.088	0.345	94.6%	0
	-1.5	-0.001	0.075	0.074	0.290	94.8%	0
	-1	-0.003	0.062	0.060	0.237	94.5%	0
	-0.5	-0.003	0.053	0.050	0.197	93.7%	0
	0.5	0.002	0.059	0.053	0.208	91.9%	0
	1	0.006	0.079	0.070	0.273	91.5%	0
	1.5	0.015	0.112	0.095	0.372	90.0%	0
	2	0.022	0.148	0.123	0.481	88.5%	0
	2.5	0.031	0.179	0.147	0.575	87.6%	0

Network-TMLE: targeted maximum likelihood estimation for dependent data, ESE: empirical standard error, ASE: average standard error, CLD: confidence limit difference, Coverage: 95% confidence interval coverage of the true parameter, Fail: estimator failed to produce an estimate.

Table A2.4.21: Network-TMLE with a single logistic model for diet data generating mechanism with a uniform random graph

		Bias	ESE	ASE	CLD	Coverage	Fail
Proportion							
	0.05	-0.004	0.058	0.057	0.222	94.8%	1568
	0.10	-0.004	0.055	0.054	0.212	95.1%	0
	0.15	-0.002	0.052	0.052	0.203	95.3%	0
	0.20	-0.001	0.051	0.050	0.195	94.9%	0
	0.25	-0.001	0.049	0.048	0.188	94.5%	0
	0.30	0.000	0.049	0.047	0.182	94.2%	0
	0.35	0.001	0.047	0.046	0.179	94.1%	0
	0.40	0.000	0.048	0.045	0.178	93.6%	0
	0.45	0.001	0.050	0.046	0.181	92.8%	0
	0.50	0.006	0.053	0.048	0.188	92.0%	0
	0.55	0.007	0.057	0.052	0.202	91.5%	0
	0.60	0.004	0.064	0.057	0.224	91.8%	0
	0.65	0.016	0.073	0.065	0.253	90.9%	0
	0.70	0.007	0.085	0.074	0.291	91.4%	0
	0.75	0.017	0.098	0.086	0.336	90.8%	0
	0.80	0.020	0.113	0.099	0.388	90.6%	0
	0.85	0.026	0.130	0.113	0.445	90.1%	0
	0.90	0.034	0.147	0.129	0.506	90.1%	0
	0.95	0.038	0.166	0.145	0.570	89.6%	0
Shift in log-odds							
	-2.5	-0.003	0.058	0.056	0.221	94.5%	963
	-2	-0.003	0.056	0.055	0.214	94.4%	0
	-1.5	-0.002	0.054	0.052	0.204	94.6%	0
	-1	-0.004	0.051	0.049	0.193	94.2%	0
	-0.5	-0.003	0.049	0.046	0.181	93.2%	0
	0.5	0.003	0.054	0.049	0.191	92.0%	0
	1	0.005	0.070	0.062	0.244	92.3%	0
	1.5	0.013	0.096	0.083	0.327	91.3%	0
	2	0.019	0.122	0.105	0.413	91.0%	0
	2.5	0.028	0.143	0.124	0.485	90.6%	0

Network-TMLE: targeted maximum likelihood estimation for dependent data, ESE: empirical standard error, ASE: average standard error, CLD: confidence limit difference, Coverage: 95% confidence interval coverage of the true parameter, Fail: estimator failed to produce an estimate.

Table A2.4.22: IID-TMLE for diet data generating mechanism with a clustered power-law random graph

		Bias	ESE	ASE	CLD	Coverage	Fail
Proportion							
	0.05	-0.948	0.156	0.213	0.835	0.0%	0
	0.10	-0.899	0.145	0.203	0.797	0.0%	0
	0.15	-0.805	0.135	0.195	0.763	0.1%	0
	0.20	-0.681	0.128	0.188	0.735	0.6%	0
	0.25	-0.528	0.123	0.182	0.712	6.7%	0
	0.30	-0.363	0.121	0.178	0.696	46.7%	0
	0.35	-0.179	0.122	0.175	0.687	91.3%	0
	0.40	0.009	0.125	0.175	0.684	99.4%	0
	0.45	0.212	0.131	0.176	0.689	83.8%	0
	0.50	0.411	0.140	0.179	0.701	33.4%	0
	0.55	0.624	0.149	0.183	0.719	4.3%	0
	0.60	0.833	0.161	0.190	0.743	0.2%	0
	0.65	1.050	0.174	0.197	0.773	0.0%	0
	0.70	1.273	0.188	0.206	0.808	0.0%	0
	0.75	1.500	0.202	0.216	0.847	0.0%	0
	0.80	1.728	0.217	0.227	0.890	0.0%	0
	0.85	1.962	0.233	0.239	0.937	0.0%	0
	0.90	2.200	0.249	0.252	0.986	0.0%	0
	0.95	2.441	0.266	0.265	1.037	0.0%	0
Shift in log-odds							
	-2.5	-0.955	0.157	0.213	0.833	0.0%	0
	-2	-0.927	0.150	0.206	0.808	0.0%	0
	-1.5	-0.851	0.141	0.198	0.774	0.0%	0
	-1	-0.684	0.130	0.187	0.733	0.4%	0
	-0.5	-0.400	0.123	0.177	0.695	33.7%	0
	0.5	0.478	0.141	0.178	0.698	19.0%	0
	1	0.979	0.167	0.193	0.756	0.0%	0
	1.5	1.449	0.196	0.212	0.832	0.0%	0
	2	1.831	0.221	0.231	0.906	0.0%	0
	2.5	2.119	0.240	0.246	0.966	0.0%	0

IID-TMLE: independent and identically distributed targeted maximum likelihood estimation, ESE: empirical standard error, ASE: average standard error, CLD: confidence limit difference, Coverage: 95% confidence interval coverage of the true parameter, Fail: estimator failed to produce an estimate.

Table A2.4.23: Network-TMLE for diet data generating mechanism with a clustered power-law random graph

		Bias	ESE	ASE	CLD	Coverage	Fail
Proportion							
	0.05	0.000	0.065	0.061	0.241	93.8%	0
	0.10	-0.001	0.061	0.058	0.228	93.6%	0
	0.15	0.001	0.058	0.055	0.214	93.3%	0
	0.20	-0.001	0.055	0.052	0.202	93.5%	0
	0.25	0.002	0.052	0.049	0.192	93.1%	0
	0.30	-0.001	0.051	0.047	0.184	92.9%	0
	0.35	0.002	0.050	0.046	0.179	92.9%	0
	0.40	-0.001	0.050	0.045	0.177	92.6%	0
	0.45	0.006	0.051	0.046	0.180	91.5%	0
	0.50	0.002	0.054	0.047	0.186	91.2%	0
	0.55	0.006	0.057	0.050	0.195	91.2%	0
	0.60	0.002	0.060	0.053	0.209	91.2%	0
	0.65	0.002	0.066	0.058	0.227	90.5%	0
	0.70	0.003	0.073	0.064	0.249	90.0%	0
	0.75	0.004	0.080	0.070	0.276	90.7%	0
	0.80	0.003	0.089	0.078	0.306	90.8%	0
	0.85	0.005	0.098	0.087	0.341	91.0%	0
	0.90	0.006	0.110	0.097	0.381	90.9%	0
	0.95	0.005	0.122	0.109	0.426	90.9%	0
Shift in log-odds							
	-2.5	-0.002	0.065	0.061	0.239	92.8%	0
	-2	-0.002	0.063	0.059	0.231	93.1%	0
	-1.5	-0.002	0.060	0.056	0.218	92.4%	0
	-1	0.001	0.055	0.051	0.200	92.9%	0
	-0.5	0.002	0.051	0.047	0.183	92.7%	0
	0.5	0.001	0.055	0.048	0.186	90.6%	0
	1	-0.001	0.064	0.056	0.220	91.2%	0
	1.5	0.007	0.079	0.069	0.269	90.6%	0
	2	0.007	0.094	0.082	0.321	91.4%	0
	2.5	0.008	0.107	0.094	0.367	91.3%	0

Network-TMLE: targeted maximum likelihood estimation for dependent data, ESE: empirical standard error, ASE: average standard error, CLD: confidence limit difference, Coverage: 95% confidence interval coverage of the true parameter, Fail: estimator failed to produce an estimate.

Table A2.4.24: Network-TMLE for diet data generating mechanism with a clustered power-law random graph restricted by degree

		Bias	ESE	ASE	CLD	Coverage	Fail
Proportion							
	0.05	-0.001	0.063	0.061	0.239	93.6%	0
	0.10	-0.003	0.060	0.058	0.227	93.8%	0
	0.15	-0.001	0.057	0.055	0.215	93.9%	0
	0.20	0.002	0.055	0.052	0.203	93.9%	0
	0.25	0.002	0.052	0.049	0.193	93.5%	0
	0.30	0.002	0.051	0.047	0.186	93.2%	0
	0.35	0.001	0.050	0.046	0.181	93.4%	0
	0.40	0.000	0.049	0.046	0.179	93.1%	0
	0.45	0.001	0.051	0.046	0.181	92.5%	0
	0.50	0.004	0.053	0.048	0.187	91.8%	0
	0.55	0.006	0.055	0.050	0.196	92.1%	0
	0.60	0.002	0.059	0.054	0.210	92.2%	0
	0.65	0.012	0.064	0.058	0.227	91.7%	0
	0.70	-0.001	0.070	0.063	0.248	91.7%	0
	0.75	0.007	0.077	0.070	0.273	92.0%	0
	0.80	0.006	0.085	0.077	0.302	91.9%	0
	0.85	0.008	0.094	0.086	0.335	92.0%	0
	0.90	0.014	0.104	0.095	0.372	92.0%	0
	0.95	0.013	0.115	0.105	0.413	92.2%	0
Shift in log-odds							
	-2.5	-0.002	0.064	0.061	0.238	93.3%	0
	-2	-0.003	0.062	0.059	0.230	93.4%	0
	-1.5	-0.001	0.059	0.055	0.218	93.0%	0
	-1	0.002	0.055	0.051	0.201	92.9%	0
	-0.5	0.002	0.051	0.047	0.185	92.6%	0
	0.5	-0.003	0.055	0.048	0.188	91.0%	0
	1	0.004	0.063	0.056	0.220	91.7%	0
	1.5	0.006	0.076	0.068	0.267	91.3%	0
	2	0.007	0.091	0.081	0.316	91.7%	0
	2.5	0.012	0.102	0.092	0.359	91.7%	0

Network-TMLE: targeted maximum likelihood estimation for dependent data, ESE: empirical standard error, ASE: average standard error, CLD: confidence limit difference, Coverage: 95% confidence interval coverage of the true parameter, Fail: estimator failed to produce an estimate.

Table A2.4.25: IID-TMLE for diet data generating mechanism with the eX-FLU network

		Bias	ESE	ASE	CLD	Coverage	Fail
Proportion							
	0.05	-1.571	0.205	0.310	1.217	0.0%	0
	0.10	-1.435	0.187	0.296	1.161	0.0%	0
	0.15	-1.208	0.171	0.284	1.113	0.0%	0
	0.20	-0.930	0.159	0.273	1.071	0.6%	0
	0.25	-0.662	0.150	0.265	1.038	16.5%	0
	0.30	-0.414	0.146	0.259	1.015	74.6%	0
	0.35	-0.183	0.147	0.255	1.001	98.9%	0
	0.40	0.028	0.153	0.254	0.997	99.6%	0
	0.45	0.226	0.163	0.256	1.003	94.5%	0
	0.50	0.407	0.177	0.260	1.020	72.5%	0
	0.55	0.571	0.194	0.267	1.046	41.5%	0
	0.60	0.730	0.212	0.276	1.081	18.4%	0
	0.65	0.871	0.233	0.287	1.124	8.5%	0
	0.70	1.013	0.255	0.300	1.175	3.6%	0
	0.75	1.137	0.277	0.314	1.232	2.0%	0
	0.80	1.259	0.300	0.330	1.294	1.3%	0
	0.85	1.380	0.325	0.347	1.361	0.9%	0
	0.90	1.497	0.349	0.365	1.432	0.8%	0
	0.95	1.612	0.374	0.384	1.507	0.6%	0
Shift in log-odds							
	-2.5	-1.567	0.200	0.308	1.207	0.0%	0
	-2	-1.486	0.188	0.298	1.170	0.0%	0
	-1.5	-1.288	0.171	0.286	1.120	0.0%	0
	-1	-0.936	0.152	0.271	1.061	0.3%	0
	-0.5	-0.486	0.139	0.257	1.006	55.5%	0
	0.5	0.461	0.173	0.259	1.014	61.3%	0
	1	0.840	0.217	0.280	1.099	8.0%	0
	1.5	1.122	0.263	0.309	1.210	1.8%	0
	2	1.334	0.302	0.336	1.318	0.7%	0
	2.5	1.482	0.332	0.359	1.406	0.5%	0

IID-TMLE: independent and identically distributed targeted maximum likelihood estimation, ESE: empirical standard error, ASE: average standard error, CLD: confidence limit difference, Coverage: 95% confidence interval coverage of the true parameter, Fail: estimator failed to produce an estimate.

Table A2.4.26: Network-TMLE for diet data generating mechanism with the eX-FLU network

		Bias	ESE	ASE	CLD	Coverage	Fail
Proportion							
	0.05	-0.004	0.077	0.069	0.271	92.0%	0
	0.10	-0.001	0.073	0.064	0.252	91.2%	0
	0.15	-0.007	0.068	0.059	0.231	90.7%	0
	0.20	0.003	0.062	0.054	0.213	91.0%	0
	0.25	0.003	0.058	0.051	0.199	91.3%	0
	0.30	0.001	0.055	0.049	0.190	91.5%	0
	0.35	0.000	0.053	0.047	0.185	92.0%	0
	0.40	-0.002	0.053	0.047	0.184	91.7%	0
	0.45	0.000	0.054	0.047	0.186	91.6%	0
	0.50	0.000	0.056	0.049	0.191	91.4%	0
	0.55	-0.003	0.057	0.051	0.199	91.2%	0
	0.60	0.001	0.061	0.053	0.210	91.6%	0
	0.65	-0.001	0.064	0.057	0.222	91.5%	0
	0.70	0.006	0.069	0.060	0.237	91.4%	0
	0.75	0.001	0.073	0.065	0.254	91.4%	0
	0.80	0.000	0.079	0.069	0.272	91.4%	0
	0.85	0.001	0.085	0.075	0.293	91.4%	0
	0.90	0.002	0.091	0.080	0.315	91.5%	0
	0.95	0.004	0.098	0.086	0.339	91.6%	0
Shift in log-odds							
	-2.5	-0.006	0.076	0.068	0.268	92.5%	0
	-2	-0.006	0.073	0.065	0.256	92.0%	0
	-1.5	-0.008	0.068	0.060	0.236	91.4%	0
	-1	-0.006	0.062	0.054	0.211	91.0%	0
	-0.5	-0.006	0.054	0.048	0.190	92.0%	0
	0.5	0.001	0.055	0.049	0.190	91.9%	0
	1	0.002	0.062	0.055	0.215	91.9%	0
	1.5	-0.002	0.072	0.063	0.247	91.6%	0
	2	0.001	0.080	0.071	0.279	91.8%	0
	2.5	0.005	0.087	0.078	0.306	91.3%	0

Network-TMLE: targeted maximum likelihood estimation for dependent data, ESE: empirical standard error, ASE: average standard error, CLD: confidence limit difference, Coverage: 95% confidence interval coverage of the true parameter, Fail: estimator failed to produce an estimate.

Table A2.4.27: Network-TMLE for diet data generating mechanism with the eX-FLU network restricted by degree

		Bias	ESE	ASE	CLD	Coverage	Fail
Proportion							
	0.05	-0.005	0.073	0.067	0.264	92.4%	0
	0.10	-0.002	0.069	0.063	0.246	92.5%	0
	0.15	-0.006	0.065	0.059	0.230	92.3%	0
	0.20	0.000	0.061	0.055	0.216	92.4%	0
	0.25	0.002	0.058	0.052	0.204	92.4%	0
	0.30	0.000	0.056	0.050	0.195	91.9%	0
	0.35	-0.002	0.054	0.049	0.190	92.4%	0
	0.40	-0.003	0.055	0.048	0.189	91.7%	0
	0.45	-0.001	0.055	0.049	0.191	91.4%	0
	0.50	-0.001	0.057	0.050	0.197	91.5%	0
	0.55	-0.004	0.059	0.052	0.206	91.1%	0
	0.60	0.001	0.063	0.055	0.217	90.9%	0
	0.65	-0.003	0.067	0.059	0.231	91.3%	0
	0.70	0.004	0.071	0.063	0.246	91.6%	0
	0.75	0.000	0.076	0.067	0.264	91.4%	0
	0.80	0.000	0.082	0.072	0.284	91.7%	0
	0.85	0.002	0.088	0.078	0.305	91.6%	0
	0.90	0.002	0.095	0.084	0.329	91.6%	0
	0.95	0.004	0.102	0.090	0.354	91.9%	0
Shift in log-odds							
	-2.5	-0.007	0.073	0.067	0.261	92.8%	0
	-2	-0.005	0.069	0.064	0.250	93.2%	0
	-1.5	-0.007	0.065	0.060	0.234	92.6%	0
	-1	-0.003	0.060	0.055	0.214	92.9%	0
	-0.5	-0.001	0.055	0.050	0.194	92.2%	0
	0.5	0.000	0.056	0.050	0.196	91.7%	0
	1	0.000	0.064	0.057	0.223	91.9%	0
	1.5	-0.001	0.073	0.066	0.257	91.8%	0
	2	0.001	0.082	0.074	0.291	92.0%	0
	2.5	0.003	0.090	0.081	0.319	92.0%	0

Network-TMLE: targeted maximum likelihood estimation for dependent data, ESE: empirical standard error, ASE: average standard error, CLD: confidence limit difference, Coverage: 95% confidence interval coverage of the true parameter, Fail: estimator failed to produce an estimate.

Table A2.4.28: IID-TMLE for vaccine data generating mechanism with a uniform random graph

	Bias	ESE	ASE	CLD	Coverage	Non-informative	Fail
Proportion							
0.05	-0.030	0.025	0.025	0.099	78.6%	0	0
0.10	-0.024	0.024	0.024	0.094	82.7%	0	0
0.15	-0.018	0.023	0.023	0.090	87.6%	0	0
0.20	-0.013	0.022	0.022	0.087	91.1%	0	0
0.25	-0.008	0.021	0.021	0.084	93.8%	0	0
0.30	-0.003	0.020	0.021	0.081	95.4%	0	0
0.35	0.001	0.020	0.020	0.079	95.6%	0	0
0.40	0.005	0.020	0.020	0.078	94.9%	0	0
0.45	0.010	0.020	0.020	0.078	93.1%	0	0
0.50	0.013	0.020	0.020	0.079	91.1%	0	0
0.55	0.016	0.020	0.020	0.080	89.1%	0	0
0.60	0.020	0.021	0.021	0.082	86.9%	0	0
0.65	0.023	0.021	0.022	0.085	85.2%	0	0
0.70	0.026	0.022	0.023	0.088	83.6%	0	0
0.75	0.028	0.023	0.024	0.092	82.3%	0	0
0.80	0.030	0.024	0.025	0.097	82.0%	0	0
0.85	0.032	0.026	0.026	0.101	81.2%	0	0
0.90	0.033	0.027	0.027	0.107	82.0%	0	0
0.95	0.034	0.028	0.029	0.112	82.6%	0	0
Shift in log-odds							
-2.5	-0.0295	0.0252	0.0251	0.0983	78.2%	0	0
-2	-0.0265	0.0245	0.0244	0.0958	81.1%	0	0
-1.5	-0.0220	0.0236	0.0236	0.0925	84.9%	0	0
-1	-0.0156	0.0226	0.0226	0.0888	89.3%	0	0
-0.5	-0.0082	0.0214	0.0216	0.0849	93.7%	0	0
0.5	0.0094	0.0200	0.0205	0.0803	94.2%	0	0
1	0.0177	0.0203	0.0209	0.0818	88.5%	0	0
1.5	0.0245	0.0215	0.0220	0.0862	82.9%	0	0
2	0.0292	0.0233	0.0236	0.0925	80.0%	0	0
2.5	0.0324	0.0251	0.0253	0.0990	79.5%	0	0

IID-TMLE: independent and identically distributed targeted maximum likelihood estimation, ESE: empirical standard error, ASE: average standard error, CLD: confidence limit difference, Coverage: 95% confidence interval coverage of the true parameter, Non-informative: the lower confidence limit was less than 0 and the upper confidence limit was greater than 1, Fail: estimator failed to produce an estimate.

Table A2.4.29: Network-TMLE with a series of logistic models for vaccine data generating mechanism with a uniform random graph

	Bias	ESE	ASE	CLD	Coverage	Non-informative	Fail
Proportion							
0.05	-0.005	0.065	0.064	0.250	94.5%	0	0
0.10	-0.004	0.050	0.049	0.191	94.5%	0	0
0.15	-0.003	0.040	0.038	0.150	94.2%	0	0
0.20	-0.002	0.032	0.031	0.122	94.4%	0	0
0.25	-0.001	0.027	0.026	0.104	94.5%	0	0
0.30	-0.001	0.024	0.024	0.094	94.7%	0	0
0.35	0.000	0.023	0.023	0.090	94.9%	0	0
0.40	0.000	0.024	0.023	0.091	94.7%	0	0
0.45	0.001	0.026	0.025	0.098	94.2%	0	0
0.50	0.001	0.030	0.028	0.109	93.8%	0	0
0.55	0.001	0.035	0.032	0.125	93.3%	0	0
0.60	0.001	0.041	0.037	0.145	93.0%	0	0
0.65	0.001	0.047	0.043	0.168	92.1%	0	0
0.70	0.001	0.054	0.049	0.193	91.6%	0	0
0.75	0.001	0.062	0.056	0.220	90.4%	0	0
0.80	0.001	0.070	0.063	0.247	89.3%	0	0
0.85	0.002	0.077	0.069	0.272	88.1%	1	1
0.90	0.002	0.086	0.075	0.295	86.0%	1	1
0.95	0.003	0.097	0.080	0.315	82.8%	0	0
Shift in log-odds							
-2.5	-0.004	0.060	0.061	0.239	95.3%	0	0
-2	-0.003	0.050	0.051	0.201	95.2%	0	0
-1.5	-0.003	0.040	0.041	0.159	95.1%	0	0
-1	-0.002	0.031	0.031	0.121	95.1%	0	0
-0.5	-0.001	0.024	0.024	0.095	94.8%	0	0
0.5	0.001	0.023	0.023	0.090	94.8%	0	0
1	0.001	0.031	0.031	0.120	94.1%	0	0
1.5	0.002	0.046	0.044	0.173	93.1%	0	0
2	0.002	0.061	0.059	0.232	92.3%	0	0
2.5	0.003	0.073	0.071	0.277	91.0%	0	0

Network-TMLE: targeted maximum likelihood estimation for dependent data, ESE: empirical standard error, ASE: average standard error, CLD: confidence limit difference, Coverage: 95% confidence interval coverage of the true parameter, Non-informative: the lower confidence limit was less than 0 and the upper confidence limit was greater than 1, Fail: estimator failed to produce an estimate.

Table A2.4.30: Network-TMLE with a single Poisson model for vaccine data generating mechanism with a uniform random graph

	Bias	ESE	ASE	CLD	Coverage	Non-informative	Fail
Proportion							
0.05	-0.003	0.046	0.035	0.136	85.7%	0	0
0.10	-0.002	0.037	0.029	0.114	87.7%	0	0
0.15	-0.002	0.031	0.026	0.101	89.8%	0	0
0.20	-0.001	0.026	0.023	0.092	91.5%	0	0
0.25	-0.001	0.024	0.022	0.087	92.6%	0	0
0.30	0.000	0.022	0.021	0.083	94.5%	0	0
0.35	0.000	0.021	0.021	0.082	94.9%	0	0
0.40	0.000	0.021	0.021	0.081	94.5%	0	0
0.45	0.000	0.022	0.021	0.082	93.1%	0	0
0.50	0.000	0.023	0.021	0.083	91.8%	0	0
0.55	0.000	0.025	0.022	0.084	89.9%	0	0
0.60	0.000	0.028	0.022	0.086	87.5%	0	0
0.65	0.000	0.030	0.023	0.089	85.0%	0	0
0.70	0.001	0.033	0.023	0.091	82.6%	0	0
0.75	0.001	0.036	0.024	0.094	79.9%	0	0
0.80	0.001	0.039	0.024	0.096	77.1%	0	0
0.85	0.001	0.042	0.025	0.098	74.6%	0	0
0.90	0.001	0.045	0.026	0.100	72.6%	0	0
0.95	0.001	0.048	0.026	0.102	70.6%	0	0
Shift in log-odds							
-2.5	-0.001	0.044	0.033	0.131	86.0%	0	0
-2	-0.001	0.038	0.030	0.118	87.4%	0	0
-1.5	-0.001	0.032	0.027	0.105	89.2%	0	0
-1	-0.001	0.027	0.024	0.093	91.5%	0	0
-0.5	-0.001	0.023	0.021	0.084	93.5%	0	0
0.5	0.000	0.021	0.020	0.078	93.2%	0	0
1	0.001	0.025	0.020	0.080	88.5%	0	0
1.5	0.002	0.030	0.022	0.085	83.4%	0	0
2	0.002	0.036	0.023	0.090	78.6%	0	0
2.5	0.002	0.040	0.024	0.094	74.8%	0	0

Network-TMLE: targeted maximum likelihood estimation for dependent data, ESE: empirical standard error, ASE: average standard error, CLD: confidence limit difference, Coverage: 95% confidence interval coverage of the true parameter, Non-informative: the lower confidence limit was less than 0 and the upper confidence limit was greater than 1, Fail: estimator failed to produce an estimate.

Table A2.4.31: IID-TMLE for vaccine data generating mechanism with a clustered power-law random graph

	Bias	ESE	ASE	CLD	Coverage	Non-informative	Fail
Proportion							
0.05	-0.032	0.026	0.026	0.101	76.9%	0	0
0.10	-0.026	0.025	0.025	0.096	81.7%	0	0
0.15	-0.020	0.024	0.023	0.092	86.4%	0	0
0.20	-0.015	0.023	0.022	0.088	89.4%	0	0
0.25	-0.010	0.022	0.022	0.085	91.7%	0	0
0.30	-0.005	0.021	0.021	0.082	93.8%	0	0
0.35	0.000	0.021	0.021	0.080	94.5%	0	0
0.40	0.004	0.021	0.020	0.079	94.1%	0	0
0.45	0.009	0.020	0.020	0.079	92.4%	0	0
0.50	0.013	0.020	0.020	0.079	90.8%	0	0
0.55	0.016	0.021	0.021	0.080	88.9%	0	0
0.60	0.020	0.021	0.021	0.082	86.6%	0	0
0.65	0.023	0.022	0.022	0.085	84.3%	0	0
0.70	0.026	0.023	0.022	0.088	82.3%	0	0
0.75	0.028	0.024	0.023	0.092	80.2%	0	0
0.80	0.030	0.025	0.025	0.096	80.0%	0	0
0.85	0.032	0.026	0.026	0.101	79.4%	0	0
0.90	0.034	0.027	0.027	0.106	79.2%	0	0
0.95	0.035	0.029	0.028	0.112	79.7%	0	0
Shift in log-odds							
-2.5	-0.031	0.026	0.025	0.099	76.5%	0	0
-2	-0.028	0.025	0.025	0.097	79.3%	0	0
-1.5	-0.023	0.024	0.024	0.093	83.1%	0	0
-1	-0.017	0.023	0.023	0.089	88.4%	0	0
-0.5	-0.009	0.021	0.022	0.084	93.0%	0	0
0.5	0.010	0.020	0.020	0.079	93.6%	0	0
1	0.019	0.020	0.021	0.081	87.9%	0	0
1.5	0.025	0.021	0.022	0.085	82.4%	0	0
2	0.030	0.022	0.023	0.092	79.1%	0	0
2.5	0.033	0.024	0.025	0.098	78.4%	0	0

IID-TMLE: independent and identically distributed targeted maximum likelihood estimation, ESE: empirical standard error, ASE: average standard error, CLD: confidence limit difference, Coverage: 95% confidence interval coverage of the true parameter, Non-informative: the lower confidence limit was less than 0 and the upper confidence limit was greater than 1, Fail: estimator failed to produce an estimate.

Table A2.4.32: Network-TMLE for vaccine data generating mechanism with a clustered power-law random graph

	Bias	ESE	ASE	CLD	Coverage	Non-informative	Fail
Proportion							
0.05	-0.001	0.059	0.038	0.148	78.1%	0	0
0.10	-0.001	0.046	0.032	0.124	82.5%	0	0
0.15	0.000	0.037	0.027	0.106	85.2%	0	0
0.20	-0.001	0.030	0.024	0.095	88.5%	0	0
0.25	-0.001	0.026	0.022	0.087	90.8%	0	0
0.30	-0.001	0.023	0.021	0.083	93.4%	0	0
0.35	0.000	0.022	0.021	0.081	94.0%	0	0
0.40	0.000	0.022	0.021	0.081	93.9%	0	0
0.45	0.000	0.023	0.021	0.081	92.6%	0	0
0.50	0.001	0.025	0.021	0.082	90.1%	0	0
0.55	0.000	0.028	0.021	0.084	86.8%	0	0
0.60	0.001	0.031	0.022	0.085	83.1%	0	0
0.65	0.001	0.035	0.022	0.087	79.0%	0	0
0.70	0.001	0.039	0.023	0.088	75.0%	0	0
0.75	0.002	0.042	0.023	0.089	70.8%	0	0
0.80	0.002	0.046	0.023	0.090	66.2%	0	0
0.85	0.002	0.050	0.023	0.090	62.5%	0	0
0.90	0.003	0.054	0.023	0.090	59.2%	0	0
0.95	0.003	0.058	0.023	0.089	55.3%	0	0
Shift in log-odds							
-2.5	-0.001	0.057	0.037	0.143	78.8%	0	0
-2	-0.001	0.048	0.033	0.129	81.7%	0	0
-1.5	-0.001	0.039	0.029	0.112	84.1%	0	0
-1	-0.001	0.031	0.025	0.097	87.9%	0	0
-0.5	-0.001	0.024	0.022	0.085	92.2%	0	0
0.5	0.000	0.022	0.020	0.078	92.2%	0	0
1	0.001	0.028	0.021	0.081	84.4%	0	0
1.5	0.002	0.036	0.022	0.084	76.1%	0	0
2	0.002	0.043	0.022	0.087	68.6%	0	0
2.5	0.003	0.049	0.023	0.089	63.5%	0	0

Network-TMLE: targeted maximum likelihood estimation for dependent data, ESE: empirical standard error, ASE: average standard error, CLD: confidence limit difference, Coverage: 95% confidence interval coverage of the true parameter, Non-informative: the lower confidence limit was less than 0 and the upper confidence limit was greater than 1, Fail: estimator failed to produce an estimate.

Table A2.4.33: Network-TMLE for vaccine data generating mechanism with a clustered power-law random graph restricted by degree

	Bias	ESE	ASE	CLD	Coverage	Non-informative	Fail
Proportion							
0.05	0.004	0.051	0.034	0.134	81.2%	0	0
0.10	0.003	0.041	0.029	0.115	83.6%	0	0
0.15	0.003	0.034	0.026	0.102	85.9%	0	0
0.20	0.003	0.029	0.024	0.093	88.8%	0	0
0.25	0.002	0.025	0.022	0.088	91.1%	0	0
0.30	0.002	0.023	0.021	0.084	93.0%	0	0
0.35	0.002	0.021	0.021	0.082	94.4%	0	0
0.40	0.001	0.021	0.021	0.081	94.3%	0	0
0.45	0.001	0.022	0.021	0.081	93.5%	0	0
0.50	0.001	0.024	0.021	0.082	91.7%	0	0
0.55	0.001	0.026	0.021	0.083	89.2%	0	0
0.60	0.000	0.028	0.022	0.084	86.1%	0	0
0.65	0.001	0.031	0.022	0.086	82.2%	0	0
0.70	0.001	0.034	0.022	0.088	78.9%	0	0
0.75	0.000	0.037	0.023	0.089	76.0%	0	0
0.80	0.001	0.040	0.023	0.091	72.5%	0	0
0.85	0.000	0.043	0.023	0.092	69.6%	0	0
0.90	0.000	0.047	0.024	0.093	67.0%	0	0
0.95	0.000	0.050	0.024	0.094	64.0%	0	0
Shift in log-odds							
-2.5	0.003	0.048	0.033	0.130	81.6%	0	0
-2	0.003	0.042	0.030	0.118	83.6%	0	0
-1.5	0.002	0.035	0.027	0.105	86.3%	0	0
-1	0.002	0.029	0.024	0.093	88.9%	0	0
-0.5	0.002	0.024	0.022	0.085	92.6%	0	0
0.5	0.002	0.021	0.020	0.078	92.9%	0	0
1	0.001	0.026	0.020	0.080	87.4%	0	0
1.5	0.001	0.032	0.021	0.083	80.9%	0	0
2	0.001	0.037	0.022	0.086	74.3%	0	0
2.5	0.001	0.042	0.023	0.089	69.5%	0	0

Network-TMLE: targeted maximum likelihood estimation for dependent data, ESE: empirical standard error, ASE: average standard error, CLD: confidence limit difference, Coverage: 95% confidence interval coverage of the true parameter, Non-informative: the lower confidence limit was less than 0 and the upper confidence limit was greater than 1, Fail: estimator failed to produce an estimate.

Table A2.4.34: IID-TMLE for vaccine data generating mechanism with the eX-FLU network

	Bias	ESE	ASE	CLD	Coverage	Non-informative	Fail
Proportion							
0.05	-0.031	0.026	0.026	0.102	78.5%	0	0
0.10	-0.025	0.025	0.025	0.097	83.2%	0	0
0.15	-0.020	0.024	0.024	0.093	87.4%	0	0
0.20	-0.014	0.023	0.023	0.089	91.0%	0	0
0.25	-0.009	0.022	0.022	0.086	93.1%	0	0
0.30	-0.004	0.021	0.021	0.084	95.0%	0	0
0.35	0.000	0.021	0.021	0.082	95.2%	0	0
0.40	0.005	0.020	0.021	0.081	95.1%	0	0
0.45	0.009	0.020	0.021	0.081	94.0%	0	0
0.50	0.013	0.021	0.021	0.082	92.2%	0	0
0.55	0.016	0.021	0.021	0.083	90.6%	0	0
0.60	0.019	0.021	0.022	0.085	89.1%	0	0
0.65	0.023	0.022	0.023	0.088	86.5%	0	0
0.70	0.026	0.023	0.023	0.092	84.9%	0	0
0.75	0.028	0.024	0.024	0.096	83.5%	0	0
0.80	0.031	0.025	0.026	0.101	82.0%	0	0
0.85	0.033	0.026	0.027	0.106	81.5%	0	0
0.90	0.035	0.028	0.028	0.111	81.5%	0	0
0.95	0.036	0.029	0.030	0.117	81.6%	0	0
Shift in log-odds							
-2.5	-0.030	0.026	0.026	0.101	78.9%	0	0
-2	-0.027	0.025	0.025	0.098	81.1%	0	0
-1.5	-0.023	0.024	0.024	0.095	84.5%	0	0
-1	-0.016	0.023	0.023	0.091	89.4%	0	0
-0.5	-0.008	0.022	0.022	0.087	93.6%	0	0
0.5	0.010	0.020	0.021	0.083	94.1%	0	0
1	0.018	0.021	0.022	0.085	89.2%	0	0
1.5	0.025	0.022	0.023	0.089	83.7%	0	0
2	0.030	0.024	0.025	0.096	81.1%	0	0
2.5	0.033	0.025	0.026	0.103	81.1%	0	0

IID-TMLE: independent and identically distributed targeted maximum likelihood estimation, ESE: empirical standard error, ASE: average standard error, CLD: confidence limit difference, Coverage: 95% confidence interval coverage of the true parameter, Non-informative: the lower confidence limit was less than 0 and the upper confidence limit was greater than 1, Fail: estimator failed to produce an estimate.

Table A2.4.35: Network-TMLE for vaccine data generating mechanism with the eX-FLU network

	Bias	ESE	ASE	CLD	Coverage	Non-informative	Fail
Proportion							
0.05	-0.004	0.058	0.037	0.146	77.1%	0	0
0.10	-0.003	0.045	0.032	0.127	82.5%	0	0
0.15	-0.003	0.036	0.028	0.111	86.4%	0	0
0.20	-0.002	0.030	0.025	0.099	89.7%	0	0
0.25	-0.002	0.025	0.023	0.091	92.4%	0	0
0.30	-0.001	0.023	0.022	0.087	94.0%	0	0
0.35	0.000	0.022	0.022	0.085	94.5%	0	0
0.40	0.000	0.023	0.022	0.086	94.0%	0	0
0.45	0.001	0.026	0.022	0.088	92.3%	0	0
0.50	0.002	0.028	0.023	0.090	89.6%	0	0
0.55	0.001	0.031	0.024	0.092	86.6%	0	0
0.60	0.002	0.034	0.024	0.094	83.0%	0	0
0.65	0.002	0.038	0.024	0.096	78.9%	0	0
0.70	0.002	0.041	0.025	0.097	75.4%	0	0
0.75	0.003	0.045	0.025	0.098	71.8%	0	0
0.80	0.003	0.048	0.025	0.098	67.8%	0	0
0.85	0.003	0.052	0.025	0.099	64.1%	0	0
0.90	0.004	0.056	0.025	0.099	60.4%	0	0
0.95	0.004	0.059	0.025	0.099	57.4%	0	0
Shift in log-odds							
-2.5	-0.005	0.057	0.036	0.143	77.9%	0	0
-2	-0.004	0.049	0.033	0.130	80.3%	0	0
-1.5	-0.003	0.040	0.029	0.115	83.7%	0	0
-1	-0.001	0.031	0.025	0.099	87.8%	0	0
-0.5	-0.001	0.025	0.022	0.088	92.3%	0	0
0.5	0.001	0.024	0.022	0.085	92.6%	0	0
1	0.001	0.031	0.023	0.090	85.8%	0	0
1.5	0.002	0.038	0.024	0.094	78.1%	0	0
2	0.002	0.045	0.025	0.097	71.0%	0	0
2.5	0.002	0.051	0.025	0.098	65.4%	0	0

Network-TMLE: targeted maximum likelihood estimation for dependent data, ESE: empirical standard error, ASE: average standard error, CLD: confidence limit difference, Coverage: 95% confidence interval coverage of the true parameter, Non-informative: the lower confidence limit was less than 0 and the upper confidence limit was greater than 1, Fail: estimator failed to produce an estimate.

Table A2.4.36: Network-TMLE for vaccine data generating mechanism with the eX-FLU network restricted by degree

	Bias	ESE	ASE	CLD	Coverage	Non-informative	Fail
Proportion							
0.05	0.002	0.054	0.039	0.154	82.6%	0	0
0.10	0.001	0.042	0.033	0.128	86.2%	0	0
0.15	0.001	0.034	0.028	0.111	89.4%	0	0
0.20	0.000	0.029	0.025	0.099	91.6%	0	0
0.25	-0.001	0.025	0.023	0.092	93.1%	0	0
0.30	-0.001	0.023	0.022	0.088	94.2%	0	0
0.35	-0.002	0.022	0.022	0.085	94.5%	0	0
0.40	-0.003	0.022	0.022	0.085	94.3%	0	0
0.45	-0.003	0.023	0.022	0.085	92.6%	0	0
0.50	-0.004	0.025	0.022	0.087	90.6%	0	0
0.55	-0.005	0.027	0.023	0.088	87.5%	0	0
0.60	-0.005	0.030	0.023	0.091	83.9%	0	0
0.65	-0.006	0.033	0.024	0.093	80.3%	0	0
0.70	-0.007	0.037	0.024	0.095	76.7%	0	0
0.75	-0.007	0.040	0.025	0.097	73.6%	0	0
0.80	-0.008	0.044	0.025	0.099	69.5%	0	0
0.85	-0.009	0.047	0.026	0.101	65.9%	0	0
0.90	-0.009	0.051	0.026	0.102	62.9%	0	0
0.95	-0.010	0.055	0.026	0.103	59.5%	0	0
Shift in log-odds							
-2.5	0.001	0.052	0.038	0.150	83.6%	0	0
-2	0.001	0.044	0.034	0.134	85.8%	0	0
-1.5	0.000	0.036	0.030	0.116	88.0%	0	0
-1	0.000	0.029	0.026	0.101	91.2%	0	0
-0.5	-0.001	0.024	0.023	0.090	93.9%	0	0
0.5	-0.003	0.023	0.021	0.084	92.9%	0	0
1	-0.004	0.028	0.022	0.088	87.3%	0	0
1.5	-0.005	0.034	0.024	0.093	80.5%	0	0
2	-0.005	0.041	0.025	0.098	73.8%	0	0
2.5	-0.006	0.047	0.026	0.102	69.0%	0	0

Network-TMLE: targeted maximum likelihood estimation for dependent data, ESE: empirical standard error, ASE: average standard error, CLD: confidence limit difference, Coverage: 95% confidence interval coverage of the true parameter, Non-informative: the lower confidence limit was less than 0 and the upper confidence limit was greater than 1, Fail: estimator failed to produce an estimate.

Appendix 2.5: Proposed Diagnostic Plot for Positivity

The following is an example of the proposed diagnostic plot for detecting potential issues regarding positivity for a policy ω. Examples were constructed using the uniform random graph (minimum degree was one and maximum was six) and the statin data generating mechanism. Figure A2.5.1A shows the observed distribution for A^s (where the summary measure is a summation of immediate contacts with $A = 1$) stratified by the individual's value for A.

Figure A2.5.1: Example of diagnostic plots for positivity issues for specific policies using the uniform random graph with statins

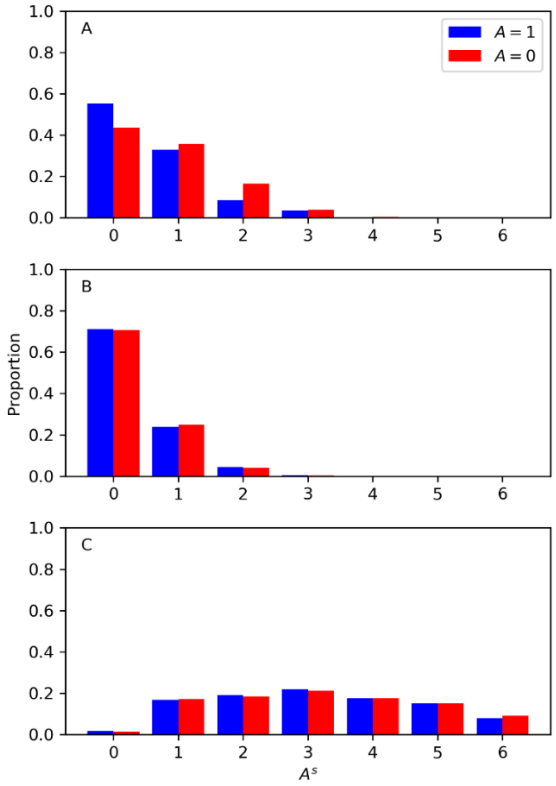

A: observed distribution of A^s by individual's A. Consists of 500 individuals.
B: distribution of A^s under policy $\alpha = 0.1$. Consists of 50,000 individuals (100 copies of the 500 individuals).
C: distribution of A^s under policy $\alpha = 0.9$. Consists of 50,000 individuals (100 copies of the 500 individuals).

These plots indicate that the ω in B has support in the data but the ω in C has little-to-no support. Therefore, the latter policy should not be estimated or it should be recognized that results are highly dependent on extrapolations from the parametric models. As shown in the simulations, this can lead to variable estimates (as indicated by the ESE) and poor CI coverage.

APPENDIX 3: CHAPTER 6 SUPPLEMENTARY MATERIALS

Figure A3.1: Diagnostic plots for MICE

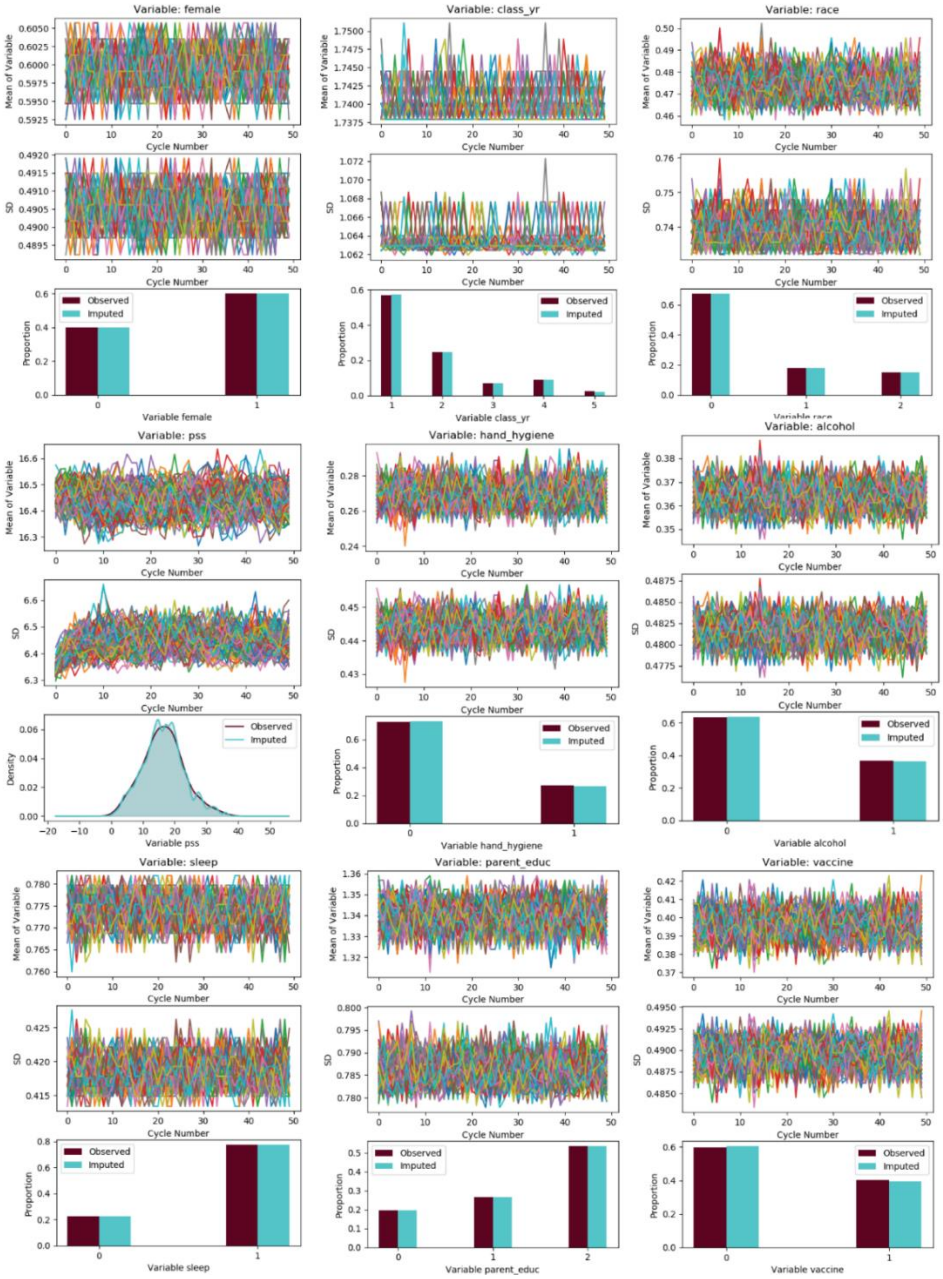

SD: standard deviation, PSS: perceived stress scale

Figure A3.2: Missing Vaccination Status Considered as Vaccinated

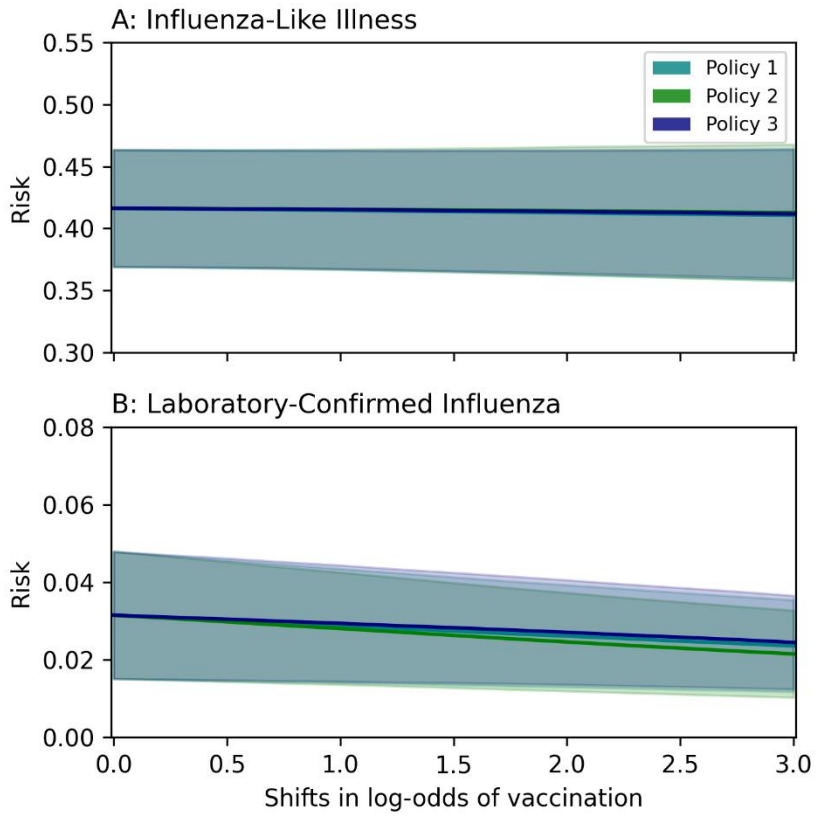

Shaded regions indicated 95% CI. All students with missing influenza vaccination status were considered as vaccinated. Influenza-like illness was defined as the presence of coughing plus at least one of the following symptoms: fever, body aches, or chills. Laboratory-confirmation of influenza was determined via quantitative polymerase chain reaction.
Policy 1: theoretical policy to emphasize benefits of the vaccine and dispelling common myths.
Policy 2: theoretical policy to address non-financial barriers to vaccination
Policy 3: theoretical policy to address financial barriers to vaccination

Figure A3.3: Missing Vaccination Status Considered as Unvaccinated

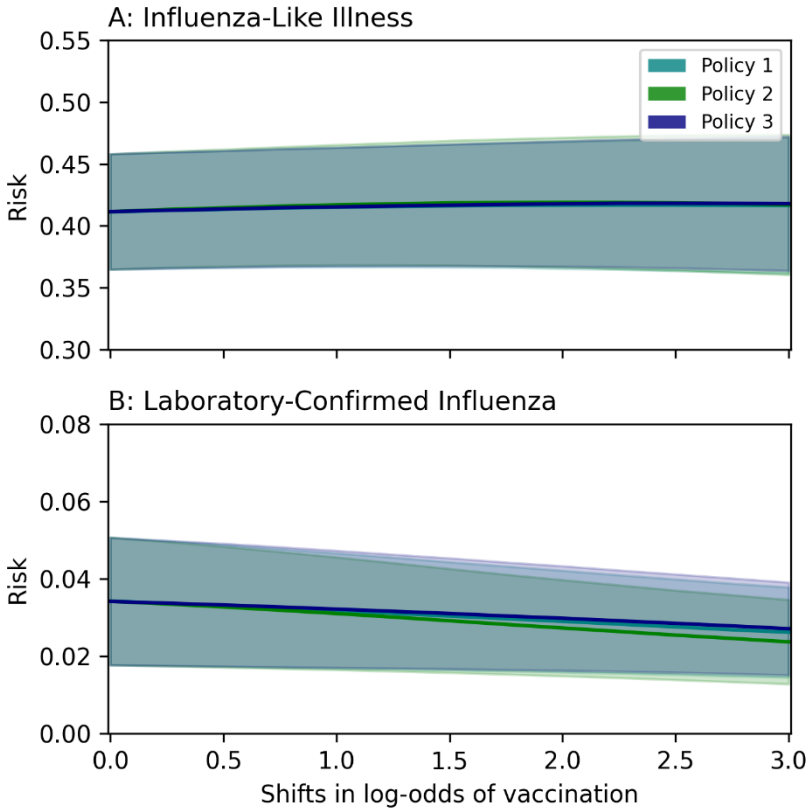

Shaded regions indicated 95% CI. All students with missing influenza vaccination status were considered as unvaccinated. Influenza-like illness was defined as the presence of coughing plus at least one of the following symptoms: fever, body aches, or chills. Laboratory-confirmation of influenza was determined via quantitative polymerase chain reaction.
Policy 1: theoretical policy to emphasize benefits of the vaccine and dispelling common myths.
Policy 2: theoretical policy to address non-financial barriers to vaccination
Policy 3: theoretical policy to address financial barriers to vaccination

REFERENCES

1. Krammer F, Smith GJD, Fouchier RAM, et al. Influenza. *Nature Reviews Disease Primers*. 2018/06/28 2018;4(1):3. doi:10.1038/s41572-018-0002-y

2. Flint J, Racaniello VR, Rall GF, Skalka AM. *Principles of Virology, Volume II: Pathogenesis & Control, Fourth Edition*. American Society of Microbiology; 2015.

3. Nelson KE, Williams CM. *Infectious Disease Epidemiology: Theory and Practice*. Jones & Bartlett Publishers; 2014.

4. Matsuzaki Y, Katsushima N, Nagai Y, et al. Clinical features of influenza C virus infection in children. *The Journal of Infectious Diseases*. May 1 2006;193(9):1229-35. doi:10.1086/502973

5. Webster RG, Bean WJ, Gorman OT, Chambers TM, Kawaoka Y. Evolution and ecology of influenza A viruses. *Microbiology and Molecular Biology Reviews*. 1992;56(1):152-179.

6. Treanor JJ, Campbell JD, Zangwill KM, Rowe T, Wolff M. Safety and immunogenicity of an inactivated subvirion influenza A (H5N1) vaccine. *New England Journal of Medicine*. 2006;354(13):1343-1351.

7. Estrada LD, Schultz-Cherry S. Development of a universal influenza vaccine. *The Journal of Immunology*. 2019;202(2):392-398.

8. Aiello AE, Coulborn RM, Perez V, Larson EL. Effect of hand hygiene on infectious disease risk in the community setting: a meta-analysis. *American Journal of Public Health*. Aug 2008;98(8):1372-81. doi:10.2105/ajph.2007.124610

9. Aiello AE, Murray GF, Perez V, et al. Mask use, hand hygiene, and seasonal influenza-like illness among young adults: a randomized intervention trial. *The Journal of Infectious Diseases*. Feb 15 2010;201(4):491-8. doi:10.1086/650396

10. Aiello AE, Perez V, Coulborn RM, Davis BM, Uddin M, Monto AS. Facemasks, hand hygiene, and influenza among young adults: a randomized intervention trial. *PloS One*. 2012;7(1):e29744. doi:10.1371/journal.pone.0029744

11. Cowling BJ, Chan K-H, Fang VJ, et al. Facemasks and hand hygiene to prevent influenza transmission in households: a cluster randomized trial. *Annals of Internal Medicine*. 2009;151(7):437-446.

12. Fong MW, Gao H, Wong JY, et al. Nonpharmaceutical measures for pandemic influenza in nonhealthcare settings—social distancing measures. *Emerging Infectious Diseases*. 2020;26(5):976.

13. Longini Jr IM, Halloran ME, Nizam A, Yang Y. Containing pandemic influenza with antiviral agents. *American Journal of Epidemiology*. 2004;159(7):623-633.

14. Marazzi I, Ho JS, Kim J, et al. Suppression of the antiviral response by an influenza histone mimic. *Nature*. 2012;483(7390):428-433.

15. Li S, Min J-Y, Krug RM, Sen GC. Binding of the influenza A virus NS1 protein to PKR mediates the inhibition of its activation by either PACT or double-stranded RNA. *Virology*. 2006;349(1):13-21.

16. Min J-Y, Krug RM. The primary function of RNA binding by the influenza A virus NS1 protein in infected cells: inhibiting the 2′-5′ oligo (A) synthetase/RNase L pathway. *Proceedings of the National Academy of Sciences*. 2006;103(18):7100-7105.

17. Conenello GM, Palese P. Influenza A virus PB1-F2: a small protein with a big punch. *Cell Host & Microbe*. 2007;2(4):207-209.

18. Graef KM, Vreede FT, Lau Y-F, et al. The PB2 subunit of the influenza virus RNA polymerase affects virulence by interacting with the mitochondrial antiviral signaling protein and inhibiting expression of beta interferon. *Journal of Virology*. 2010;84(17):8433-8445.

19. Steens A, Waaijenborg S, Teunis PF, et al. Age-dependent patterns of infection and severity explaining the low impact of 2009 influenza A (H1N1): evidence from serial serologic surveys in the Netherlands. *American Journal of Epidemiology*. 2011;174(11):1307-1315.

20. Yu X, Tsibane T, McGraw PA, et al. Neutralizing antibodies derived from the B cells of 1918 influenza pandemic survivors. *Nature*. 2008;455(7212):532-536.

21. Heaton NS, Sachs D, Chen C-J, Hai R, Palese P. Genome-wide mutagenesis of influenza virus reveals unique plasticity of the hemagglutinin and NS1 proteins. *Proceedings of the National Academy of Sciences*. 2013;110(50):20248-20253.

22. Wilkinson TM, Li CK, Chui CS, et al. Preexisting influenza-specific CD4+ T cells correlate with disease protection against influenza challenge in humans. *Nature Medicine*. 2012;18(2):274-280.

23. Warren-Gash C, Smeeth L, Hayward AC. Influenza as a trigger for acute myocardial infarction or death from cardiovascular disease: a systematic review. *The Lancet Infectious Diseases*. 2009;9(10):601-610.

24. Sellers SA, Hagan RS, Hayden FG, Fischer WA. The hidden burden of influenza: a review of the extra-pulmonary complications of influenza infection. *Influenza and Other Respiratory Viruses*. 2017;11(5):372-393.

25. Zangrillo A, Biondi-Zoccai G, Landoni G, et al. Extracorporeal membrane oxygenation (ECMO) in patients with H1N1 influenza infection: a systematic review and meta-analysis including 8 studies and 266 patients receiving ECMO. *Critical Care*. 2013;17(1):1-8.

26. Li T, Liu Y, Di B, et al. Epidemiological investigation of an outbreak of pandemic influenza A (H1N1) 2009 in a boarding school: serological analysis of 1570 cases. *Journal of clinical virology : the official publication of the Pan American Society for Clinical Virology*. Mar 2011;50(3):235-9. doi:10.1016/j.jcv.2010.11.012

27. Gurav YK, Pawar SD, Chadha MS, et al. Pandemic influenza A(H1N1) 2009 outbreak in a residential school at Panchgani, Maharashtra, India. *The Indian Journal of Medical Research*. Jul 2010;132:67-71.

28. Carrat F, Vergu E, Ferguson NM, et al. Time lines of infection and disease in human influenza: a review of volunteer challenge studies. *American Journal of Epidemiology*. Apr 1 2008;167(7):775-85. doi:10.1093/aje/kwm375

29. Launes C, de-Sevilla MF, Selva L, Garcia-Garcia JJ, Pallares R, Munoz-Almagro C. Viral coinfection in children less than five years old with invasive pneumococcal disease. *The Pediatric Infectious Disease Journal*. Jun 2012;31(6):650-3. doi:10.1097/INF.0b013e31824f25b0

30. Wolter N, Tempia S, Cohen C, et al. High nasopharyngeal pneumococcal density, increased by viral coinfection, is associated with invasive pneumococcal pneumonia. *The Journal of Infectious Diseases*. Nov 15 2014;210(10):1649-57. doi:10.1093/infdis/jiu326

31. Kwong JC, Schwartz KL, Campitelli MA, et al. Acute myocardial infarction after laboratory-confirmed influenza infection. *New England Journal of Medicine*. 2018;378(4):345-353.

32. Stowe J, Andrews N, Wise L, Miller E. Investigation of the temporal association of Guillain-Barre syndrome with influenza vaccine and influenzalike illness using the United Kingdom General Practice Research Database. *American Journal of Epidemiology*. Feb 1 2009;169(3):382-8. doi:10.1093/aje/kwn310

33. Sivadon-Tardy V, Orlikowski D, Porcher R, et al. Guillain-Barré syndrome and influenza virus infection. *Clinical Infectious Diseases*. 2009;48(1):48-56.

34. Grohskopf LA, Sokolow LZ, Broder KR, et al. Prevention and Control of Seasonal Influenza with Vaccines. *MMWR Recommendations and reports : Morbidity and mortality weekly report Recommendations and reports*. Aug 26 2016;65(5):1-54. doi:10.15585/mmwr.rr6505a1

35. Disease Burden of Influenza. Centers for Disease Control and Prevention. Updated February 19, 2019. Accessed July 15, 2019, 2019. https://www.cdc.gov/flu/about/burden/index.html

36. Zhou H, Thompson WW, Viboud CG, et al. Hospitalizations associated with influenza and respiratory syncytial virus in the United States, 1993-2008. *Clinical Infectious Diseases*. May 2012;54(10):1427-36. doi:10.1093/cid/cis211

37. Thompson M, Shay D, Zhou H, et al. Estimates of deaths associated with seasonal influenza-United States, 1976-2007. *Morbidity and Mortality Weekly Report*. 2010;59(33):1057-1062.

38. Molinari NA, Ortega-Sanchez IR, Messonnier ML, et al. The annual impact of seasonal influenza in the US: measuring disease burden and costs. *Vaccine*. Jun 28 2007;25(27):5086-96. doi:10.1016/j.vaccine.2007.03.046

39. Yan J, Grantham M, Pantelic J, et al. Infectious virus in exhaled breath of symptomatic seasonal influenza cases from a college community. *Proceedings of the National Academy of Sciences*. 2018;doi:10.1073/pnas.1716561115

40. Zivich PN, Gancz AS, Aiello AE. Effect of hand hygiene on infectious diseases in the office workplace: A systematic review. *American Journal of Infection Control*. Apr 2018;46(4):448-455. doi:10.1016/j.ajic.2017.10.006

41. Anderson G, Palombo EA. Microbial contamination of computer keyboards in a university setting. *American Journal of Infection Control*. Aug 2009;37(6):507-9. doi:10.1016/j.ajic.2008.10.032

42. Thompson K-A, Bennett A. Persistence of influenza on surfaces. *Journal of Hospital Infection*. 2017;95(2):194-199.

43. Oxford J, Berezin EN, Courvalin P, et al. The survival of influenza A (H1N1) pdm09 virus on 4 household surfaces. *American Journal of Infection Control*. 2014;42(4):423-425.

44. Zhao J, Eisenberg JE, Spicknall IH, Li S, Koopman JS. Model analysis of fomite mediated influenza transmission. *PloS One*. 2012;7(12):e51984.

45. Asadi S, ben Hnia NG, Barre RS, Wexler AS, Ristenpart WD, Bouvier NM. Influenza A virus is transmissible via aerosolized fomites. *Nature Communications*. 2020;11(1):1-9.

46. Ip DK, Lau LL, Leung NH, et al. Viral shedding and transmission potential of asymptomatic and paucisymptomatic influenza virus infections in the community. *Clinical Infectious Diseases*. 2017;64(6):736-742.

47. Patrozou E, Mermel LA. Does influenza transmission occur from asymptomatic infection or prior to symptom onset? *Public Health Reports*. 2009;124(2):193-196.

48. Davis BM, Foxman B, Monto AS, et al. Human coronaviruses and other respiratory infections in young adults on a university campus: Prevalence, symptoms, and shedding. *Influenza and Other Respiratory Viruses*. 2018;12(5):582-590.

49. Grohskopf LA, Olsen SJ, Sokolow LZ, et al. Prevention and control of seasonal influenza with vaccines: recommendations of the Advisory Committee on Immunization Practices (ACIP) -- United States, 2014-15 influenza season. *MMWR*. Aug 15 2014;63(32):691-7.

50. Osterholm MT, Kelley NS, Sommer A, Belongia EA. Efficacy and effectiveness of influenza vaccines: a systematic review and meta-analysis. *The Lancet Infectious Diseases*. Jan 2012;12(1):36-44. doi:10.1016/s1473-3099(11)70295-x

51. Rondy M, El Omeiri N, Thompson MG, Levêque A, Moren A, Sullivan SG. Effectiveness of influenza vaccines in preventing severe influenza illness among adults: A systematic review and meta-analysis of test-negative design case-control studies. *The Journal of infection*. Nov 2017;75(5):381-394. doi:10.1016/j.jinf.2017.09.010

52. Yamayoshi S, Kawaoka Y. Current and future influenza vaccines. *Nature Medicine*. 2019/02/01 2019;25(2):212-220. doi:10.1038/s41591-018-0340-z

53. Skowronski DM, Janjua NZ, De Serres G, et al. Low 2012–13 influenza vaccine effectiveness associated with mutation in the egg-adapted H3N2 vaccine strain not antigenic drift in circulating viruses. *PloS One*. 2014;9(3):e92153.

54. Cianci R, Newton EE, Pagliari D. Efforts to Improve the Seasonal Influenza Vaccine. Multidisciplinary Digital Publishing Institute; 2020.

55. Maassab HF, Bryant ML. The development of live attenuated cold-adapted influenza virus vaccine for humans. *Reviews in Medical Virology*. 1999;9(4):237-244.

56. Maassab H. Adaptation and growth characteristics of influenza virus at 25 C. *Nature*. 1967;213(5076):612-614.

57. Sridhar S, Brokstad KA, Cox RJ. Influenza vaccination strategies: comparing inactivated and live attenuated influenza vaccines. *Vaccines*. 2015;3(2):373-389.

58. Harper SA, Fukuda K, Cox NJ, Bridges CB. Using live, attenuated influenza vaccine for prevention and control of influenza. *MMWR*. 2003;52:1-8.

59. Anand A. Advisory Committee on Immunization Practices (ACIP) summary report: June 22-23, 2016, Atlanta, Georgia. 1916;

60. Chung JR, Flannery B, Ambrose CS, et al. Live Attenuated and Inactivated Influenza Vaccine Effectiveness. *Pediatrics*. 2019;143(2):e20182094. doi:10.1542/peds.2018-2094

61. Piedra PA. Live Attenuated Influenza Vaccine: Will the Phoenix Rise Again? *Pediatrics*. 2019;143(2):e20183290. doi:10.1542/peds.2018-3290

62. Grohskopf LA, Sokolow LZ, Broder KR, et al. Prevention and Control of Seasonal Influenza with Vaccines: Recommendations of the Advisory Committee on Immunization Practices - United States, 2017-18 Influenza Season. *MMWR*. Aug 25 2017;66(2):1-20. doi:10.15585/mmwr.rr6602a1

63. Grohskopf LA, Sokolow LZ, Fry AM, Walter EB, Jernigan DB. Update: ACIP Recommendations for the Use of Quadrivalent Live Attenuated Influenza Vaccine (LAIV4) - United States, 2018-19 Influenza Season. *MMWR*. 2018;67(22):643-645. doi:10.15585/mmwr.mm6722a5

64. McLean HQ, Thompson MG, Sundaram ME, et al. Influenza Vaccine Effectiveness in the United States During 2012–2013: Variable Protection by Age and Virus Type. *The Journal of Infectious Diseases*. 2015;211(10):1529-1540. doi:10.1093/infdis/jiu647

65. Castilla J, Godoy P, Dominguez A, et al. Influenza vaccine effectiveness in preventing outpatient, inpatient, and severe cases of laboratory-confirmed influenza. *Clinical Infectious Diseases*. Jul 2013;57(2):167-75. doi:10.1093/cid/cit194

66. Ridenhour BJ, Campitelli MA, Kwong JC, et al. Effectiveness of inactivated influenza vaccines in preventing influenza-associated deaths and hospitalizations among Ontario residents aged >/= 65 years: estimates with generalized linear models accounting for healthy vaccinee effects. *PloS One*. 2013;8(10):e76318. doi:10.1371/journal.pone.0076318

67. Zivich PN, Tatham L, Lung K, Tien J, Bollinger CE, Bower JK. Influenza vaccination status and outcomes among influenza-associated hospitalizations in Columbus, Ohio (2012–2015). *Epidemiology and Infection*. 2017:1-10. doi:10.1017/S0950268817002163

68. Ainslie KEC, Haber MJ, Malosh RE, Petrie JG, Monto AS. Maximum likelihood estimation of influenza vaccine effectiveness against transmission from the household and from the community. *Statistics in Medicine*. Mar 15 2018;37(6):970-982. doi:10.1002/sim.7558

69. Loeb M, Russell ML, Moss L, et al. Effect of influenza vaccination of children on infection rates in Hutterite communities: a randomized trial. *JAMA*. Mar 10 2010;303(10):943-50. doi:10.1001/jama.2010.250

70. Wang B, Russell ML, Moss L, et al. Effect of Influenza Vaccination of Children on Infection Rate in Hutterite Communities: Follow-Up Study of a Randomized Trial. *PloS One*. 2016;11(12):e0167281. doi:10.1371/journal.pone.0167281

71. Kwong JC, Pereira JA, Quach S, et al. Randomized evaluation of live attenuated vs. inactivated influenza vaccines in schools (RELATIVES) cluster randomized trial: Pilot results from a household surveillance study to assess direct and indirect protection from influenza vaccination. *Vaccine*. Sep 11 2015;33(38):4910-5. doi:10.1016/j.vaccine.2015.07.044

72. Glezen WP, Gaglani MJ, Kozinetz CA, Piedra PA. Direct and Indirect Effectiveness of Influenza Vaccination Delivered to Children at School Preceding an Epidemic Caused by 3 New Influenza Virus Variants. *The Journal of Infectious Diseases*. 2010;202(11):1626-1633. doi:10.1086/657089

73. Piedra PA, Gaglani MJ, Kozinetz CA, et al. Herd immunity in adults against influenza-related illnesses with use of the trivalent-live attenuated influenza vaccine (CAIV-T) in children. *Vaccine*. Feb 18 2005;23(13):1540-8. doi:10.1016/j.vaccine.2004.09.025

74. Sugaya N. A review of the indirect protection of younger children and the elderly through a mass influenza vaccination program in Japan. *Expert review of vaccines*. Dec 2014;13(12):1563-70. doi:10.1586/14760584.2014.951036

75. Sullender W, Fowler K, Krishnan A, et al. Design and initiation of a study to assess the direct and indirect effects of influenza vaccine given to children in rural India. *Vaccine*. Jul 27 2012;30(35):5235-9. doi:10.1016/j.vaccine.2012.06.002

76. Hobson D, Curry RL, Beare AS, Ward-Gardner A. The role of serum haemagglutination-inhibiting antibody in protection against challenge infection with influenza A2 and B viruses. *J Hyg (Lond)*. 1972;70(4):767-777. doi:10.1017/s0022172400022610

77. Noah DL, Hill H, Hines D, White EL, Wolff MC. Qualification of the Hemagglutination Inhibition Assay in Support of Pandemic Influenza Vaccine Licensure. *Clinical and Vaccine Immunology*. 2009;16(4):558-566. doi:10.1128/cvi.00368-08

78. Ainslie KEC, Haber M, Orenstein WA. Challenges in estimating influenza vaccine effectiveness. *Expert review of vaccines*. 2019;18(6):615-628. doi:10.1080/14760584.2019.1622419

79. Halloran ME, Longini IM, Struchiner CJ. *Design and Analysis of Vaccine Studies*. Springer New York; 2009.

80. Thomas RE. Is influenza-like illness a useful concept and an appropriate test of influenza vaccine effectiveness? *Vaccine*. Apr 17 2014;32(19):2143-9. doi:10.1016/j.vaccine.2014.02.059

81. Merckx J, Wali R, Schiller I, et al. Diagnostic accuracy of novel and traditional rapid tests for influenza infection compared with reverse transcriptase polymerase chain reaction: a systematic review and meta-analysis. *Annals of Internal Medicine*. 2017;167(6):394-409.

82. Arriola CS, Anderson EJ, Baumbach J, et al. Does Influenza Vaccination Modify Influenza Severity? Data on Older Adults Hospitalized With Influenza During the 2012-2013 Season in the United States. *The Journal of Infectious Diseases*. Oct 15 2015;212(8):1200-8. doi:10.1093/infdis/jiv200

83. Chaves SS, Lynfield R, Lindegren ML, Bresee J, Finelli L. The US Influenza Hospitalization Surveillance Network. *Emerging Infectious Diseases*. Sep 2015;21(9):1543-50. doi:10.3201/eid2109.141912

84. Ohmit SE, Petrie JG, Malosh RE, Fry AM, Thompson MG, Monto AS. Influenza vaccine effectiveness in households with children during the 2012–2013 season: assessments of prior vaccination and serologic susceptibility. *The Journal of Infectious Diseases*. 2014;211(10):1519-1528.

85. Malosh R, Ohmit SE, Petrie JG, Thompson MG, Aiello AE, Monto AS. Factors associated with influenza vaccine receipt in community dwelling adults and their children. *Vaccine*. 2014;32(16):1841-1847.

86. Feng S, Cowling BJ, Kelly H, Sullivan SG. Estimating Influenza Vaccine Effectiveness With the Test-Negative Design Using Alternative Control Groups: A Systematic Review and Meta-Analysis. *American Journal of Epidemiology*. Feb 1 2018;187(2):389-397. doi:10.1093/aje/kwx251

87. Sullivan SG, Tchetgen Tchetgen EJ, Cowling BJ. Theoretical Basis of the Test-Negative Study Design for Assessment of Influenza Vaccine Effectiveness. *American Journal of Epidemiology*. Sep 1 2016;184(5):345-53. doi:10.1093/aje/kww064

88. Dean NE, Halloran ME, Longini JIM. Temporal Confounding in the Test-Negative Design. *American Journal of Epidemiology*. 2020;189(11):1402-1407. doi:10.1093/aje/kwaa084

89. Westreich D, Hudgens MG. Invited Commentary: Beware the Test-Negative Design. *American Journal of Epidemiology*. 2016;184(5):354-356. doi:10.1093/aje/kww063

90. Fiore AE, Shay DK, Haber P, et al. Prevention and control of influenza. Recommendations of the Advisory Committee on Immunization Practices (ACIP), 2007. *MMWR*. Jul 13 2007;56(Rr-6):1-54.

91. Fiore AE, Uyeki TM, Broder K, et al. Prevention and control of influenza with vaccines: recommendations of the Advisory Committee on Immunization Practices (ACIP), 2010. *MMWR*. Aug 6 2010;59(Rr-8):1-62.

92. Lu PJ, Santibanez TA, Williams WW, et al. Surveillance of influenza vaccination coverage--United States, 2007-08 through 2011-12 influenza seasons. *MMWR*. Oct 25 2013;62(4):1-28.

93. Ratnapradipa KL, Norrenberns R, Turner JA, Kunerth A. Freshman Flu Vaccination Behavior and Intention During a Nonpandemic Season. *Health Promotion Practice*. Sep 2017;18(5):662-671. doi:10.1177/1524839917712731

94. Shropshire AM, Brent-Hotchkiss R, Andrews UK. Mass media campaign impacts influenza vaccine obtainment of university students. *Journal of American College Health*. 2013;61(8):435-43. doi:10.1080/07448481.2013.830619

95. Monn JL. An Evidence-based Project to Improve Influenza Immunization Uptake. *The Journal for Nurse Practitioners*. 2016/04/01/ 2016;12(4):e159-e162. doi:https://doi.org/10.1016/j.nurpra.2015.11.030

96. Nichol KL, D'Heilly S, Ehlinger EP. Influenza vaccination among college and university students: impact on influenzalike illness, health care use, and impaired school performance. *Archives of Pediatrics & Adolescent Medicine*. Dec 2008;162(12):1113-8. doi:10.1001/archpedi.162.12.1113

97. Wilson SL, Huttlinger K. Pandemic flu knowledge among dormitory housed university students: a need for informal social support and social networking strategies. *Rural and Remote Health*. Oct-Dec 2010;10(4):1526.

98. Bednarczyk RA, Chu SL, Sickler H, Shaw J, Nadeau JA, McNutt L-A. Low uptake of influenza vaccine among university students: evaluating predictors beyond cost and safety concerns. *Vaccine*. 2015;33(14):1659-1663.

99. Poehling KA, Blocker J, Ip EH, Peters TR, Wolfson M. 2009–2010 Seasonal Influenza Vaccination Coverage Among College Students From 8 Universities in North Carolina. *Journal of American college health : J of ACH*. 2012;60(8):541-547. doi:10.1080/07448481.2012.700973

100. Ravert RD, Fu LY, Zimet GD. Reasons for low pandemic H1N1 2009 vaccine acceptance within a college sample. *Advances in Preventive Medicine*. 2012;2012

101. Sobal J, Loveland FC. Infectious disease in a total institution: a study of the influenza epidemic of 1978 on a college campus. *Public Health Reports (Washington, DC : 1974)*. Jan-Feb 1982;97(1):66-72.

102. Pons VG, Canter J, Dolin R. INFLUENZA A/USSR/77 (H1N1) ON A UNIVERSITY CAMPUS. *American Journal of Epidemiology*. 1980;111(1):23-30. doi:10.1093/oxfordjournals.aje.a112871

103. Layde PM, Engelberg AL, Dobbs HI, et al. Outbreak of influenza A/USSR/77 at Marquette University. *The Journal of Infectious Diseases*. Sep 1980;142(3):347-52.

104. Iuliano AD, Reed C, Guh A, et al. Notes from the field: outbreak of 2009 pandemic influenza A (H1N1) virus at a large public university in Delaware, April-May 2009. *Clinical Infectious Diseases*. Dec 15 2009;49(12):1811-20. doi:10.1086/649555

105. Kar-Purkayastha I, Ingram C, Maguire H, Roche A. The importance of school and social activities in the transmission of influenza A(H1N1)v: England, April - June 2009. *Euro Surveillance*. Aug 20 2009;14(33)

106. Tsuang WM, Bailar JC, Englund JA. Influenza-like symptoms in the college dormitory environment: a survey taken during the 1999-2000 influenza season. *Journal of Environmental Health*. Apr 2004;66(8):39-42, 44.

107. Hashmi S, D'Ambrosio L, Diamond DV, Jalali MS, Finkelstein SN, Larson RC. Preventive behaviors and perceptions of influenza vaccination among a university student population. *Journal of Public Health*. 2016;38(4):739-745. doi:10.1093/pubmed/fdv189

108. Uchida M, Kaneko M, Tsukahara T, Washizuka S, Kawa S. Evaluation of the spread of pandemic influenza A/H1N1 2009 among Japanese university students. *Environmental Health and Preventive Medicine*. 2014;19(5):315.

109. Virk RK, Gunalan V, Lee HK, et al. Molecular evidence of transmission of influenza A/H1N1 2009 on a university campus. *PloS One*. 2017;12(1):e0168596.

110. Murray CJL, Lopez AD, Chin B, Feehan D, Hill KH. Estimation of potential global pandemic influenza mortality on the basis of vital registry data from the 1918–20 pandemic: a quantitative analysis. *The Lancet*. 2006/12/23/ 2006;368(9554):2211-2218. doi:https://doi.org/10.1016/S0140-6736(06)69895-4

111. Mullins J, Cook R, Rinaldo C, Yablonsky E, Hess R, Piazza P. Influenza-like illness among university students: symptom severity and duration due to influenza virus infection compared to other etiologies. *J Am Coll Health*. 2011;59(4):246-51. doi:10.1080/07448481.2010.502197

112. Uddin M, Cherkowski GC, Liu G, Zhang J, Monto AS, Aiello AE. Demographic and socioeconomic determinants of influenza vaccination disparities among university students. *J Epidemiol Community Health*. Sep 2010;64(9):808-13. doi:10.1136/jech.2009.090852

113. Benjamin SM, Bahr KO. Barriers associated with seasonal influenza vaccination among college students. *Influenza Research and Treatment*. 2016;2016

114. Agarwal V. A/H1N1 Vaccine Intentions in College Students: An Application of the Theory of Planned Behavior. *Journal of American College Health*. 2014/08/18 2014;62(6):416-424. doi:10.1080/07448481.2014.917650

115. Boiron K, Sarazin M, Debin M, et al. Opinion about seasonal influenza vaccination among the general population 3 years after the A(H1N1)pdm2009 influenza pandemic. *Vaccine*. Nov 27 2015;33(48):6849-54. doi:10.1016/j.vaccine.2015.08.067

116. Ramsey MA, Marczinski CA. College students' perceptions of H1N1 flu risk and attitudes toward vaccination. *Vaccine*. Oct 13 2011;29(44):7599-601. doi:10.1016/j.vaccine.2011.07.130

117. Yang ZJ. Too scared or too capable? Why do college students stay away from the H1N1 vaccine? *Risk Analysis: An International Journal*. 2012;32(10):1703-1716.

118. Lawrence HY. Healthy bodies, toxic medicines: college students and the rhetorics of flu vaccination. *Yale J Biol Med*. 2014;87(4):423-437.

119. Nowak GJ, Sheedy K, Bursey K, Smith TM, Basket M. Promoting influenza vaccination: insights from a qualitative meta-analysis of 14 years of influenza-related communications research by U.S. Centers for Disease Control and Prevention (CDC). *Vaccine*. Jun 4 2015;33(24):2741-56. doi:10.1016/j.vaccine.2015.04.064

120. Byrne C, Walsh J, Kola S, Sarma KM. Predicting intention to uptake H1N1 influenza vaccine in a university sample. *British Journal of Health Psychology*. 2012;17(3):582-595.

121. Nowak GJ, Gellin BG, MacDonald NE, Butler R. Addressing vaccine hesitancy: The potential value of commercial and social marketing principles and practices. *Vaccine*. Aug 14 2015;33(34):4204-11. doi:10.1016/j.vaccine.2015.04.039

122. Lee Y-I, Jin Y, Nowak G. Motivating Influenza Vaccination Among Young Adults:The Effects of Public Service Advertising Message Framing and Text Versus Image Support. *Social Marketing Quarterly*. 2018;24(2):89-103. doi:10.1177/1524500418771283

123. Marotta C, Raia DD, Ventura G, et al. Improvement in vaccination knowledge among health students following an integrated extra curricular intervention, an explorative study in the University of Palermo. *J Prev Med Hyg*. 2017;58(2):E93-E98.

124. Control CfD, Prevention. Mumps outbreak on a university campus--California, 2011. *MMWR*. 2012;61(48):986-989.

125. Clemmons NS, Redd SB, Gastañaduy PA, Marin M, Patel M, Fiebelkorn AP. Characteristics of Large Mumps Outbreaks in the United States, July 2010–December 2015. *Clinical Infectious Diseases*. 2018;68(10):1684-1690. doi:10.1093/cid/ciy779

126. McLean HQ, Fiebelkorn AP, Temte JL, Wallace GS. Prevention of measles, rubella, congenital rubella syndrome, and mumps, 2013: summary recommendations of the Advisory Committee on Immunization Practices (ACIP). *MMWR*. 2013;62(4):1-34.

127. Weinberg GA, Szilagyi PG. Vaccine Epidemiology: Efficacy, Effectiveness, and the Translational Research Roadmap. *The Journal of Infectious Diseases*. 2010;201(11):1607-1610. doi:10.1086/652404

128. Belongia EA, Simpson MD, King JP, et al. Variable influenza vaccine effectiveness by subtype: a systematic review and meta-analysis of test-negative design studies. *The Lancet Infectious Diseases*. 2016/08/01/ 2016;16(8):942-951. doi:https://doi.org/10.1016/S1473-3099(16)00129-8

129. Nichol KL, D'Heilly S, Ehlinger EP. Influenza Vaccination Among College and University Students: Impact on Influenzalike Illness, Health Care Use, and Impaired School Performance. *Archives of Pediatrics & Adolescent Medicine*. 2008;162(12):1113-1118. doi:10.1001/archpedi.162.12.1113

130. Splawa-Neyman J, Dabrowska DM, Speed T. On the application of probability theory to agricultural experiments. Essay on principles. Section 9. *Statistical Science*. 1990:465-472.

131. Rubin DB. Estimating causal effects of treatments in randomized and nonrandomized studies. *Journal of Educational Psychology*. 1974;66(5):688.

132. Robins J. A new approach to causal inference in mortality studies with a sustained exposure period—application to control of the healthy worker survivor effect. *Mathematical Modelling*. 1986;7(9-12):1393-1512.

133. Hudgens MG, Halloran ME. Toward Causal Inference With Interference. *Journal of the American Statistical Association*. Jun 2008;103(482):832-842. doi:10.1198/016214508000000292

134. Cox DR. Planning of experiments. 1958;

135. Rubin DB. Randomization analysis of experimental data: The Fisher randomization test comment. *Journal of the American Statistical Association*. 1980;75(371):591-593.

136. Ross R. An Application of the Theory of Probabilities to the Study of a priori Pathometry. Part I. *Proceedings of the Royal Society of London Series A*. 1916;92(638):204-230. doi:10.1098/rspa.1916.0007

137. Halloran ME, Haber M, Longini IM, Jr., Struchiner CJ. Direct and indirect effects in vaccine efficacy and effectiveness. *American Journal of Epidemiology*. Feb 15 1991;133(4):323-31.

138. Vanderweele TJ, Tchetgen Tchetgen EJ. Effect partitioning under interference in two-stage randomized vaccine trials. *Stat Probab Lett*. 2011;81(7):861-869. doi:10.1016/j.spl.2011.02.019

139. Halloran ME, Hudgens MG. Dependent Happenings: A Recent Methodological Review. *Current Epidemiology Reports*. Dec 2016;3(4):297-305. doi:10.1007/s40471-016-0086-4

140. Tchetgen EJT, VanderWeele TJ. On causal inference in the presence of interference. *Statistical Methods in Medical Research*. 11/10 2012;21(1):55-75. doi:10.1177/0962280210386779

141. Perez-Heydrich C, Hudgens MG, Halloran ME, Clemens JD, Ali M, Emch ME. Assessing effects of cholera vaccination in the presence of interference. *Biometrics*. Sep 2014;70(3):731-44. doi:10.1111/biom.12184

142. Baird S, Bohren JA, McIntosh C, Ozler B. Designing Experiments to Measure Spillover Effects. 2014;

143. Liu L, Hudgens MG, Becker-Dreps S. On inverse probability-weighted estimators in the presence of interference. *Biometrika*. 2016;103(4):829-842. doi:10.1093/biomet/asw047

144. Tchetgen Tchetgen EJ, VanderWeele TJ. On causal inference in the presence of interference. *Stat Methods Med Res*. Feb 2012;21(1):55-75. doi:10.1177/0962280210386779

145. Liu L, Hudgens MG, Saul B, Clemens JD, Ali M, Emch ME. Doubly robust estimation in observational studies with partial interference. *Stat*. 2019;8(1):e214.

146. VanderWeele TJ, Tchetgen Tchetgen EJ, Halloran ME. Interference and Sensitivity Analysis. *Statistical Science*. Nov 2014;29(4):687-706. doi:10.1214/14-sts479

147. Aronow PM, Samii C. Estimating average causal effects under general interference, with application to a social network experiment. *The Annals of Applied Statistics*. 2017;11(4):1912-1947.

148. Bowers J, Fredrickson MM, Panagopoulos C. Reasoning about interference between units: A general framework. *Political Analysis*. 2013;21(1):97-124.

149. Tchetgen Tchetgen EJ, Fulcher IR, Shpitser I. Auto-G-Computation of Causal Effects on a Network. *Journal of the American Statistical Association*. 2020:1-12. doi:10.1080/01621459.2020.1811098

150. Ogburn EL, Sofrygin O, Diaz I, van der Laan MJ. Causal inference for social network data. *arXiv preprint arXiv:170508527*. 2017;

151. Sofrygin O, van der Laan MJ. Semi-Parametric Estimation and Inference for the Mean Outcome of the Single Time-Point Intervention in a Causally Connected Population. *Journal of Causal Inference*. 2017;5(1):20160003. doi:10.1515/jci-2016-0003

152. van der Laan MJ. Causal Inference for a Population of Causally Connected Units. *Journal of Causal Inference*. Mar 2014;2(1):13-74. doi:10.1515/jci-2013-0002

153. Mossong J, Hens N, Jit M, et al. Social contacts and mixing patterns relevant to the spread of infectious diseases. *PLoS Medicine*. Mar 25 2008;5(3):e74. doi:10.1371/journal.pmed.0050074

154. Aiello AE, Simanek AM, Eisenberg MC, et al. Design and methods of a social network isolation study for reducing respiratory infection transmission: The eX-FLU cluster randomized trial. *Epidemics*. Jun 2016;15:38-55. doi:10.1016/j.epidem.2016.01.001

155. Mastrandrea R, Fournet J, Barrat A. Contact Patterns in a High School: A Comparison between Data Collected Using Wearable Sensors, Contact Diaries and Friendship Surveys. *PloS one*. 2015;10(9):e0136497. doi:10.1371/journal.pone.0136497

156. Smieszek T, Barclay VC, Seeni I, et al. How should social mixing be measured: comparing web-based survey and sensor-based methods. *BMC Infectious Diseases*. Mar 10 2014;14:136. doi:10.1186/1471-2334-14-136

157. Smieszek T, Burri EU, Scherzinger R, Scholz RW. Collecting close-contact social mixing data with contact diaries: reporting errors and biases. *Epidemiology and Infection*. Apr 2012;140(4):744-52. doi:10.1017/s0950268811001130

158. Smieszek T, Castell S, Barrat A, Cattuto C, White PJ, Krause G. Contact diaries versus wearable proximity sensors in measuring contact patterns at a conference: method comparison and participants' attitudes. *BMC Infectious Diseases*. Jul 22 2016;16:341. doi:10.1186/s12879-016-1676-y

159. Leecaster M, Toth DJ, Pettey WB, et al. Estimates of Social Contact in a Middle School Based on Self-Report and Wireless Sensor Data. *PloS One*. 2016;11(4):e0153690. doi:10.1371/journal.pone.0153690

160. Borgatti SP, Carley KM, Krackhardt D. On the robustness of centrality measures under conditions of imperfect data. *Social Networks*. 2006/05/01/ 2006;28(2):124-136. doi:https://doi.org/10.1016/j.socnet.2005.05.001

161. Frantz TL, Cataldo M, Carley KM. Robustness of centrality measures under uncertainty: Examining the role of network topology. *Computational and Mathematical Organization Theory*. 2009;15(4):303.

162. Wang DJ, Shi X, McFarland DA, Leskovec J. Measurement error in network data: A re-classification. *Social Networks*. 2012;34(4):396-409.

163. Huisman M. Imputation of missing network data: some simple procedures. *Encyclopedia of Social Network Analysis and Mining*. 2014:707-715.

164. Peixoto TP. Reconstructing Networks with Unknown and Heterogeneous Errors. *Physical Review X*. 10/16/ 2018;8(4):041011. doi:10.1103/PhysRevX.8.041011

165. Young J-G, Cantwell GT, Newman M. Bayesian inference of network structure from unreliable data. *Journal of Complex Networks*. 2020;8(6):cnaa046.

166. Cole SR, Chu H, Greenland S. Multiple-imputation for measurement-error correction. *International Journal of Epidemiology*. 2006;35(4):1074-1081. doi:10.1093/ije/dyl097

167. Edwards JK, Cole SR, Westreich D. All your data are always missing: incorporating bias due to measurement error into the potential outcomes framework. *International Journal of Epidemiology*. 2015;44(4):1452-1459. doi:10.1093/ije/dyu272

168. Edwards JK, Cole SR, Westreich D, et al. Multiple imputation to account for measurement error in marginal structural models. *Epidemiology (Cambridge, Mass)*. 2015;26(5):645-652. doi:10.1097/EDE.0000000000000330

169. Wang C, Butts CT, Hipp JR, Jose R, Lakon CM. Multiple Imputation for Missing Edge Data: A Predictive Evaluation Method with Application to Add Health. *Soc Networks*. Mar 1 2016;45:89-98. doi:10.1016/j.socnet.2015.12.003

170. *An Introduction to Exponential Random Graph Modeling*. 2014. Accessed 2019/05/14. https://methods.sagepub.com/book/an-introduction-to-exponential-random-graph-modeling

171. Koskinen JH, Robins GL, Pattison PE. Analysing exponential random graph (p-star) models with missing data using Bayesian data augmentation. *Statistical Methodology*. 2010;7(3):366-384.

172. Koskinen JH, Robins GL, Wang P, Pattison PE. Bayesian analysis for partially observed network data, missing ties, attributes and actors. *Social Networks*. 2013;35(4):514-527.

173. Handcock MS, Gile KJ. Modeling social networks from sampled data. *The Annals of Applied Statistics*. 2010;4(1):5.

174. Lu P-j, Santibanez TA, Williams WW, et al. Surveillance of influenza vaccination coverage—United States, 2007–08 through 2011–12 influenza seasons. *MMWR*. 2013;62(4):1-28.

175. McIntyre AF, Gonzalez-Feliciano AG, Bryan LN, et al. Seasonal Influenza Vaccination Coverage—United States, 2009–10 and 2010–11. *MMWR*. 2013;62(suppl 3):65-68.

176. Lipsitch M, Jha A, Simonsen L. Observational studies and the difficult quest for causality: lessons from vaccine effectiveness and impact studies. *International Journal of Epidemiology*. Dec 1 2016;45(6):2060-2074. doi:10.1093/ije/dyw124

177. Tchetgen EJT, Fulcher I, Shpitser I. Auto-G-Computation of Causal Effects on a Network. *arXiv preprint arXiv:170901577*. 2017;

178. Girvan M, Newman MEJ. Community structure in social and biological networks. *Proceedings of the National Academy of Sciences*. 2002;99(12):7821-7826. doi:10.1073/pnas.122653799

179. Thursky K, Cordova SP, Smith D, Kelly H. Working towards a simple case definition for influenza surveillance. *Journal of Clinical Virology*. 2003;27(2):170-179.

180. Health UDo, Services H. FDA clears new CDC test to detect human influenza. *Washington, DC: US Department of Health and Human Services*. 2008;

181. McLean HQ, Thompson MG, Sundaram ME, et al. Influenza vaccine effectiveness in the United States during 2012-2013: variable protection by age and virus type. *The Journal of Infectious Diseases*. May 15 2015;211(10):1529-40. doi:10.1093/infdis/jiu647

182. Puig-Barberà J, Natividad-Sancho A, Launay O, et al. 2012-2013 seasonal influenza vaccine effectiveness against influenza hospitalizations: results from the global influenza hospital surveillance network. *PloS One*. 2014;9(6):e100497.

183. Skowronski D, Janjua N, De Serres G, et al. Interim estimates of influenza vaccine effectiveness in 2012/13 from Canada's sentinel surveillance network, January 2013. *Eurosurveillance*. 2013;18(5):20394.

184. Debin M, Colizza V, Blanchon T, Hanslik T, Turbelin C, Falchi A. Effectiveness of 2012–2013 influenza vaccine against influenza-like illness in general population: Estimation in a French web-based cohort. *Human Vaccines & Immunotherapeutics*. 12/16 2014;10(3):536-543. doi:10.4161/hv.27439

185. Cohen S, Kamarck T, Mermelstein R. A Global Measure of Perceived Stress. *Journal of Health and Social Behavior*. 1983;24(4):385-396. doi:10.2307/2136404

186. Walt Svd, Colbert SC, Varoquaux G. The NumPy Array: A Structure for Efficient Numerical Computation. *Computing in Science & Engineering*. 2011/03/01 2011;13(2):22-30. doi:10.1109/MCSE.2011.37

187. Virtanen P, Gommers R, Oliphant TE, et al. SciPy 1.0: fundamental algorithms for scientific computing in Python. *Nature Methods*. 2020;17(3):261-272.

188. Seabold S, Perktold J. Statsmodels: Econometric and statistical modeling with python. 2010

189. Smith N. Patsy: describing statistical models in Python using symbolic formulas. 2018.

190. Hagberg AA, Schult DA, Swart PJ. Exploring network structure, dynamics, and function using NetworkX. 2008:11-15.

191. Pedregosa F, Varoquaux G, Gramfort A, et al. Scikit-learn: Machine Learning in Python. *Journal of Machine Learning Research*. 2011;12:2825-2830.

192. Servén D, Brummitt C. pyGAM: generalized additive models in python. *Zenodo DOI*. 2018;10

193. Goodreau SM, Handcock MS, Hunter DR, Butts CT, Morris M. A statnet tutorial. *Journal of Statistical Software*. 2008;24(9):1.

194. Hunter DR, Handcock MS, Butts CT, Goodreau SM, Morris M. ergm: A package to fit, simulate and diagnose exponential-family models for networks. *Journal of Statistical Software*. 2008;24(3):nihpa54860.

195. Team SD. RStan: the R interface to Stan. R package version 2.21.2. http://mc-stan.org/

196. Farine DR. Measuring phenotypic assortment in animal social networks: weighted associations are more robust than binary edges. *Animal Behaviour*. 2014;89:141-153.

197. Clemente GP, Grassi R, Clemente MGP. Package 'DirectedClustering'. *Chaos, Solitons and Fractals*. 2018;107:26-38.

198. Rubin DB. *Multiple imputation for nonresponse in surveys*. vol 81. John Wiley & Sons; 2004.

199. Newman ME. Mixing patterns in networks. *Physical Review E*. 2003;67(2):026126.

200. Watts DJ, Strogatz SH. Collective dynamics of 'small-world' networks. *Nature*. Jun 4 1998;393(6684):440-2. doi:10.1038/30918

201. Quenouille MH. Approximate tests of correlation in time-series. *Journal of the Royal Statistical Society Series B (Methodological)*. 1949;11(1):68-84.

202. Tukey J. Bias and confidence in not quite large samples. *Ann Math Statist*. 1958;29:614.

203. Miller RG. The jackknife-a review. *Biometrika*. 1974;61(1):1-15.

204. Snijders TA, Borgatti SP. Non-parametric standard errors and tests for network statistics. *Connections*. 1999;22(2):161-170.

205. Lin Q, Lunde R, Sarkar P. On the Theoretical Properties of the Network Jackknife. *arXiv preprint arXiv:200408935*. 2020;

206. Holme P, Kim BJ. Growing scale-free networks with tunable clustering. *Physical Review E*. 2002;65(2):026107.

207. Green TC, Ray M, Bowman SE, McKenzie M, Rich JD. Two cases of intranasal naloxone self-administration in opioid overdose. *Substance Abuse*. 2014;35(2):129-132.

208. Christakis NA, Fowler JH. The spread of obesity in a large social network over 32 years. Article. *New England Journal of Medicine*. 2007;357(4):370-379. doi:10.1056/NEJMsa066082

209. Smith NR, Zivich PN, Frerichs L. Social Influences on Obesity: Current Knowledge, Emerging Methods, and Directions for Future Research and Practice. *Current Nutrition Reports*. 2020/03/01 2020;9(1):31-41. doi:10.1007/s13668-020-00302-8

210. Rose S. Mortality risk score prediction in an elderly population using machine learning. *American journal of epidemiology*. 2013;177(5):443-452.

211. Van der Laan MJ, Polley EC, Hubbard AE. Super learner. *Statistical Applications in Genetics and Molecular Biology*. 2007;6(1)

212. Hastie TJ. Generalized additive models. *Statistical models in S*. Routledge; 2017:249-307.

213. Rumelhart DE, Hinton GE, Williams RJ. Learning representations by back-propagating errors. *Nature*. 1986;323(6088):533-536.

214. Breiman L. Random forests. *Machine learning*. 2001;45(1):5-32.

215. Zou H, Hastie T. Regularization and variable selection via the elastic net. *Journal of the Royal Statistical Society: Series B (statistical methodology)*. 2005;67(2):301-320.

216. Azur MJ, Stuart EA, Frangakis C, Leaf PJ. Multiple imputation by chained equations: what is it and how does it work? *International Journal of Methods in Psychiatric Research*. 2011;20(1):40-49.

217. Gelman A, Jakulin A, Pittau MG, Su Y-S. A weakly informative default prior distribution for logistic and other regression models. *The Annals of Applied Statistics*. 2008;2(4):1360-1383.

218. Shen Z. *Nested multiple imputations*. Harvard University; 2000.

219. McGinniss J, Harel O. Multiple imputation in three or more stages. *Journal of Statistical Planning and Inference*. 2016;176:33-51.

220. Holland PW, Leinhardt S. The structural implications of measurement error in sociometry. *Journal of Mathematical Sociology*. 1973;3(1):85-111.

221. Vaquera E, Kao G. Do You Like Me as Much as I Like You? Friendship Reciprocity and Its Effects on School Outcomes among Adolescents. *Social Science Research*. 2008;37(1):55-72. doi:10.1016/j.ssresearch.2006.11.002

222. Wiese J, Min J-K, Hong JI, Zimmerman J. " You Never Call, You Never Write" Call and SMS Logs Do Not Always Indicate Tie Strength. 2015:765-774.

223. Sprinzak E, Sattath S, Margalit H. How Reliable are Experimental Protein–Protein Interaction Data? *Journal of Molecular Biology*. 2003/04/11/ 2003;327(5):919-923. doi:https://doi.org/10.1016/S0022-2836(03)00239-0

224. H. KR, R. WI. A toolkit for measurement error correction, with a focus on nutritional epidemiology. *Statistics in Medicine*. 2014;33(12):2137-2155. doi:doi:10.1002/sim.6095

225. Edwards JK, Cole SR, Troester MA, Richardson DB. Accounting for Misclassified Outcomes in Binary Regression Models Using Multiple Imputation With Internal Validation Data. *American Journal of Epidemiology*. 2013;177(9):904-912. doi:10.1093/aje/kws340

226. Edwards JK, Cole SR, Fox MP. Flexibly Accounting for Exposure Misclassification With External Validation Data. *American Journal of Epidemiology*. 2020;doi:10.1093/aje/kwaa011

227. Young J-G, Cantwell GT, Newman M. Robust Bayesian inference of network structure from unreliable data. *arXiv preprint arXiv:200803334*. 2020;

228. Newman MEJ. Network structure from rich but noisy data. *Nature Physics*. 2018/06/01 2018;14(6):542-545. doi:10.1038/s41567-018-0076-1

229. Harris JK. *An introduction to exponential random graph modeling*. vol 173. Sage Publications; 2013.

230. Hoff PD. Additive and multiplicative effects network models. *arXiv preprint arXiv:180708038*. 2018;

231. Smith JA, Moody J. Structural Effects of Network Sampling Coverage I: Nodes Missing at Random(1). *Social networks*. 2013;35(4):10.1016/j.socnet.2013.09.003. doi:10.1016/j.socnet.2013.09.003

232. Yan B, Gregory S. Finding missing edges and communities in incomplete networks. *Journal of Physics A: Mathematical and Theoretical*. 2011;44(49):495102.

233. Costenbader E, Valente TW. The stability of centrality measures when networks are sampled. *Social Networks*. 2003;25(4):283-307.

234. Marsden PV. The reliability of network density and composition measures. *Social Networks*. 1993;15(4):399-421.

235. Kossinets G. Effects of missing data in social networks. *Social Networks*. 2006;28(3):247-268.

236. Smith JA, Moody J, Morgan JH. Network sampling coverage II: The effect of non-random missing data on network measurement. *Social Networks*. 2017/01/01/ 2017;48:78-99. doi:https://doi.org/10.1016/j.socnet.2016.04.005

237. Miller M, Neaigus A. Sex partner support, drug use and sex risk among HIV-negative non-injecting heroin users. *AIDS care*. 2002/12/01 2002;14(6):801-813. doi:10.1080/0954012021000031877

238. Miller M. The dynamics of substance use and sex networks in HIV transmission. journal article. *Journal of Urban Health*. September 01 2003;80(3):iii88-iii96. doi:10.1093/jurban/jtg086

239. Paluck EL, Shepherd H, Aronow PM. Changing climates of conflict: A social network experiment in 56 schools. *Proceedings of the National Academy of Sciences*. 2016;113(3):566-571.

240. Zhang S, de la Haye K, Ji M, An R. Applications of social network analysis to obesity: a systematic review. *Obesity Reviews*. 2018;19(7):976-988.

241. Holtz D, Zhao M, Benzell SG, et al. Interdependence and the cost of uncoordinated responses to COVID-19. *Proceedings of the National Academy of Sciences*. 2020;117(33):19837. doi:10.1073/pnas.2009522117

242. Li Y, Undurraga EA, Zubizarreta JR. Effectiveness of Localized Lockdowns in the SARS-CoV-2 Pandemic. *medRxiv*. 2020:2020.08.25.20182071. doi:10.1101/2020.08.25.20182071

243. Seamans MJ, Carey TS, Westreich DJ, et al. Association of Household Opioid Availability and Prescription Opioid Initiation Among Household Members. *JAMA Intern Med*. 2018;178(1):102-109. doi:10.1001/jamainternmed.2017.7280

244. Jarvis MJ, Feyerabend C, Bryant A, Hedges B, Primatesta P. Passive smoking in the home: plasma cotinine concentrations in non-smokers with smoking partners. *Tobacco Control*. 2001;10(4):368-374.

245. Du Y, Cui X, Sidorenkov G, et al. Lung cancer occurrence attributable to passive smoking among never smokers in China: a systematic review and meta-analysis. *Transl Lung Cancer Res*. 2020;9(2):204-217. doi:10.21037/tlcr.2020.02.11

246. Foster EM. Causal inference and developmental psychology. *Developmental Psychology*. 2010;46(6):1454.

247. Sobel ME. What Do Randomized Studies of Housing Mobility Demonstrate?: Causal Inference in the Face of Interference. *Journal of the American Statistical Association*. 2006;101(476):1398-1407.

248. Newman MEJ, Park J. Why social networks are different from other types of networks. *Physical Review E*. 09/22/ 2003;68(3):036122. doi:10.1103/PhysRevE.68.036122

249. Badham J, Kee F, Hunter RF. Network structure influence on simulated network interventions for behaviour change. *Social Networks*. 2021/01/01/ 2021;64:55-62. doi:https://doi.org/10.1016/j.socnet.2020.08.003

250. Schuler MS, Rose S. Targeted maximum likelihood estimation for causal inference in observational studies. *American Journal of Epidemiology*. 2017;185(1):65-73.

251. Van der Laan MJ, Rose S. *Targeted Learning: Causal Inference for Observational and Experimental Data*. Springer Science & Business Media; 2011.

252. Kennedy EH. Semiparametric theory and empirical processes in causal inference. *Statistical Causal Inferences and their Applications in Public Health Research*. Springer; 2016:141-167.

253. Zivich PN, Breskin A. Machine learning for causal inference: on the use of cross-fit estimators. *arXiv preprint arXiv:200410337*. 2020;

254. Schomaker M, Luque-Fernandez MA, Leroy V, Davies M-A. Using longitudinal targeted maximum likelihood estimation in complex settings with dynamic interventions. *Statistics in Medicine*. 2019;38(24):4888-4911.

255. Muñoz ID, van der Laan M. Population Intervention Causal Effects Based on Stochastic Interventions. *Biometrics*. 2012;68(2):541-549. doi:10.1111/j.1541-0420.2011.01685.x

256. Cole SR, Frangakis CE. The consistency statement in causal inference: a definition or an assumption? *Epidemiology*. 2009;20(1):3-5.

257. Hernán MA, Robins JM. Estimating causal effects from epidemiological data. *Journal of Epidemiology and Community Health*. 2006;60(7):578-586. doi:10.1136/jech.2004.029496

258. Balzer LB, Petersen ML, van der Laan MJ, Collaboration S. Targeted estimation and inference for the sample average treatment effect in trials with and without pair-matching. *Statistics in Medicine*. 2016;35(21):3717-3732.

259. Ference BA, Ginsberg HN, Graham I, et al. Low-density lipoproteins cause atherosclerotic cardiovascular disease. 1. Evidence from genetic, epidemiologic, and clinical studies. A consensus statement from the European Atherosclerosis Society Consensus Panel. *European Heart Journal*. 2017;38(32):2459-2472. doi:10.1093/eurheartj/ehx144

260. Buhaescu I, Izzedine H. Mevalonate pathway: A review of clinical and therapeutical implications. *Clinical Biochemistry*. 2007/06/01/ 2007;40(9):575-584. doi:https://doi.org/10.1016/j.clinbiochem.2007.03.016

261. Grundy SM, Stone NJ, Bailey AL, et al. 2018 AHA/ACC/AACVPR/AAPA/ABC/ACPM/ADA/AGS/APhA/ASPC/NLA/PCNA guideline on the management of blood cholesterol: a report of the American College of Cardiology/American Heart Association Task Force on Clinical Practice Guidelines. *Journal of the American College of Cardiology*. 2019;73(24):e285-e350.

262. Rudd RA, Aleshire N, Zibbell JE, Matthew Gladden R. Increases in Drug and Opioid Overdose Deaths—United States, 2000–2014. *American Journal of Transplantation*. 2016/04/01 2016;16(4):1323-1327. doi:10.1111/ajt.13776

263. Wilson N. Drug and opioid-involved overdose deaths—United States, 2017–2018. *MMWR*. 2020;69

264. Handal KA, Schauben JL, Salamone FR. Naloxone. *Annals of Emergency Medicine*. 1983;12(7):438-445.

265. Dwyer K, Walley AY, Langlois BK, et al. Opioid education and nasal naloxone rescue kits in the emergency department. *West J Emerg Med*. 2015;16(3):381-384. doi:10.5811/westjem.2015.2.24909

266. Clark AK, Wilder CM, Winstanley EL. A Systematic Review of Community Opioid Overdose Prevention and Naloxone Distribution Programs. *Journal of Addiction Medicine*. 2014;8(3):153-163. doi:10.1097/adm.0000000000000034

267. Binswanger IA, Blatchford PJ, Mueller SR, Stern MF. Mortality after prison release: opioid overdose and other causes of death, risk factors, and time trends from 1999 to 2009. *Annals of Internal Medicine*. 2013;159(9):592-600.

268. Zedler B, Xie L, Wang L, et al. Risk Factors for Serious Prescription Opioid-Related Toxicity or Overdose among Veterans Health Administration Patients. *Pain Medicine*. 2014;15(11):1911-1929. doi:10.1111/pme.12480

269. Lemmens VEPP, Oenema A, Klepp K-I, Henriksen HB, Brug J. A systematic review of the evidence regarding efficacy of obesity prevention interventions among adults. *Obesity Reviews*. 2008;9(5):446-455.

270. Halloran ME, Haber M, Longini Jr IM. Interpretation and estimation of vaccine efficacy under heterogeneity. *American Journal of Epidemiology*. 1992;136(3):328-343.

271. Ogburn EL, VanderWeele TJ. Vaccines, contagion, and social networks. *Annals of Applied Statistics*. 2017/06 2017;11(2):919-948. doi:10.1214/17-AOAS1023

272. Edwards JK, Cole SR, Lesko CR, et al. An Illustration of Inverse Probability Weighting to Estimate Policy-Relevant Causal Effects. *American Journal of Epidemiology*. 2016;184(4):336-344. doi:10.1093/aje/kwv339

273. Westreich D. From exposures to population interventions: pregnancy and response to HIV therapy. *American Journal of Epidemiology*. 2014;179(7):797-806. doi:10.1093/aje/kwt328

274. Kennedy EH. Nonparametric causal effects based on incremental propensity score interventions. *Journal of the American Statistical Association*. 2019;114(526):645-656.

275. Zimmerman RK, Nowalk MP, Raymund M, et al. Tailored interventions to increase influenza vaccination in neighborhood health centers serving the disadvantaged. *American Journal of Public Health*. 2003;93(10):1699-1705. doi:10.2105/ajph.93.10.1699

276. Stinchfield PK. Practice-proven interventions to increase vaccination rates and broaden the immunization season. *The American Journal of Medicine*. 2008;121(7):S11-S21.

277. Díaz I, van der Laan MJ. Stochastic treatment regimes. *Targeted Learning in Data Science*. Springer; 2018:219-232.

278. Munoz ID, van der Laan MJ. Super learner based conditional density estimation with application to marginal structural models. *The International Journal of Biostatistics*. 2011;7(1)

279. Cox DR. *Planning of experiments*. vol 20. Wiley Series in Probability and Statistics. Wiley; 1958.

280. Sävje F, Aronow PM, Hudgens MG. Average treatment effects in the presence of unknown interference. *arXiv preprint arXiv:171106399*. 2017;

281. Halloran ME, Struchiner CJ, Longini IM, Jr. Study designs for evaluating different efficacy and effectiveness aspects of vaccines. *American Journal of Epidemiology*. Nov 15 1997;146(10):789-803.

282. Sofrygin O, van der Laan MJ. Causal Inference in Longitudinal Network-Dependent Data. *Targeted Learning in Data Science*. Springer; 2018:349-371.

283. DiGuiseppi GT, Meisel MK, Balestrieri SG, et al. Resistance to peer influence moderates the relationship between perceived (but not actual) peer norms and binge drinking in a college student social network. *Addictive Behaviors*. May 2018;80:47-52. doi:10.1016/j.addbeh.2017.12.020

284. Cori A, Valleron A-J, Carrat F, Tomba GS, Thomas G, Boëlle P-Y. Estimating influenza latency and infectious period durations using viral excretion data. *Epidemics*. 2012;4(3):132-138.

285. Chernozhukov V, Chetverikov D, Demirer M, et al. Double/debiased machine learning for treatment and structural parameters. Oxford University Press Oxford, UK; 2018.

286. Grimaldi-Bensouda L, Aubrun E, Leighton P, et al. Agreement between patients' self-report and medical records for vaccination: the PGRx database. *Pharmacoepidemiology and Drug Safety*. 2013;22(3):278-285. doi:10.1002/pds.3401

287. Lochner KA, Wynne MA, Wheatcroft GH, Worrall CM, Kelman JA. Medicare claims versus beneficiary self-report for influenza vaccination surveillance. *American Journal of Preventive Medicine*. Apr 2015;48(4):384-91. doi:10.1016/j.amepre.2014.10.016

288. Grohskopf LA, Bresee JS, Cox N, Shimabukuro TT. Prevention and control of influenza with vaccines: recommendations of the Advisory Committee on Immunization Practices (ACIP)--United States, 2012-13 influenza season. 2012;

289. Helmeke C, Gräfe L, Irmscher H-M, Gottschalk C, Karagiannis I, Oppermann H. Effectiveness of the 2012/13 Trivalent Live and Inactivated Influenza Vaccines in Children and Adolescents in Saxony-Anhalt, Germany: A Test-Negative Case-Control Study. *PloS One*. 2015;10(4):e0122910. doi:10.1371/journal.pone.0122910

290. Buchan SA, Booth S, Scott AN, et al. Effectiveness of live attenuated vs inactivated influenza vaccines in children during the 2012-2013 through 2015-2016 influenza seasons in Alberta, Canada: a Canadian Immunization Research Network (CIRN) study. *JAMA pediatrics*. 2018;172(9):e181514-e181514.

291. VanderWeele TJ. On Well-defined Hypothetical Interventions in the Potential Outcomes Framework. *Epidemiology*. 2018;29(4):e24-e25. doi:10.1097/ede.0000000000000823

292. VanderWeele TJ, Hernan MA. Causal inference under multiple versions of treatment. *Journal of Causal Inference*. 2013;1(1):1-20.

293. Wanis KN, Madenci AL, Dokus MK, et al. The meaning of confounding adjustment in the presence of multiple versions of treatment: an application to organ transplantation. *European Journal of Epidemiology*. 2019;34(3):225-233.

294. Kasamba I, Sully E, Weiss HA, Baisley K, Maher D. Extraspousal partnerships in a community in rural Uganda with high HIV prevalence: a cross-sectional population-based study using linked spousal data. *Journal of Acquired Immune Deficiency Syndromes (1999)*. Sep 1 2011;58(1):108-14. doi:10.1097/QAI.0b013e318227af4d

295. Mah TL, Halperin DT. Concurrent sexual partnerships and the HIV epidemics in Africa: evidence to move forward. *AIDS and behavior*. Feb 2010;14(1):11-6; dicussion 34-7. doi:10.1007/s10461-008-9433-x

296. Lurie MN, Rosenthal S. Concurrent Partnerships as a Driver of the HIV Epidemic in sub-Saharan Africa? The Evidence is Limited. *AIDS and behavior*. 06/02 2010;14(1):10.1007/s10461-009-9583-5. doi:10.1007/s10461-009-9583-5

297. Kretzschmar M, Morris M. Measures of concurrency in networks and the spread of infectious disease. *Mathematical Biosciences*. 1996/04/15/ 1996;133(2):165-195. doi:https://doi.org/10.1016/0025-5564(95)00093-3

298. Morris M, Kretzschmar M. Concurrent partnerships and the spread of HIV. *AIDS (London, England)*. 1997;11(5):641-648.

299. Morris M. Barking up the Wrong Evidence Tree. Comment on Lurie & Rosenthal, "Concurrent Partnerships as a Driver of the HIV Epidemic in Sub-Saharan Africa? The Evidence is Limited". *AIDS and behavior*. 12/09 2010;14(1):31-33. doi:10.1007/s10461-009-9639-6

300. Mah TL, Halperin DT. The Evidence for the Role of Concurrent Partnerships in Africa's HIV Epidemics: A Response to Lurie and Rosenthal. journal article. *AIDS and behavior*. February 01 2010;14(1):25-28. doi:10.1007/s10461-009-9617-z

301. Pines HA, Wertheim JO, Liu L, Garfein RS, Little SJ, Karris MY. Concurrency and HIV transmission network characteristics among MSM with recent HIV infection. *AIDS (London, England)*. Nov 28 2016;30(18):2875-2883. doi:10.1097/qad.0000000000001256

302. Howard J, Huang A, Li Z, et al. An evidence review of face masks against COVID-19. *Proceedings of the National Academy of Sciences*. 2021;118(4)

303. Cheng KK, Lam TH, Leung CC. Wearing face masks in the community during the COVID-19 pandemic: altruism and solidarity. *The Lancet*. 2020;

304. Xiao J, Shiu EY, Gao H, et al. Nonpharmaceutical measures for pandemic influenza in nonhealthcare settings—personal protective and environmental measures. *Emerging Infectious Diseases*. 2020;26(5):967.

305. Pleil JD, Beauchamp JD, Risby TH, Dweik RA. The scientific rationale for the use of simple masks or improvised facial coverings to trap exhaled aerosols and possibly reduce the breathborne spread of COVID-19. *J Breath Res*. 2020;14(3):030201-030201. doi:10.1088/1752-7163/ab8a55

306. Leung NH, Chu DK, Shiu EY, et al. Respiratory virus shedding in exhaled breath and efficacy of face masks. *Nature Medicine*. 2020;26(5):676-680.

307. Lee Y, Ogburn EL. Network Dependence Can Lead to Spurious Associations and Invalid Inference. *Journal of the American Statistical Association*. 2020:1-15. doi:10.1080/01621459.2020.1782219

308. Benjamin-Chung J, Arnold BF, Berger D, et al. Spillover effects in epidemiology: parameters, study designs and methodological considerations. *International Journal of Epidemiology*. Feb 1 2018;47(1):332-347. doi:10.1093/ije/dyx201

309. Halloran ME. The Minicommunity Design to Assess Indirect Effects of Vaccination. *Epidemiologic Methods*. Aug 01 2012;1(1):83-105. doi:10.1515/2161-962x.1008